Design and operation of a Fixed Bed Pyrolizer for thermochemical conversion of municipal solid waste and its product applications

A thesis submitted

in partial fulfillment of the requirement for the degree of

Doctor of Philosophy

By

Silvia Saikia

School of Agro and Rural Technology

Indian Institute of Technology Guwahati

Guwahati-781039, Assam, India

March-2025

In loving gratitude to

My beloved parents

whose unwavering love, blessings, and continual encouragement have been the guiding light leading to my achievements and growth

School of Agro and Rural Technology
Indian Institute of Technology Guwahati
Guwahati – 781039, Assam, India

Dr. Ajay Kalamdhad

Professor

Email: kajay@iitg.ac.in

Phone: +91-361-258-2431

CERTIFICATE

This is to certify that the thesis entitled **"Design and operation of a fixed bed pyrolizer for thermochemical conversion of municipal solid waste and its product applications"** submitted by Silvia Saikia (196154104), a Research Scholar of School of Agro and Rural Technology, Indian Institute of Technology Guwahati, for the award of the degree of Doctor of Philosophy, is a record of an original research work carried out by under my supervision and guidance. The thesis has fulfilled all requirements as per the regulations of the institute and, in my opinion, has reached the standard needed for submission. The results embodied in this thesis have not been submitted to any other University or Institute for the award of any degree or diploma to the best of my knowledge and belief.

Date: 26-03-2025
Place: IIT Guwahati

Prof. Ajay Kalamdhad

School of Agro and Rural Technology
Indian Institute of Technology Guwahati
Guwahati – 781039, Assam, India

STATEMENT

I, Silvia Saikia, declare that this thesis titled **"Design and operation of a fixed bed pyrolizer for thermochemical conversion of municipal solid waste and its product applications"** and the work presented in it are my own. I confirm that:

- This work was done wholly while in candidature for a research degree at this Institute.
- In full or in portions, the contents of this thesis have not been submitted to any other University or Institute for the award of any degree or diploma.
- Where I have consulted the published work of others, this is always clearly attributed.
- Where I have quoted from the work of others, the source is always given. With the exception of such quotations, this thesis is entirely my own work.
- I have acknowledged all main sources of help.
- Where the thesis is based on work done by myself jointly with others, I have made clear exactly what was done by others and what I have contributed myself.

Date: 26.03.2025

Signed: Silvia Saikia

Silvia Saikia

Registration No.: 196154104

ACKNOWLEDGEMENT

I am truly privileged to have this opportunity to express my profound gratitude to the individuals who have wholeheartedly supported me in my journey toward the completion of this thesis. I firmly believe that without their support, the successful completion of this work would not have been possible.

First and foremost, I am profoundly grateful to my supervisor, **Prof. Ajay Kalamdhad**, for his exceptional guidance and mentorship throughout my research journey. His invaluable expertise, constructive feedback, and unwavering encouragement have played a pivotal role in shaping the direction of this thesis and driving me to reach my fullest potential. His dedication, patience, and commitment to excellence have been a constant source of inspiration, and I consider myself incredibly fortunate to have had such an outstanding supervisor who believed in my capabilities and nurtured my academic and personal growth. Working under his supervision has been an honour, and I am deeply indebted to him for his significant contribution to my overall development.

I would also take this opportunity to thank my Doctoral Committee Members, **Dr. Siddhartha Singha** (Chairman), **Dr. Meena Khwairakpam**, and **Dr. Bimlesh Kumar**, for their exceptional suggestions and encouragement in propelling my research work forward. Their thought-provoking questions have inspired me to explore my research from diverse perspectives, leading to a more comprehensive and enriched study. I also express my sincere thanks to **Prof. Sudip Mitra**, Head of the School of Agro and Rural Technology for providing me with the necessary research facilities.

I express my gratitude to **Prof. Devendra Jalihal**, Director of IITG, for providing necessary facilities and creating a conducive academic environment within the institution that facilitated my research journey. Additionally, I acknowledge the Central Instrument Facility, Department of Civil Engineering, Mechanical Workshop, and Lakshminath Bezbaroa Central Library at IIT Guwahati for offering state-of-the-art infrastructure for conducting advanced research in the field of study.

I extend my sincere appreciation to all the members of the **Waste Management Research Group (WMRG)** for their invaluable support, engaging research discussions, and assistance in my laboratory work. Being a part of the WMRG family has enriched my research experience in countless ways. Words will fall short of expressing my gratitude to Mr. Sujit and Mr. Raju for their constant assistance during the experimental setup and sample collection.

I would also appreciate the efforts of **Ms. Anagha V**, **Mr. Harsh Prit**, and **Mr. Sajan Kumar Dansena**, former master's students of IIT Guwahati, for their contribution during my academic journey, especially while assisting in the experimental work. I extend my best wishes to them for their future endeavours.

I must take this opportunity to thank my seniors, **Dr. Maturi Krishna Chaitanya, Dr. Shinjini Paul Choudhury, Dr. Suryateja Pottipati**, **Dr. Jayeeta Hazarika, Dr. Izharul Haq, Dr. Gaurav Goel**, **Dr. Jiwan Singh, Dr. Mayur Shirish Jain, Dr. Chejarla Venkatesh Reddy**, **Dr. Mandefroth Dubale**, **Dr. Heena Kauser, Dr. Ankit Goswami, and Dr. Saswati Ray,** for their support and mentorship during my journey.

I must say thanks to my supportive friends, juniors, and labmates, **Ms. Vaishnavi Jahagirdar, Ms. Jyoti Beniwal, Ms. Phularaitpam Sujata Devi, Ms. Ashmita Kundu, Ms. Sanjana Sinha, Ms. Nidhi Chhabra, Ms. Sumona Koley, Ms. Bwenele Tep, Ms. Rajkumari Joyshree Devi, Mr. Prakash Singh**, **Mr. Arun Sathyan**, **Mr. Induchoodan T.G.**, **Mr. Monish Goswami, Mr. Zamminsion**, **Mr. Ankit Kumar**, **Mr. Sayan Saha, Mr. Sagar Aditya,** and **Mr. Kiran Venkatesh** whose support and respect during my research journey at IITG have been encouraging.

Lastly, I am deeply grateful and indebted to my mother, **Mrs. Biva Saikia**, my father, **Mr. Sanjib Saikia**, and my sister**, Ms. Chinmoyee Saikia,** for their unconditional love, unwavering support, continuous encouragement, and blessings throughout my years of study and the entire research journey leading up to this thesis. Their presence has been the cornerstone of my achievements, and I cannot thank them enough for existing in my life. Above all, I humbly acknowledge the **ALMIGHTY** for bestowing upon me the wisdom, strength, and patience to undertake this research and complete it with His divine grace and blessings.

Silvia Saikia

ABSTRACT

Pyrolysis provides an effective approach for municipal solid waste (MSW) management, enabling energy recovery and resource utilization. This study evaluated the pyrolysis of MSW and legacy waste, demonstrating their potential as renewable energy sources with heating values of 37,737.89 kJ/kg and 40,432.84 kJ/kg, respectively. Proximate analysis confirmed their suitability for pyrolysis without auxiliary fuel, and lignin content (47.6% in MSW, 44.16% in legacy waste) supported char production. Thermal degradation resulted in mass losses of 68% and 82%, with MSW exhibiting lower activation energy (5.72 kJ/mol), suggesting faster reactions.

A fixed-bed reactor was designed and optimized using Central Composite Design (CCD) to maximize char yield. The highest char yield (72.62%) was achieved at 250°C, a 10°C/min heating rate, 50 mm particle size, and 180-minute residence time. A p-value of <0.05 from ANOVA indicated that each process parameter was statistically significant. The operating temperature for pyrolysis was the most influential variable for achieving the highest char yield based on the F-value derived from ANOVA.

MSW char produced at different temperatures exhibited changes in physicochemical properties. The 250°C char retained the highest fuel potential. Activated carbon derived from MSW char (250°C) using KOH showed over 90% Pb(II) removal from water, following the Langmuir isotherm (R^2 = 0.99), with reusability up to two cycles. Composting trials incorporating MSW char improved compost quality, with the 5% char amendment enhancing nitrogen (+2.35%) and phosphorus (+23.48 mg/kg) while lowering the C/N ratio (10).

Soil amendment studies over 120 days showed that MSW char and compost improved soil health by reducing bulk density (-12%), enhancing organic matter, and increasing cation exchange capacity. While heavy metal bioavailability initially rose with compost, it was mitigated with MSW char. In mine tailing soil, MSW char (10%) increased pH (+45.44%), while a 5% char–30% vermicompost mix

improved nutrient retention and reduced heavy metal leachability (Ni -30%, Pb -61%).

Overall, MSW pyrolysis presents a sustainable waste management strategy, producing biochar that enhances soil health, supports composting, and reduces heavy metal contamination. This study underscores MSW char's role in advancing circular economy goals and environmental sustainability.

Keywords: *Municipal solid waste; Pyrolysis; Char; Heavy metal; Adsorbent; Activated carbon; Soil amendment; Compost; Vermicompost; Mine tailing soil*

TABLE OF CONTENT

LIST OF FIGURES

Chapter 10

LIST OF TABLES

Chapter 1

INTRODUCTION

1.1 INTRODUCTION

The anticipated worldwide rise in overall waste production could surge by 70%, amounting to approximately 3.40 billion metric tons by 2050 (Kaza et al., 2018). The United States, China, and India rank as the leading producers of waste (Law et al., 2020). As outlined in the Global Waste Management Outlook 2024, the global solid waste output amounts to 2.1 billion tonnes, with 0.76 kg/person/day as of 2020, and will reach 0.88 kg/person/day by 2030 (UNEP, 2024). Projections suggest a 56% increase in annual waste production by 2050, reaching 3.88 billion tonnes, driven by population growth and urbanization (UNEP, 2024). Within this amount, 13.5% of waste is subjected to recycling, 5.5% undergoes composting, and 40% is disposed of improperly through dumping or neglect. According to the Press Information Bureau, in the Indian context, the generated waste annually is 62 million tons, out of which 60% is being collected and 15% is being treated. Projections indicate that waste production in India is set to rise from 60 million tons to 150 million tons by 2030, as highlighted by the Press Information Bureau in 2021 (Cheela et al., 2021). This increase can be attributed to the swift industrialization, urbanization, and economic expansion in India, which has resulted in rural-to-urban migration, subsequently contributing to an escalation in MSW generation on a per kilogram per capita daily basis (Vikramarjun et al., 2020).

Management of MSW through sustainable technology is challenging as these wastes are heterogeneous and change their composition and generation rate over time. If the waste is not controlled appropriately, it could negatively affect the environment and climate (Sharma et al., 2019). In India, the management of MSW is governed by the guidelines outlined in the Solid Waste Management Rules, 2016. These regulations encompass various aspects such as waste generation, collection, transportation, treatment, and disposal (Gupta et al., 2016). Many Urban Local Bodies (ULBs) lag behind in the proper collection and treatment of this massive

waste generated due to improper collection systems (Sharholy et al., 2008). Due to the lack of a transportation system, the loading of waste to the landfill becomes difficult (TERI, 2014). The lack of reuse and recycling facilities results in the disposal of reusable and recyclable plastics, metals, and glass in the dumpsite (Gupta et al., 2015). Also, due to improper scientific treatment facilities (Kaushal et al., 2012) and the technology gap (Sahu et al., 2014), the treatment of this waste in large quantities has not been achieved yet. The disposal capacity of waste in the landfill is low due to the massive generation of this waste as compared to the space available for disposal (Periathamby et al., 2012). Additionally, the shortage of financial means (Sharholy et al., 2008) and labor resources (Upadhyay et al., 2012) contributes to hindrances in the effective collection of waste from the source of generation.

In India, most landfills or dumpsites are still operational even after exhausting their capacity due to the lack of landfills (Ghosh and Kartha, 2024). Examples of such exhausted landfills are at Deonar in Mumbai, Ghazipur, Bhalswa, and Okhla in Delhi (Kumar et al., 2013). Such over-dumping can lead to landfill collapse due to slope failure (Koelsch et al., 2005). The investigation and analysis of all the old and operational dumpsites were made necessary in India according to Solid Waste Management Rule 2016 for determining the potential and feasibility for reclamation, biomining, and bioremediation of the dumpsites (Bhatnagar et al., 2017). About 21% of the total waste comprises combustible fractions, with 2% of paper/cardboard and 4% of textile fractions that are not recyclable, as these waste fractions are highly contaminated. The plastic fraction in this legacy waste requires sub-segregation and pretreatment for recycling. It should meet permissible standards for heavy metals, and recycling these plastics requires an initial investment, which is economically not feasible (Alghobar et al., 2017). Moreover, recycling of these plastic wastes by physical and chemical processes emits 1 to 1.5 tons of carbon (Simon et al., 2021). The most appropriate option for the treatment of unsegregated MSW is thermal treatment. Pyrolysis of these wastes is a feasible option while taking Waste to Energy and the environment into account (Bosmans et al., 2013).

Pyrolysis is a thermal degradation of feedstock in the absence of air, which gives products such as solid char, liquid oil/tar, and gas. For thousands of years, pyrolysis has been done using biomass as feedstock for the production of charcoal. Accordingly, the conditions of operation for pyrolysis of a feedstock can also be optimized according to the product requirement, such as char, oil/tar, or gas. Numerous non-biodegradable MSW components can be processed using pyrolysis. Pyrolysis is an environmentally preferable method since it emits less greenhouse gases and toxic pollutants than incineration, gasification, or combustion. It has a reduced carbon footprint as compared to other technologies for the treatment of solid waste (Saravanakumar et al., 2024). The energy recovery potential from pyrolysis is higher than any other thermochemical conversion process (Sipra et al., 2018). The syngas produced during pyrolysis can be used as a fuel for the combustion process or for the generation of electricity, thus contributing to the production of renewable energy. Also, the quality of char and pyrolysis oil produced is eligible to be utilized as a value-added product (Saffarzadeh et al., 2006). The amount of feedstock used in pyrolysis is flexible, unlike incineration, which operates on kiloton per day. Currently, the demand for pyrolysis of MSW is increasing to prevent waste transportation over a long distance and reduce incineration and landfilling of MSW due to lack of site availability. The valorization of waste is becoming an interesting area of research at the industry level as it is environmentally and economically sustainable (Moustakas et al., 2020). There are many studies on pyrolysis of an individual component of MSW (Chen et al., 2015; Wong et al., 2015; Al-Salem et al., 2017; Barampouti et al., 2019; Elkhalifa et al., 2019), but significantly less on pyrolysis of comingled MSW, which is much needed because, in most of the developing countries, waste handling is not effective as there is no segregation of waste at the source.

The thermal degradation of the material during pyrolysis can be divided into drying, primary stage, secondary stage, and charring. In the first stage, the moisture content of the material is eliminated at 100 to 200°C. In this stage, the water in the raw material evaporates, preparing for the processes of thermal degradation thereafter. In the devolatilization or primary stage, the organic parts of the material

start to break down into volatile molecules. The long-chain hydrocarbons break down into gases, vapors that condense into bio-oil, and solid residues into biochar at 200 to 500°C. The heating rate, particle size, feedstock type, and temperature profile strongly influence the quantity of yield and product composition. During the secondary cracking stage, the vapors formed in the devolatilization stage are further broken down into smaller molecules, stable compounds, and lighter gases. The amount and quality of the pyrolysis oil and gases are determined at this step. A combination of hydrogen, carbon monoxide, and methane, known as syngas, is produced more readily at higher temperatures. In the char formation stage, after the volatile is driven off, the solid residues are turned into char (Hasan et al., 2021).

1.2 TYPES OF PYROLYSIS PROCESSES

The pyrolysis process is categorized based on factors like operational temperature, residence time, and heating rate. Also, depending on the product targeted, such as char, syngas, and oil, the type of pyrolysis varies.

1.2.1 Slow pyrolysis

Slow pyrolysis is executed at an operational temperature of 400°C, with a gradual heating rate of 0.1 to 1°C/s. This method primarily focuses on generating char. The duration of this process spans more than 30 minutes. The resulting product distribution consists of 35% biochar (solid), 30% bio-oil (liquid), and 35% syngas (gas) (Onay and Kockar, 2003). Literature also exists concerning the production of bio-oil through the process of slow pyrolysis (Stamatov et al., 2006). Slow pyrolysis has been historically employed for carbonizing feedstock to produce charcoal. The output of bio-oil and biochar is significantly influenced by the characteristics of the feedstock used for pyrolysis, such as temperature, moisture content, ash content, volatile matter, and fixed carbon. Optimal moisture content in the feedstock falls within the range of 15 to 20%, as identified by Vitolo et al. (2001) and Bridgwater and Peacocke (2000), as ideal for biochar production via pyrolysis. Furthermore, the slow pyrolysis process can accommodate a wide variety of feedstock sizes.

1.2.2 Fast Pyrolysis

Fast pyrolysis is characterized by an operational temperature of 500°C and a rapid heating rate ranging from 1 to 200°C per second. This method features a brief residence time of 10 to 20 seconds. The primary objective of this pyrolysis variant is to achieve the highest possible yield of bio-oil, succeeded by syngas and biochar. The product distribution resulting from fast pyrolysis consists of 20% biochar (solid), 50% bio-oil (liquid), and 30% syngas (gas), as reported by Bridgwater and Peacocke in 2000. In fast pyrolysis, the feedstock commonly involves finely ground particles, and the reaction time within the reactor is shorter compared to slow pyrolysis. Heat and mass transfer rates, chemical kinetics, and transitional phenomena principally influence the composition of the produced yield. According to existing literature, the optimal temperature for generating the maximum amount of bio-oil is 500°C (Demirbas et al., 2007; Jones et al., 2009; Iribarren et al., 2012; Lira et al., 2013) with a yield of 70 wt% bio-oil (Xiu et al., 2012; Lehto et al., 2013).

1.2.3 Flash pyrolysis

Flash pyrolysis entails an operational temperature of 700 to 900°C or higher, accompanied by an exceedingly swift heating rate exceeding 1000°C per second, within a residence time of just one second. The resulting product distribution through flash pyrolysis includes 13% syngas (gas), 2% biochar (solid), and 75% bio-oil (liquid) (Marcilla et al., 2013) Given the demanding heating rate of flash pyrolysis, the feedstock's particle size should be extremely diminutive (Kataki et al., 2018). This method allows for utilizing around 80% of the feedstock to produce energy-dense materials with greater density compared to the original feedstock (Maliutina et al., 2017). However, the bio-oil derived from this pyrolysis process contains elevated levels of oxygen, which leads to corrosion, along with substantial quantities of heavy metals and nitrogen. Addressing these pollutants necessitates a significant amount of hydrogen, which can prove to be financially challenging (Fang et al., 2018).

1.3 TYPES OF PYROLYSIS REACTORS

There are several types of pyrolizers, but the most commonly used are fixed-bed, fluidized-bed, ablative, auger or screw, and rotary kiln. For pyrolysis to be effective, design parameters like higher heat transfer and short residence time must be ensured (Musale et al., 2013). The pyrolysis reactors are operated according to the product requirement. A high heat transfer rate and low residence time are preferable for producing a high quantity of bio-oil. Whereas if the objective is to produce large quantities of biochar and syngas, then heat transfer to the feedstock must be low with high residence time. Some of the pyrolysis reactors commonly used for the production of biochar, bio-oil, and syngas from MSW have been discussed below.

1.3.1 Fluidized-bed reactor

Fluidized-bed reactors are very popular reactors used for pyrolysis in the laboratory and industrial scale, primarily to produce chemicals and oil. These reactors have a high heat transfer rate and continuous feeding, and the process can be controlled. There are two types of fluidized bed reactors: bubbling fluidized bed reactors and circulating fluidized bed reactors.

In a bubbling fluidized bed reactor, the hot sand bed is used, which is fluidized by an inert gas, and the feeding is done after shredding the MSW into the size of 2 to 6 mm (Beheshti et al., 2015). In most cases, for high heat transfer to the feedstock, sand is used. The heating inside the reactor is done by combustion of the product gas and sometimes by combustion of biochar produced by pyrolysis (Ding et al., 2016). The drawback of this type of reactor is that if the feedstock used is heterogeneous, i.e., mixed MSW, the separation of biochar from the volatile is difficult. Moreover, the sand used in this type of reactor also leads to corrosion.

In a circulating fluidized bed reactor, the fluidizing bed is expanded, and the sand is circulated inside the reactor (Grace et al., 1997). The advantage of this type of reactor is that it provides uniform mixing of a large quantity of feedstock with controllable temperature. Also, the biochar produced in this reactor is easy to separate from the bubbling fluidized bed reactor.

1.3.2 Fixed-bed reactor

It is a batch type reactor that is considered adequate for pyrolysis of material with uniform size. Heat is supplied externally for thermal degradation of the feedstock. The gaseous product formed due to pyrolysis flows out of the reactor due to volume expansion of gaseous material, and the biochar formed remains inside the reactor. For efficient removal of syngas, sweep gas is also used in some fixed bed reactors (Onay et al., 2007). The primary products in these types of pyrolysis reactors are biochar and syngas. There are some drawbacks in this type of reactor, such as long residence time and temperature inside the reactor is not uniform, resulting in non-uniform heating of ample quantity feedstock.

1.3.3 Rotary kiln reactor

This type of reactor is primarily suitable for heterogeneous waste and is commonly used on an industrial scale. This type of reactor features a low heating rate and adjustable residence time of the solid phase that can reach up to 1 hour (Fantozzi et al., 2007). In the case of heating feedstock, a rotary kiln reactor heats more uniformly than a fixed bed reactor (Fantozzi et al., 2007). The rotation mechanism of the kiln enhances the mixing of the waste for uniform heating. This type of reactor is reported to be the most commonly used reactor in the case of pyrolysis of MSW (Chen et al., 2015).

1.3.4 Screw or Auger reactor

This is a continuous tubular shape reactor provided with a screw that rotates and transports the feedstock to the reactor, and heat transfer occurs through the reactor's tubular wall. The inert gas is purged into the hopper feedstock to make the feedstock free from oxygen. The pyrolysis vapour moves through a slight positive pressure exerted by the inert gas. The heat required to increase the temperature of the tubes is fulfilled by the heat supplied from outside, but if the amount of feedstock is more than it requires very high temperature hot solid carriers such as steel or ceramic pellets (Bortolamasi et al., 2001). Like any other pyrolysis reactor, here also, the vapour is condensed to produce bio-oil. The advantage of an auger or screw reactor is that it is compact and portable and can be used at the feedstock

generation site making it economical by reducing transportation costs to the treatment site (Badger et al., 2006).

1.3.5 Ablative reactor

In an ablative reactor, high pressure is created inside the reactor between reactor walls and feedstock, enabling heat transfer from the reactor wall to feedstock, resulting in heating water in the feedstock to remove the moisture. This type of reactor has a high heating rate and low residence time (Peacocke et al., 1994), leading to the production of 80% bio-oil (Solantausta et al., 1993). Large sizes of feedstock can be processed at a time in this type of reactor.

1.3.6 Other pyrolysis reactors and technologies

The above-discussed reactors are single-stage reactors, and the products from the pyrolysis in these types of reactors require post-treatment for utilization. There are also multi-stage pyrolysis reactors whose products do not require treatment and produce an improved quality of products. Ohmukai et al. (2008) used a two-stage tube reactor to study the influence of steam reforming on the tar generated in the first stage of the reactor, since the two stages can be regulated under different conditions. Cao et al. (2011) described a three-stage reactor for a similar purpose, in which the first stage is for HCl extraction, the second stage is for volatile extraction, and the third stage is for product reformation. The multi-stage reactors allow the pyrolysis reactor to operate independently. Traditional thermal pyrolysis uses hot flue gas in the reactor to provide process heat, although there are also pyrolysis methods such as plasma pyrolysis (Hrabovsky et al., 2006) and microwave pyrolysis (Beneroso et al., 2017), in which the process heat is supplied by volumetric heating. Plasma pyrolysis is the process of heating trash to above 1000°C in the absence of air using plasma torches, converting waste into a synthetic gas (mostly CO and H_2) and other value-added end-products. It has a very high efficiency in providing heat that modifies the physical and chemical composition of waste materials, allowing it to adjust the operating temperature, heating rate, decreased reaction volume, and optimal syngas composition. The products are also harmless in terms of public health and the environment (Huang et al., 2007). The disadvantage of the plasma pyrolysis technique is that it takes a considerable

quantity of secondary energy. Plasma pyrolysis is now mostly used to remediate hazardous waste. Even if a facility is present, a life cycle assessment comparison of the entire process with a thermal cracking system is advised for its MSW implementation. Microwave pyrolysis is mostly utilized for homogeneous wastes such as sludge, shredded plastics, and tyres. These types of reactors use microwave dielectric heating technology. It is notable for its efficient in-core volumetric heating for direct coupling of microwave energy with the molecules present in the reactants. It can simply manage and maintain the desired temperature for pyrolysis based on the product, such as maintaining a lower temperature on the material's surface and a higher temperature inside the material (Baghurst et al., 1992). However, to achieve the required rapid heating rate, the feedstock particle size must be very fine, and to reach the required temperature in a microwave reactor, accurate dielectric data in the microwave frequency range is required, which is not available for most waste components. In order to reduce secondary tar cracking, the vapor must be swiftly swept out of a microwave reactor (Yin et al., 2012). Microwave pyrolysis of heterogeneous MSW is not a viable solution in the future due to its limited treatment capacity. There is also pyrolysis technology based on the employment of several catalysts to boost the yield of the product from municipal plastic waste pyrolysis (MPW). The benefits of utilizing catalysts in the pyrolysis process over the typical thermal degradation method are lower energy consumption, shorter reaction times, and improved selectivity to higher-value compounds. Furthermore, the liquid products of pyrolysis utilizing catalysts have a boiling point in the range of commercial motor engine fuel, opening the door to future applications (Gulab et al., 2010).

1.4 BACKGROUND

Char is a carbon-rich substance produced from the pyrolysis of biomass and has garnered significant attention for its wide range of applications in environmental management, agriculture, and industry (Masud et al., 2023). Since organic waste makes up some portion of solid waste, there is a lot of potential for producing char from the pyrolysis of MSW (Hu et al., 2017; El-Naggar et al., 2019). The resulting char is a very rich carbon source that is generated when it is pyrolyzed in an

inert atmosphere (Lehmann and Joseph, 2009; Mohanty et al., 2018). Char has special qualities that make it useful for a variety of applications, including a wide surface area, high porosity, functional groups, a high cation exchange capacity, and stability. A few benefits of char are its quick and simple production, eco-friendliness, cost-effectiveness, and reusability (Hemavathy et al., 2020; Gayathri et al., 2021). Numerous researchers have been interested in biochar due to its effectiveness in eliminating a wide range of pollutants. The yield of char is mostly determined by the operational parameters (Babu and Chaurasia, 2003). The primary factor influencing char's characteristics is temperature (Kambo and Dutta, 2015). To produce biochar, thermochemical processes such as torrefaction, hydrothermal treatment, gasification, pyrolysis, and flash carbonization are frequently employed (Bridgwater, 2012). Pyrolysis is the most generally employed process of all of them for producing biochar (Yaashikaa et al., 2019). Despite the fact that char is entirely composed of carbon and ash, its elemental content and properties vary depending on the variety of feedstock, the circumstances of the reaction, and the kind of reactors used in the pyrolysis process. Therefore, the kind of feed used to produce char determines the use and effectiveness of char in different domains. Determining the elemental composition, surface functional groups, stability, and structure of char requires careful characterization. Many contemporary methods, including Thermo Gravimetric Analysis (TGA), X-ray diffraction (XRD), Raman spectroscopy, Brunauer Emmett Teller (BET), nuclear magnetic resonance (NMR), Fourier transform infrared spectrometer (FTIR), and scanning electron microscopy (SEM) can be used to characterize the char (Lou et al., 2012). Adsorption is the process by which heavy metals and other pollutants are adsorbed by char. The physicochemical characteristics of char, such as surface area, functional groups, and cation exchange capacity, are closely correlated with its adsorptive performance. The application of oxidizing, alkalizing, or acidic chemicals to char enhances its physicochemical characteristics (Kumar et al., 2011). The treatment of char with acid can be used for modifying the surface area.

The extensive literature on the characteristics of char and the methods used to

analyze and contribute to the efficiency of char in a variety of industries. Char has been used to address a wide range of environmental problems because of its various benefits and sustainability, including the adsorption of heavy metals (Saravanan et al., 2018), catalysts (Lee et al., 2017), composting (He et al., 2017), soil remediation (Liu et al., 2017), the reduction of greenhouse gas emissions (Awasthi et al., 2017), production of energy (Shen, 2015), and treatment of wastewater (Wang et al., 2017). Char has also been used in agricultural areas to remove contaminants from the soil. Biochar has been made from a variety of agricultural leftovers, including scrap wood (Yargicoglu et al., 2015), rice straw (Luo et al., 2019), corn cobs (Duan et al., 2019), wheat straw (Qian et al., 2019), etc. Char is commonly used as a soil amendment to increase soil fertility. It improves the availability of nutrients, water retention, and soil structure. The soil retains more water and nutrients because of the porous nature of char, which can lessen the need for artificial fertilizers (Lehmann and Joseph, 2009). To neutralize the pH of acidic soil, char is applied to make it suitable for plant growth (Lehmann and Joseph, 2009). Because of its durability in soil, char is useful for the long-term storage of carbon. char lowers the amount of CO_2 in the atmosphere, which helps to slow down climate change by storing carbon in soils (Woolf et al., 2010). Pollutants are extracted from water and wastewater using char. Heavy metals, chemical compounds, and other pollutants can be effectively adsorbed due to their wide surface area and porous structure (Mohan et al., 2017). Thus, the production of char and its application for various purposes is also more cost-effective than the upgradation of pyrolysis oil for its utilization (Gao et al., 2022).

1.5 OBJECTIVE OF THE STUDY

The main objective of this study is the design and operation of a fixed bed pyrolizer for the thermochemical conversion of MSW and legacy waste. Also, the characterization and application of pyrolysis product (char) was studied. The objective of the study is limited to the:

- Seasonal sampling and characterization of MSW and legacy waste.
- Design and fabrication of the fixed bed pyrolizer for pyrolysis of MSW.

- Operation of the pyrolizer by varying the operating temperature, heating rate, holding time, and particle size of feedstock for maximum yield of char.
- Characterization of MSW char and its utilization in adsorption, soil amendment, during composting and with compost.

1.6 NEED FOR THE STUDY

Pyrolysis of MSW in a fixed-bed reactor presents a promising solution for mitigating disposal challenges and reducing the volume of waste sent to landfills while also enabling resource recovery. Typically, the wet waste fraction of MSW undergoes biological treatments such as composting and anaerobic digestion, while dry and combustible waste is incinerated. Recyclable materials are processed in recycling facilities, and metals and glass are reused through melting. However, incineration of MSW generates significant amounts of toxic gases, such as nitrogen oxides (NO_x) and sulfur oxides (SO_x), making emission control a complex task. Additionally, the recycling process necessitates the segregation and cleaning of waste before it reaches the recycling facility, reducing the feasibility of recycling unsegregated waste, which often ends up in landfills for extended periods. Although much research has been conducted on biomass pyrolysis, studies focused on the design and operation of pyrolizers capable of handling heterogeneous MSW are limited. The demand for MSW pyrolysis is increasing as it offers a solution to the challenges of long-distance waste transportation, incineration, and landfilling, especially in the face of pollution concerns and limited landfill space. With landfills rapidly reaching capacity due to high waste generation rates, there is a pressing need for research into novel pyrolizer designs that can address the emission of toxic gases and environmental pollution associated with landfill and thermal waste treatment while also reducing disposal issues. Furthermore, research in pyrolysis technology is necessary to develop pyrolizers that can effectively process heterogeneous MSW with flexibility in feedstock quantities.

1.7 SCOPE OF THE STUDY

This study primarily focused on the design and fabrication of a lab-scale pyrolizer that can be used for pyrolysis of unsegregated dry fraction of MSW in

large quantities as a feedstock as compared to the capacity of existing lab-scale pyrolizer. In the first phase, both fresh MSW and legacy waste were collected from Boragaon dumpsite, Guwahati, Assam (North Eastern part India), seasonally throughout the year. The physicochemical characterization and thermodynamic study were performed to investigate the feasibility of MSW and legacy waste for pyrolysis. In the second phase, the pyrolizer was designed and fabricated. The pyrolysis of the MSW was carried out along by varying the operating parameters such as temperature, heating rate, holding time, and particle size of the sample and optimization of the pyrolysis process in the fixed bed reactor for maximum char yield. In the third phase, the physicochemical characterization of the MSW char produced at different temperatures was done to determine the most potent char for application. The further application of MSW char for adsorption, soil amendment, co-composting, and addition with compost was studied.

1.8 THESIS ORGANIZATION

The current thesis is divided into eleven chapters with suitable headings, subheadings, references, and study results. Following is a synopsis of these chapters in brief:

- **Chapter 1** is on the introduction of waste generation worldwide and the management of MSW globally and in India. MSW treatment through pyrolysis, pyrolysis processes, and reactors, production of char, objectives, need, and scope of the study.
- **Chapter 2** gives a thorough literature review on the management system of MSW in accordance with the functional element of MSW management, the current status of MSW management in India, a systematic literature review by scientometric analysis, research trend and current status, science mapping of the journals, countries active in the domain of pyrolysis of MSW, pyrolysis of individual fraction of MSW, application of char as an adsorbent, during composting and with compost, application of char for soil remediation and concluding remark from the literature review.

- **Chapter 3** describes the materials and methods of the study, work flow chart, collection of samples for the entire study, methods involved for seasonal characterization of MSW in phase I, design and operation of the fixed bed pyrolizer in phase II, characterization and application of char in phase III.
- **Chapter 4** gives the results and discussion of the feasibility study of MSW for pyrolysis in accordance with the season and age of waste dumped in the dumpsite. The potential of the unsegregated MSW was assessed by physicochemical and thermochemical characterization.
- **Chapter 5** is all about the design and operation of the fixed bed pyrolizer, optimization of the process parameter for maximizing the yield of char, and calculation of the energy consumed and cost of production of char.
- **Chapter 6** details about the results of characterization of MSW char produced at different temperatures and discussion of its potential as an adsorbent and in soil amendment.
- **Chapter 7** describes the results and detail discussion of the application of MSW char as an activated carbon and adsorption study by using MSW char derived activated carbon for Pb(II) adsorption form water.
- **Chapter 8** gives a detail of the results and discussions on the effect of application of MSW char during co-composting with vegetable waste.
- **Chapter 9** is about the application of MSW char and compost in alluvial soil and its effect on plants growth.
- **Chapter 10** discuss about the application of MSW char and vermicompost in mine tailing soil and its effect with the due course of time.
- **Chapter 11** gives the overall conclusion of the study and future recommendations in the domain of pyrolysis of MSW.

Chapter 2

LITERATURE REVIEW

2.1 MSW MANAGEMENT SYSTEM

Municipal solid waste (MSW) is the waste collected by the municipality or the waste disposed at the municipal waste disposal site or landfill. It includes day-to-day waste from residents, institutions, industries, commercial sectors, municipal, construction, and demolition waste (Hoornweg, 2015). The activities associated with the management of solid waste from the point of generation to final disposal have been grouped into the six functional elements as shown in Fig. 2.1. These functional elements of MSW have been discussed briefly as follows

- **Waste generation:** Waste generation encompasses activities in which materials are identified as no longer being of value and are either thrown away or gathered together for disposal.
- **Waste handling and storage:** They involve the activities associated with the management of wastes until they are placed in storage containers for collection.
- **Collection:**

  Primary Collection: It includes the gathering of solid wastes and recyclable materials from the sources. but also, the operation of collection vehicles at landfill disposal sites.

  Secondary Collection: This includes the operation of collection vehicles from the dustbin areas to landfill disposal sites.
- **Processing and transformation of solid wastes:** It is a very important function of solid waste management but is often ignored.
- **Transfer and transport:** Two steps:

  (i) The transfer of wastes from the smaller collection vehicle to the larger transport equipment

  (ii) The subsequent transport of the wastes to disposal sites.
- **Disposal:** Today, the disposal of wastes by landfilling is the ultimate fate of all solid waste.

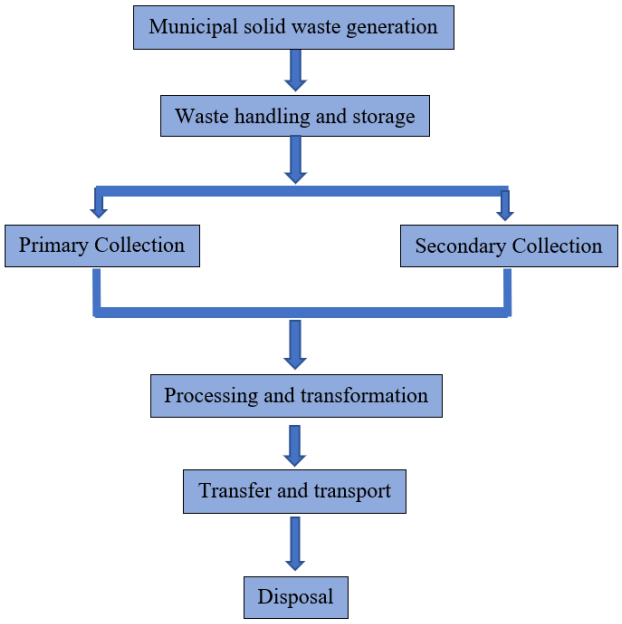

Fig. 2.1. Functional elements of MSW management

2.2 CURRENT STATUS OF MSW MANAGEMENT

In India, approximately 82% (50 million tons) of MSW is collected, while the remaining 18% (12 million tons) represents scattered litter. Out of the total waste generated, only 28% (14 million tons) undergoes treatment, with 72% (36 million tons) being openly disposed of in urban regions. According to the Central Pollution Control Board (CPCB), towns and cities with populations below 0.2 million exhibit a daily MSW generation of 200 to 300 grams per capita. It was also reported that cities with a population of 200,000 to 500,000 generate 300 to 350 g per capita per day of MSW, and those with a population of more than 1 million generate MSW of 400 to 600 g per capita per day (Karajgi et al., 2012; CPCB, 2016;). Of the MSW generated, approximately 40 to 60% are compostable, 30 to 50% are inert, and 10 to 30% are recyclable (Vikramarjun et al., 2020). In India, the practice of house-to-house waste collection is operational in 18 states, while waste segregation at its origin has been executed in just 5 states (CPCB, 2022). Of the 553 ULBs in operation, around 173 are engaged in composting and vermicomposting the organic portion of MSW (CPCB, 2022). Furthermore, the country hosts 11,100 small-scale biogas plants and 6 BioCNG plants (PIB, 2023). However, most of the Waste-to-

Energy plants fail due to the high moisture content of the waste and low heating value, compounded by the lack of segregation at the source (Komilis et al., 2012). As per the Earth Engineering Centre's findings in 2012, metropolitan areas serve as the primary generators of urban waste in India, followed by regions in the North, South, West, and East. Among the categories, organic waste constitutes a significant portion at 47 to 50% of total waste generation, recyclables make up 17 to 20%, while inert waste contributes 25% (Meena et al., 2023). A typical MSW management process is shown in Fig. 2.2.

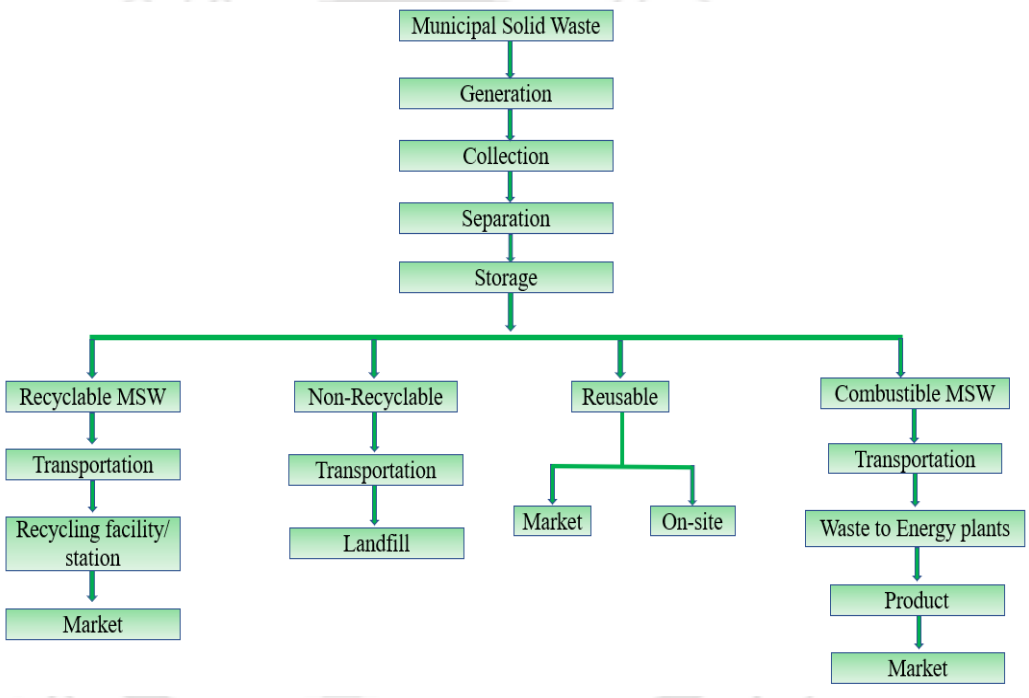

Fig. 2.2. A typical MSW management process

2.3 LITERATURE SEARCH

A systematic literature review was carried out in the domain of pyrolysis of municipal solid waste, which included the keywords and information sources from the academic database Scopus, as it included a wide range of journals as well as recently published journals as compared to other academic database search engines (Chadegani et al., 2013). A total of 1633 documents were shown initially. The following protocols were taken into account while searching for scientific research

articles: (a) publications between the years 1971 to 2024 were considered, (b) the keywords "pyrolysis" AND "municipal solid waste" had to appear in the title and abstract (c) the papers had to be science citation indexed (d) articles falling under the scope of "Environmental Science", "Energy", "Engineering", "Chemical Engineering", "Chemistry", "Material Science", "Earth and Planetary Science", "Agricultural and Biological Science" and "Social Sciences" were considered as the scope of the study is limited to these areas (e) articles published in the English language were only considered (f) book chapters and conference papers were excluded. Thus, a more specific search was conducted, which resulted in 53 documents.

2.4 SCIENTOMETRIC ANALYSIS

The screening process was followed by scientometric analysis, which included more relevant documents focusing on the research area. The scientometric analysis was done using a data mining tool called VOSViewer (Van Eck and Waltman, 2010), where VOS stands for visualization of similarities used for maps containing a moderately large number of items, through which bibliometric maps are constructed and viewed. The nodal distance between them reflects their proximity. The following objectives have been obtained through *VOSViewer* (i) exporting the documents from Scopus to *VOSviewer* (ii) computation, analysis, and visualization of the impact of various articles, journals, authors, and countries that are active in the research area of pyrolysis of MSW (iii) study of the papers that involves the keywords and their relationship with the pyrolysis of MSW (iv) documents with the title or abstract that lack the relation to pyrolysis of MSW were excluded.

The documents extracted from Scopus were studied thoroughly, and a summary was produced while considering the following strategies: pyrolysis of organic fraction of MSW, plastic, paper, mixed MSW, different types of pyrolysis reactors used, pyrolysis products, the effect of temperature, pressure, and pH on pyrolysis,

the gap in the research area and suggestion of future scope in the area of pyrolysis of MSW.

2.4.1 Research trend and current status

The literature published up to 2024 has been analyzed using scientometric methods, as shown in Fig. 2.3. The data extracted from Scopus shows the trend of research in the area of pyrolysis of MSW. It was observed that there was not much publication of papers in the early 1970s, but it started increasing in 2014 and reached the highest peak in the year 2024 with 9 publications in the domain of pyrolysis of MSW, as depicted in Fig. 2.3 (a). It is expected that there will be an expansion of research in the domain of pyrolysis of MSW with the development of pyrolysis technology. The scientometric research has also been done according to the study area. It was observed as shown in Fig. 2.3 (b), that about 16.7% were published in the area of Energy, 9.4% in Engineering, 17.7% were published in the subject area of environmental science, 22.9% were published in the area of Chemical Engineering, 17.7% in Chemistry, 2.1% in Earth and Planetary Sciences, 5.2% in Agricultural and Biological Sciences, 4.2% in Material Science, and 2.1% in Multidisciplinary. This shows that major studies in the domain of pyrolysis of MSW have been carried out in the areas of Energy, Environmental Sciences, Chemical Engineering, and Chemistry. There has also been work carried out in the subject areas of mathematics, Business, Management and Accounting, medicine, Immunology, Microbiology, Economics, Econometrics, and finance, etc., but these subject areas are not within the scope of the current work, and so, they are excluded for further. But this also shows that the pyrolysis of MSW can be expanded in a broad research area.

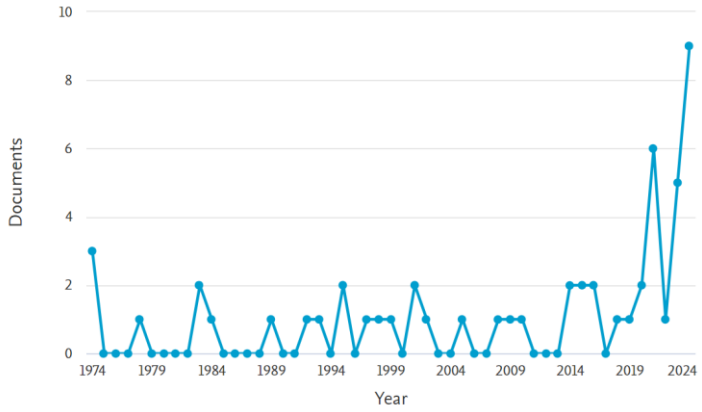

(a) Number of publications per year

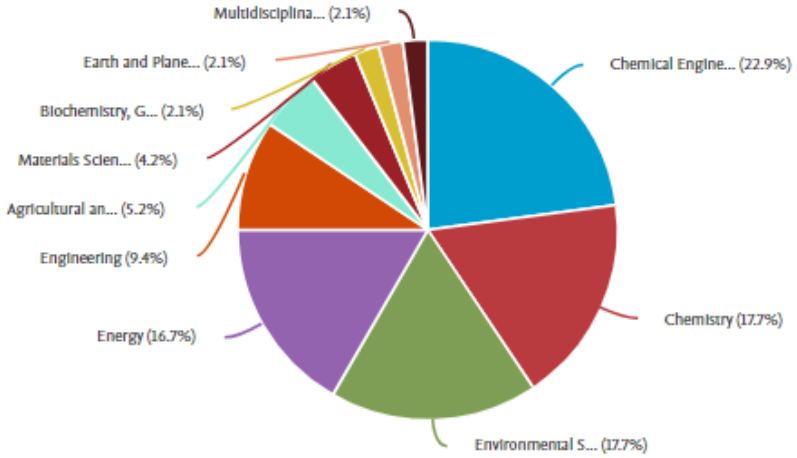

(b) Publications as per subject area

Fig. 2.3. Result of scientometric analyses

2.4.2 Science-mapping of the journals

In this study, the journals that are related to the publication of articles in the area of pyrolysis of MSW were evaluated and anticipated. The result of the science mapping of the journals involved in the research of pyrolysis of MSW has been shown in Table 2.1 and Fig. 2.4. The analysis in VOSViewer was done by setting a minimum of one article and at least one citation in which out of 216 sources of journals, 24 journals meet the threshold. Fig. 2.4. shows the mapping of the mainstream journals in the domain of pyrolysis of MSW with 11 clusters of journals and the relative closeness between them through connected lines. The size of the

nodes and fonts of the journals denotes the number of publications in that particular journal. The bigger the size of the nodes and fonts, the more the number of publications in that journal. The connecting lines and the colour of the clusters indicate the journals' proximity. The greater the density of the connecting lines and the colour of the clusters, the greater the relative proximity of the journals in terms of reciprocal citations. From Fig. 2.4, it was observed that journals like Waste Management, Energy Conversion and Management, Journal of Analytical and Applied Pyrolysis, Bioresource Technology, Fuel, Progress in Energy and Combustion Science contributed significantly to the research area in the domain of pyrolysis of MSW.

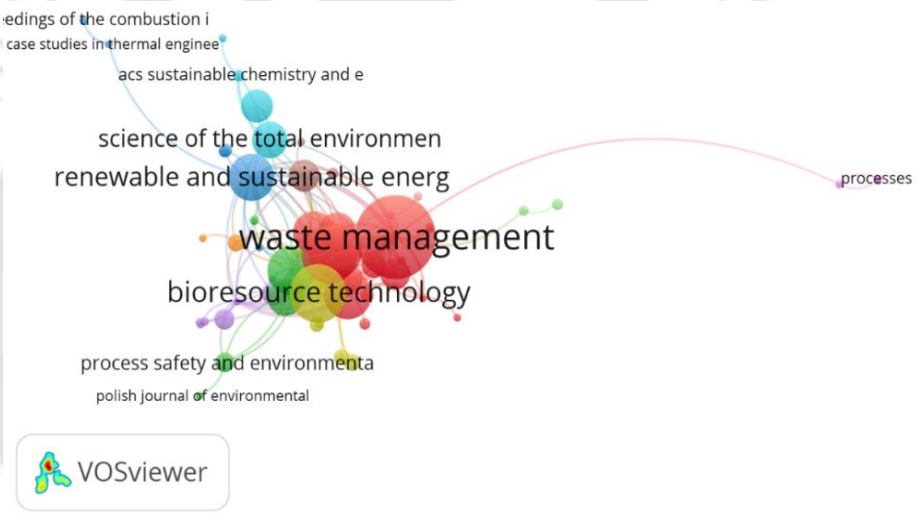

Fig. 2.4. Mapping of journals in the domain of pyrolysis of MSW

Most of these journals have dense connectivity networks, indicating their relative closeness with each other with respect to the mutual citations. Also, it was observed from Fig. 3 that the link strength of the journal Progress in Energy and Combustion Science is 0, with the least number of published articles of 2 but with a higher number of citations of 1004 compared to other journals with a higher number of published articles but with fewer citations. However, all the journal sources were not clearly visible; therefore, a more quantitative study was done, which is shown in Table 2.1.

Table 2.1. Quantitative study of the journal sources in the domain of pyrolysis of MSW

Source	Number of documents	Number of citations	Average citations	Normalized citations	Average Normalized Citations
Waste Management	17	2981	175.35	31.49	1.85
Journal of Analytical and Applied Pyrolysis	15	792	52.8	41.92	2.79
Bioresource Technology	13	684	52.62	19.59	1.51
Energy and Fuels	13	505	38.85	17.24	1.33
Fuel	13	731	56.23	27.74	2.13
Waste Management and Research	12	586	48.83	14.3	1.19
Energy Conversion and Management	12	442	36.83	12.95	1.08
Journal of Hazardous Materials	12	626	52.17	24.04	2.00
Applied Energy	11	226	20.55	8.33	0.78
Energy	10	264	26.4	16.72	1.67
Renewable and Sustainable Energy Reviews	9	392	43.56	12.09	1.34
Environmental Science and Technology	7	159	22.71	6.38	0.91
Fuel Processing Technology	7	162	23.14	7.73	1.1
Journal of Environmental Management	6	31	5.17	1.7	0.28
Chemical Engineering Journal	5	84	16.8	1.88	0.38
Science of the Total Environment	4	40	10	1.85	0.46
Chemosphere	3	25	8.33	1.74	0.58

Industrial and Engineering Chemistry Research	3	162	54	4.13	1.38
Renewable Energy	3	12	4	0.86	0.29
Chemical Engineering Transactions	2	7	3.5	0.52	0.26
Environmental Science and Pollution Research	1	1	1	0.54	0.54

Table 2.1 has been organized based on the count of published documents, with a minimum of one document published. It presents a quantitative evaluation of journal sources related to the subject of MSW pyrolysis. The table includes the number of documents published within a journal source, the total citation count, average citations, normalized citations, and average normalized citations. The average citation metric signifies the journal's impact in terms of both productivity and significance within the research domain. This value is obtained by dividing the total number of citations by the total number of published articles. Normalized citations, generated using *VOSViewer*, are utilized to assess citation counts within the same journal. The average normalized citation is computed by dividing the number of normalized citations by the total documents published within the journal. This metric offers insight into the most influential papers across various journals within the research field. A journal with the most document publications or the most citations may not have the highest average citation score. From Table 5, it was observed that even though the number of documents published and number of citations is higher for the journal, *Energy* but the average citation is highest for the journal, *Renewable and Sustainable Energy Reviews* with an average citation score of 43.56, which indicates that this journal has strongest influence in terms of productivity and research in the domain of pyrolysis of MSW. Whereas normalized citation is highest for the *Journal of Analytical and Applied Pyrolysis,* which is about 41.92, indicating the highest number of citations of all the documents published within the journal. Also, the average normalized citation is highest for *the Journal of Analytical and Applied Pyrolysis* with an average normalized score

of 2.79, which depicts this journal as the most influential publication in the research of pyrolysis of MSW.

2.4.3 Co-occurrence of keywords in the domain area

The keyword in research provides a broad idea about the topics that have been studied in detail in the domain of a research area. The interrelationship between the keywords and the relative closeness between them is provided by a network of all the selected keywords (Van Eck and Waltman, 2010). The study was done in *VOSViewer* by using *the "Authors keywords" and "Fractional counting" methods* for analysis. The minimum number of occurrences was set as 5, which yielded 1157 keywords, and 43 keywords met the threshold. The 43 keywords were then filtered by removing the repetitive keywords such as "Municipal Solid Waste", "Biochar", "Waste-to-Energy", "Catalyst", "Refused Derived Fuel" etc., and 49 keywords were selected, which are given in Table 2.2.

Fig. 2.5 shows the mapping of keywords, where the size of the nodes indicates the frequency of occurrence. The keywords such as "Municipal Solid Waste", "Pyrolysis", "Gasification" and "Biochar" shows bigger size nodes, indicating a higher frequency of occurrence with a number of occurrences of 201, 166, 46, and 41, respectively. Also, the single colors of the nodes indicate the relative closeness with each other and are categorized into 8 clusters. For example, as shown in Fig. 2.5 (b), "Municipal Solid Waste", "Renewable Energy", "Waste-to-Energy", "Thermal treatment", and "Energy recovery" are seen to have the same color indicating their relative closeness between them. Fig. 2.5 (c) shows the relative closeness between keywords such as "Biomass", "Biofuel", "Syngas", "Catalyst", "Biogas" and "Fuel". Fig. 2.5 (d) shows the relative closeness between "Municipal Solid Waste", "Biomass", "Activated carbon", "Adsorption", "Biochar", "RDF" and "Steam gasification". From cluster analysis of all the keywords, the overall research can be categorized based on pyrolysis of MSW, pyrolysis of plastic waste, product from pyrolysis of MSW, and its utilization, which is discussed in detail below.

Table 2.2. Co-occurrence of the keywords

Keyword	Occurrences
Municipal solid waste	201
Pyrolysis	166
Gasification	46
Biochar	41
Waste-to-Energy	34
Biomass	32
Syngas	25
Incineration	20
Co-pyrolysis	18
Combustion	17
Waste management	16
Sewage sludge	15
Bio-oil	14
Kinetics	14
Thermogravimetric analysis	14
Heavy metals	13
Waste	13
Recycling	12
Refuse-derived fuel	11
Tar	10
Life cycle assessment	9
Renewable energy	9
Thermal degradation	9
Energy recovery	8
Plastics	8
Sustainability	8
Biofuel	7
Energy	7
Thermal treatment	7
Activated carbon	6

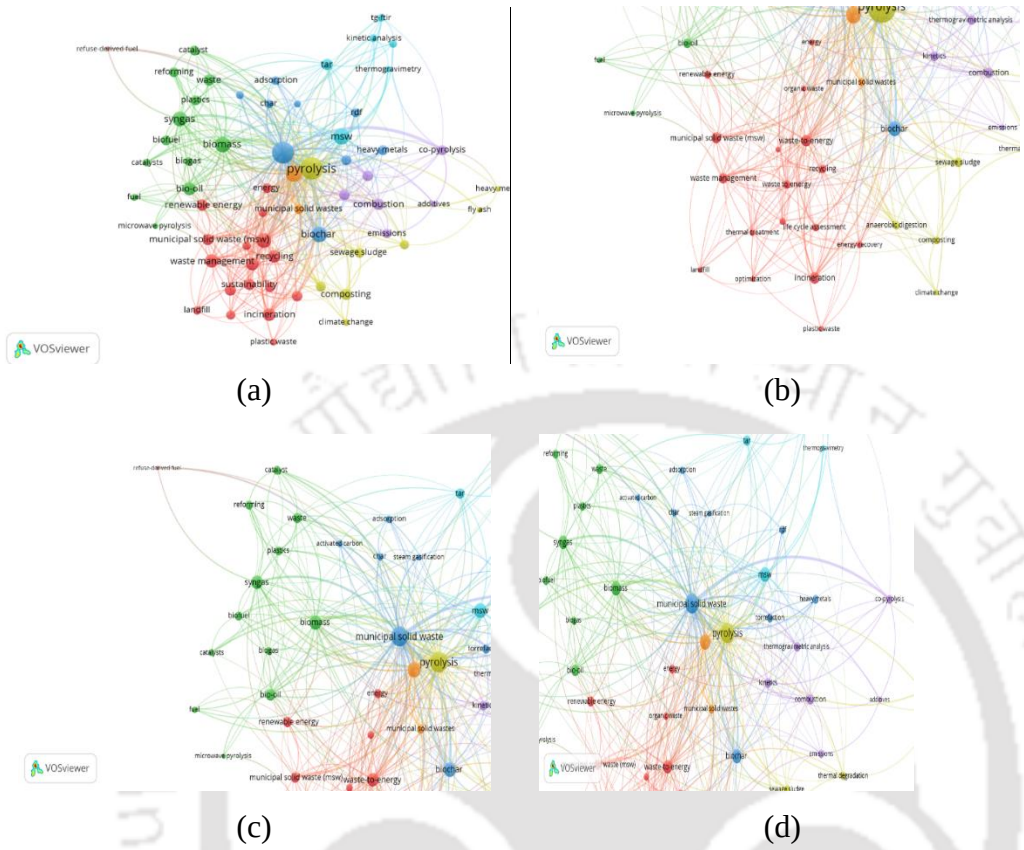

Fig. 2.5. Keywords appeared in published articles in the field of MSW pyrolysis

2.4.4 Countries active in the domain of pyrolysis of MSW

The scientometric analysis of the countries active in the research of pyrolysis of MSW is shown in Fig. 2.6. Mapping of countries that are active in the domain of pyrolysis of MSW was done by using *VOSViewer*. It was observed that countries like China, the United States (Lee et al., 2020; Rasheed et al., 2021), United Kingdom (Williams et al., 1999; Buah et al., 2007; Al-Salem et al., 2009; Wang et al., 2018; Iannello et al., 2020), and India (Chauhan et al., 2008; Gedam and Regupathi, 2012; Zaman, 2013; Agarwal et al., 2015; Bhavanam et al., 2015; Ghosh et al., 2018; Saqib et al., 2019; Shastri, et al., 2020; Bhatt et al., 2021; Chhabra et al., 2021; Goli et al., 2021) have higher contribution towards the research of pyrolysis of MSW. This also shows that both developed and developing countries are involved in the research of pyrolysis of MSW.

In China, work has been done on the treatment of medical waste, whose production increased rapidly due to covid-19 pandemic. Various treatment methods have been studied, and one such method is pyrolysis incineration (Zhao et al., 2021). Pyrolysis experiment has also been performed on the organic fraction of MSW, especially on agricultural waste like rice husk, wood chips, rice straw, animal waste, etc. (Zheng et al., 2009; Liu et al., 2017; Liu et al., 2020; Rasheed et al., 2021) and on plastic waste from MSW (Xu et al., 2019). Pyrolysis by mixing different components of MSW and MSW sewage sludge by using different kinds of reactors was also studied in various parts of China (Li et al., 1999; Yufeng et al., 2003; Mohee et al., 2015; Wang et al., 2019; Tugov et al., 2021). Also, in China, pyrolysis experiments have been reported by using synthetic MSW samples as feedstock to study the characteristics of pyrolysis products and their utilization (Dong et al., 2016).

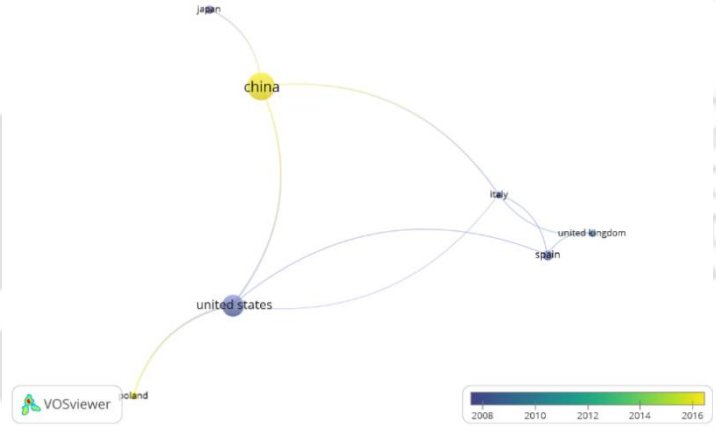

Fig. 2.6. Science mapping of the countries active in the domain of pyrolysis of MSW

Table 2.3. Quantitative study of the countries active in the domain of pyrolysis of MSW

Country	Documents	Citations	Average citations	Normalized citations	Average Normal Citation
China	32	558	17.43	41.07	1.28
United States	25	266	10.64	20.06	0.80
Italy	8	275	34.37	8.69	1.08
Poland	8	70	8.75	9.56	1.19
Spain	12	343	28.58	21.99	1.83
United Kingdom	9	152	16.88	10.17	1.13
Japan	10	155	15.5	5.70	0.57

Table 2.3 shows a quantitative study of the countries around the world that are active in the research of pyrolysis of MSW. The average citations, normalized citations and average normalized citations were calculated by using data from *VOSViewer*. It was observed that the number of publications (32) and citations (558) are more from China, but the average citation is highest for Italy with a value of 34.37, which indicated the most influential country in terms of productivity and research in the area of pyrolysis of MSW. Normalized citation is highest for China, indicating that they have the highest number of citations of all the articles within the same journal. The average normalized citation is highest for Spain, about 1.83, which indicates that Spain is the most influential country that is active in the domain of pyrolysis of MSW.

2.5 PYROLYSIS OF SPECIFIC COMPONENTS OF MSW

MSW has the potential to be used as a feedstock for pyrolysis for the generation of value-added products and to increase the operational efficiency of large-scale pyrolysis plants (Ohmukai et al., 2008). Pyrolysis of individual waste like organic waste, paper waste, and plastic waste has been done for the production of bio-oil, char, and syngas (Hrabovsky et al., 2006). The main aim of the pyrolysis of MSW is energy recovery, as the product from pyrolysis of MSW has similar properties to

fuel. Pyrolysis of treated MSW sludge with a moisture content of less than 10% was done in a furnace (Koyo Lindberge Co. Ltd.) using a retort for carbonization (Shinogi et al., 2003). The furnace was equipped with a programmable temperature controller. The carbonization was carried out at a temperature of 250, 300, 400, 500, 600, and 800°C and at a heating rate of 2°C/min for 2 h, after which the furnace was turned off, and the retort was allowed to cool. The physical and chemical characteristics of the products were found to compare the difference in product properties of the four types of waste pyrolysis. According to the findings, increasing the carbonization temperature increased the surface area, total carbon, ash content, and pH but lowered the yield.

Pyrolysis of combustible fraction of MSW (RDF) and pyrolysis of organic fraction of MSW blended with coal at different ratios was done in a fixed bed horizontal tube furnace where the sample to be heated was kept inside a quartz tube, both in the presence of air and inert gases (Tokmurzin et al., 2019). The sample taken for pyrolysis was 20 g in each test, the maximum operating temperature was 800°C, and the heating rate was 20°C/min. It was observed from TGA that the volatile content from the organic fraction of MSW and RDF starts emitting at 180 to 200°C and loses all the volatile content at 500°C and 700°C and below 500°C, pyrolysis of the organic fraction of MSW only produces tar. Also, it was observed that pyrolysis performed on the blending of organic fraction of MSW with coal yielded a higher concentration of methane, about 35-37%, as compared to pyrolysis of MSW or coal alone at 800°C.

Pyrolysis of MSW was reported by Font et al. (1993) in a fluidized bed reactor made of stainless steel, which was heated in a cylindrical refractory oven at operating temperatures for pyrolysis was 700, 750, 800, and 850°C. The inert atmosphere inside the reactor was created by using helium gas with a discharge velocity of 3.6 cm/s. The amount of sample taken as feedstock was 0.8 to 5 g and kinetic study of the sample was done using TGA at a heating rate of 1.5 to 200°C/min.

In a study by Song et al. (2018), the pyrolysis of MSW constituents, including wood, polyethylene, paper, biomass, and other components, was investigated. This

pyrolysis process was conducted in a fixed-bed reactor and involved mixing the MSW materials with CaO, plastic, and MSW char. The reactor utilized a quartz tube with dimensions of 35 mm in diameter and 700 mm in length, serving as the feeding point. The pyrolysis was conducted within a temperature range of 400 to 700°C, employing a heating rate of 20°C/min. The experiments were conducted in a nitrogen environment with a gas flow rate of 40 mL/minute.

Rajaeifar et al. (2017) determined the potential of pyrolysis of MSW for the generation of electricity. Chen et al. (2014) reported pyrolysis of three components of MSW, i.e., paper, bamboo, and polyethylene in a fixed bed reactor. The feedstock components, paper, bamboo, and polyethylene, were purchased from the local market. The pyrolysis experiment was done in a quartz tube of length 700 mm and diameter of 40 mm inside the fixed bed reactor. The maximum temperature of operation was 900°C with feeding of 4 g of the sample in each batch. The inert atmosphere inside the reactor was maintained by surging nitrogen gas with a flow rate of 2 L/min, and Calcium Oxide (CaO) was added at different ratios in different tests. This study was done to investigate the effect of moisture content and CaO on the pyrolysis of MSW. the result showed a lower production of Hydrogen and higher tar yield with the increase in moisture content and a higher production of hydrogen and a decrease in tar yield with the increase in the addition of CaO.

A synthetic, simulated MSW sample was prepared by (2016) as a feedstock for pyrolysis in a fluidized bed reactor equipped with a cyclone for cleaning flue gas. The diameter of the reactor was 60 mm, and the height of the reactor was 1100 mm. To monitor the temperature inside the reactor at the top, middle, and bottom, three K-type thermocouples were used. The pyrolysis was done at a temperature of 550, 650, 750 and 850°C.

Fang et al. (2016) used thermogravimetric analysis to study the effect of additives such as MgO, Al_2O_3, and ZnO on co-pyrolysis of MSW components such as food waste, wood, PVC, and paper sludge. This study showed that additives reduce the initial temperature and activation energy during pyrolysis. However,

there was also a change in the effect of pyrolysis even after using the same additive with a different ratio of mixing of MSW and paper sludge.

Pyrolysis of three key components of MSW, such as paper, bamboo, and polyethylene, was done individually by Zheng et al. (2019) in a fixed bed reactor to study the effect of tar formed during pyrolysis with the addition of CaO. The pyrolysis was done using a pyrolizer equipped with Gas Chromatography/ Mass Spectrometry (Py-GC/MS) with a model named CDS-5200-type pyrolizer. The maximum temperature for pyrolysis was 900°C at a heating rate of 10°C/ms (ms in abbreviation of millisecond) in an inert atmosphere created by surging Helium. The amount of feedstock taken was 5 mg of powdered sample in a quartz capillary of 25 mm length and 1.9 mm diameter. Also, by taking the same samples, pyrolysis was conducted by using a type of fixed bed reactor, where the sample was fed into a quartz tube with a length of 700 mm and an inner diameter of 40 mm. The reactor was heated externally by using an electric heater. The inert atmosphere inside the reactor was maintained by purging nitrogen at a flow rate of 2 L/min, and the amount of feedstock taken was 4 g, along with the addition of CaO in each experiment. It was found from the study that with the addition of CaO, the tar formation during pyrolysis decreases, and also, there was a change in the chemical composition of the tar formed from the pyrolysis of each of the three components of MSW.

Fang et al. (2017) reported a co-pyrolysis study of MSW mixed with paper sludge at different ratios and with the addition of additives using a TGA/DSC thermal analyzer. The amount of sample taken for the study was 5 ± 2 mg, and the experiment was carried out at a temperature of 110 to 900°C in a nitrogen atmosphere at a heating rate of 20, 30, and 40°C/min. This experiment was done to study the characteristics of co-pyrolysis of the MSW and paper sludge at different ratios with the existence of additives such as MgO and activated carbon.

Most of the studies on the characterization of pyrolysis products have been done by using the thermogravimetric analyzer. There are pyrolysis experiments done using different reactors of different sizes with varying quantities of feedstock and operating temperatures with varying heating rates (Guo et al., 2001, Buah et al.,

2007, Hwang et al., 2007; Zhou et al., 2013; Nilai et al., 2017; Zaini et al., 2019). There are also pyrolysis experiments that have been done by preparing synthetic MSW samples to study the pyrolysis characteristics, pyrolysis product, and chemical distribution of the products (Chakraborty et al., 2013; Peces et al., 2014; Huang et al., 2015; Suriapparao et al., 2015; Jung et al., 2019; Lu et al., 2019; Tang et al., 2020).

2.6 PYROLYSIS OF ORGANIC WASTE

Pyrolysis of plant waste such as sugarcane bagasse and rice husk and biosolid of cow and its product characterization was done by Shinogi et al. (2003). Manyà et al. (2016) studied the effect of the addition of additives and rejected material from municipal waste composting and the effect of pressure on the pyrolysis of two-phase olive mill waste in a fixed bed pyrolizer at a peak temperature of 600°C, consisting of a vertical cylindrical reactor of 140 mm diameter and 465 mm length. The pyrolysis was done at Normal Temperature and Pressure (NTP) conditions, and pressure was adjusted from 0.1 to 1.0 MPa for 60 minutes in a nitrogen environment. It was observed that the biochar produced at atmospheric pressure was more stable with the addition of additives ($CaO + K_2CO_3$) than that produced at 1 MPa. The stability of biochar appeared to be the highest and most effective from the pyrolysis of a mixture of olive mill waste and rejected municipal waste compost at any pressure.

Shao et al. (2019) conducted a pyrolysis experiment by using Municipal Sewage Sludge (MSS) as feedstock which was collected from the wastewater treatment plant of Qiubin, and another feedstock was prepared by using MSS mixed with wood chips in a rotary kiln at 800°C for 1 h. About 65% of the feedstock was converted to biochar and was used for soil amendment. Hu et al. (2017) studied the effect of chlorine on the pyrolysis product char derived from an organic fraction of MSW. The sample for the study was prepared using rice powder and wood chips as feedstock for pyrolysis. The experiment was done in a fixed bed reactor in a

horizontal quartz tube of length 600 mm and diameter 50 mm in an inert atmosphere of nitrogen at a flow rate of 0.15 L/min at a temperature of 500°C for 60 min.

Jin et al. (2014) reported pyrolysis of organic waste fraction of MSW at a temperature of 400, 500, and 600°C in a nitrogen atmosphere at a flow rate of 100 mL/min and pressure less than 10 psi for 20 min. The amount of feeding for pyrolysis was 150 g in each experiment. This pyrolysis experiment was done to utilize the product char for the removal of arsenic after activation and without activation of the char produced from pyrolysis.

Hamilton et al. (2020) designed a solar-driven pyrolysis technology as a waste-to-fuel technology. In this model, the Fresnel Reflector Concentrated Solar panel was used as the solar power collector from where the power generated was used to run the pyrolysis reactor. It was specially designed for the pyrolysis of waste biomass, and a comparative study was done to investigate the performance of the solar-integrated pyrolysis technology by using two sources of light, such as a natural source of light from the sun and an artificial source of light.

There are a number of studies carried out on the pyrolysis of organic fraction of MSW to study the effect on product yield, either in the existence of additives or without additives and combined pyrolysis/gasification (Demirbaş et al., 2001; Phan et al., 2008; Demirbas et al., 2011; Klemetsrud et al., 2016; Taherymoosavi et al., 2017; Yang et al., 2018; Ayiania et al., 2019; Šuhaj et al., 2019; Kosakowski et al., 2020; Tokmurzin et al., 2020; Akyürek, et al., 2021).

2.7 PYROLYSIS OF PLASTIC/PAPER/CARDBOARD WASTE

Bi et al. (2015) reported pyrolysis of polyvinylchloride in a two-stage reactor to a maximum temperature of 900°C at a heating rate of 10°C/min in a nitrogen environment at a flow rate of 200 mL/min. Co-pyrolysis of combustible components of MSW with or without the addition of additives such as CaO, $CuCl_2$, and MnO_2 was reported by Fan et al. (2018) to study the effect of additives on the pyrolysis product yield, heating value, and change in chemical composition of the product. Co-pyrolysis of biomass and polyvinyl chloride waste was done by (Xu et

al., 2019) to prepare magnetic chlorinated biochar for the removal of mercury at a temperature of 600, 700, and 800°C.

Han et al. (2021) did a pyrolysis experiment by modeling an MSW feedstock using polyvinyl chloride, which is a source of chlorine, mixed with poplar as a source of PAH (Polycyclic Aromatic Hydrocarbon) in a tubular furnace. The inert atmosphere in the reactor was maintained by surging nitrogen gas at a flow rate of 1 L/min, and the reactor was purged for 10 min to remove the air before pyrolysis. Pyrolysis was done to a maximum temperature of 900°C with a heating rate of 20°C/min. The amount of feeding was 10 g per batch inserted in a quartz tube and heated for 1 h. In this study, torrefaction was done as a pretreatment of the feedstock for pyrolysis to reduce the production of dioxins during pyrolysis. The dioxin in the pyrolysis product was determined by High-Resolution Mass Spectrometry. The result of torrefaction showed that about 98.63% of the total dioxins and 99.09% of the toxic can be removed from the pyrolysis product.

Most of the pyrolysis experiments have been done in batch mode to study the effect of pyrolysis product and characteristics of pyrolysis of plastics, paper, and cardboard with different kinds of additives (Wu et al., 1998; Al-Salem et al., 2017; Blanco et al., 2014; Sotoudehnia et al., 2020; Quesada et al., 2019).

2.8 APPLICATION OF CHAR AS AN ADSORBENT

The char produced from pyrolysis holds potential applications as an adsorbent due to its significant surface area, pH, iodine number, and various surface functional groups. There are many studies conducted on biochar characterization and application for adsorption (Yaashikaa et al., 2020). Addressing the removal of heavy metals from wastewater is particularly critical due to their non-biodegradable nature and significant threat to public health, even at very low concentrations (Vidu et al., 2020). Utilizing adsorption techniques presents a promising approach for wastewater treatment, wherein industries can implement methods to capture metal ions from their effluents (Briffa et al., 2020). Hoslett et al., (2019) studied the adsorption of Cu from water by using biochar prepared from pyrolysis of a combination of meat, paper, plastic, and food wastes, such as bread, at 300°C for 12 hours. The maximum capacity of adsorption of the biochar was 4 to 5 mg/g.

Biochar prepared from pineapple peel, municipal sewage sludge, tea waste, and sweet lime peel by pyrolysis at less than 450°C was also used for the removal of heavy metals such as Cd(II) and Cr(VI) from wastewater (Fan et al., 2018; Shakya and Agarwal, 2019; Shakya et al., 2019). The use of char generated from the pyrolysis of a plastic component of MSW for the removal of heavy metals was documented by Saravanakumar et al., (2024). An increasing amount of research is showing that heavy metals can be successfully removed from water and wastewater using char made from waste plastic and biomass (Higashikawa et al., 2016; Inyang et al., 2016; Tan et al., 2016). The char derived from plastic was used for the adsorption of Cu and Zn (Bogusz et al., 2015), and char from tires was used for phenolic compounds removal from water (Kuśmierek et al., 2020). The plastic-derived char was also efficient in the removal of ammonia (Tang et al., 2019), hazardous heavy metals (Calugaru et al., 2019; Yonglin Liu et al., 2020), and char derived from sewage sludge was efficient in the removal of methylene blue (Hu et al., 2021) from wastewater. The maximum removal percentage of heavy metals such as Fe, Cr, Pb, Cu, and Cd from water contaminated with heavy metals was achieved to be 99.9% by using char produced synthetically from plastic waste and biomass (Singh et al., 2021). Studies have been reported on the application of plastic-derived char activated by using zinc nitrate for the removal of As^{3+} (Vinh et al., 2015). Table 2.4 provides an overview of the application of char produced from fractions of MSW in the adsorption system to remove pollutants from water.

Table 2.4. Adsorption of contaminants from water by char generated from MSW

Raw material	Temperature of pyrolysis (°C)	Pollutant	Removal (%)	Char dosage (g/L)	Contact time (h)	Reference
Bones of pork	500	Pb(II)	8.5	0.5	5	(Wang and Luo, 2020)
Pork bone and microcrystalline cellulose	500	Pb(II)	9.4	0.5	1.5	
Waste colored paper	300	Pb(II)	50	2	10	(Xu et al., 2017)

Organic fraction of MSW	450	Ciprofloxacin	88.4	1	3.3	(Sarkar, et al., 2019)
Organic fraction of MSW and bentonite	450	Ciprofloxacin	89.8	1	6.6	(Adassooriya, et al., 2019)
MSW (components not specified)	600-650	Phosphate	3.5	1	10	(Takaya et al., 2016)
	400-450	Ammonium	13.7	1	10	

2.9 APPLICATION OF CHAR DURING COMPOSTING

Char can boost compost stability by accelerating the breakdown of organic matter and enhancing the humification process, which will shorten the time required to attain compost maturity. A number of studies have demonstrated that introducing biochar to compost can speed up the process of composting by improving the stability and maturity of the finished product (Hassanzadeh et al., 2023). Char and organic wastes can be co-composted to increase the retention of nutrients, decrease nitrogen losses, and speed up the organic matter stabilization. This improves microbial habitats during composting and provides compost with higher quality (Nguyen et al., 2022). Biochar's properties and effects during composting are greatly influenced by the kind of raw materials used to make it. The effects of various biochar feedstocks on compost quality, microbial activity, nutrient retention, and heavy metal immobilization have been investigated in a number of researches which are discussed in Table 2.5.

Table 2.5. Application of char during composting

Raw material for production of		Pyrolysis temperature (°C)	Dosage		Time of study	Effects	Reference
Char	Compost		Char	Composting material			
Pine chips	Poultry litter	400	5 and 20%	95 and 80%	213 days	Moisture content decreased, pH increased, and peak CO_2 and temperatures with higher dosage of biochar	(Steiner et al., 2010)
Holm oak	Poultry manure and barley straw	650	3%	90% Poultry manure and 10% barley straw	140 days	Reduction of volatile organic compounds	(Monedero et al., 2019)
Coconut shells	Grain waste	700-900	5-20%	5.5 kg	65 days	accelerated the microbial activity during composting, reduced nitrogen loss	(Wang et al., 2021)
Corn straw	Chicken manure	400	1 g	Not specified	50 days	Reduced the bioavailability of heavy metals	(Chen et al., 2022)
Tobacco and bamboo	Food waste mature compost	600	10%	1:3:1.3	42 days	increase in degradation rate during composting	(Li et al., 2023)
Wood chips	Chicken manure	500-650	10% of the mixture	4:1	42 days	Reduction of gaseous pollutant	(Dang et al., 2024)

2.10 APPLICATION OF CHAR FOR SOIL REMEDIATION

The potential of char generated from a variety of feedstocks to boost microbial activity, improve soil structure, and adsorb pollutants has led to extensive research on its use in soil remediation. The type of raw material used for biochar production plays a crucial role in determining its properties and effectiveness in remediating different soil pollutants. Some of the studies conducted on the application of biochar for soil remediation have been shown in Table 2.6. Numerous researches have indicated that using biochar for soil remediation has produced encouraging outcomes. Biochar, made from a variety of raw materials, including wood, agricultural residues, manure, sewage sludge, bamboo, coconut shells, and organic waste, has been shown to be beneficial in lowering organic pollutants, promoting soil health, and immobilizing heavy metals (Nguyen et al., 2023). The feedstock utilized in the formation of the biochar greatly affects its properties, including surface area, porosity, and nutrient content. These factors also affect the biochar's capacity to absorb pollutants and improve soil fertility.

Table 2.6. Application of char in soil amendment

Raw material	**Pyrolysis temperature (°C)**	**Char dosage**	**Duration of study**	**Effects**	**Reference**
Chicken manure	500	10%	14 days	Reduction in availability of Cu	(Meier et al., 2017)
Corn straw and bamboo	300 and 700	2% each	150 days	Bioavailability of PAHs was reduced	(Ni et al., 2017)
Rice husk (Sulphur modified biochar)	550	1, 2 and 5%	5 days	Reduction in leachability of Hg	(O'Connor et al., 2018)
Rice hull and wheat straw	480-660 and 350-450	24 t and 72 t/ha	120 days	Reduced Hg mobility in pore water of soil, and Hg content in rice grain	(Xing et al., 2019)
Sewage sludge	600	5%	110 days	Reduction in accumulation of methylmercury in rice	(Zhang et al., 2019)

Casuarina	500	4%	Not Defined	Reduced the availability of Cd, Co, Cr, Cu, Ni, Pb and Zn	(Ibrahim et al., 2022)

As the char and compost work well together to improve soil quality, immobilize pollutants, and increase microbial activity, applying them together has become a potential technique for the rehabilitation of soil. While compost increases microbial diversity and supplies vital nutrients, char uses its high porosity and surface area to absorb pollutants and strengthen soil structure. By lowering organic contaminants and heavy metals and enhancing soil nutrients, this mixture helps clean up polluted soils. Table 2.7 shows a review of the literature on the use of biochar and compost in soil remediation.

Table 2.7. Remediation of soil with the combined application of char and compost

Raw material for production of		**Pyrolysis temperature**	**Dosage**		**Study duration**	**Effects**	**Reference**
Char	**Compost**	**(°C)**	**Char**	**Compost**			
Orchard pruning	Olive husk	500	10%	5%	28 days	Decreased metal solubility in mine soil and reduced toxicity, assessed by bio-assays.	(Beesley et al., 2014)
Rice husk, corn cob, sugarcane bagasse	cow manure, “blotong”, plant litter, lime, bran, and starter (EM-4)	Not available	15 t/ha	20 t/ha	Not available	Reduction of Cd and residue of mancozeb in soil in shallot cultivation	(Zu’amah et al., 2024)
Willow wood	bagasse, green waste, and chicken manure	Not available	2.5 t/ha	25 t/ha	140 days	Improved the physicochemical properties of the soil and plant growth	(Agegnehu et al., 2016)

Palm fruit bunches	Plant straw and chicken manure	600	8 t/ha	40 t/ha	669 days	Reduction of nutrients leaching and heavy metals in excessively fertilized soils, suppress plant-parasitic nematode infestation	(Cao et al., 2018)
Holm oakwood	Rabbit and horse manure, fruit wastes, pruning residues, and seaweeds	400	5%	95%	45 days	Improved the physicochemical properties and availability of metals	(Rodrígu ez-Vila et al., 2016)

2.11 CONCLUDING REMARKS

Various pyrolysis systems utilized for the thermal conversion of simulated or individual fractions of MSW have been examined, including rotary, fixed-bed, fluidized bed, auger or screw, and ablative reactors. Given the present trend of escalating waste generation rates, pyrolysis emerges as a plausible solution to address the challenge of landfill waste accumulation. Since MSW consists of a diverse array of waste types, pyrolysis stands out as a robust method for managing mixed waste. Among the various reactor options, rotary and fixed-bed reactors are the most prevalent choices for MSW pyrolysis. The resultant pyrolysis products, such as biochar and syngas, serve as readily usable and marketable fuels. Particularly, polymer materials present in MSW yield high-quality bio-oil, suitable for employment as liquid fuel and chemicals. The char produced from pyrolysis holds potential applications as an adsorbent and soil amendment due to its significant surface area, pH, iodine number, and various surface functional groups. Most existing research has centered on utilizing biomass or organic waste-derived biochar for heavy metal adsorption. However, there's limited literature on the mixed MSW-derived char for the adsorption of heavy metals. Additionally, there is a noticeable absence of studies investigating the adsorption capabilities of activated carbon derived from MSW char. The pyrolysis of MSW to generate char, coupled

with heavy metal removal from wastewater using activated carbon derived from MSW, not only helps in reducing waste volume in landfills but also presents a viable approach for heavy metal remediation in wastewater, contributing to resource utilization efforts. Co-composting of biochar, employed as a soil amendment, has demonstrated excellent efficacy in enhancing soil properties and promoting plant growth, as evidenced by studies (Awasthi et al., 2017; Oldfield et al., 2018; Wang et al., 2019). Several studies have demonstrated the effectiveness of biochar in remediating contaminated soils. Biochar has shown the ability to adsorb and immobilize various contaminants, including heavy metals, organic compounds, and pesticides (Nobile et al., 2022). The application of char in soil remediation shows promising results, but several challenges and considerations need to be addressed. Factors such as char type, pyrolysis conditions, particle size, and application rate can influence its effectiveness (Albalasmeh et al., 2024). Moreover, the long-term stability and persistence of char in the soil, as well as its potential impact on soil microbial communities, require further investigation (Yang et al., 2024). Standardized protocols and guidelines for char application in different soil types and contamination scenarios are also needed. However, further research is required to optimize char production, application methods, and long-term stability in the soil. Additionally, the potential ecological implications and economic feasibility of char-based soil remediation should be carefully evaluated. The application of unsegregated MSW char and compost in remediating soil presents a promising strategy for tackling soil contamination, improving nutrient properties, and making better use of landfill waste. Therefore, considering the heterogeneous composition of MSW, the prospect of energy production, the generation of value-added materials, environmental compatibility, and economic viability, pyrolysis stands as an innovative avenue to effectively tackle the MSW disposal predicament.

Chapter 3

MATERIALS AND METHODS

Various experimental techniques were employed to achieve the specified goals. Using the designed fixed bed pyrolizer and unsegregated MSW as a feedstock for the char production process, the study was conducted in three phases. The following is a summary of the thorough methodology.

3.1 WORK FLOW CHART

The work was done in three phases to accomplish the objectives, which are summarized in Fig. 3.1.

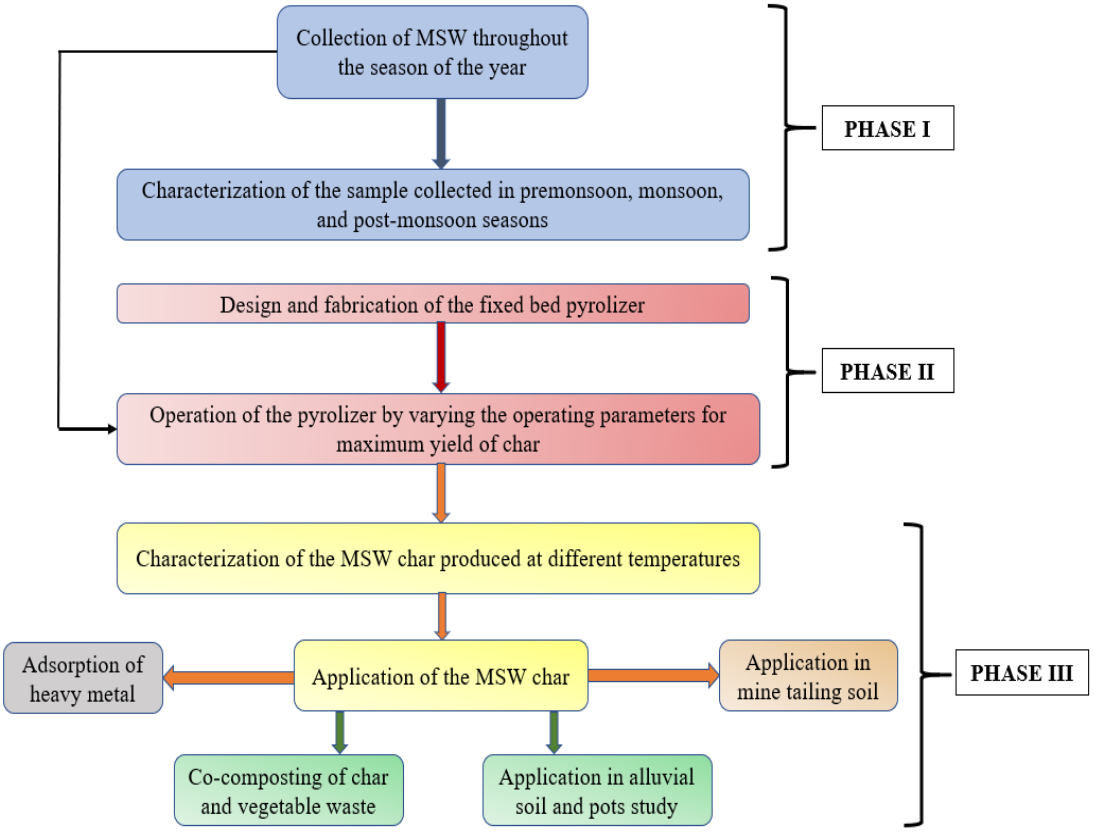

Fig. 3.1. Experimental flow chart of the work

In phase I, MSW (both fresh and legacy waste) was collected throughout the year during three seasons, viz. pre-monsoon, monsoon, and post-monsoon season, and physicochemical and thermal characterization was done to determine the feasibility

of pyrolysis. In phase II, a fixed bed pyrolizer of 3 kg capacity was designed and fabricated. It was then operated by varying the pyrolysis process parameters for maximum char yield. In phase III, the char produced at different temperatures was characterized to find the most potent MSW char for its application. The char was then applied as an adsorbent for heavy metal removal from water, co-composted with vegetable waste to enhance the properties of matured compost, applied in mine tailing soil and alluvial soil for soil remediation, and pot study was done by mixing char and compost at different ratios.

3.2 STUDY AREA AND SAMPLE COLLECTION

MSW and legacy waste were gathered from Guwahati, an urban center in India, characterized by a population of approximately 1,260,419 (as per the 2011 census). This city produces 500 metric tons of waste, with a per capita daily generation of 0.39 kg (Joshi et al., 2016). Out of the entire waste generated, approximately 85% to 90% is collected and directed to a dumpsite (Nithikul et al., 2007). The MSW disposal site in Guwahati is situated in West Boragaon, as shown in Fig. 3.2, and is adjacent to a wetland known as Deepor Beel, designated as a Ramsar site (Gohain and Bordoloi, 2021). At the Boragaon dumpsite, MSW is deposited without separation and in an exposed area, lacking compliance with the requirements outlined in MSW Rules 2000. Also, the dumpsite does not have a geomembrane lining beneath its base, leachate, or gas collecting system, causing an ecological threat, and disposal of waste has been continuing for 15 years (Gohain and Bordoloi, 2021). The solid wastes were collected from 10 locations within the dumpsite, consisting of wastes from fresh to 13 years old in three seasons throughout the year: pre-monsoon, monsoon, and post-monsoon. The waste in the dumpsite that was 6 months to 13 years old was considered legacy waste. In Assam, the pre-monsoon season starts in March-May, the monsoon season in July-September, and the post-monsoon season in October-December. In total, 30 MSW samples were collected, consisting of combustible and incombustible products. The waste sample was sun-dried and shredded into different sizes of 5, 10, 20, and 50 mm by mechanical shredder and manual shredding for optimization study. These

samples were then consistently utilized for physicochemical and thermochemical analysis, and uniform composition was maintained throughout the analyses.

For co-composting, vegetable wastes were collected from the different hostel messes of the Indian Institute of Technology Guwahati (IITG), and fresh cow dung was used as an inoculum for enhancing the microbial activity in the study. The moisture content of Vegetable waste and cow dung was very high, so to avoid the probability of generation of leachate, a bulking agent such as grass cutting, dry leaves (collected from the vicinities of IITG) and sawdust (collected from sawmill located in Amingaon, Guwahati, Assam) were mixed during composting process (Varma and Kalamdhad, 2015).

The alluvial soil was collected from the bank of the Brahmaputra River around Amingaon, North Guwahati, in the neighborhood of the Indian Institute of Technology Guwahati, Assam, India. The color of this soil ranges from moderately deep to very deep with grey to molted grey color.

The mine tailing soil samples were collected from Ledo Coalfield of Assam, India. The sample was manually examined, and undesirable particles like pieces of rocks, stones, and bits of wood were separated. The soil was cleaned, dried, crushed, and put through a mesh sieve of 2 mm before analysis. Oven-dried samples were carefully stored in a dry area for testing and analysis. The samples that were ready for various tests were kept in the lab refrigerator at 4°C until the analysis was completed.

Fig. 3.2. Sampling sites and collection of MSW from Boragaon dumpsite

3.3 PHASE I: SEASONAL CHARACTERIZATION OF MSW

The composition and characteristics of fresh MSW and legacy waste change with season, age of waste, and geographical location of sampling. Therefore, sample preparation and characterization are critical steps for the end use of the recovered material (Korai et al., 2016). A detailed physicochemical and thermal characterization of MSW and legacy waste of North-East India (Guwahati, Assam) was done to determine its potential to generate energy materials such as solid (char), liquid (pyrolysis oil), and gaseous (syngas) fuel by using pyrolysis technology (Reddy et al., 2016).

3.3.1 Physical composition of MSW

The composition analysis of MSW and legacy waste was done by the quartering method. The waste collected was emptied on a horizontal surface of 4×4 m^2 to form a heap. The sample was then mixed until it was homogenized. These were then divided into four equal sections, and weight was taken. The waste in each section was segregated into different fractions and the weight of each fraction was taken to determine the percentage composition of MSW and legacy waste (Valencia and Aguilar, 2012).

3.3.2 Physicochemical analysis

The proximate analysis was done to determine the moisture content, ash content, volatile matter, and fixed carbon of the MSW sample collected in the three seasons throughout the year using the standard methods of ASTM E949:1996, ASTM E830:2004, ASTM E790:2015, and ASTM E897:1998, respectively, on a dry basis. The ultimate analysis of MSW and legacy waste was determined using a CHN analyzer (Perkin Elmer, 2400 Series-II). The difference determined the oxygen content. The theoretical high heating value (HHV) was determined through C, H, N, S, and ash content in the sample (Kalivodová et al., 2022), and the instrumental heating value of MSW and legacy waste was determined using Bomb Calorimeter (LECO, AC 350 LECO model). The biochemical analysis determined the composition of extractive, hemicelluloses, lignin, and cellulose in MSW and legacy waste by gravimetric method (Ayeni et al., 2015). The bulk density of the

MSW and legacy waste sample was determined by ASTM D-1895. The calculation was done by using the expression as given in equation (1) and (2).

$$\text{Bulk density} = \frac{\text{Mass of the sample}}{\text{Volume of the cylinder}} \quad (1)$$

The porosity was calculated as follows:

$$\text{Porosity}, \eta = \frac{\text{Volume of void}}{\text{Volume of the cylinder in which the sample is filled}} \quad (2)$$

Thermogravimetric-differential analysis (TG-DTA) was carried out on MSW and legacy waste samples using a Thermal Analyzer (NETZSCH STA 449F3) within an argon atmosphere at a flow rate of 100 mL/min and temperature range spanning from 20 to 800°C, employing a heating rate of 10 K/min.

3.3.3 Kinetic analysis through the Arrhenius kinetic model

The reaction kinetics parameters were calculated from the TG/DTG profile. The TG/DTG graph was divided into three stages based on different temperature ranges through which combustion kinetics were studied. Stage I, which is ≤100°C, shows the dehydration stage. The combustion of the MSW sample starts at stage I, and the combustion of the char begins at stage III. Based on the DTG curves, the onset of stage III aligns with the temperature at the beginning of stage III (T_i), while the conclusion of stage III corresponds to the point of maximum weight loss rate (R_{max}) observed at the peak temperature (T_{max}). The activation energy (E_a), and pre-exponential factor (A) for the MSW and legacy waste were determined using the Arrhenius equation (3).

$$k = A \exp\left(-\frac{Ea}{RT}\right) \quad (3)$$

$$\log k = \log A - \frac{Ea}{2.303RT} \quad (4)$$

$$k = -\frac{\left(\frac{dW}{dt}\right)}{W} \quad (5)$$

Where k is the specific reaction rate, A is the preexponential factor (s^{-1}), R is the universal gas constant (8.314 $JK^{-1}mol^{-1}$), T is the instantaneous absolute

temperature (K), W is the weight of unburned combustible (kg), dW/dt is the instantaneous rate of weight loss per minute (%/min) from DTG curve.

The equation (4) can be expressed as

$$y = mx + c \quad (6)$$

Where m is the slope and c is the y-intercept, m and c can be determined by the Arrhenius plot of 1/T versus log k value from stage III of the TG/DTG graph (Weil et al., 1980).

3.3.4 Thermodynamic analysis

The thermodynamic analysis of the MSW and legacy waste sample was done by calculating the thermodynamic parameters such as change in enthalpy (ΔH kJ.mol^{-1}), Gibb's free energy (ΔG kJ.mol^{-1}) and entropy (ΔS kJ.mol^{-1} K^{-1}) by using the following equations (7), (8) and (9) (Dhyani et al., 2017)

$$\Delta H = E_a - RT_\alpha \quad (7)$$

$$\Delta G = E_a + RT \ln \frac{K_B.T_m}{h.A} \quad (8)$$

$$\Delta S = (\Delta H - \Delta G)/T_m \quad (9)$$

Where T_α is the final temperature (K) of stage III, K_B is the Boltzmann constant (1.3819×10^{-23} JK^{-1}), h is the Plank's constant (6.6269×10^{-34} Js), T_m is the peak temperature.

3.3.5 Statistical analysis

The analysis results were contrasted utilizing OriginLab® OriginPro software with the application of analysis of variance (ANOVA), and subsequently, the Tukey test was employed, where a significance level of $p<0.05$ was considered indicative of statistical significance.

3.4 PHASE II: DESIGN, FABRICATION, AND OPERATION OF THE PYROLIZER

In this phase, a fixed bed pyrolizer was designed and fabricated with a feeding capacity of 3 kg. The process parameter optimization of the pyrolysis of MSW

through Response Surface Methodology (RSM) has been done. This study considered four operational parameters during pyrolysis such as temperature, rate of heat, feed particle size, and residence time. The interaction between the processing parameters and optimization based on RSM for maximum yield of char from mixed MSW pyrolysis has been studied in phase II.

3.4.1 Design and fabrication of the pyrolysis reactor

The pyrolizer designed for the pyrolysis of MSW was a lab-scale fixed-bed type reactor. A schematic diagram of the pyrolysis setup and the pyrolizer is depicted in Fig. 3.3 (a) and (d), respectively. The materials used for framing the furnace of the pyrolizer setup were stainless steel sheet (1.5 mm thickness), stainless steel pipes, grate, electricity conducting rods, and valves. The experimental design comprises a PID controller, a nitrogen cylinder, and a condenser. The outer dimension of the reactor is 900 mm × 400 mm × 400 mm, and the inner dimension is 700 mm × 200 mm × 200 mm with an insulation thickness of 200 mm, and the reactor is heated electrically. A temperature controller with an Al/Rh thermocouple controlled the temperature inside the pyrolizer. The sample feeding is done on the movable grate inside the reactor. The maximum feed quantity in a batch was up to 3 kg, and char formed from pyrolysis was collected from the grate, as shown in Fig. 3.3 (b). The pyrolysis oil formed from condensable gas is collected in a glass apparatus, which is connected to a gas outlet valve and is kept in ice-cold water for condensation, and the non-condensable gas is collected through the outlet pipe as depicted in Fig. 3.3 (c).

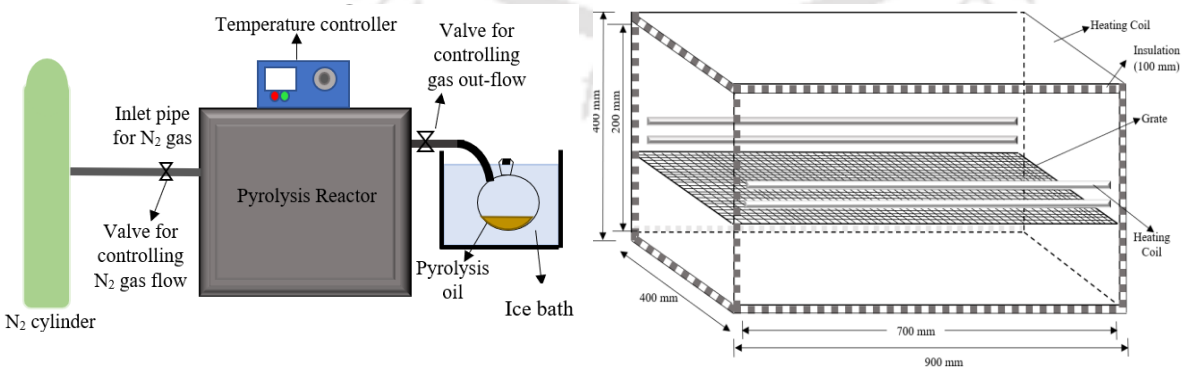

(a) (b)

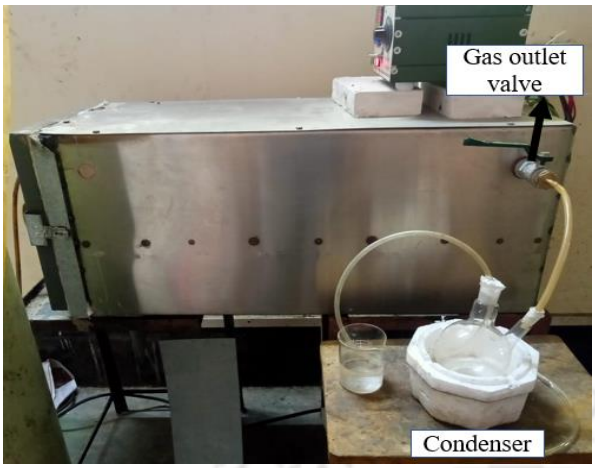

(c)

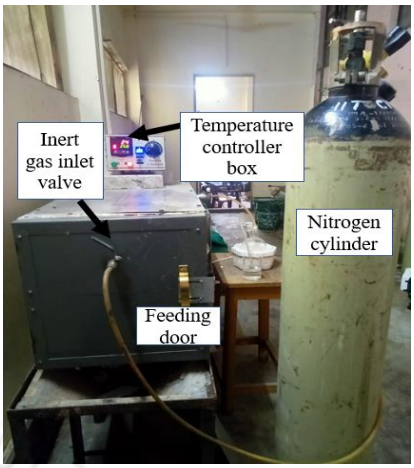

(d)

Fig. 3.3. (a) Schematic of the Pyrolysis setup (b) Inside view of the pyrolysis reactor (c) Side view and (d) Front view of the experimental setup of the pyrolizer

3.4.2 Operation of the Pyrolizer

In the experimental process, 3 kg of mixed MSW sample was fed on the movable grate inside the reactor. An inert atmosphere was maintained in the reactor by purging nitrogen gas through a gas inlet valve, and the gas outlet of the reactor was connected to a condenser. The reactor was powered on and adjusted to the required temperature and ramp rate. The pyrolysis experiment was conducted at four-terminal temperatures, i.e., 250, 350, 450, and 550°C and at a rate of heat 10 to 40°C/min according to the thermogravimetric analysis of MSW. The experiment was done by varying the particle sizes of the feedstock and residence time from 30 to 180 minutes after reaching the required terminal temperature. The product formed was char, gas, and condensate liquid-pyrolysis oil, which was heterogeneous, consisting of a heavy and aqueous fraction. The aqueous solution was brownish with the appearance of oil as a black, tarry substance floating in the solution. The product was then collected for further analysis, and the temperature at which the maximum char yield was found was considered for analysis and characterization of the sample. The MSW waste conversion (%) through pyrolysis to three products, viz; char, pyrolysis oil, and gas, was calculated as shown below in equation (9), (10) and (11) (Mohamed et al., 2014):

$$\text{Char yield (\%)} = \frac{\text{weight of the char produced}}{\text{initial weight of the sample}} \times 100\% \quad (9)$$

$$\text{Yield of pyrolysis oil (oil+aqueous)} = \frac{\text{weight of the pyrolysis oil produced}}{\text{initial weight of the sample}} \times 100\% \quad (10)$$

$$\text{Yield of gas (\%)} = 100 - (\text{char\%} + \text{pyrolysis oil\%}) \quad (11)$$

3.4.3 Optimization of the process parameters for maximizing the yield of char

The current study used Response Surface Methodology (RSM) as a statistical approach to optimize the operational parameters to generate maximum char, pyrolysis oil, and gas yield while using different factors as operating parameters. The regression analysis and optimization of the independent factors were done using *Design Expert 11* software. The software recommends using Face-Centered Central Composite Design (FCCCD) to analyze the influence of independent factors on the responses. Table 3.1 lists the coded levels of the four independent input parameters.

Table 3.1. Code of the independent factors and their range

Independent factors	Code	Unit	- alpha	Low	High	+ alpha
Temperature	A	°C	250	250	550	550
Rate of heat	B	°C/min	10	10	40	40
Feed particle size	C	mm	5	5	50	50
Residence time	D	min	30	30	180	180

The RSM suggested that a quadratic and linear model fit the study best. Statistical analysis was done using ANOVA, incorporating quadratic equations. Using FCCCD in RSM, the process parameters were optimized. The parameters examined were temperature, rate of heat, feed particle size, and time for holding after reaching the desired temperature. The lowest and highest values of the independent factors are

displayed in Table 3.1, as suggested by RSM. There were 31 experimental runs recommended by CCD using different process parameter conditions as shown in Table 3.2. Using ANOVA, all experiment findings were thoroughly examined.

Table 3.2. CCD experimental setup for pyrolysis experiment

Std	Run	Space Type	Factor 1 A:Temperature °C	Factor 2 B:Heating rate °C/min	Factor 3 C:Feed particle size mm	Factor 4 D:Residence time min
1	6	Factorial	250	10	5	30
2	16	Factorial	550	10	5	30
3	7	Factorial	250	40	5	30
4	30	Factorial	550	40	5	30
5	24	Factorial	250	10	50	30
6	3	Factorial	550	10	50	30
7	15	Factorial	250	40	50	30
8	11	Factorial	550	40	50	30
9	25	Factorial	250	10	5	180
10	14	Factorial	550	10	5	180
11	5	Factorial	250	40	5	180
12	4	Factorial	550	40	5	180
13	27	Factorial	250	10	50	180
14	1	Factorial	550	10	50	180
15	2	Factorial	250	40	50	180
16	23	Factorial	550	40	50	180
17	8	Axial	250	25	27.5	105
18	29	Axial	550	25	27.5	105
19	10	Axial	400	10	27.5	105
20	28	Axial	400	40	27.5	105
21	26	Axial	400	25	5	105
22	17	Axial	400	25	50	105
23	20	Axial	400	25	27.5	30
24	19	Axial	400	25	27.5	180
25	9	Center	400	25	27.5	105
26	12	Center	400	40	27.5	180
27	21	Center	400	40	27.5	30
28	22	Center	400	10	27.5	30
29	18	Center	400	10	27.5	180
30	13	Center	400	40	5	105
31	31	Center	400	40	50	105

3.5 PHASE III: CHARACTERIZATION OF MSW CHAR AND ITS APPLICATION

In phase III, pyrolysis of unsegregated and non-shredded MSW at four different terminal temperatures and evaluating the quality of the resulting char through physicochemical analysis and microplastic identification with the aim of potential applications such as adsorption, combustible fuel, or as an amendment in soil. The

most potent char was applied as an activated carbon for the adsorption of heavy metals, co-composting with vegetable waste and for remediation of alluvial soil and mine tailing soil.

3.5.1 Characterization of char produced at different temperatures

i. Proximate analysis

The proximate analysis was performed to determine the moisture content, volatile matter, ash content, and fixed carbon on a dry basis of the four-char samples produced by pyrolysis of MSW using ASTM E949:1996, ASTM E790:2015, ASTM E830:2004, and ASTM E897:1998, respectively.

ii. Elemental composition and calorific value

The carbon, nitrogen, oxygen, hydrogen, and sulphur content in the MSW char was analyzed by a CHN analyzer (maker: Perkin Elmer, 2400 Series-II). The calorific value was determined using the Bomb Calorimeter (LECO, AC 350 LECO model). The theoretical heating value was calculated as shown in equations (12) and (13) according to Schwanecke (1976) (Götze et al., 2016):

$$H_{high} = H_{low} + (W + H \times 8.937) \times 24.45 \text{ kJ/kg} \quad (12)$$

$$H_{low} \text{ (kJ/kg)} = 348\ C + 939\ H + 105\ S + 63\ N - 108\ O - 24.5\ H_2O \quad (13)$$

Where C, H, N, S, O, and H_2O are the percentage weight of Carbon, Hydrogen, Nitrogen, Sulphur, Oxygen, and moisture content, respectively, in the MSW char.

iii. Fourier transform infrared (FTIR) spectroscopy

The functional group present in the MSW char was determined in the resolution and range of 4 cm^{-1} and 400-4000 cm^{-1}, respectively, by FTIR spectroscopy using FTIR-system-2000, Perkin Elmer, USA.

iv. Determination of bulk density, porosity, pH, and iodine number

The bulk density of the MSW char samples was determined by ASTM D-1895. The pH of the char was determined according to IS:10158-1982 using a pH meter of model μ pH system 361. The iodine number of the MSW char was determined using the Gimba and Musa (Adeolu et al., 2016) method. In this method, an iodine solution was prepared using iodine (2.7 g) and potassium iodide (4.1 g) in 1 litre of

distilled water. The standardization of the iodine solution was done using sodium thiosulphate. An amount of 0.5 g of char was taken and mixed with 10 ml of 5% V/V hydrochloric acid. The sample was then mixed with 100 ml of the iodine stock solution and agitated quickly for 60 minutes. The mixture was then filtered and 20 ml of the aliquot portion was titrated with 0.1 M of sodium thiosulphate. The concentration of iodine absorbed by char at ambient temperature was calculated by equation (13).

$$\text{I mg/g} = \frac{(B - S)}{B} \times \frac{V \times m}{W} \times 253.81 \quad (14)$$

Where,

B = thiosulphate solution required for blank (mL)

S = sample titrated (mL)

W = mass of char (g)

m = iodine solute (mol)

253.81 = iodine atomic mass

V = volume of aliquote (20 mL)

v. Brunauere Emmette Teller (BET) surface area

The specific surface area and size of the pore of char were determined by Autosorb-1 (Quantachrome, USA) using low-temperature nitrogen adsorption. The experiment was performed on dry char samples via N_2 adsorption at 150K on a Surface Area Analyzer. The degasified temperature was kept at 150°C for 5 hours.

vi. Field Emission Scanning Electron Microscope (FESEM) and Energy Dispersive X-ray (SEM-EDX) analysis

The surface morphology of char was observed under by Gemini Field Emission Scanning Electron Microscope (FESEM). The oven-dried char was placed on the carbon tape, and the gold coating was done to prevent sample charging. The chemical and elemental properties of char were analyzed using SEM-EDX analysis in Zeiss-Sigma 300, which provides detailed insights into the composition of the material. This study examined the EDX spectra of MSW char samples to understand their chemical and elemental characteristics.

vii. X-ray diffractometer (XRD)

The crystallographic characteristics were identified through X-ray diffraction. The identification of different minerals present in the char was accomplished through XRD analysis, employing a Single-crystal X-ray diffractometer with an intensity range at 2-theta value from 0 to 80. The crystallinity index was computed by using equation (15) (Rojith et al., 2013);

$$\text{Crystallinity index (\%)} = \frac{\text{Area of all the crystalline peaks}}{\text{Area of all the crystalline and amorphous peaks}} \quad (15)$$

viii. Atomic Absorption Spectroscopy (AAS) analysis

The concentration of heavy metal in MSW char was determined through AAS analysis, employing an Atomic Absorption Spectrometer (Varian-Spectra 55B).

ix. Microplastic analysis of MSW char

Over time, larger plastic materials undergo a process of degradation and subsequent fragmentation, resulting in the creation of smaller fragments (Shah et al., 2010). A specific category of plastic waste known as microplastics refers to particles with sizes below 5mm, as defined arbitrarily. When plastic particles reach sizes smaller than 0.1μm or 1 μm, they are called Nano plastics, although some recent studies suggest that the lower limit for microplastics could be as small as 1 nm (Cutroneo et al., 2021). The commonly utilized polymer types, such as polyethylene (PE) and polypropylene (PP), possess elevated molecular weights and exhibit non-biodegradable characteristics (Shah et al., 2010). Microplastic detection in every product produced is crucial for protecting the environment, safeguarding human health, maintaining product quality, and complying with regulations. It ropes to take proactive measures to minimize microplastic pollution, ensuring a more sustainable and healthier future.

a. Microplastic analysis through FTIR

The functional group present in the char generated from MSW has been analyzed to understand the presence of plastic by FTIR spectroscopy.

b. Density separation; flotation and elutriation

By exploiting the density differences, it is possible to distinguish plastics (with a density range of 0.8-1.6 g cm^{-3}) from sediment (Tirkey and Upadhyay, 2021). The

density separation method utilizing NaCl (1.2 g cm^{-3}) was employed to remove microplastic from char. NaCl is a commonly used salt for density separation due to its wide availability, cost-effectiveness, and environmentally friendly nature (Cutroneo et al., 2021). In this process, the MSW char was mixed with 140 gL^{-1} of NaCl and agitated for 10 mins. Then, the char was allowed to settle down at the bottom of the beaker so that light-density microplastic particles floated on the surface of the solution. To recover the floating plastic, the supernatant was filtered out with Whatman ® GF/C with a pore of 1 mm and 47 mm diameter. The filtered plastic was kept for drying in a glass-covered petri dish for 24 hours at room temperature. The petri dish was then observed under a stereomicroscope, and images were captured (Abidli et al., 2018).

3.5.2 Application of char as an activated carbon

i. Activation of MSW char

Chemical activation was employed to activate municipal solid waste (MSW) char using $ZnCl_2$, KOH, and NaCl, resulting in the production of three different types of activated carbon. In the case of activation by $ZnCl_2$, 70 grams of MSW char was mixed with 100 cm^3 of a 10% w/v $ZnCl_2$ solution. The mixture was then heated at a consistent 80°C using a heating mantle until it formed a paste. Subsequently, the paste underwent further heating in a furnace for one hour at 300°C. The paste formed was washed after cooling with distilled water until it reached a neutral state followed by oven drying (Ekpete et al., 2017). The resultant dried sample was stored in an airtight moisture-free container for subsequent analysis. The chemical activation using KOH involved blending 1 N KOH with MSW char and subjecting it to heating for 2 hours at 200°C. After cooling, the mixture was washed to neutralize and subsequently dried in the oven until reaching a constant weight (Hendrawan et al., 2019). Activation with NaCl entailed mixing char with 0.5 M NaCl and then heating it at 300°C in a muffle furnace.

ii. Adsorption study by using MSW-derived activated carbon (MSW-AC)

The heavy metal adsorption capacity by different activated carbon was studied by batch adsorption experiment. In this study, one gram of the MSW-AC was added

to 20 mL of heavy metal concentration, viz. 50, 100, 150, 200, 500 and 1000 mg/L and sonication for 20 minutes at 150 rpm. The filtrate was collected by filtration after the solids were allowed to settle down. The atomic adsorption spectroscopy was used to find the metal concentration. The removal capacity of the heavy metal was determined by the subsequent calculation using equations (16) and (17) (Zabihi et al., 2009).

$$\text{Removal } \% = \frac{c_i - c_e}{c_i} \times 100 \tag{16}$$

$$Q_e = \frac{(c_i - c_e)v}{m} \tag{17}$$

Q_e represents metal concentration uptake by MSW-AC in equilibrium (mg/g), the initial and the final concentration of a metal ion in the solution is expressed as c_i and c_e, respectively in mg/L, the volume of the solution denoted by v in litres, m is the grams of adsorbent.

iii. Adsorption Kinetics of heavy metal adsorption by MSW-AC

The kinetics study offers an important understanding of both the mechanism and effectiveness of the adsorption process. In this study, pseudo-first and second-order kinetics models of Lagergren were employed to analyze experimental data and determine their fit. The experiments were conducted under optimal parameters such as pH, duration of contact, metal dosage, and activated carbon quantity. In this experiment, different time intervals were considered with 1000 ppm Pb(II) solution for kinetic modeling. One gram of the MSW-AC was added to 20 mL of metal solution and was put into the horizontal shaker. The solution was observed for Pb(II) solution using atomic adsorption spectroscopy to find the capacity of activated carbon against heavy metal. The linear forms of Lagergren's pseudo-first and second-order kinetics equations were utilized, as shown in equation (18) and (19), respectively (Buah and Williams, 2010).

$$\log(q_e - q_t) = \log q_e - \frac{k_1}{2.303} t \tag{18}$$

$$\frac{1}{q_t} = \frac{1}{q_e} + \frac{1}{k_2 q_e^2 t} \tag{19}$$

Where q_e and q_t represent the capacity of adsorption at equilibrium and at time t (min) in mg/g, respectively, k_1 and k_2 is the pseudo-first-order and second-order rate constant, respectively.

iv. Adsorption Isotherm

The quantitative assessment of metal adsorbed is conducted through equilibrium isotherms (Puranik and Paknikar, 1999; Namasivayam and Kavitha, 2002). In the literature, two widely recognized linearized adsorption isotherm models are commonly employed: Langmuir and Freundlich, as indicated by equations (20) and (21), respectively. The Langmuir adsorption isotherm assumes that the adsorbate is monolayerly covered over the adsorbent's surface and that each adsorption site is identical. This model offers insights into uptake capacity, reflecting the behavior of the equilibrium process (Langmuir, 1918). On the other hand, the Freundlich model establishes an association between the capacity of metal uptake (qe in mg/g) and the residual (equilibrium) concentration of metal ions (C_e in mg/L) (Mushtaq et al., 2023). The objective of this research was to evaluate the best interaction of MSW-AC for metal immobilization based on varying concentrations and time. The Pb solutions were prepared with concentrations of 50, 100, 150, 200, 500, and 1000 mg/L. Then, activated carbon (1 g) was added to a 20 mL metal solution and put on a horizontal shaker. The solution was observed for Pb solution using atomic adsorption spectroscopy capacity against heavy metal.

$$q_e = \frac{q_{max} K_L C_e}{1 + K_L C_e} \tag{20}$$

$$q_e = K_F C_e^{1/2} \tag{21}$$

q_e (mg/g) is the metal ion concentration adsorbed by MSW-AC, C_e represents the metal concentration in the solution at equilibrium (mg/L), the adsorption capacity at the monolayer is denoted by q_{max} (mg/g), K_L is the Langmuir constant which relates the adsorption energy and capacity, the Freundlich constant is K_F, and ½ is the intensity of adsorption.

v. Cycle study

The cycle study allows to investigate the effectiveness of the adsorbent in

removing target contaminants during repeated adsorption-desorption cycles. It helps determine if the adsorbent retains its adsorption capacity and efficiency after multiple cycles or if there is any loss in its performance. Cycle study in adsorption studies is essential for understanding the long-term performance, reusability, and regenerability of the adsorbent material, contributing to the development of sustainable and cost-effective adsorption processes for wastewater treatment (Badran et al., 2023).

vi. Desorption study

The desorption was conducted to evaluate how effectively contaminants could be removed from the adsorbent material for potential reuse. Following the adsorption process, pollutants become attached to the surface of the adsorbent. Desorption entails releasing these pollutants from the adsorbent, typically achieved through the use of a desorbing agent or altering environmental conditions. In this particular study, desorption was performed using 0.1 M solutions of HNO_3, H_2SO_4, and HCl. A desorbing solution of 20 mL was employed for a duration of 2 h (Vishan et al., 2019). The pH level and duration of contact emerged as critical factors influencing desorption efficiency (Badran et al., 2023). Consequently, optimization of these parameters was also undertaken.

3.5.3 Application of MSW char during co-composting of vegetable waste

i. Co-composting of MSW char and vegetable waste

Co-composting was done utilizing in-vessel composting in the rotary drum composter (RDC), which outperforms all other composting methods in terms of degradation rate and waste materials stabilization (Singh and Kalamdhad, 2016; Sharma et al., 2017). Therefore, a retention period of 20 days was selected for the experiment. The lab-scale RDC had a volume capacity of 550 L and operated in batch mode, as shown in Fig. 3.5. The apparatus is affixed to a metal frame with four rubber rollers and is mechanically rotated using a handle. The main body of the drum was made from mild steel and has dimensions of 1.022 meters in length and 0.76 meters in diameter. Inside the drum, 40×40 mm angles are welded along its length to facilitate proper blending, stirring, and aeration of feedstock during

rotation. Additionally, two head-to-head holes, each 10 cm in diameter, are positioned at the top to allow for the drainage of additional water. Rotation of the RDC was done manually every 24 hours to ensure appropriate aeration. Three different composting ratios of vegetable waste, sawdust, cow dung, and MSW char were added in three different rotary drum composters comprising 100 kg of waste materials. Vegetable wastes were cut into 2 to 5 cm in size by the mechanical shredder for the uniform blending of the composting material. The optimal blend consisting of cow dung, vegetable waste, and sawdust was prepared as shown in Fig. 3.4, taking into account their respective mixing ratios as documented in previous studies on the RDC of vegetable waste Varma and Kalamdhad, 2015). The addition of more than 20% of the MSW char is not recommended as it may interfere with the biodegradation of organic waste (Camps and Tomlinson, 2015). As shown in Table 3.3, 2.5% and 5% (w/w) MSW char was added to the 100 kg of waste material, and it was homogenized and mixed before it was put in the rotary drum.

(a) (b) (c) (d)

Fig. 3.4. (a) Vegetable waste (b) cow dung (c) saw dust (d) MSW char

Table 3.3. Mix proportion of composting material and MSW char

Trial Name	Mixed proportions	Vegetable waste (kg)	Cow dung (kg)	Saw dust (kg)	Total (kg)	MSW char (%) added
Control	4:1	50	40	10	100	0
Trial 1	4:1	50	40	10	100	2.5
Trial 2	4:1	50	40	10	100	5

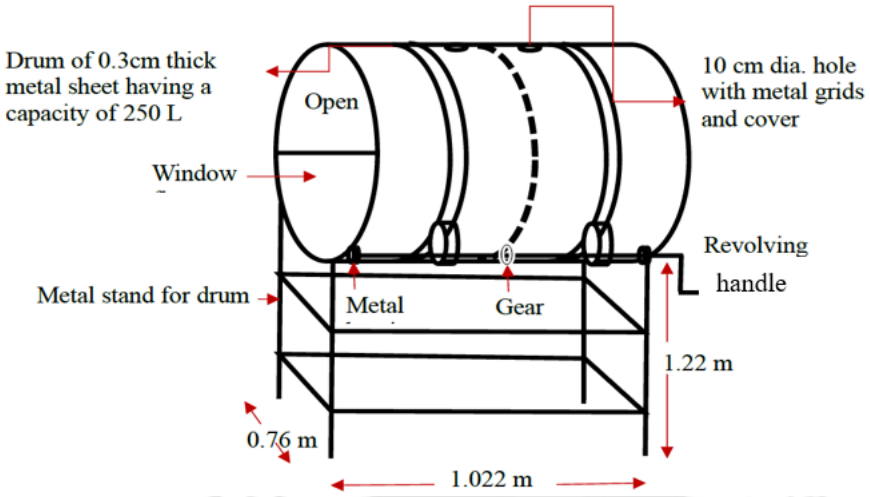

(a)

(b) (c)

Fig. 3.5. (a) Schematic diagram of Rotary Drum Composter and (b) and (c) Rotary drum composter (Kalamdhad et al., 2008)

ii. Sampling

Sampling was conducted on even alternative days throughout the 20 days. From each reactor, triplicate samples were collected at three specific locations, each 20 cm from the surface and distinct from one another. A portion of the samples was kept at 4°C for immediate biological examination, while some were air-dried, crushed, and sieved for subsequent physicochemical analysis.

iii. Physicochemical and Nutritional Parameters

The temperature was monitored every six hours with the help of a digital thermometer. To measure pH and electrical conductivity, approximately 10 g of the compost sample, which was sieved through a 0.22 mm sieve, was mixed with 100

mL of distilled water in a 1:10 ratio (w/v). The mixture was then subjected to horizontal shaking for 2 hours at 120 rpm. Subsequently, the pH of the suspension was determined using the pH meter. The conductivity of the suspension was measured using the EC meter. To measure volatile solids, approximately 10 g of the compost was placed in a crucible (W_1), which was subsequently placed in a muffle furnace for 2 hours at 550°C. After this duration, the final weight of the sample was recorded as W_2. The measurement of volatile solids in the sample was calculated using equation (22) according to the APHA (2017) standard method.

$$VS = \frac{(10-(W2-W1))}{10} \times 100 \quad (22)$$

Total Organic Carbon was determined by dividing the value of the volatile solids by factor 1.8, according to the APHA (2017) standard method (Maturi et al., 2022). The ash content and TKN was measured in similar method as done for MSW char.

The Nitrate (NO_3-N) and ammonical nitrogen (NH_4-N) were determined spectrophotometrically after extraction with 2 M KCl solution (Varma et al., 2018). Determination of Available phosphorus and Total phosphorus is done by colorimetric method according to APHA (2017) standard method (Kauser et al., 2020). The overall concentration of sodium, potassium, and calcium was assessed using a flame photometer (Systronic 128) after digestion of the 0.2 g sample in a block digester with 10 mL of mixed acid (H_2SO_4 and $HClO_4$ in ratio 5:1) (Kauser et al., 2020).

iv. Heavy Metal Analysis

Total concentrations of heavy metals such as iron (Fe), lead (Pb), manganese (Mn), zinc (Zn), chromium (Cr), copper (Cu), and nickel (Ni) were determined by atomic adsorption spectrometer (AAS) (Varian Spectra 55B).

v. Biological Analysis

Evolution of CO_2

According to Kalamdhad et al. (2008) the direct approach to assess the stability of compost is CO_2 evolutions measured by static measurement method. About 10 g of soda lime was oven-dried and mixed with 25 g of fresh compost inside a

container. The evolution of CO_2 was calculated as given in equation (23) (Kalamdhad et al., 2008):

$$CO_2 \text{ evolution (mg/gVS/day)} = \frac{W_2 - W_1}{W \times T} \times 1000 \quad (23)$$

In equation (23), W_1 and W_2 represent the initial and final weight of the soda-lime (in grams) after incubated at 25°C and oven-dried, respectively, W denotes the weight of the compost sample (in grams), and T indicates the period of incubation (in hours).

Soluble Biochemical oxygen demand (sBOD) (APHA, 2005)

The sample was diluted in a ratio of 1:10 and placed on a horizontal shaker for 2 hours. Following this, the solution was filtered, and the resulting supernatant was collected for analysis of BOD using the BOD5 test and calculated using equation (24).

$$\text{sBOD} = \frac{D_1 - D_2}{P} \times DF \quad (24)$$

In this context, D_1 and D_2 represent the initial and final levels of dissolved oxygen in the sample after 5 days of incubation, measured in mg/L, P denotes the volume of the sample diluted to a total volume of 300 mL with dilution water, DF = Dilution factor.

Soluble Chemical oxygen demand (sCOD) (APHA, 2005)

The sCOD analysis was conducted by diluting the compost in 1:10 ratio, and the resulting filtrate was analyzed using closed reflux method. In this method, 1.5 mL of $K_2Cr_2O_7$ and 3.5 mL of H_2SO_4 reagent were mixed with 2.5 mL of the filtered sample in a COD vial. The mixture was then digested for 2 hours at 150°C and subsequently cooled to ambient temperature. It was then titrated against ferrous ammonium sulfate ($FeH_8N_2O_8S_2$) using a ferroin indicator until the color changed from green to deep red hue (Kauser et al., 2020) and calculated as given in equation (25).

$$\text{sCOD} = \frac{(\text{A} - \text{B}) \times \text{M} \times 8000}{\text{mL of sample}} \quad (25)$$

In this scenario, A and B represent the volume of $FeH_8N_2O_8S_2$ used for the blank and sample, respectively; M denotes the molarity of $FeH_8N_2O_8S_2$, and 8000 signifies the milliequivalent weight of oxygen multiplied by 1000 mL/L.

vi. Microbial Analysis

10 grams of fresh samples were placed into 100 mL of sterile distilled water in an Erlenmeyer flask. The solution is mechanically mixed at 220 rpm in a horizontal shaker. The diluted samples were inoculated in culture media tubes to measure the amount of total and Fecal coliform using the most probable number (MPN) (APHA 2012). Total counts of heterotrophic bacteria were determined by inoculation of diluted samples in culture media Petri dish using the pour plate method (APHA, 2015).

3.5.4 Application of MSW char in alluvial soil and its effect on plant growth

i. Experimental setup

Table 3.4. Experimental setup for the study of the effect of char and compost in alluvial soil

Treatment	Weight of soil (kg)	Weight of vermicompost (kg)	Weight of char (kg)	Total weight (kg)
1% char (C1)	4	0	0.04	4.04
5% char (C5)	4	0	0.2	4.2
10% char (C10)	4	0	0.4	4.4
20% compost + 1% char (CM1)	4	0.8	0.04	4.84
20% compost + 5% char (CM5)	4	0.8	0.2	5
20% compost + 10% char (CM10)	4	0.8	0.4	5.2

The MSW char and a combination of MSW char and compost were applied to the alluvial soil and to assess its effects, a quadrimester study was conducted in pots of volume 0.012 m^3. The MSW char was mixed with alluvial soil at rates of 1, 5,

and 10%, respectively. In another three pots, the percentage of compost in the alluvial soil was fixed, and then MSW char was mixed at a rate of 1, 5, and 10% with the alluvial soil, as shown in Table 3.4. The pot study was conducted in the hard-plastic material reactor. The bottom layer (10-20 cm) was filled with aggregates having size (4-16 mm). The next layer (30-40 cm) was placed with a homogenized mixture of soil mixed with the compost and MSW char. For soil quality assessment, *Abelmoschus esculentus (Okra)* was grown.

ii. Sampling

For each reactor, sampling was carried out in duplicates immediately after placing the reactors (referred to as day 0 samples) and then after 15, 30, 45, 60, 90 and 120 days. Sampling was done at a random depth of 10 cm with the help of a soil auger. The collected samples are dried in a hot air oven for 24 hours at 105°C and ground through a 212 μm sieve.

iii. Physiochemical and Nutritional Parameters

The pH and electrical conductivity (EC) were measured according to APHA (2017). Total Kjeldahl nitrogen (TKN) was determined using the stannous chloride method according to the APHA (2017) standard method (Jain and Kalamdhad, 2018). The Nitrate (NO_3-N) and ammoniacal nitrogen (NH_4-N) were determined spectrophotometrically after extraction with 2M KCl solution (Varma et al., 2018). Determination of available phosphorus was done using the colorimetric method (Kauser et al., 2020). The total concentration of Na, K, Ca, and Mg was determined by flame photometer (Systronics 128) and atomic adsorption spectrometer (AAS) (Varian spectra 55B) after digestion of the 0.2 g sample in a block digester with 10 mL of mixed acid (H_2SO_4 and $HClO_4$ in ratio 5:1). The soil organic matter (SOM) was determined in accordance with the ASTM D 2974. Soil organic carbon (SOC) was determined using the Walkley and Black oxidation method (FAO, 2019). In this procedure, 0.5 to 1 g of dried sample passed through a 0.22 mm sieve was mixed with 10 mL of $K_2Cr_2O_7$, followed by mixing with 20 mL of concentrated H_2SO_4 and swirled until the soil and reagents were mixed. The mixture was allowed to cool for 30 mins and diluted to 200 mL. The diluted sample was then mixed with

10 mL of 85% H_3PO_4, 0.2 g of NaF, and 15 drops of diphenylamine indicator. The solution was titrated with 0.5 N Ferrous Ammonium Sulfate (FAS). The soil organic carbon is calculated by the formula given in equation (26):

$$\% \text{ SOC} = (\text{B} - \text{S}) \times \text{N} \times 0.003 \times \frac{100}{Weight\ of\ dry\ soil} \quad (26)$$

B = mL of standard 0.5 N ferrous ammonium sulphate required for the blank.

S= mL of standard 0.5 N ferrous ammonium sulphate required for blank sample

N = Normality of standard FAS (0.5 N)

The correction factor 1.3 is multiplied according to the Walkley and Black oxidation method.

iv. Specific gravity of the sample

The specific gravity was measured according to ASTM-D854 and calculated using equations (28).

$$\rho_s = \frac{(W_3 - W_1) \times \rho_w}{(W_2 - W_1) - (W_4 - W_3)} \quad (27)$$

$$S_g = \frac{\rho_s}{\rho_w} \quad (28)$$

Where ρ_s denotes the specific density of the sample (g/cm^3), W_1 is the weight of the empty volumetric flask (g), W_2 represents the weight of the volumetric flask filled with distilled water up to the graduation mark (g), the density of water is denoted as ρ_w (g/cm^3), W_3 is the weight of the sample with the volumetric flask (g), W_4 represents the weight of the flask filled with sample and distilled water up to 2/3rd of the flask (g), S_g is the specific gravity of the sample.

v. Water Holding Capacity (WHC)

A sample with a known moisture content (S_i) was placed in a beaker and let to soak in water for one to two days. After draining the extra water through Whatman 2 No. filter paper, the soaked sample's weight (S_s) was recorded. Equation (29) was used to compute the amount of water that the dry sample absorbed. The following formula can be used to calculate the WHC (g water/g dry material) (Klute, 1986)

$$WHC = \frac{(Ss - Si) + MC \times Si}{(1 - W) \times Si} \quad (29)$$

Where,

W is the moisture content (g), S_i denotes the initial weight (g), and S_s is the final weight (g) of the sample.

vi. Exchangeable Cations

5 g of air-dried soil sample (passed through a 0.22 mm sieve) was taken in the conical flask. 50 mL of 1 N ammonium acetate was added to the sample. The mixture was kept in a horizontal shaker for 2 hours at 100 rpm. After shaking, the extracted solution from the solid residue was separated using Whatman 42 No. filter. The exchangeable cation was measured from the extraction using a Flame photometer and atomic adsorption spectrophotometer.

vii. Bioavailability of Metals

Diethylenetriamine Penta acetic Acidic Fraction (DTPA)

About 40 mL of 0.1 M triethanolamine, 0.01 M $CaCl_2$, and 0.005 M DTPA of pH 7.3 were added to 4 g of the sample shaking at 100 rpm (Kulikov, 2016). The concentration of heavy metals in the extracted solution was measured using AAS.

3.5.5 Application of MSW char in mine tailing soil

i. Experimental setup for char, vermicompost, and mine tailing soil

The char prepared at 350°C and 10°C/min heating rate was used along with vermicompost for application in mine tailing soil. To prepare the vermicompost (VC), rotary drum composting followed by vermicomposting was done. In this process vegetable waste was collected from hostels of the Indian Institute of Technology Guwahati, Assam, India. Saw dust was applied as a bulking agent, and cow dung was used for microbial inoculum. The proportion of shredded waste, inoculum, and bulking agent were combined in a ratio of 5:4:1, respectively (Varma and Kalamdhad, 2015). The composting process was mainly carried out in a 550 L capacity RDC. The RDC received 100 kg of the feed, and aeration was maintained by rotating the drum once a day during the process of composting. In the current

combined method for vermicomposting, *E. fetida* was utilized. The earthworms were obtained from Krishi Vigyan Kendra (KVK), Guwahati, and cultivated in the laboratory before being applied to the waste that has been predegraded. Following the RDC's first 7 days of operation, 2.5 kg of predegraded waste was extracted, and VC was obtained after 20 days (Pottipati et al., 2022).

The MTS was air dried at 20-25°C for two weeks, sieved to <2 mm, and any biological debris was removed. The soil was then homogenized and thoroughly hand-mixed with MSW char and vermicompost in the following proportions, and sampling was done on the 0^{th}, 30^{th}, and 45^{th} day:

Control (MTS + 0% C + 0% VC)

MTS + 10% C

MTS + 20% C

MTS + 20% VC + 5% C

MTS + 30% VC + 5% C

Where MTS is mine tailing soil, C is the MSW char, and VC is the vermicompost.

ii. Total heavy metals

The total metals were determined by using a 0.1 g sample and digested with 10 mL of H_2SO_4 and $HClO_4$ (5:1) in a digester for 2 hours at 300°C. The sample that was digested was used to determine the total concentration of heavy metals through an atomic absorption spectrometer (AAS) (Varian Spectra 55B).

iii. Extraction of Water-Soluble Heavy Metals

To determine the water-soluble metals, the sample was extracted using distilled water in the ratio of 1:20 (sample: distilled water) at room temperature using a bath shaker for 2 hours at 100 rpm (Singh and Kalamdhad, 2012). The mixture was kept for 5 mins at 10,000 rpm and filtered through the Whatman No. 42 filter paper. The heavy metal analysis of the supernatant was done by AAS.

iv. Extraction of Heavy Metals with Diethylene Triamine Penta-Acetic Acid (DTPA)

Approximately 4 g of the sample was taken in powder form, and 40 mL of 0.1 M triethanolamine, 0.01 M $CaCl_2$, and 0.005 M DTPA were added to the sample with pH 7.3 shaking at 100 rpm (Kulikov, 2016). The concentration of heavy metals in the extracted solution was measured using AAS.

v. Leachability of Heavy Metals

The standard toxicity characteristic leaching procedure (TCLP) method (US EPA, 1992) was performed on the sample to find the leachability of heavy metals from the MTS. In this procedure, 5 g of the sample was mixed with 100 mL of acetic acid at pH 5, which was adjusted using 1 N NaOH, maintaining a sample-to-solution ratio of 1:20 at ambient temperature using a bath shaker for 18 hours at 30 rpm. The remaining procedure was similar to the extraction of water-soluble heavy metals.

vi. Metal Speciation

A sequential extraction of the heavy metals was carried out by the method of Tessier et al. (1979). These authors reported the five forms of fractions as Exchangeable fraction (F1), Carbonate fraction (F2), Reducible fraction (F3), Organically bound fraction (F4), and Residual fraction (F5). The extraction was performed with an initial oven-dried sample of 1.0 g in polypropylene centrifuge tubes of 50 mL capacity. In the process of sequential extraction of F1, 8 mL of 1.0 M $MgCl_2$ was used as an extractant, which is then agitated at 220 rpm for 1 hour at 25°C. The extraction of F2 was done by using 8 mL 1.0 M NaOAc (pH was adjusted to 5 by concentrated HOAc) and was agitated for 5 hours. 20 mL of 0.04 M $NH_2OH.HCl$ in 25% HOAc (v/v) was used as an extractant for extraction of F3, which was then put in a water bath shaker for 6 hours at 96°C with irregular agitation. The F4 was extracted at first by using 3 mL 0.02 M HNO_3 and 5 mL 30% H_2O_2 (pH adjusted to 2 with concentrated HNO_3), followed by heating at 85°C for 2 hours. After 2 hours, 3 mL of 30% H_2O_2 was added and then heated at 85°C for 3 hours with occasional stirring. As the mixture was cooled, 5 mL of 3.2 M

NH_4OAc in 20% (v/v) HNO_3 was added and agitated for 0.5 hours at 25°C. The F5 was extracted by using an extractant solution consisting of 10 mL of H_2SO_4 and $HClO_4$ (5:1) mixture, followed by heating at 300°C for 2 hours. After each successive extraction, the supernatant liquid was separated with a pipette after centrifugation at 10,000 rpm for 5 minutes and diluted for heavy metal analysis. The residue is washed (except residual fraction) with 20 mL of Milli Q water by shaking for 15 minutes, followed by centrifugation without loss of solids. The extracts are stored in plastic reagent bottles for heavy metal analysis by AAS.

The soil matrix actively holds some metals together in their certain chemical forms, while some are weakly bound and are soluble in acidic solutions or through basic redox reactions with the change in pH. The first three fractions of Tessier's sequential extraction method, F1, F2, and F3, contain examples of such metals. Based on the absolute and relative amount of metal fractions that are loosely attached to the soil components, metal mobility in the soil matrix can be ascertained. Equation (30) was used to calculate the metal mobility index as a "mobility factor" as given below (Narwal et al., 1999)

$$MF = \frac{(F1 + F2 + F3) \times 100}{F1 + F2 + F3 + F4 + F5} \quad (30)$$

where,

F4= Fraction 4

F5= Fraction 5

The level of risk based on the type of metal, chemical species, and ecological risk is denoted by the Risk assessment code (RAC). RAC determines the availability of metals in sediments and soils by considering the metal in the carbonate and exchangeable fractions (%) (Amini et al., 2024). If the percentage of metal in carbonate and exchangeable fraction is <1, then it is considered as no risk; 1-10 is low risk, 11-30 is medium risk, 31-50 is high risk, and >50 is very high risk. The RAC is calculated as given in equation (31) (Kabata-Pendias, 1984):

$$RAC = \frac{(F1 + F2) \times 100}{F1 + F2 + F3 + F4 + F5} \quad (31)$$

Chapter 4

SEASONAL CHARACTERIZATION OF MSW

4.1 PHYSICAL COMPOSITION OF FRESH MSW AND LEGACY WASTE

The MSW of Boragaon dumpsite includes paper/cardboard, plastic, rubber, leather, glass, metal, inert (street sweepings, stones, soil, and construction and demolition waste), and biodegradable wastes (vegetable peels, leaves, wood, tree branches, coconut husk, shells) as shown in Fig. 4.1. The legacy waste mostly consists of plastics, textiles, and inert waste. The proportion of plastic waste in the MSW was highest during the monsoon season (34.18%) and slightly lower in both the pre-monsoon (30.74%) and post-monsoon (32.46%) season periods, as shown in Fig. 4.1 (a). The paper/cardboard fraction remained relatively consistent across the different seasons. The rubber/leather fraction sees a decrease during the monsoon season (0.50%) and an increase during the post-monsoon (0.83%) period. The proportion of clothes in MSW remains relatively stable, with a slight decrease during the monsoon season (10.59%). The inert fraction decreases during the monsoon season (17.65%) and slightly increases during the post-monsoon (15.72%) period. The biodegradable and glass/metal fractions remain relatively consistent, with a slight increase during the monsoon season (37.38% and 0.78%, respectively). These prepared samples were then used for physicochemical analysis to check the feasibility of the samples for pyrolysis.

In legacy waste, the plastic fraction constitutes the major proportion and remains relatively consistent throughout the seasons, as shown in Fig. 4.1 (b). The paper/cardboard fraction is minimal but experiences slight fluctuations across the seasons. The rubber/leather fraction shows some variation, with a peak during the monsoon season. The proportion of clothes in the legacy waste remains relatively stable, with a slight increase during the monsoon season. The inert fraction shows variations across the seasons, with a decrease during the monsoon season and an increase during the post-monsoon period. The biodegradable fraction is minimal and almost negligible, except for a slight increase during the monsoon season. The

glass/metal fraction experiences fluctuations, with a notable decrease during the monsoon season.

The overall data provides insight into how the composition of different waste fractions within MSW and legacy waste changes during different seasons. From the study, it was observed that plastic, clothes, and inert materials are the most prominent components of this waste category, while other fractions, such as paper/cardboard, rubber/leather, and glass/metal, exhibit varying levels of presence with some seasonal fluctuations. The negligible presence of biodegradable waste in this context is also noteworthy, whereas most of the studies have reported with higher percentage composition of biodegradable waste, followed by paper, cardboard, and plastic waste (Singhal et al., 2022). Therefore, the coexistence of mixed flammable, biodegradable, textile, and inert waste within MSW can undergo thermal treatment following the segregation of metal/glass components, resulting in the production of energy resources. In contrast, the predominance of the combustible portion in legacy waste indicates the potential use of waste with limited preliminary processing and sorting. This investigation into physical composition examined the viability of employing MSW and legacy waste as a solid fuel in thermochemical procedures, providing an alternative approach to waste management. Additionally, it aimed to spark innovation in finding alternative avenues for utilizing rejected waste, thereby extending landfill lifespans, promoting circular economy principles, and considering the socio-environmental responsibilities associated with waste generation.

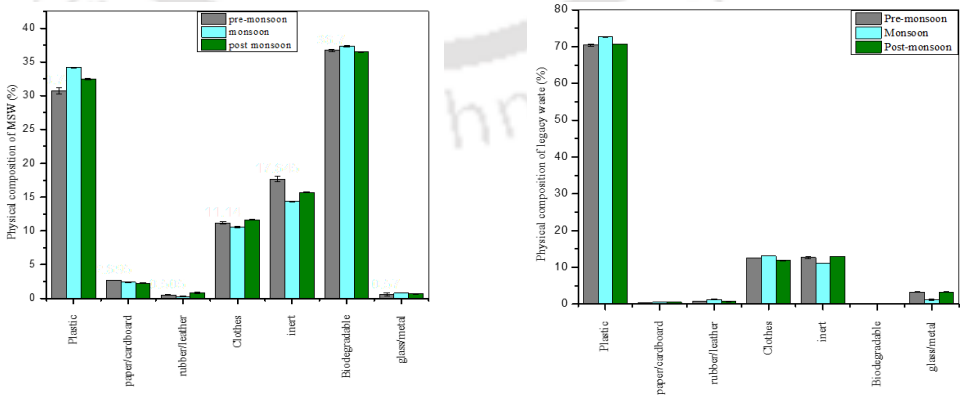

(a) (b)

Fig. 4.1. Physical composition (%) of (a) MSW and (b) legacy waste

4.2 RESULT OF PROXIMATE ANALYSIS

The moisture content in different categories of MSW, namely plastics, paper/cardboard, rubber/leather/clothes, and inert and biodegradable waste, were analyzed for characterization, as shown in Table 4.1. The plastic portion within MSW exhibited low moisture content because plastics are hydrophobic, a characteristic stemming from the lower surface tension of their components compared to that of water (Tiburcio et al., 2021). The inert portion of MSW comprises street sweepings, soil, sand, construction and demolition waste, and pebbles. Inert waste typically accumulates with fresh MSW, including clothes, paper/cardboard, and organic waste, absorbing the moisture from other waste fractions. As a result, the moisture level in the inert section of newly generated MSW surpasses that found in the organic waste portion.

Table 4.1. Proximate analysis of individual fractions of MSW

Fraction	**Total moisture content (wt. %, wet basis)**	**Ash content (wt. %, dry basis)**	**Volatile matter (wt. %, dry basis)**	**Fixed Carbon (wt. %, dry basis)**
Plastic	1.11 ± 0.02 [a]	3.49 ± 1.06 [a]	32.23 ± 14.39 [a]	25.16 ± 11.25 [a]
Paper/cardboard	14.11 ± 0.05 [a]	13.87 ± 0.16 [b]	32.35 ± 9.25 [a]	27.34 ± 7.31 [a]
Rubber/leather/ clothes	8.24 ± 0.13 [a]	7.79 ± 0.23 [a, b]	30.19 ± 11.21 [a]	26.23 ± 8.53 [a]
Inert	33.40 ± 0.54 [a]	26.40 ± 3.14 [c]	27.98 ± 2.18 [a]	24.99 ± 2.25 [a]
Biodegradable waste	20.28 ± 0.20 [a]	11.59 ± 3.89 [a, b]	32.61 ± 10.81 [a]	24.99 ± 8.92 [a]

[*]Using the Tukey test, different letters show significant variation, $p<0.05$.

As depicted in Table 4.2, the variation in the range of moisture, ash content, volatile matter, and fixed carbon values illustrates the diverse product compositions present in the fractions of MSW, influenced by seasonal changes. During the pre-monsoon period, there was an 83.84% reduction in moisture content across the sample years. This decrease was primarily attributed to the degradation of the fresh organic waste fraction within MSW over time. Conversely, in the monsoon season, the moisture

content of the newly generated waste sample rose significantly to 51.09%, markedly surpassing the moisture content of the fresh waste (8.29%) collected in the pre-monsoon period. However, the moisture content also displayed a decline as the waste aged during the monsoon season. A similar pattern was observed for waste collection in the post-monsoon season, where the moisture content of the freshly collected waste was 30.26%, which was much lower than that of studies that have reported a moisture content of 65% during the post-monsoon season (Singhal et al., 2022). Notably, the moisture content from fresh waste to legacy waste exhibited a substantial decrease of 89.59%.

The trend in the ash content of the MSW was varying during the pre-monsoon season mainly due to its more variation in the waste collected from different locations. The percentage of ash content was less in the range of 4.42 to 7.12% compared to monsoon (9.04 to 26.7%) and post-monsoon season (8.76 to 25.05%). Higher ash content results in the corrosion of the reactor and affects the radiative heat transfer (Patumsawad et al., 2002). Also, high ash content results in a slow heating rate, which is favorable for char production, but the quantity of char yield will be less. High ash content results in the disturbance of the combustion process, resulting in higher emissions of CO (Verla et al., 2012). The higher ash content also reduces the sample's calorific value and combustion efficiency (Verla et al., 2012). So, the MSW collected during the pre-monsoon season is preferable for pyrolysis technology due to low ash content for a high char yield.

The percentage of volatile matter during the pre-monsoon season was 53.23 to 64.64%, much higher than that of the MSW sample collected during monsoon and post-monsoon season, which was in the range of 41.24 to 22.13% and 47.37 to 59.25%, respectively. In the present study, the percentage of volatile matter was comparatively lower than that of a similar study which reported volatile matter of 79.5% (Singhal et al., 2022). The higher volatile matter of the sample for pyrolysis indicates more formation of pyrolysis oil. It reduces the time of ignition required for combustion and char production (Suriapparao et al., 2015).

The proportion of fixed carbon directly influences the quantity of char obtained from pyrolysis. A greater fixed carbon percentage corresponds to increased char

production (Charvet et al., 2021). In the pre-monsoon period, the fixed carbon content of MSW and legacy waste (13 years old) was 20.06 and 40.87%, respectively, which is quite comparable to the waste collected in the monsoon season, measuring 10.19% and 44.87%, respectively. The results of the proximate analysis of MSW and legacy waste were not similar and comparable with other available studies conducted on the characterization of MSW in Guwahati city. The current study suggests that the MSW and legacy waste collected during the pre-monsoon seasons and legacy waste collected during the monsoon period are suitable for char production through pyrolysis.

Table 4.2. Proximate analysis of mixed MSW sample during pre-monsoon, monsoon, and post-monsoon season from 10 locations.

Age of waste collected from different locations	**Moisture content (%)**	**Ash content (%)**	**Volatile matter (%)**	**Fixed carbon (%)**
		Pre-monsoon season		
0 day	8.29 ± 0.16^{a}	6.84 ± 0.66^{a}	64.64 ± 0.06	20.23 ± 0.16^{a}
7 days	8.13 ± 0.15^{a}	6.82 ± 0.60^{a}	63.37 ± 1.21	20.68 ± 0.14^{b}
6 months	8.16 ± 0.21^{a}	7.05 ± 0.51^{a}	64.73 ± 0.71	20.06 ± 0.22^{a}
1 year	8.24 ± 0.16^{a}	7.17 ± 0.48^{a}	63.66 ± 0.40	$20.93 \pm 0.14^{a, b, c}$
3 years	5.55 ± 0.24^{b}	5.94 ± 0.22^{a}	64.15 ± 0.19	24.36 ± 0.24^{d}
4 years	$5.15 \pm 0.15^{c, b}$	5.76 ± 0.28^{a}	63.68 ± 0.20	25.41 ± 0.21^{e}
7 years	3.40 ± 0.22^{d}	5.12 ± 0.78^{a}	62.69 ± 0.41	28.52 ± 0.15^{f}
8 years	$3.46 \pm 0.25^{e, d}$	5.47 ± 0.92^{a}	53.23 ± 0.24	37.84 ± 0.20^{g}
10 years	2.39 ± 0.21^{f}	5.01 ± 1.18^{a}	53.39 ± 0.48	$39.21 \pm 0.22^{h, f}$
13 years	1.34 ± 0.18^{g}	4.42 ± 1.38^{a}	53.37 ± 0.42	40.87 ± 0.18^{i}
		Monsoon season		
0 day	51.09 ± 0.12^{a}	9.04 ± 0.21^{a}	29.65 ± 0.17^{a}	10.19 ± 0.03^{a}
7 days	50.29 ± 0.07^{a}	10.02 ± 0.16^{a}	28.94 ± 0.09^{a}	10.69 ± 0.06^{a}
6 months	32.33 ± 0.09^{a}	11.16 ± 0.59^{a}	28.16 ± 0.1^{b}	28.40 ± 0.05^{b}
1 year	30.30 ± 0.13^{a}	13.19 ± 0.41^{b}	26.31 ± 0.09^{c}	30.33 ± 0.13^{c}

3 years	25.44 ± 0.21 [a]	14.55 ± 0.23 [c, b]	25.22 ± 0.01 [d]	34.68 ± 0.12 [d]
4 years	23.38 ± 0.14 [a]	15.25 ± 0.21 [d, c, b]	24.62 ± 0.34 [e, d]	36.86 ± 0.11 [e]
7 years	13.50 ± 0.19 [a]	19.12 ± 0.15 [e]	41.24 ± 0.21 [f]	26.10 ± 0.05 [f]
8 years	11.85 ± 0.11 [a]	19.97 ± 0.19 [f, e]	39.7 ± 0.14 [g]	28.36 ± 0.12 [g]
10 years	10.66 ± 0.06 [a]	20.68 ± 0.13 [g]	36.08 ± 0.12 [h]	43.58 ± 0.15 [h]
13 years	6.30 ± 0.02 [a]	26.70 ± 0.04 [h]	22.13 ± 0.13 [i, h]	44.87 ± 0.17 [i]
Post-monsoon season				
0 day	30.26 ± 0.22 [a]	8.76 ±0.13 [a]	59.25 ± 0.26 [a]	1.53 ± 0.08 [a]
7 days	22.51 ± 0.26 [b]	16.77 ±0.21 [a]	57.59 ± 0.16 [b]	3.14 ± 0.62 [a]
6 months	15.65 ± 0.37 [c]	18.17 ±0.14 [b]	55.03 ± 0.16 [c]	11.16 ± 0.07 [b]
1 year	10.43 ± 0.19 [d]	19.52 ±0.26 [c]	54.75 ± 0.19 [d, c]	14.80 ± 0.40 [c]
3 years	9.85 ± 0.18 [e, f]	21.94 ±0.22 [d]	53.53 ± 0.25 [e]	14.69 ± 0.29 [d, c]
4 years	8.42 ± 0.15 [f]	20.59 ± 0.26 [e, c]	51.50 ± 0.23 [f]	19.50 ± 0.17 [e]
7 years	5.87 ± 0.11 [g]	24.86 ± 0.19 [f]	49.43 ± 0.21 [g]	20.10 ± 0.34 [f, e]
8 years	5.35 ± 0.12 [h, g]	24.14 ± 0.24 [g, f]	49.30 ± 0.14 [h, g]	21.23 ± 0.22 [g, e, f]
10 years	4.87 ± 0.20 [i, g, h]	24.28 ± 0.31 [h, f, g]	48.37 ± 0.23 [i, h, g]	22.50 ± 0.12 [h, g, e, f]
13 years	3.15 ± 0.12 [j]	25.05 ± 0.29 [i, f, g, h]	47.37 ± 0.20 [j, i, h, g]	24.44 ± 0.36 [h]

*Using the Tukey test, different letters show significant variation, $p<0.05$.

4.3 TANNER DIAGRAM

The evaluation of the combustion process of incinerated solid waste was proposed by Tanner, (1965) by correlating the moisture, ash, and combustible material contents. The Tanner diagram, as shown in Fig. 4.2, was used to evaluate the potential of various types of waste for pyrolysis without requiring auxiliary fuel. The data obtained from proximate analysis of MSW during pre-monsoon, monsoon, and post-monsoon season was plotted in the Tanner diagram. It was found that the pre-monsoon MSW sample was the most potent fuel for pyrolysis, followed by post monsoon sample because the moisture content was <50%, ash content <60%, and combustible material >25%, which were within Tanner's limits as shown in Fig. 4.2 (a), (b) and (c).

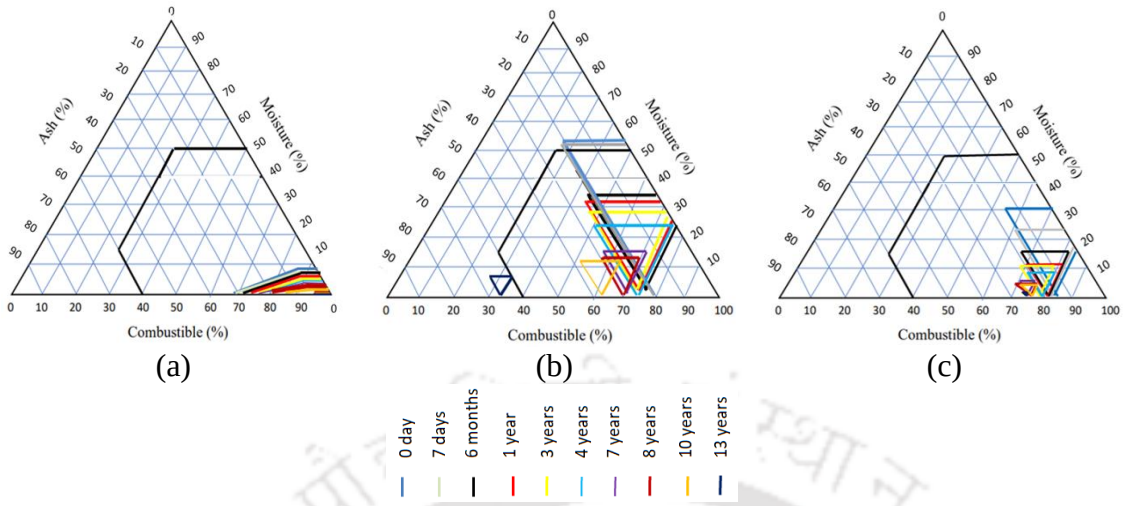

Fig. 4.2. Tanner diagram of MSW correlating between moisture, ash, and combustible content (%) during (a) pre-monsoon, (b) monsoon, and (c) post-monsoon season

4.4 ULTIMATE ANALYSIS AND CALORIFIC VALUE

The comprehensive examination of MSW and legacy waste collected in the pre-monsoon period revealed that carbon and oxygen were the predominant elements in both samples, while nitrogen and sulfur content were relatively low. This implies that NO_x and SO_x emissions from the combustion of MSW could be low (Moroń and Rybak, 2015). In the case of legacy waste, it was found that the percentage of carbon was higher than that in mixed MSW. This data is critical for designing the treatment of flue gas and recirculation systems in pyrolizers (Moroń and Rybak, 2015). The sulfur content is due to the combustible fraction constituted in the MSW and legacy waste (Eze et al., 2021). The plastics investigated in this research were sourced from practical applications, differing from pure polymer, and could potentially contain additives within the samples. The MSW samples tested include 70.59% carbon and 11.96% hydrogen, while the legacy samples have 78.37% carbon and 11.7% hydrogen, which was comparatively higher than that of similar studies reported for MSW (Singhal et al., 2022). Such qualities enabled effective pyrolysis and the production of high-quality solid residue char.

The elevated nitrogen content found in legacy waste compared to MSW can lead to a decline in oxygen and carbon dioxide levels (Deng et al., 2017). The H/C

ratio indicates the aromaticity and stability and O/C indicates the aging of the sample. The study found that both H/C and O/C molecular ratios for MSW are higher than legacy waste. The H and O-containing functional group in MSW vanishes with the increase in the aging of waste due to decarboxylated dehydrogenation (Wang et al., 2021). The molecular ratio of H/C in MSW and legacy waste was 2.03 and 1.79, respectively, while the O/C ratio of MSW compared to legacy waste decreased from 0.11 to 0.04. The higher H/C ratio observed in MSW signifies the presence of aromatic organic components, which tend to exhibit biological instability, whereas the opposite holds for legacy waste (Yang et al., 2007). The decline in the O/C ratio from MSW to legacy waste indicates the degradation of carbon compounds and also serves as an indicator of waste half-life, with a half-life exceeding 1000 years when the O/C value is <0.2. Both MSW and legacy waste exhibit an O/C molecular ratio of less than 0.2, suggesting the non-biodegradability in the landfill (Wang et al., 2021).

The heating value assessment of the samples collected in the pre-monsoon season was conducted both theoretically (Kalivodová et al., 2022) and instrumentally, as outlined in Table 4.3. The heating value of legacy waste surpassed that of MSW due to its higher carbon content and lower moisture levels. The diminished heating value of MSW can be attributed to its heterogeneous composition, which possesses elevated moisture and ash content. In contrast, legacy waste is unsuitable for recycling but holds promise as a potential pyrolysis feedstock, given its low moisture content and high heating value as compared to MSW characterization reported by other studies (Chiemchaisri et al., 2010; Singhal et al., 2022).

Table 4.3. Ultimate analysis and calorific value of MSW and legacy waste

Analysis	**Sample**	
	MSW	**Legacy waste**
C (%)	70.59 ± 0.01	78.37 ± 0.13
H (%)	11.96 ± 0.08	11.7 ± 0.09
N (%)	0.15 ± 0.04	0.86 ± 0.03

S (%)	4.47 ± 0.25	0.30 ± 0.01
O (%)	10.83 ± 0.57	4.35 ± 0.49
H/C	2.03 ± 0.01	1.79 ± 0.02
O/C	0.11 ± 0.01	0.04 ± 0.00
Lower Heating Value (LHV) (kJ/kg)	34903.89 ± 11.75	37835.14 ± 15.85
High Heating Value (HHV) (kJ/kg)	37717.89 ± 11.1	40432.84 ± 4.42
Instrumental Heating Value ($HHV_{instrumental}$) (kJ/kg)	35216.82 ± 6.27	39812.13 ± 7.58

4.5 BIOCHEMICAL ANALYSIS OF MSW

The biochemical analysis of the mixed MSW and legacy waste collected during the pre-monsoon season is shown in Table 4.4. A higher percentage of lignin content indicates high char production and a high percentage of hemicellulose and cellulose content signifies a high pyrolysis oil yield (Rangabhashiyam et al., 2019). The percentage of lignin content of the MSW sample collected was higher (47.6%) than that of hemicellulose (13.4%) and cellulose content (24.12%) as compared to most of the lignocellulosic biomass (Rangabhashiyam et al., 2019). This study shows that the MSW sample can be a potential feedstock for char production through pyrolysis. Similarly, the percentage of lignin content (44.16%) in the legacy waste also reveals the feasibility of char production.

According to the linear correlation between absorbance and gas concentration, as stated by Beer-Lambert's law, it is possible to ascertain the gas production resulting from the thermal degradation of both MSW and legacy waste. Typically, the degradation of cellulose and hemicellulose leads to the creation of carbonyl groups, which in turn gives rise to the production of CO and CO_2 (Yang et al., 2007). There is also a likelihood that cellulose generates increased CO through secondary reactions involving primary volatiles and the breaking of aldehyde groups (Pasangulapati et al., 2012). In contrast, the breakdown of lignin has been linked to the generation of methane due to the fragmentation of the methoxy groups in the lignin molecule (Yang et al., 2007). Therefore, a higher presence of lignin in

MSW compared to legacy waste results in a considerably elevated emission of methane gas.

Table 4.4. Biochemical constituent of MSW and legacy waste

Biochemical constituent	Percentage composition (%)	
	MSW (%)	Legacy waste (%)
Extractive	8.21 ± 0.27	7.47 ± 0.21
Hemicellulose	13.4 ± 0.45	14.66 ± 0.89
Lignin	47.6 ± 0.66	44.16 ± 0.45
Cellulose	24.12 ± 0.33	13.63 ± 1.06

4.6 BULK DENSITY AND POROSITY

The bulk density of the MSW and legacy waste sample was determined by ASTM D 1895 and was found to be 132.05 and 95.78 kg/m^3, respectively. The bulk density helps determine the space requirement for storing the feeding material. The quantity of feedstock that can be fed inside the pyrolysis reactor can be determined through bulk density (Shrivastava et al., 2023). The porosity of MSW and legacy was 59.16 and 61.11%.

4.7 THERMOGRAVIMETRIC AND DERIVATIVE THERMOGRAVIMETRIC ANALYSIS

Fig. 4.3 (a) and (b) depict the thermogravimetric (TG) and derivative thermogravimetry (DTG) analyses of both MSW and legacy waste, respectively. These curves were utilized to determine various parameters such as the maximum rate of pyrolysis, initial temperature, peak temperature, termination temperature, rate of weight loss during the reaction, and other pertinent values, extensively detailed in Table 5. The point where the tangent intersects the horizontal curve on the TG graph aligns with the peak on the DTG curve. The initial temperature is identified as the point where the tangent line meets the flat horizontal curve line (Lin et al., 2014). The termination temperature was identified as the temperature at which the mass loss reached 68% for MSW and 82% of the overall quality loss for legacy waste (Mu et al., 2015), also representing the temperature at the peak mass loss rate in the DTG curves, outlining the three distinct pyrolysis phases for both

waste types. The initial stage involves eliminating water content between room temperature and 100°C. Stage II shows the MSW sample undergoing thermal degradation between approximately 240 and 310°C, while for legacy waste, thermal degradation occurs between 100 and 370°C, accounting for about 10% of the total quality loss. The third stage (stage III) involves char combustion, occurring around 315 to 425°C for MSW and 220 to 360°C for legacy waste. Considering that MSW, excluding plastics, mainly comprises biomass components such as cellulose, hemicellulose, and lignin (Zhou et al., 2015a), plastic components contain higher levels of chlorine and hydrocarbon content (Li et al., 2005). Hemicellulose decomposition happens within the range of 198 to 398°C, rapid cellulose decomposition occurs between 300 to 350°C, and lignin decomposition transpires approximately within the range of 410 and 540°C (Fisher et al., 2002). Chlorine is released between 220 to 380°C, while hydrocarbon degradation starts at temperatures ranging from 380 to 550°C (Fisher et al., 2002).

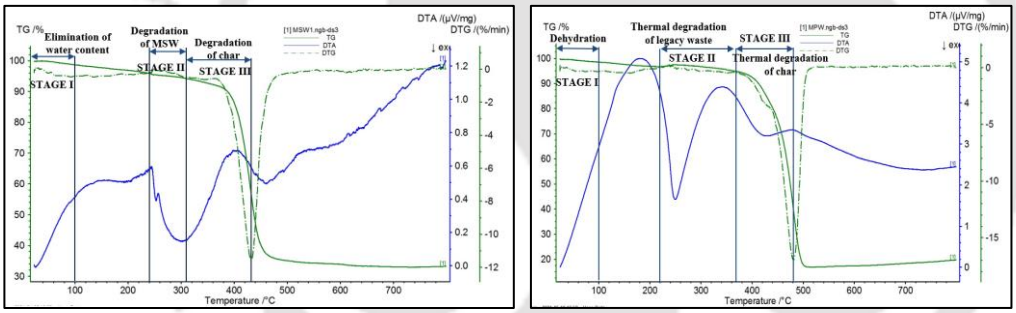

(a) (b)

Fig. 4.3. Thermogravimetric and derivative thermogravimetric analysis of (a) MSW and (b) Legacy waste

4.8 KINETIC STUDY THROUGH ARRHENIUS KINETIC MODEL AND THERMODYNAMIC ANALYSIS

The Arrhenius plot of MSW and legacy waste sample showed a linear correlation between log k and 1/T, where the r value for MSW and legacy waste was 0.9862 and 0.9603, respectively, as shown in Fig. 4.4. According to Evans correlation guide, if the r value is more significant than 0.8, it is considered a 'very strong' correlation. But this linearity disappears when the r value ranges from

0.0245 to 0.5753, indicating a 'very weak' to 'moderate' correlation as per Evans classification.

The results of the thermodynamic analysis are illustrated in Table 4.5. The activation energy of the analyzed MSW and legacy waste sample was lower, about 5.72 and 14.96 kJ/mol, respectively, than that of fossil fuel like coal, which has an activation energy of about 128–140 kJ/mol (Khare et al., 2014). The lower activation energy of the sample indicates a higher reaction rate. This also depicts that the energy required for thermal processing of MSW is lower than that of legacy waste. It is beneficial for pyrolysis from an energy conservation point of view but poses a risk of fire hazards at the elevated landfill temperature. Enthalpy changes (ΔH) for the kinetic model under investigation were positive, demonstrating the necessity for external energy for the system for the reactants to enter a transition state. It was observed that the potential energy barrier between ΔE_a and ΔH in the case of legacy waste was considerably smaller (5.42 kJ/mol) than MSW (113.86 kJ/mol), indicating the production of activated complexes and the reactions will proceed more quickly (Kaur et al., 2018). The value of Gibb's free energy denotes the useful energy available from the sample to perform the work and convert it into an activated complex (Song et al., 2019). It also indicates how favorable a chemical reaction is, whether spontaneous (when $\Delta G<0$) or non-spontaneous (when $\Delta G>0$), according to the first and second laws of thermodynamics (Liu et al., 2022). The MSW sample has a higher ΔG value (170.37 kJ/mol) than legacy waste (2.45 kJ/mol), indicating that the reactions are spontaneous and more useful energy is available for thermal conversion of MSW to valuable products than legacy waste. The range of ΔG value for MSW was within the range of lignocellulosic biomass (Song et al., 2019). Thermal cracking was explored using positive and negative entropy (ΔS) values, and positive ΔS values of legacy wastes show that the decomposition processes are not spontaneous, indicating that the material underwent some physical and chemical changes (Kaur et al., 2018). The negative ΔS value of MSW indicated that the sample was faster in attaining its thermodynamic equilibrium because of its high reactivity and easier generation of the activated complex.

The preexponential factor (A) of MSW and legacy waste $<10^9$, suggested the possibility of a process involving highly branched and linear molecules. The thermal cracking of legacy waste exhibits the highest value of A, which indicates the highest value of E_a, leading to a slower and more challenging degradation (Bhardwaj et al., 2021). From the thermodynamic study of the MSW and legacy waste, it can be deduced that these wastes in the landfill can be used as potential feedstock for pyrolysis with product (char, pyrolysis oil, and gas) valorization.

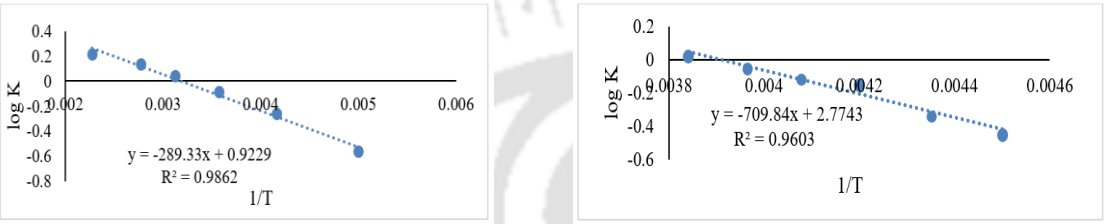

(a) (b)

Fig. 4.4. Arrhenius plot of (a) MSW and (b) legacy waste

Table 4.5. Combustion parameters and thermodynamic analysis determined from TG/DTG profile

Thermodynamic parameter	**Sample**	
	MSW	**Legacy waste**
T_i (°C)	240	240
T_α (°C)	400	380
T_b (°C)	620	500
T_m (°C)	430	480
R_{max} (%/min)	11.5	17
t_b (min)	48.3	50
Total weight loss (%)	68	82
Activation energy (ΔE_a) (kJ/mol)	5.71	14.96
Enthalpy (ΔH) (kJ/mol)	119.57	9.54
Gibb's Free Energy (ΔG) (kJ/mol)	170.37	2.45
Entropy (ΔS) (kJ/mol)	-0.072	0.009
Preexponential factor, A (s^{-1})	8.54×10^1	1.16×10^3

***T_b** is the burn-out temperature, R_{max} is the maximum rate of weight loss, and t_b is burn-out time.

The physical composition analysis of both MSW and legacy waste indicated that the proportion of biodegradable waste was considerably lower in legacy waste due to degradation with time. The elevated percentage of dry combustible materials in both MSW and legacy waste suggests the potential for thermal treatment, such as incineration and gasification. However, in the current unsegregated condition of waste and considering environmental concerns related to flue gas emissions and high energy consumption, this treatment method is not advisable. Pyrolysis stands out as a significant technology for managing unsegregated dry waste, offering opportunities for waste-to-wealth initiatives and addressing energy consumption and environmental concerns.

In many developing countries, waste is typically segregated as dry and wet. The sub-segregation of the dry waste poses significant challenges. The non-combustible fraction of dry waste can be segregated within the dumpsite at a large scale. For the unsegregated combustible dry waste, decentralized pyrolysis presents a viable option for treatment. The uniqueness of the pyrolysis technology is its ability to operate with samples from any season for the production of char, oil, and gas. The MSW can be fed into a pyrolizer without the need for segregation and grinding. Nowadays, pyrolysis technology is used in many industrial applications for producing charcoal, activated carbon, and methanol. It curbs gas emissions arising from landfills and dumpsites, lessens pollution, and emerges as a promising avenue for waste valorization. The resultant pyrolysis products, such as char and syngas, serve as readily usable and marketable fuels. Particularly, polymer materials present in mixed MSW yield high-quality bio-oil, suitable for employment as liquid fuel and chemicals. The char generated through MSW pyrolysis also holds potential as fertilizer, soil conditioner, and activated carbon. Therefore, considering the heterogeneous composition of MSW, the prospect of energy production, the generation of value-added materials through pyrolysis, environmental compatibility, and economic viability, pyrolysis stands as an innovative avenue to effectively tackle the MSW disposal predicament.

4.9 CONCLUSION FROM THE MSW CHARACTERIZATION STUDY

The critical findings of this study indicate that pyrolysis shows promise for managing MSW and legacy waste, aiding resource recovery, and aligning with the Tanner diagram for direct energy recovery. The high heating value of MSW suggests suitability as a solid fuel, given its higher bulk density for easier transportation. TGA indicates MSW's lower mass loss than legacy waste at increasing temperatures. Lower activation energy, positive enthalpy, and Gibb's free energy signify faster reactions and increased available energy. Despite limited adoption in India, pyrolysis emerges as a cleaner alternative, evolving "third generation" technologies and offering commercialized fuel options to reduce landfill emissions.

Chapter 5

OPERATION OF THE PYROLIZER

5.1 PRODUCT YIELD FROM PYROLYSIS OF MSW ACCORDING TO EXPERIMENTAL SETUP OF CCD

Table 5.1 displays the results of the pyrolysis responses. The development of regression equations and the ANOVA for char, pyrolysis oil, and gas yields were discussed. To show the impact of process factors during pyrolysis, parametric studies of all responses were thoroughly discussed.

Table 5.1. CCD experimental arrangement for pyrolysis of MSW

Std	**Factor 1** **A:Temperature** °C	**Factor 2** **B:Heating rate** (°C/min)	**Factor 3** **C:Feed particle size** (mm)	**Factor 4** **D:Residence time** (min)	**Response 1** **Char** (%)	**Response 2** **Pyrolysis oil** (%)	**Response 3** **Gas** (%)
1	250	10	5	30	56.71	37.23	6.06
2	550	10	5	30	37.47	14.79	47.74
3	250	40	5	30	62.06	25.17	12.77
4	550	40	5	30	24.28	20.67	45.05
5	250	10	50	30	64.21	13.76	22.03
6	550	10	50	30	38.87	13.86	47.27
7	250	40	50	30	66.91	22.22	10.87
8	550	40	50	30	36.77	14.12	49.11
9	250	10	5	180	67.13	12.36	20.51
10	550	10	5	180	33.32	15.71	50.97
11	250	40	5	180	68.26	18.55	13.19
12	550	40	5	180	17.76	14.03	68.21
13	250	10	50	180	72.97	3.81	23.22
14	550	10	50	180	34.64	14.13	51.23
15	250	40	50	180	70.18	9.89	19.93
16	550	40	50	180	35.43	14.55	50.02
17	250	25	27.5	105	65.21	15.68	19.11
18	550	25	27.5	105	22.22	16.02	61.76
19	400	10	27.5	105	49.02	15.11	35.87
20	400	40	27.5	105	47.17	15.25	37.58
21	400	25	5	105	38.25	25.67	36.08
22	400	25	50	105	51.67	14.18	34.15
23	400	25	27.5	30	52.98	15.22	31.8
24	400	25	27.5	180	47.16	14.76	38.08
25	400	25	27.5	105	49.66	15.77	34.57
26	400	40	27.5	180	47.02	15.25	37.73
27	400	40	27.5	30	52.43	14.28	33.29
28	400	10	27.5	30	52.05	15.11	32.84
29	400	10	27.5	180	47.54	15.63	36.83
30	400	40	5	105	44.28	14.8	40.92
31	400	40	50	105	51.32	14.21	34.47

5.2 ANOVA FOR QUADRATIC MODEL FOR CHAR YIELD

Using CCD, a link was formed between the actual values of the parameters (A, B, C, and D) and responses and the char yield (%) throughout the pyrolysis process. ANOVA was utilized to assess a suitable model, and it was discovered that the quadratic model best matched the empirical values. The following equation (31) displays the regression equation for char production as a function of coded process parameters:

$$\text{Char (\%)} = 48.64 - 17.39\,A - 1.48\,B + 4.08\,C - 0.5195\,D \quad (31)$$

A is the operating temperature, B is the rate of heat, C is the feed particle size, and D is the residence time. ANOVA was performed to determine how operational conditions affect char yield, as shown in Table 5.2. A p-value of <0.0001 from ANOVA indicated that each process parameter was statistically significant. The operating temperature for pyrolysis was the most influential variable for achieving the highest char yield based on the F-value derived from ANOVA. The p-value was <0.0001, showing the model is statistically significant.

Table 5.2. ANOVA for Quadratic model **(**Response 1: Char)

Source	**Sum of Squares**	**df**	**Mean Square**	**F-value**	**p-value**	
Model	5835.64	4	1458.91	82.15	< 0.0001	significant
A-Temperature	5445.16	1	5445.16	306.62	< 0.0001	
B-Heating rate	52.03	1	52.03	2.93	0.0989	
C-Feed particle size	332.52	1	332.52	18.72	0.0002	
D-Residence time	5.94	1	5.94	0.3344	0.5681	
Residual	461.72	26	17.76			
Cor Total	6297.37	30				

The order of impact of the four operational parameters on the model for maximum char yield was operating temperature (A) > feed particle size (C) > rate of heat (B) > residence time (D). The p-values for temperature (A) and feed particle size were <0.05, indicating that the independent parameters were significant. F-value typically illustrates the effects of operating parameters on the responses, whereas the p-value denotes the model's validity (Shahbaz et al., 2017). The

operating temperature (A) has the highest F-value of 306.62. So, factor A was considered the most influential parameter among all values for the significant factors from ANOVA for maximum char production.

Fig. 5.1 shows the surface plot, demonstrating how operational factors affected char production. From Fig. 5.1 (a), it can be seen that char yield increased to about 72.97% at the lowest operating temperature of 250°C and a heat rate of 10°C/min, the feed particle size of 50 mm, and a residence time of 180 min. It decreased to approximately 17.76% with a further increase of pyrolysis operating temperature at 550°C and an increase in rate of heat of 40°C/min. Fig. 5.1 (b) shows the interaction between factor A and factor C on char yield. The percentage char yield was highest at the lowest temperature of 250°C and the largest feed particle size of 50 mm. The F-value was the largest for factor A, which signifies that residence time was the most influential operating parameter and feed particle size was the second most influential parameter to char production. The interaction between factors A and D, B and C, B, and D, and C and D shows a significant effect on char yield, as shown in Fig. 5.1. The char yield also showed a corresponding trend with rising operating temperature, feed particle size, rate of heat, and residence time. The percentage of char yield decreased with the increase in operating temperature, rate of heat, and residence time. However, the percentage of char yield was increased with the increase in feed particle size at low operating temperature (250°C), rate of heat (10°C/min), and residence time (180 mins). A similar trend was observed with Mohamed et al. (2014) and Kasim et al. (2018), which reported that temperature and time were the most influential variables for pyrolysis product yield. The multiple phases of lignocellulosic material breakdown may account for the decrease in the proportion of char yield and the rise in gas yield with rising operating temperature. Hemicellulose and cellulose begin to break down at temperatures <400°C to produce light volatile compounds, whereas lignin breaks down at temperatures >400°C, producing a more significant char production at lower working temperatures (Sembiring et al., 2015). The results of this investigation may be explained by the fact that pyrolysis vapour cracked at high temperatures and

that, under these operating circumstances, the severity of the cracking was higher (Ruengvilairat et al., 2012).

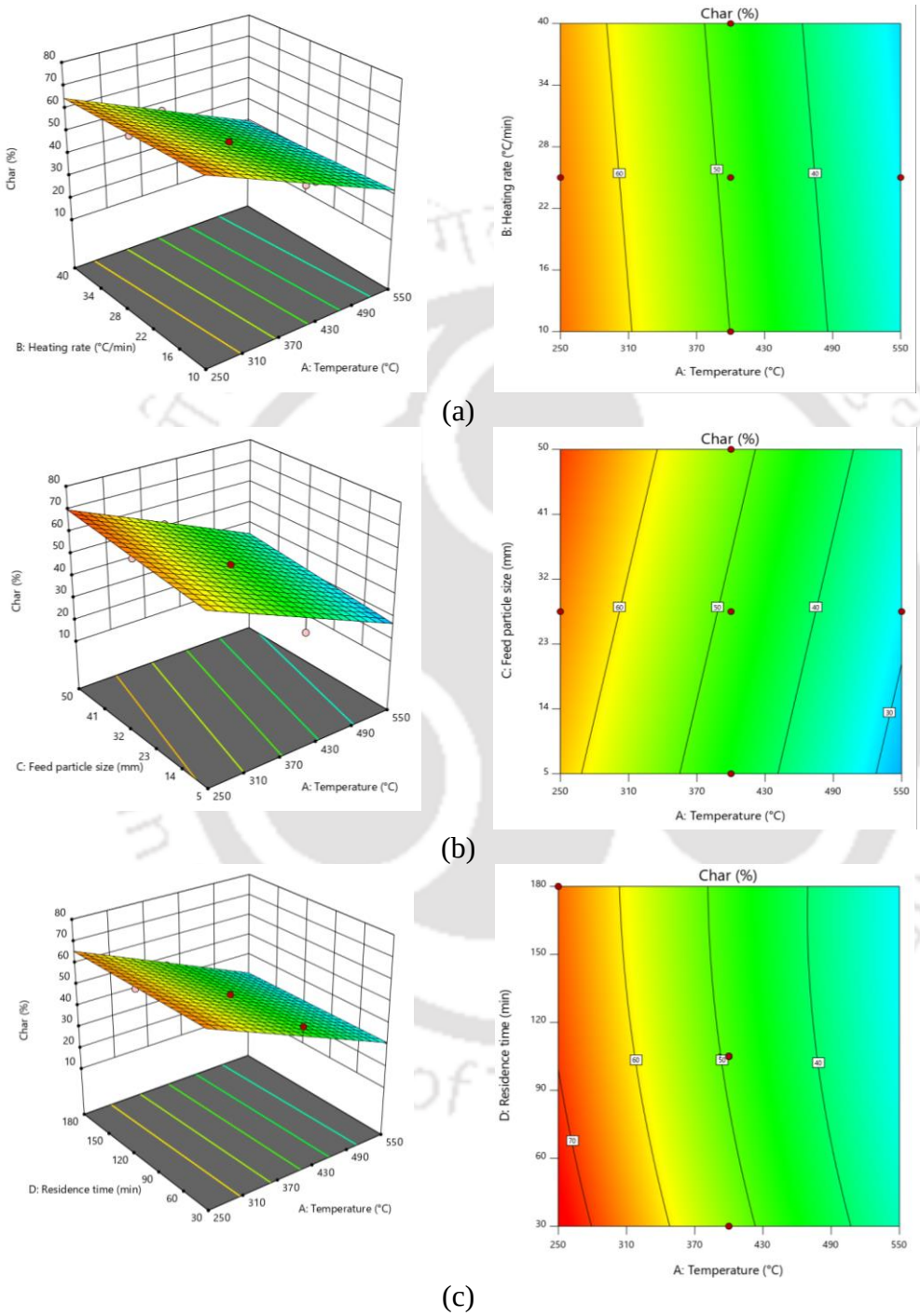

Fig. 5.1. Surface plot of char yield and the following factors: (a) temperature and rate of heat; (b) temperature and feed particle size (c) temperature and residence time

5.3 ANOVA FOR QUADRATIC MODEL FOR PYROLYSIS OIL YIELD

Equation (33) illustrates the regression equation created using CCD to generate pyrolysis oil. ANOVA was used to examine the impact of independent factors on the generation of pyrolysis oil. The quadratic model was the best fit for pyrolysis oil production and is depicted using coded components in equation (33).

$$\text{Pyrolysis oil \%} = 16.18 - 1.16\,A + 0.0639\,B - 2.95\,C - 2.97\,D + 0.4863\,AB + 1.47\,AC + 3.77\,AD + 1.12\,BC + 0.5455\,BD + 0.8525\,CD \quad (33)$$

A is the operating temperature for pyrolysis, B is the rate of heat, C is feed particle size, and D is the residence time.

From the findings of the ANOVA analysis for the production of pyrolysis oil, the F-value of 5.43 and p-value of 0.0007 infer that the model was significant, as shown in Table 5.3. In this case, factor C influenced the pyrolysis oil yield because of a larger F-value of 16.76, followed by a residence time (D) and temperature (A) with an F-value of 12.29 and 2.33, respectively, and smaller p-value of <0.05. The residence time (D) was insignificant for pyrolysis oil production. On the subject of pyrolysis oil output, the actual values and expected responses were compared, and it was discovered that the regression was statistically relevant.

Table 5.3. ANOVA for quadratic model: Response 2 (pyrolysis oil)

Source	Sum of Squares	df	Mean Square	F-value	p-value	Remark
Model	686.35	10	68.63	5.43	0.0007	significant
A-Temperature	29.49	1	29.49	2.33	0.0424	
B-Heating rate	0.0040	1	0.0040	0.0003	0.9860	
C-Feed particle size	206.35	1	206.35	16.76	0.0006	
D-Residence time	161.06	1	161.06	12.29	0.0019	
AB	2.10	1	2.10	0.1662	0.6878	
AC	40.64	1	40.64	3.21	0.0882	
AD	212.72	1	212.72	16.82	0.0006	
BC	26.60	1	26.60	2.10	0.1625	
BD	3.99	1	3.99	0.3153	0.5807	
CD	15.25	1	15.25	1.21	0.2852	
Residual	252.94	20	12.65			
Cor Total	939.28	30				

5.4 PARAMETRIC ANALYSIS OF PYROLYSIS OIL PRODUCTION

The four operating parameters (A, B, C, and D) and the pyrolysis oil production have been examined using 3-D plots as shown in Fig. 5.2. According to the results of ANOVA analyses for the process parameter as shown in Table 5.3, A, B, C, and AD are found to be significant model terms in terms of production of maximum pyrolysis oil. The pyrolysis oil yield obtained was a maximum of about 25.67% at a temperature of 400°C, a rate of heat of 25°C/min, and a feed particle size of 5 mm because of more significant primary decomposition of the sample followed by secondary decomposition of the char into pyrolysis oil (Aysu et al., 2014). In comparison, at the lowest operating temperature of 250°C, the pyrolysis oil was produced with a minimum of 3.81% at the maximum feed particle size of 50 mm, a lower rate of heat of 10°C/min, and a holding period of 180 min as shown in Fig. 5.2. The production of char is observed to rise, whereas the production of pyrolysis oil and gas decreases because hemicellulose decomposes at lower temperatures of pyrolysis (Anca et al., 2016). According to the findings, there is no apparent influence of interaction between feed size, rate of heat, and residence time on the output of pyrolysis oil. In contrast, there was an influence of interaction between temperature and rate of heat, temperature, and feed particle size on pyrolysis oil yield.

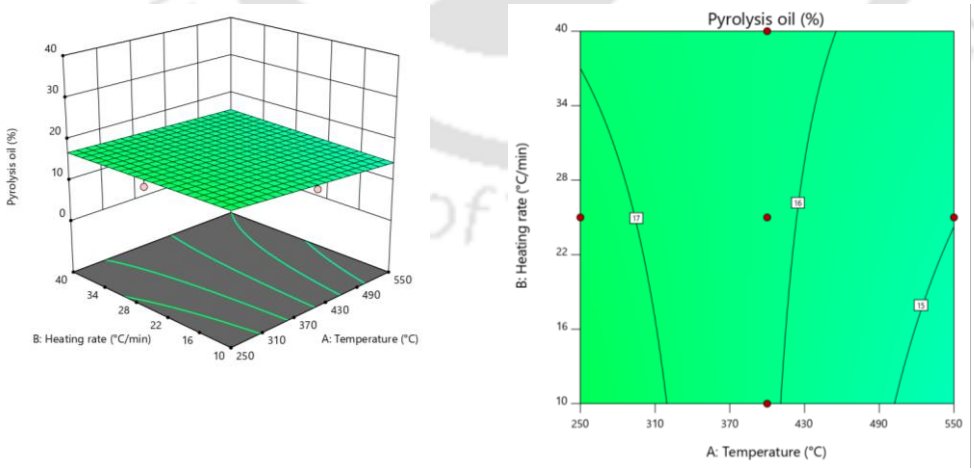

(a)

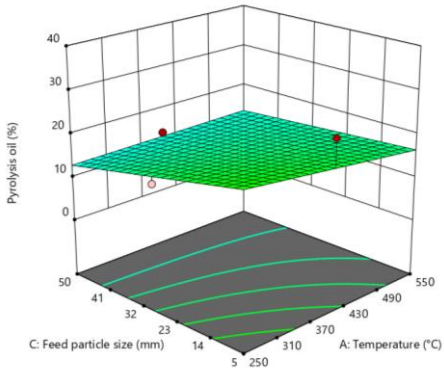
Pyrolysis oil (%)
40
30
20
10
0
50
41
32
23
14
5
C: Feed particle size (mm)
250
310
370
430
490
550
A: Temperature (°C)

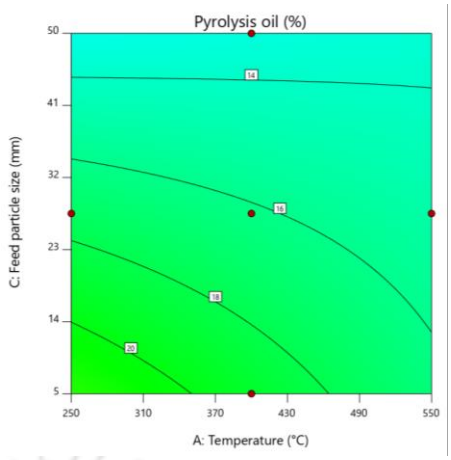
Pyrolysis oil (%)
50
41
32
23
14
5
C: Feed particle size (mm)
14
16
18
20
250
310
370
430
490
550
A: Temperature (°C)

(b)

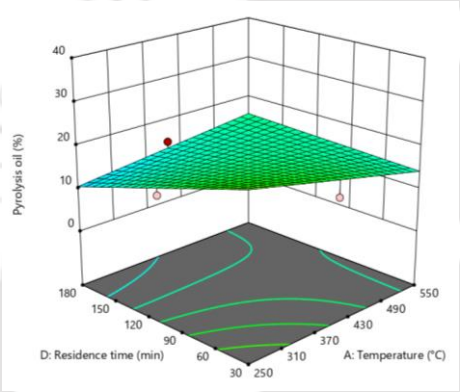
Pyrolysis oil (%)
40
30
20
10
0
180
150
120
90
60
30
D: Residence time (min)
250
310
370
430
490
550
A: Temperature (°C)

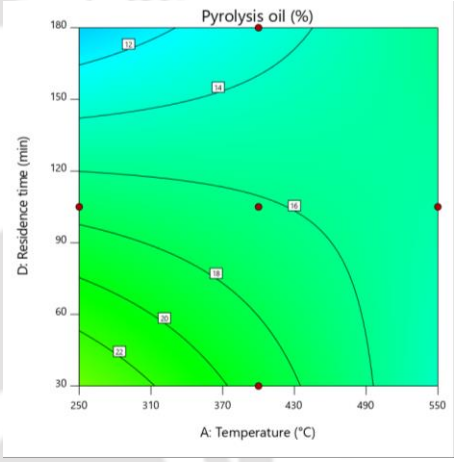
Pyrolysis oil (%)
180
150
120
90
60
30
D: Residence time (min)
12
14
16
18
20
22
250
310
370
430
490
550
A: Temperature (°C)

(c)

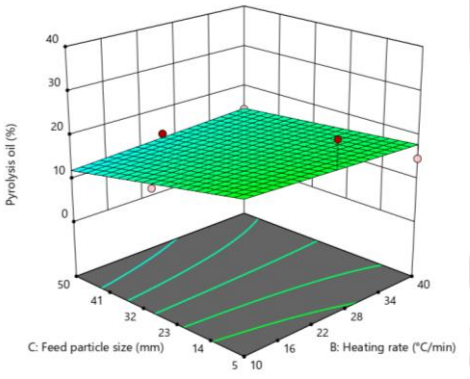
Pyrolysis oil (%)
40
30
20
10
0
50
41
32
23
14
5
C: Feed particle size (mm)
10
16
22
28
34
40
B: Heating rate (°C/min)

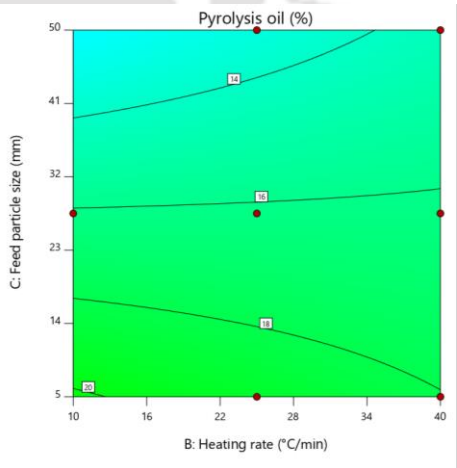
Pyrolysis oil (%)
50
41
32
23
14
5
C: Feed particle size (mm)
14
16
18
20
10
16
22
28
34
40
B: Heating rate (°C/min)

(d)

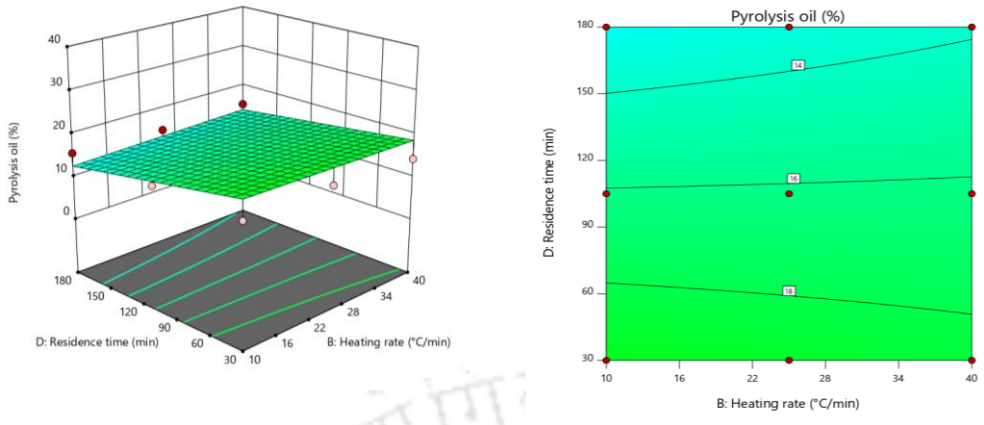

(e)

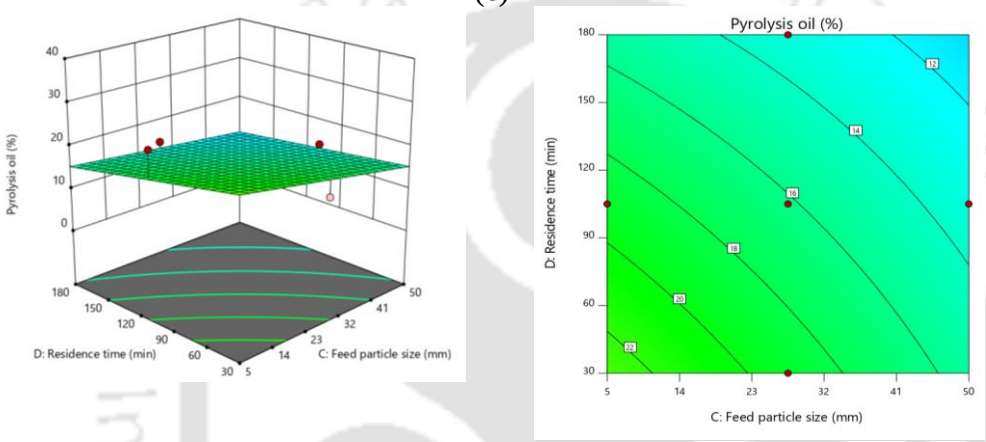

(f)

Fig. 5.2. Surface plot of (a) temperature and rate of heat, (b) temperature and feed particle size, (c) temperature and residence time, (d) rate of heat and feed size, and (e) rate of heat and residence time, and (f) feed particle size and residence time

5.5 ANOVA AND REGRESSION EQUATION DEVELOPMENT FOR PYROLYSIS GAS YIELD

A mathematical model for pyrolysis gas production using a coded equation has been built using RSM to ascertain the impact of independent factors on pyrolysis gas yield. RSM suggested a linear model be the best fit for modeling pyrolysis gas yield. Equation (34) displays the linear model equation. The F-value of this linear model was 86.84, which implies that the model was significant, as shown in Table 5.4. A p-value of <0.0001 also validated a considerable model. The actual values

were compared with the predicted responses by the linear model for pyrolysis gas generation, and the R^2 value of 0.9255 was obtained, indicating the model's fit.

$$\text{Pyrolysis gas (\%)} = 34.95 + 18.12\ A + 1.10\ B - 0.8435\ C + 4.03\ D \quad (34)$$

The most influential operating parameters on pyrolysis gas yield were temperature, with an F value of 325.26, and residence time, with an F value of 19.71.

Table 5.4. ANOVA for linear model: Response 3 (pyrolysis gas)

Source	**Sum of Squares**	**df**	**Mean Square**	**F-value**	**p-value**	
Model	6309.29	4	1577.32	86.84	< 0.0001	significant
A-Temperature	5908.21	1	5908.21	325.26	< 0.0001	
B-Heating rate	28.74	1	28.74	1.58	0.2196	
C-Feed particle size	14.23	1	14.23	0.7834	0.3842	
D-Residence time	358.11	1	358.11	19.71	0.0001	
Residual	472.28	26	18.16			
Cor Total	6781.57	30				

5.6 PARAMETRIC STUDY OF PYROLYSIS GAS PRODUCTION

Using a 3D response surface plot, the impact of operating parameters on the output of pyrolysis gas generation was examined, as shown in Fig. 5.3. A surface plot was used to determine how the operating temperature and rate of heat affected the generation of pyrolysis gas. Pyrolysis gas yield was a minimum of about 6.06% at a lower operating temperature of 250°C and rate of heat of 10°C/min. However, at the highest operating temperature of 550°C and rate of heat of 40°C/min, the gas yield percentage was highest, approximately 68.21%. Due to subsequent cracking processes of the pyrolysis vapour and degradation of the char during the process, pyrolysis gas yields rise with increasing operating temperature and decreasing feed particle size (Aysu et al., 2014). According to the surface plot, the lowest pyrolysis gas yield (3.81%) was achieved at the lowest temperature of 250°C. Consequently,

the findings showed that operating temperature (A) and residence time (D) have more impact on pyrolysis gas yield.

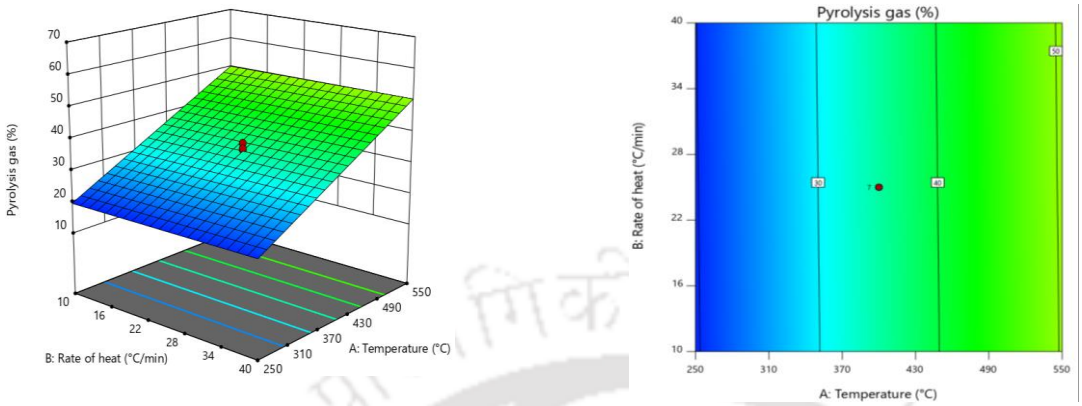

(a)

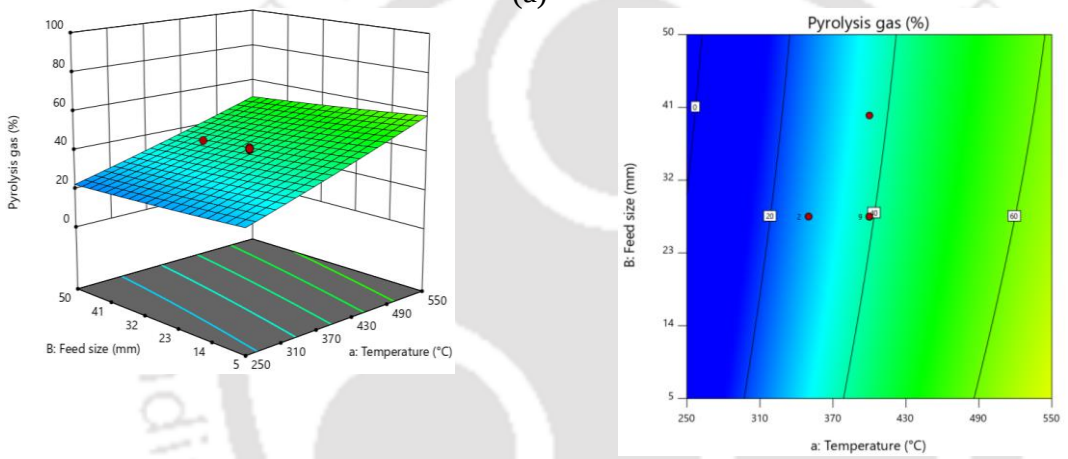

(b)

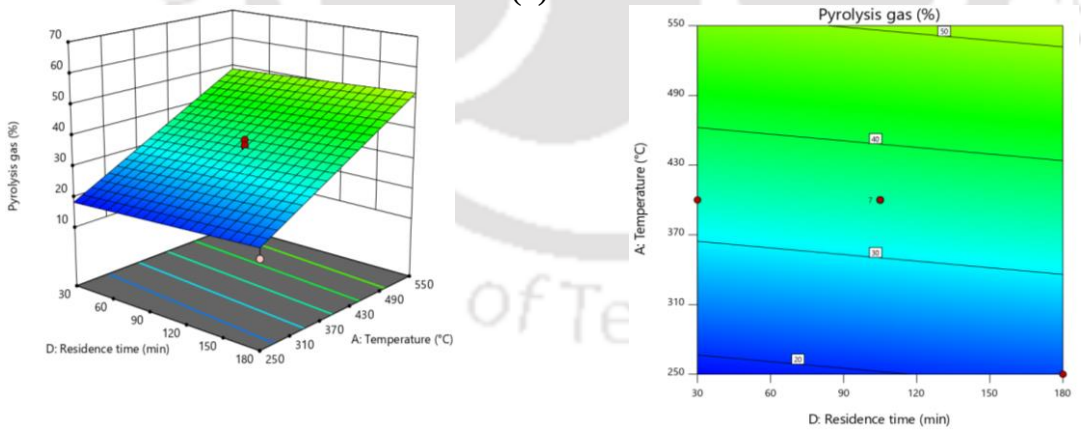

(c)

Fig. 5.3. Surface plot of (a) temperature and rate of heat; (b) temperature and feed particle size; (c) temperature and residence time.

5.7 CONFIRMATION TEST OF THE PREDICTED VALUES OF THE MSW PYROLYSIS EXPERIMENT

From RSM experimental findings, the optimization of the pyrolysis operating parameters for MSW in the fixed bed pyrolysis reactor was accomplished. Using an ANOVA, it was determined that the optimal operating conditions for maximum char yield were a temperature of 250°C, a rate of heat of 10°C/min, a feed particle size of 50 mm, and a residence time of 180 min. Through these conditions, the predicted values of the three responses were 72.77% of char, 4.8% of pyrolysis oil, and 20.89% of gas. The optimization condition recommended by RSM was carried out along with three confirmation experiments, and the mean and standard deviation were determined, as shown in Table 5.5. The percentage of pyrolysis product char, pyrolysis oil, and gas yield were 72.62%, 5.25%, and 22.13%, respectively. The standard deviation between the confirmation experiment of char yield and the predicted char yield was 0.11, which implies that the model was significant.

Table 5.5. Validation experiment of the optimized parameter

Factors			
Temperature (°C)	**Rate of heat (°C/min)**	**Particle size of feed (mm)**	**Residence time (min)**
250	10	50	180
Responses			
	Char (%)	**Pyrolysis oil (%)**	**Pyrolysis gas (%)**
Predicted value	72.77	4.8	20.89
Confirmation test 1	73.03	5.15	21.82
Confirmation test 2	72.16	5.37	22.47
Confirmation test 3	72.67	5.22	22.11
Mean	72.62	5.25	22.13
Std dev.	0.11	0.32	0.88

5.8 ENERGY CONSUMED DURING PYROLYSIS, EFFICIENCY AND COST OF OPERATION OF THE PYROLIZER

5.8.1 Energy consumed during the pyrolysis process

The energy consumed during the pyrolysis process at a terminal temperature of 250°C, heating rate of 10°C/min, and holding time of 180 minutes was calculated as follows

Initial temperature, T_i = 25°C

Terminal temperature, T_f = 250°C

Heating rate, HR = 10°C/min

Holding time = 180 mins

So, the time required to reach 250°C = $\frac{T_f - T_i}{HR}$ = 22.5 mins

Total time = 22.5 + 180 = 202.5 mins

Given, power of the heating coil = 4 kW

Therefore, energy during heating for 22.5 mins = 4000 W× (22.5×60) s = 5.4 MJ

Energy consumed during the holding time = 4000 W × (180×60) = 43.2 MJ

The total energy consumed = 5.4 + 43.2 = 48.6 MJ

The energy consumed during pyrolysis was 48.6 MJ, which corresponds to 16.2 MJ per kg of MSW processed in the fixed-bed reactor at 250°C, 10°C/min heating rate, and 180-minute residence time.

5.8.2 Efficiency of the Pyrolizer

The efficiency of the fixed bed pyrolizer for pyrolysis of MSW can be calculated as follows:

Energy consumed during the pyrolysis process = 48.6 MJ

Energy output in terms of the heating value of the pyrolysis product: char (72.66% of 3 kg), pyrolysis oil (5.25% of 3 kg), and syngas (22.13% of 3 kg).

Heating value of char = 5.025 MJ/kg

Heating value of pyrolysis oil = 10 MJ/kg

Heating value of syngas = 8 MJ/kg

Therefore, total energy output = (5.025×72.66% of 3 kg) + (10×5.25% of 3 kg) + (8×22.13% of 3 kg) = 17.84 MJ

Efficiency, $\eta = \frac{Energy\ output}{Energy\ input} \times 100\% = \frac{17.48\ MJ}{48.6\ MJ} \times 100\% = 36.7\%$

Thus, if all the products are considered, the efficiency of the fixed bed pyrolizer is 36.7%.

5.8.3 Cost of operation of the pyrolizer

Cost of 1 unit or 1 kWh of electricity = Rs. 5.25

Energy consumed in kWh = 48.6 MJ × 0.2778 kWh/MJ = 13.5 kWh

Total cost of electricity for the production of MSW char = 13.5 kWh × Rs 5.25/kWh = Rs. 71.25

The market price of biochar is Rs 25 to 40/kg (www.amazon.in).

So, the cost of production of MSW char in the fixed bed reactor is Rs. 31.67/kg.

5.9 CONCLUSION FROM THE OPTIMIZATION STUDY

The pyrolysis of commingled MSW in a fixed bed reactor with varying operational factors was performed successfully, and the optimum condition of operating factors for maximum char yield was determined using CCD in RSM. From ANOVA, the ideal condition was obtained at a temperature of 250°C, rate of heat at 10°C/min, particle feed size of 50 mm, and residence time of 180 min for a high yield of char of about 72.62% with 5.25% of pyrolysis oil, and 22.13% of gas through pyrolysis of 3 kg of commingled MSW. The ANOVA indicated that the operational parameters best fit the quadratic model for char and pyrolysis oil yield. But for pyrolysis gas yield, RSM suggested the linear model best fit. The order of most influential process parameters on char yield was found to be temperature (A) > feed particle size (C) > rate of heat (B) > residence time (D). A high char yield could be achieved at low operating temperature, low rate of heat, large feed particle size, and low residence time. Moreover, the char produced at 250°C consumes less energy and is more economically feasible than conventional biochar production at higher temperatures.

Chapter 6

CHARACTERIZATION OF MSW CHAR

6.1 TG AND DTG ANALYSIS OF MSW-DERIVED CHAR

The TGA of MSW char produced at 250°C, as depicted in Fig. 6.1, showed a mass reduction of 0.64% from room temperature to 100°C, primarily due to evaporation of moisture content. Subsequently, at 220°C, the degradation of cellulose and hemicellulose began, leading to a 1.54% reduction in char mass (Amalina et al., 2022). Interestingly, within the temperature range of 219 to 221°C, there was a consistent mass loss, indicating a buffer phase in which complete char formation occurred. However, beyond 222°C, the MSW char underwent thermal degradation, resulting in the loss of carbonaceous material and the production of gas.

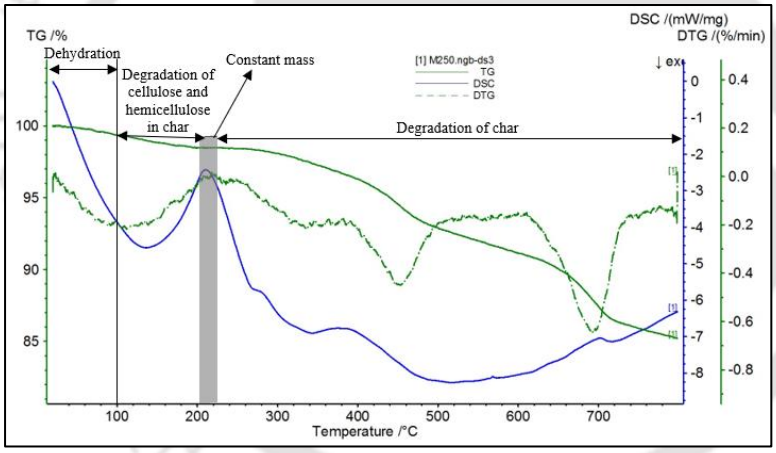

Fig. 6.1. Thermogravimetric and derivative thermogravimetric analysis of (a) MSW and (b) char

6.2 PROXIMATE ANALYSIS OF CHAR

The moisture content of the char produced at 250°C was 1.17%, which decreased to 0.68% at 550°C. The volatile matter decreased from 27.80 to 6.90%, while the ash content increased from 1.90 to 30.91%. The fixed carbon decreased from 70.13% to 61.51%. Results show that the parameters of the proximate analysis

of char were within the limit and resembled the properties of biochar (Enders et al., 2012). When the temperature at which the MSW char was produced increased, moisture content, volatile matter, and fixed carbon decreased, whereas the ash content increased. The higher moisture content of char results in higher energy consumption, for which the feasibility of the material to be used as combustible material decreases. Also, higher ash content results in a decrease in the adsorption capacity (Ambaye et al., 2021). Char with higher volatile matter is a good source of fuel for combustion due to low energy consumption to start ignition (Miao et al., 2021). The higher fixed carbon content in char is a potential source for combustion, but the capacity of the char as an adsorbent decreases (Sun et al., 2017). The result of the proximate analysis of the char produced is shown in Table 6.1. It was observed that the moisture content and ash content of the four types of char were within the limit of the tanner diagram, as shown in Fig. 6.2 (moisture content<50% and ash content<60%), but the combustible matter was less for char produced at a temperature of 350, 450 and 550°C which should be >25% (Lombardi et al., 2015). So, it can be deduced from this study that MSW char produced at 250°C is a potential material to be used as a combustible material without the requirement of auxiliary fuel for combustion.

Table 6.1. Proximate analysis of MSW char

Sample	**Moisture content (%)**	**Ash content (%)**	**Volatile matter (%)**	**Fixed carbon (%)**
250°C	1.17 ± 0.20^{a}	1.90 ± 0.09^{a}	27.80 ± 0.03^{a}	70.13 ± 0.20^{a}
350°C	1.15 ± 0.02^{a}	16.88 ± 0.30^{b}	18.73 ± 0.08^{a}	64.24 ± 0.30^{a}
450°C	0.96 ± 0.06^{a}	22.69 ± 0.13^{b}	12.48 ± 0.10^{a}	63.87 ± 0.50^{a}
550°C	0.68 ± 0.08^{a}	30.91 ± 0.09^{a}	6.90 ± 0.05^{a}	61.51 ± 0.20^{a}

Note: *Significant variation, indicated by different letters, was observed using the Tukey test at a significance level of $p < 0.05$. The data is presented in *xx* ± *yy* format where xx denotes the average value *yy* denotes the standard deviation.

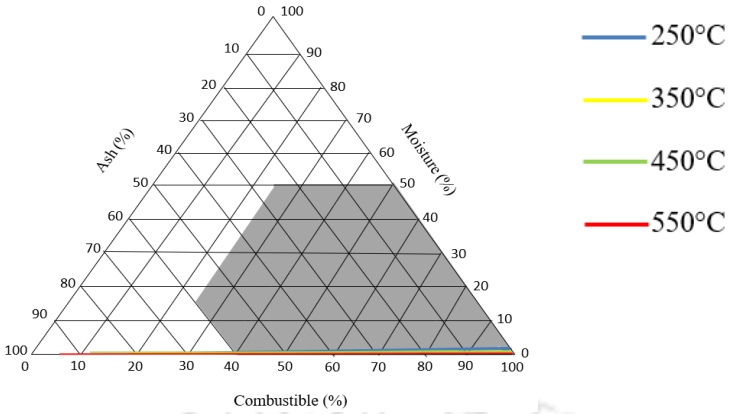

Fig. 6.2. Tanner diagram of MSW char

6.3 ELEMENTAL STUDY AND HEATING VALUE OF CHAR

The ultimate analysis and heating value of the char is presented in Table 6.2. The elemental analysis of MSW char generated at different temperatures shows that the percentage of C content in the char decreased from 9.91 to 3.68% as the temperature increased from 250 to 550°C. The percentage of H decreased from 1.79 to 0.36%, and N from 0.36 to 0.03% in char with the increase in temperature due to the degradation of weaker bonds in char (Sun et al., 2014). The char with higher N content can reduce oxygen and carbon dioxide. In contrast, the carbon content in char can be used for adsorption (Deng et al., 2017). The O/C specifies the aging of char, and the H/C ratio designates stability and aromaticity (Moiseenko et al., 2021). The study found that H/C molecular ratios decreased from 2.17 to 1.17 with the increased temperature at which the char was produced. The higher H/C molecular ratio of char prepared at 250°C indicates the occurrence of aromatic organic matter, which tends towards biological variability, whereas vice versa for char produced at 550°C (Yang et al., 2007;). As the temperature increases the H and O-containing functional groups in char vanish due to decarboxylated dehydrogenation (Windeatt et al., 2014).

The O/C ratio increased from 0.74 to 2.30 as the temperature of the char produced increased from 250 to 550°C, representing higher oxidation and instability, which predicts the potential of MSW char for its application in soil and agriculture (Bakshi et al., 2020). Char produced at 250°C has higher carbon compounds than char prepared at 550°C. The O/C molecular ratio also depicts the

half-life of char. When the O/C is <0.2, half-life is more than 1000 years, 100 to 1000 years when the O/C value is from 0.2 to 0.6, and <100 years when the O/C value is > 0.6. The O/C molecular ratio of prepared char was > 0.6, indicating the potential of MSW char for carbon sequestration (Crombie et al., 2013; Wang et al., 2021).

The theoretical Low Heating Value (LHV) and High Heating Value (HHV) were determined from elemental analysis and compared with the instrumental HHV. It was found that there was not much difference between the values obtained from theoretical and instrumental HHV. The LHV and HHV decreased with the increase in temperature of the produced MSW char. The LHV and HHV of the char produced at 250°C were the highest, with heating values of 4199.43 and 4830.89 kJ/kg, respectively, and the instrumental HHV was 5025.46 kJ/kg. The heating values of MSW char were much lower than those of biochar produced from slow pyrolysis (Himbane et al., 2022; Rathod et al., 2023). The decreasing heating value with the increase in temperature synchronized the decreasing fixed carbon value of MSW char. The char derived from MSW does not meet the necessary criteria for combustion because, according to the Municipal Solid Waste Management manual, a material should have a minimum heating value of 6276 kJ/kg (1500 kCal/kg) to utilize it as a combustible material (Ministry of Urban Development, 2016).

Table 6.2. Ultimate analysis and heating value of char

Analysis	MSW char produced at 250°C	350°C	450°C	550°C
C (%)	9.91 ± 0.03[a]	9.15 ± 0.21[b]	6.19 ± 0.02[a]	3.68 ± 0.25 [a]
H (%)	1.79 ± 0.06[a]	0.97 ± 0.00[a]	0.77 ± 0.02[a]	0.36 ± 0.03 [a]
N (%)	0.36 ± 0.04[a]	0.34 ± 0.03[a]	0.27 ± 0.04[a]	0.03 ± 0.01 [a]
S (%)	1.33 ± 0.01[a]	0.92 ± 0.01[a]	0.99 ± 0.00[a]	0.81 ± 0.00 [a]
O (%)	9.83 ± 0.02[b]	12.33 ± 0.02[a]	9.76 ± 0.00[a]	11.68 ± 0.00 [a]
H/C	2.17 ± 0.06[a]	1.27 ± 0.03[a]	1.5 ± 0.03[a]	1.17 ± 0.17[a]
O/C	0.74 ± 0.00[a]	1.01 ± 0.02[a]	1.18 ± 0.0[a]	2.39 ± 0.17[a]

LHV (kJ/kg)	4199.43 ± 71.46[a]	2853.30 ± 74.69[a]	1926.42 ± 31.47[a]	427.36 ± 64.19[a]
HHV (kJ/kg)	4830.89 ± 83.32[a]	3366.51 ± 73.9[a]	2334.22 ± 35.71[a]	791.36 ±58.28[a]
$HHV_{instrumental}$ (kJ/kg)	5025.46 ± 9.98[a]	3574.75 ± 7.59[a]	2621.22 ± 11.95[a]	849.83 ± 10.84[a]

6.4 FTIR SPECTROSCOPY OF MSW CHAR

The functional group present in char produced at different temperatures has been determined using FTIR analysis and is shown in Fig. 6.3. It was observed that there were peaks between 3600 to 3000 cm^{-1} representing the presence of the -OH group in carboxylic acids, phenols, and alcohols (Qiu et al., 2022). However, the peaks were weaker with the increase in the final temperature of the char produced, indicating the vanishing of the hydroxyl and carbonyl functional group in the char produced at 350 to 550°C. The peak at 2927.57 cm^{-1} in char produced at 250°C depicts C-H groups in methylene (CH_2) and methyl (CH_3), which is absent in char formed at higher temperatures at 350, 450, and 550°C (Qiu et al., 2022). The peaks 1421.05, 1415.74, 1429.74, and 1422.24 cm^{-1} in char produced at 250, 350, 450, and 550°C indicated the presence of -CH_3 stretching (Qiu et al., 2022). These peaks were stronger with the increased temperature of the char produced. The peaks at 1010.18, 1007.96, 1007.15, and 1021.29 cm^{-1} showed the existence of C-O groups. The peaks below 1007.15 cm^{-1} specified the occurrence of esters and ethers in char. Because of the existence of hydroxyl and carbonyl groups in MSW char produced at 250°C can be used as an adsorbent (Qiu et al., 2022).

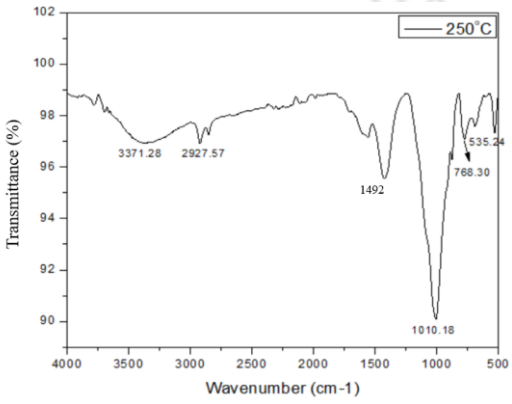

(a)

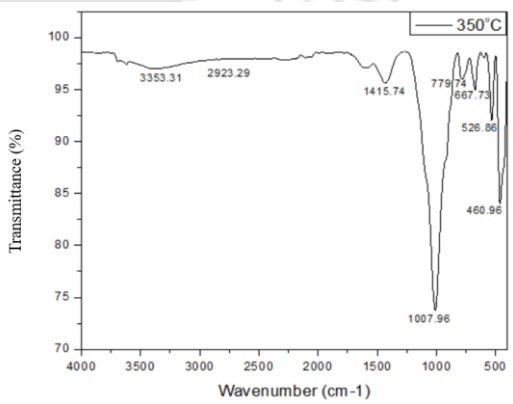

(b)

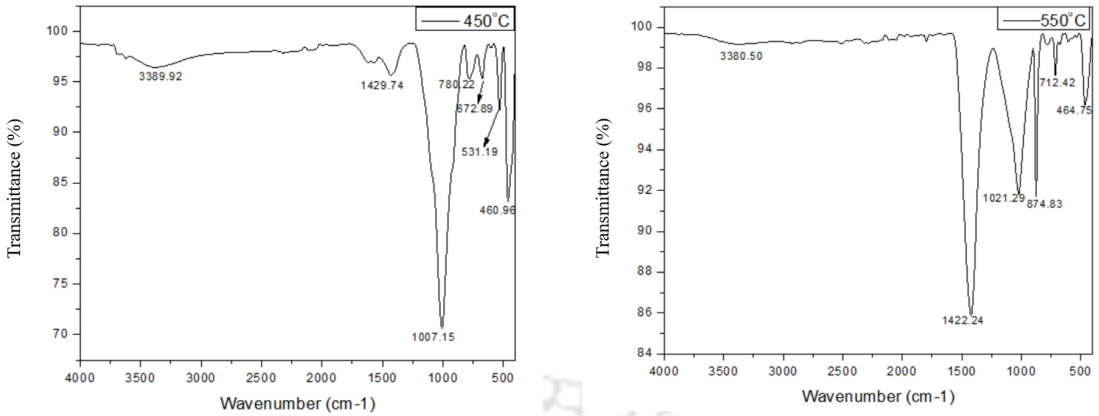

(c) (d)

Fig. 6.3. FTIR Spectroscopy of char produced at (a) 250, (b) 350, (c) 450, and (d) 550°C

6.5 BULK DENSITY, POROSITY, PH, IODINE NUMBER, AND BET SURFACE AREA OF MSW CHAR

The bulk density, porosity, and pH of the MSW char produced at 250, 350, 450, and 550°C were found and presented in Table 6.3. The bulk density of char decreased while the porosity increased with the temperature at which char was produced. The bulk density was 0.63 to 0.67 g/cc, resembling biochar's bulk density ≤ 0.6. The porosity of the MSW char was 74 to 86%, which was within the range of porosity of biochar (70 to 90%) (Blanco et al., 2017). This implies the potential of MSW char for soil application, like biochar, having its wide application in soil conditioning (Blanco et al., 2017). Moreover, some literature reported that the higher the bulk density of char, the higher the adsorbing capacity (Nuraisyah et al., 2020).

The pH of the MSW char increased from 7.44 to 7.85 with the increased temperature of the char produced. The more the basic nature of char, the higher the adsorption (Nuraisyah et al., 2020). The application of char in the soil increases the soil's pH and microbial activity, reducing the exchangeable capacity of aluminium, hydrogen, and acidity of the soil (Geng et al., 2022) and emissions of greenhouse gas (Chandra et al., 2019). Thus, from bulk density, porosity, and pH study, it can be inferred that just like biochar, MSW char produced at temperatures 250, 350, 450, and 550°C has the potential for application in the soil and as an adsorbent.

The iodine number of chars decreased with the increase in temperature at which char was produced and was in the range of 243.66 to 101.52 mg/g, which was within the range of iodine number of biochar (214.67 to 154.16 mg/g) (Powar et al., 2015).

The BET surface area of the char produced at 250, 350, 450, and 550°C is shown in Table 3. The specific surface area decreased, and the pore volume and pore diameter of the char increased with the increase in temperature. The specific surface area was in the range of 5.38 to 9.4 m^2/g, and the pore volume was in the range of 0.027 to 0.086 cm^3/g. The larger the specific area of the char surface ensures a larger quantity of active sites for adsorption (Lu et al., 2018). The char produced at 250°C has the highest surface area of 9.4 m^2/g as the volume and diameter of the pore is the smallest. The pore diameter of the MSW char was 3.74 to 3.99 µm, within the range of pore diameter of biochar, which is 1.5 to 15 µm (Lu et al., 2018). These characteristics of MSW char resemble the characteristics of biochar, which was within the range of surface area and pore volume of biochar (Leng et al., 2021). Thus, the char produced from pyrolysis of mixed MSW can be applied as an adsorbent and used for soil amendment.

Table 6.3. Bulk density, porosity, pH, iodine number, and BET surface area of MSW char

Parameters	**250°C**	**350°C**	**450°C**	**550°C**
Bulk density (g/cc)	0.66 ± 0.03^a	0.64 ± 0.01^a	0.63 ± 0.04^a	0.63 ± 0.01^a
Porosity (%)	74 ± 0.01^a	79 ± 0.01^b	83 ± 0.02^a	86 ± 0.01^a
pH	7.44 ± 0.11^a	7.55 ± 0.02^a	7.56 ± 0.01^a	7.85 ± 0.04^a
Iodine number (mg/g)	243.66 ± 0.56^b	142.13 ± 0.16^a	121.83 ± 0.08^a	101.52 ± 0.30^a
Specific surface area (m^2/g)	9.4 ± 0.32^a	9.12 ± 0.29^a	8.79 ± 0.13^a	5.38 ± 0.73^a
Pore volume (cm^3/g)	0.027 ± 0.01^a	0.043 ± 0.01^a	0.058 ± 0.00^a	0.086 ± 0.01^a
Pore diameter (µm)	3.74 ± 0.01^b	3.81 ± 0.06^a	3.94 ± 0.06^a	3.99 ± 0.01^a

6.6 FESEM AND SEM-EDX ANALYSIS OF MSW CHAR

The FESEM images of the char produced at 250, 350, 450, and 550°C are shown in Fig. 6.4. It was observed that the char produced at different temperatures shows different topography of the surface. Among the four char types, the char produced at 450 and 550°C had more porous structures than that produced at 250°C as most organic volatiles evolved, leaving behind the ruptured char surface. The rough surfaces of char images were mostly due to the heterogeneity of the components of MSW. However, as shown in Fig. 6.4 (a) and (b), there were fewer micropores but had a large surface area compared to char produced at 450 and 550°C.

The EDX analysis of MSW char is shown in Fig. 6.4 (e), (f), and (g) to determine the concentration of elements such as O, C, Si, Fe, Ca, Al, and K in MSW char. It was observed that the char contains higher carbon and oxygen concentrations, indicating the possibility of C-O bond formation. The C-O bond is commonly found in organic compounds, including plastics, but this does not necessarily indicate the presence of plastic (Kondoh et al., 2018). This also inferred the presence of compounds such as carbohydrates, alcohols, ethers, and esters (Qiu et al., 2022), further confirmed by FTIR spectroscopy.

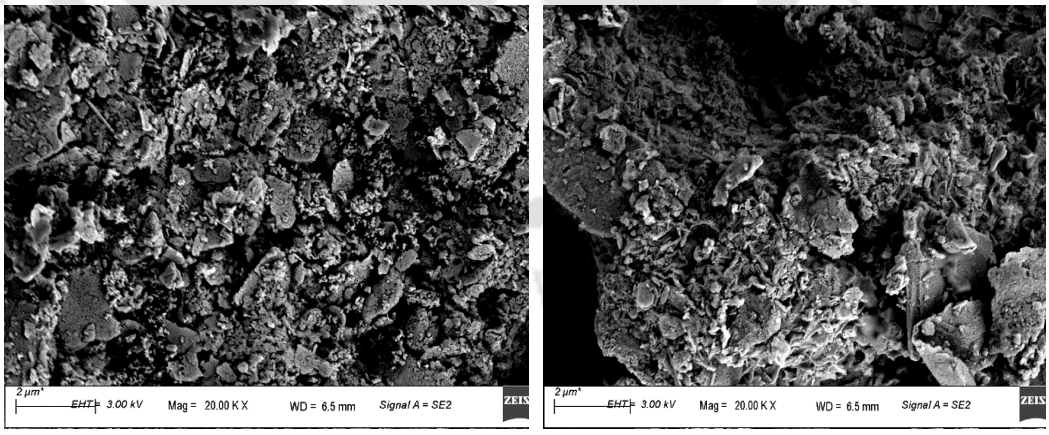

(a) (b)

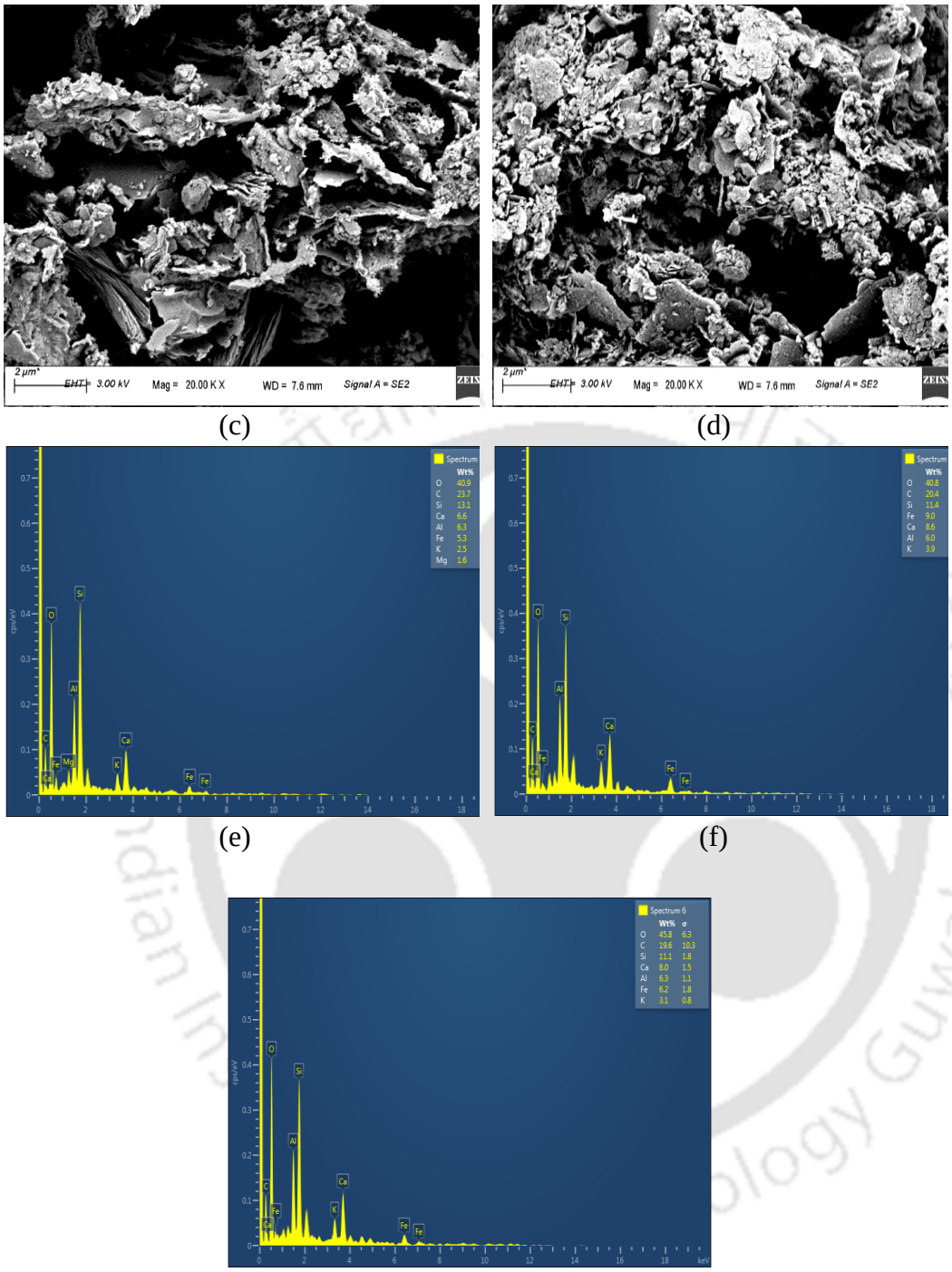

Fig. 6.4. FESEM images of MSW char produced at (a) 250°C, (b) 350°C, (c) 450°C and (d) 550°C and SEM-EDX of char produced at € 250°C, (f) 350°C and (g) 450°C

6.7 XRD ANALYSIS OF CHAR

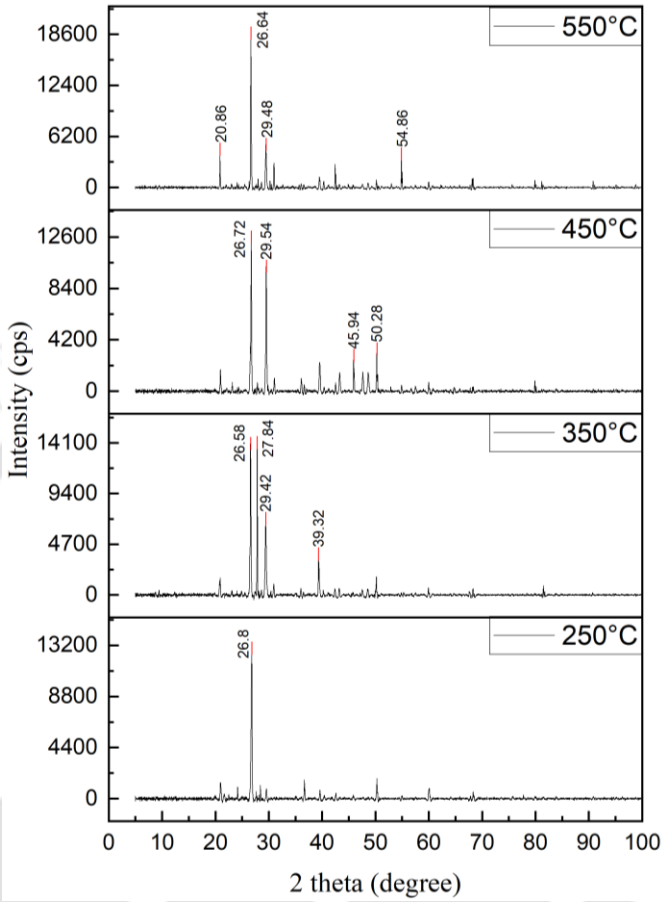

Fig. 6.5. XRD analysis of MSW char produced at different temperatures

The XRD spectroscopy of char produced at 250, 350, 450, and 550°C was analyzed and shown in Fig. 6.5. The chemical composition, crystallography, and physical properties of char were determined through XRD analysis. The peaks at 20°, 26°, 29°, 36° and 39° indicates the presence of SiO_2 (Mészáros et al., 2007). There was an increase in the crystallinity of the MSW char formed at high temperatures. With the increase in temperature, the amorphous silicates were converted into crystalline silicates (Hidayat et al., 2023). The peaks at 24° in char produced at 250 and 350°C represent the (002) crystallographic planes, and 42° and 43° represent the (100) crystallographic planes of graphite carbon. These planes inferred the amorphous carbon structure of MSW char (Zhang et al., 2022). The

crystallinity index was calculated for all four types of MSW char, and it was found that the crystallinity index increased by 53.36%. Thus, due to the amorphous nature of MSW char produced at a lower temperature (250 and 350°C), it can be used for heavy metal removal as an adsorbent from wastewater and as a carbon precursor for soil amendment.

6.8 HEAVY METAL ANALYSIS BY AAS

The AAS study was to determine the heavy metal concentration of the four MSW chars since MSW comprised heterogeneous waste. Heavy metal such as Pb, Ni, Fe, Mn, and Cd was determined in this analysis. It was found that there was some concentration of Pb (6 to 25.5 mg/kg), Fe (196.24 to 166.88 mg/kg), and Mn (154.87 to 196.24 mg/kg), whereas no traces of Ni and Cd were found in the MSW char as shown in Fig. 6.6. These heavy metals were within the permissible limit (Pb 250-500 mg/kg, Ni 75-150 mg/kg, Fe 400-500 mg/kg, and Cd 3-6 mg/kg) for soil application (Alghobar et al., 2017).

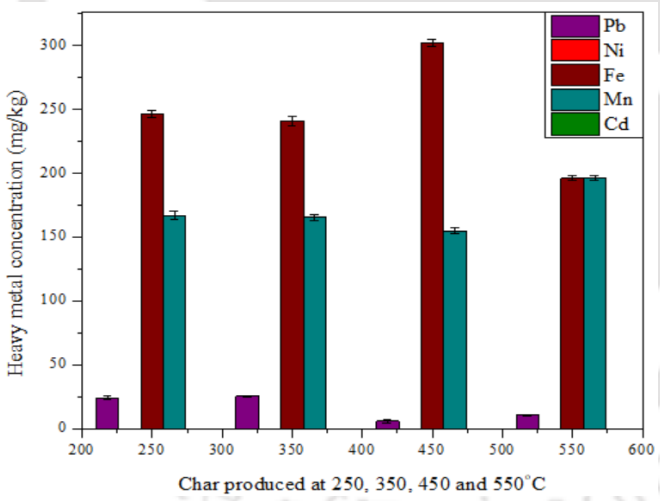

Fig. 6.6. Heavy metal analysis of MSW char produced at different temperatures

6.9 IDENTIFICATION OF MICROPLASTIC IN MSW CHAR

The FTIR spectroscopy identified three distinguish peaks in the char produced at 250°C, as depicted in Fig. 6.3 (a). The peak 1492 cm^{-1} indicates C=C stretching vibrations, which reveals the presence of aromatic structures (Stefanidis et al., 2014). The peak at 1004 cm^{-1} defines the functional groups that contain oxygen,

such as methoxy or hydroxyl, that are formed during the pyrolysis process (Gopinath et al., 2021). Most of the literature demonstrated that the presence of microplastics was identified through peaks such as CH stretching ranging from 2980-2780 cm-1, CO stretching from 1760-1670 cm-1, and CH deformation from 1480-1400 cm^{-1} (Xu et al., 2019). The non-appearance of these peaks in the MSW char specified no trace of microplastic.

After the density separation test using NaCl, the filtered particles were subjected to microscopic examination. Fig. 6.7 (a) and (b) display the microscopic images obtained by the density separation process. Notably, the microscopic investigation did not reveal any evidence of the plastic presence in the char produced at 250°C. Therefore, the likelihood of microplastic presence in the char produced at a temperature exceeding 250°C is negligible.

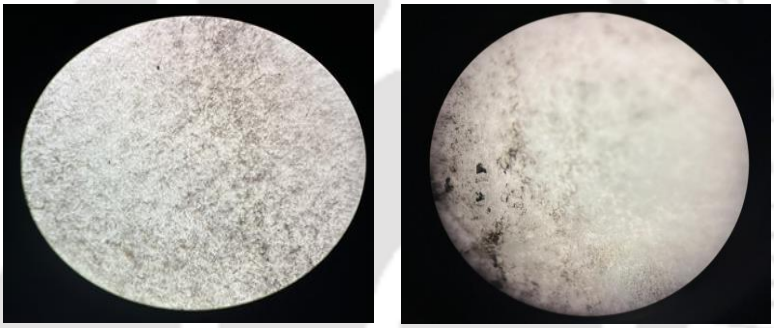

(a) (b)

Fig. 6.7. Stereomicroscopic images after density separation

6.10 CONCLUSION FROM CHARACTERIZATION OF MSW CHAR PRODUCED AT DIFFERENT TEMPERATURES

The pyrolysis of mixed MSW for char production in a fixed-bed reactor was comparable to biomass pyrolysis for biochar production. About 72.66% of MSW char was produced at 250°C. According to the characterization research employed on MSW char, it was identified that, like biochar having diverse applications as a natural resource, mixed MSW char can also be used for various applications as an adsorbent and soil amendment. The properties of MSW char, such as lower moisture content, ash content, high fixed carbon, and presence of hydroxyl and carbonyl group in char produced at 250°C, marks a significant character as an

adsorbent. The morphological analysis, bulk density, porosity, iodine number, surface area, and elemental analysis of the char produced at 250°C and 350°C can be compared with biochar produced from biomass, which made a remarkable contribution in the area of heavy metal adsorption study as well as in soil application. Moreover, no trace of microplastic was identified in the char. Consequently, producing a substantial quantity of high-quality char from MSW at low temperatures can be beneficial due to its versatility as a carbon precursor for various applications. This study approach is a way to produce char by utilizing waste resources and reducing waste dumped in landfills.

Chapter 7

APPLICATION OF CHAR AS AN ACTIVATED CARBON

7.1 PROXIMATE ANALYSIS OF ACTIVATED CARBON

The proximate analysis was conducted on activated carbon derived from MSW char produced at temperatures of 250 and 350°C, as detailed in Table 7.1. The moisture content of AC_NaCl_250°C was initially 1.27% and decreased to 0.24% at 350°C. Volatile matter decreased from 20.74 to 10.39%, while ash content increased from 8.5 to 9.05%. Fixed carbon increased from 69.5 to 80.33%. For AC_KOH_250°C, moisture content was 1.21% at 250°C, decreasing to 0.86% at 350°C. Volatile matter decreased from 22.66 to 10.21%, and ash content increased from 5.71 to 9.23%. Fixed carbon increased from 70.42 to 79.71%. AC_$ZnCl_2$_250°C had a moisture content of 1.43%, decreasing to 0.38% at 350°C. Volatile matter decreased from 15.5 to 11.23%, and ash content increased from 9.4 to 12.12%. Fixed carbon increased from 73.68 to 76.27%. Compared to commercial activated carbon, these samples generally exhibited similar properties with values falling within the range. Increasing char production temperature led to decreased moisture content and volatile matter, with a corresponding increase in ash content and fixed carbon. Higher ash content and fixed carbon reduced adsorption capacity (Sun et al., 2017; Ambaye et al., 2021). Additionally, while higher fixed carbon content suggests combustion potential, it diminishes adsorption capacity. Consequently, activated carbon produced at 250°C with NaCl and KOH shows promising results as an adsorbent for heavy metal removal.

Table 7.1. Proximate analysis of MSW-AC

Sample	Moisture content (%)	Ash content (%)	Volatile matter (%)	Fixedcarbon (%)
AC_NaCl_250°C	1.27 ± 0.09	8.5 ± 0.13	20.74 ± 0.09	69.5 ± 0.05
AC_NaCl_350°C	0.24 ± 0.06	9.05 ± 0.21	10.39 ± 0.12	80.33 ± 0.04
AC_KOH_250°C	1.21 ± 0.16	5.71 ± 0.15	22.66 ± 0.27	70.42 ± 0.27
AC_KOH_350°C	0.86 ± 0.08	9.23 ± 0.25	10.21 ± 0.16	79.71 ± 0.01
AC_$ZnCl_2$_250°C	1.43 ± 0.18	9.4 ± 0.42	15.5 ± 0.32	73.68 ± 0.08
AC_$ZnCl_2$_350°C	0.38 ± 0.16	12.12 ± 0.31	11.23 ± 0.24	76.27 ± 0.09
AC (Commercial)	1.66 ± 0.22	8.5 ± 0.14	19.15 ± 0.07	70.69 ± 0.16

7.2 FTIR SPECTROSCOPY OF MSW CHAR-ACTIVATED CARBON

FTIR spectroscopy reveals the presence of functional groups on the surface of activated carbon, as depicted in Fig. 7.1. Notably, three prominent adsorption bands appear within the ranges of 1421-1427, 1000-1010, and 460-535 cm^{-1}, accompanied by a broad peak at 3464 cm^{-1} indicating the presence of the O-H stretching mode of hydroxyl groups (Al-Qodah and Shawabkah, 2009). Peaks at 1421, 1442, and 1427 cm^{-1} suggest -CH_3 stretching, while those at 1000, 1004, 1007, 1009, and 1010 cm^{-1} indicate the presence of C-O groups. Within the 460-535 cm^{-1} range, vibrations depict in and out-of-plane aromatic ring deformations, with the 535 cm^{-1} band corresponding to out-of-plane C-H bending (Al-Qodah and Shawabkah, 2009). The presence of hydroxyl and carbonyl groups suggests the potential utility of MSW char-activated carbon as an adsorbent (Qiu et al., 2022). This analysis by FTIR spectroscopy provides clear evidence of activated carbon formation.

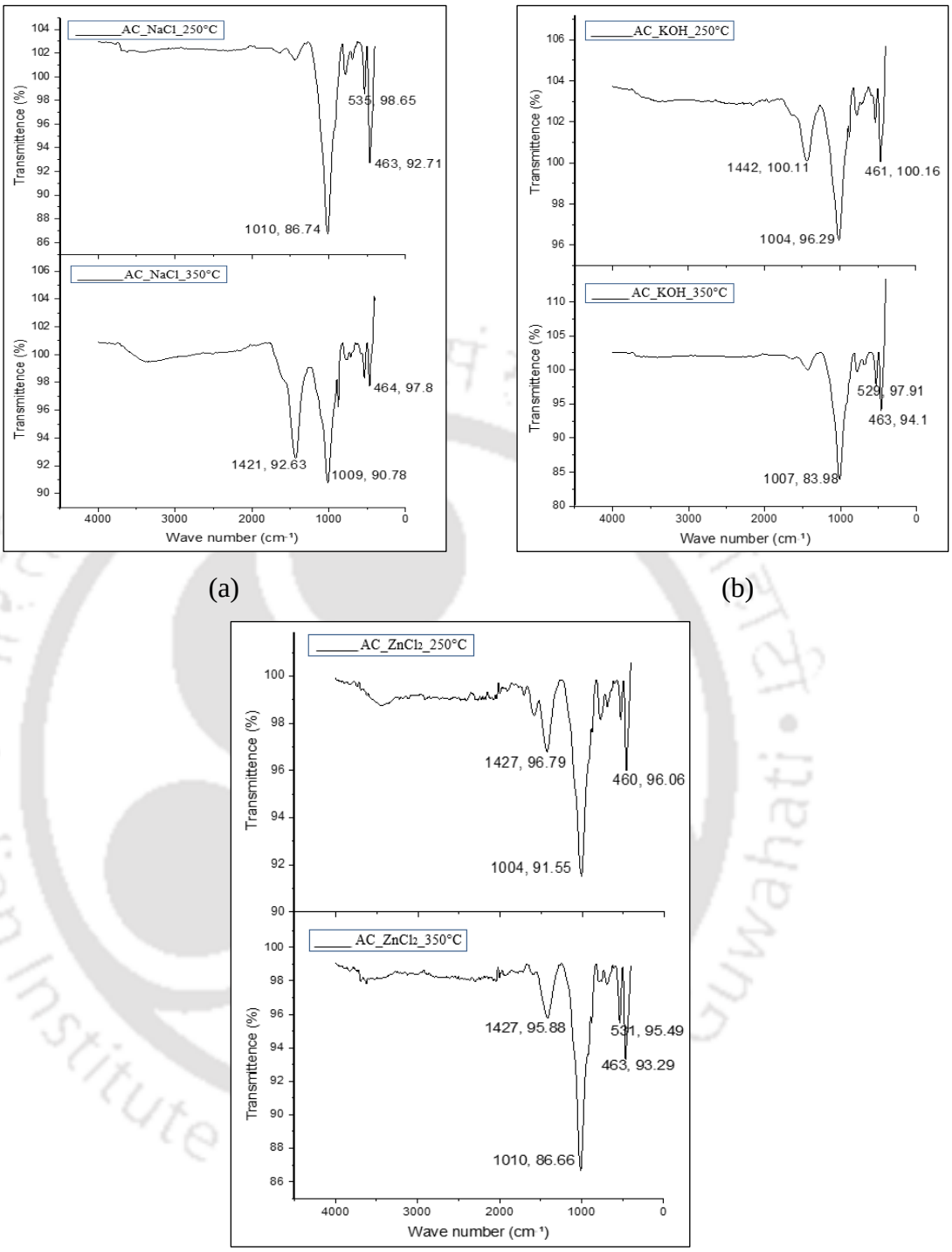

Fig. 7.1. FTIR spectroscopy of MSW char-activated carbon (a) AC_NaCl (b) AC_KOH and (c) AC_ZnCl_2

7.3 pH, IODINE NUMBER, AND BET SURFACE AREA OF MSW CHAR-ACTIVATED CARBON

When MSW char undergoes activation, its pH tends to lean towards alkalinity. Similar to commercially available activated carbon, all activated carbon produced tends to be alkaline. According to Table 7.2, AC_KOH_250°C exhibits a high pH value, making it effective as a cationic pollutant adsorbent. This is because higher pH results in a decrease of H+ ions and, hence, fewer positively charged particles on the activated carbon, reducing repulsion with cationic pollutants and allowing for increased adsorption (Nizam et al., 2021).

The iodine number indicates the capacity of adsorption in the micropores of the carbon. The adsorption capacity of MSW char-derived activated carbon at 250 and 350°C was determined by calculating the iodine number. The iodine number of the activated carbon was found to decrease with the increase in the MSW char produced at higher temperatures. At high temperatures, the pore volume becomes high due to the destruction of pores. This causes a decrease in the specific surface area and iodine number (Maulina and Iriansyah, 2018). The iodine number of MSW char-activated carbon was compared with that of commercial-activated carbon. It was observed that the activated carbon produced with KOH at 250°C closely resembled commercial activated carbon. Among the tested samples, the highest iodine number was recorded for the char produced at 250°C and activated with KOH. Consequently, based on the findings in Table 7.2, it can be inferred that AC_KOH_250°C is the most suitable adsorbent for Pb(II) adsorption compared to other MSW char-activated carbon samples.

From BET analysis, as detailed in Table 7.2, it was found that with an increase in the temperature of MSW char production, there was a corresponding decrease in specific surface area, alongside an increase in pore volume and diameter of the activated carbon. The specific surface area ranged from 5.99 to 15.52 m^2/g, while pore volume and diameter ranged from 0.020 to 0.026 cm^3/g and 3.45 nm, respectively. A larger surface area of the char implies a greater number of active sites available for adsorption. Notably, activated carbon produced from MSW char at 250°C using KOH exhibited the highest specific surface area of 15.52 m^2/g.

However, it's worth mentioning that the surface area of this activated carbon was relatively smaller compared to commercial activated carbon and activated carbon derived from biochar (Lu and Zong, 2018). While increasing the pyrolysis temperature can augment the surface area of activated carbon, it comes at the expense of reduced char yield and heightened energy consumption (Leng et al., 2021). Therefore, considering its lower energy consumption and higher quantity of activated carbon produced, AC_KOH_250°C emerges as the most promising activated carbon for further adsorption studies.

Table 7.2. Characterization of MSW char-activated carbon

	AC_KOH		**AC_NaCl**		**AC_$ZnCl_2$**		**Commercial Activated carbon**
	250°C	**350°C**	**250°C**	**350°C**	**250°C**	**350°C**	
pH	7.6 ± 0.09	6.93 ± 0.08	8.15 ± 0.01	8.05 ± 0.05	7.00 ± 0.04	6.94 ± 0.04	7.94 ± 0.03
Iodine number (mg/g)	467.45 ± 0.59	325.05 ± 0.23	474.39 ± 0.25	346.52 ± 0.36	142.15 ± 0.03	101.30 ± 0.33	503.52 ± 0.36
Specific surface area (m^2/g)	15.52	10.62	8.02	7.13	6.60	5.99	590
Pore volume (cc/g)	0.024	0.025	0.022	0.020	0.026	0.023	0.466
Pore diameter (nm)	3.05	3.34	3.06	3.45	3.24	3.06	5.26

7.4 FESEM ANALYSIS OF MSW-AC

The surface texture and morphological structure of activated carbon are shown in Fig. 7.2. The images reveal the presence of rough and tumble heterogeneous surfaces in the composite. The AC_KOH_250°C had the largest pore compared to other activated carbon. Based on the size of its pores and morphology, the largest pore should be the most effective in the study of heavy metal adsorption (Nizam et al., 2021).

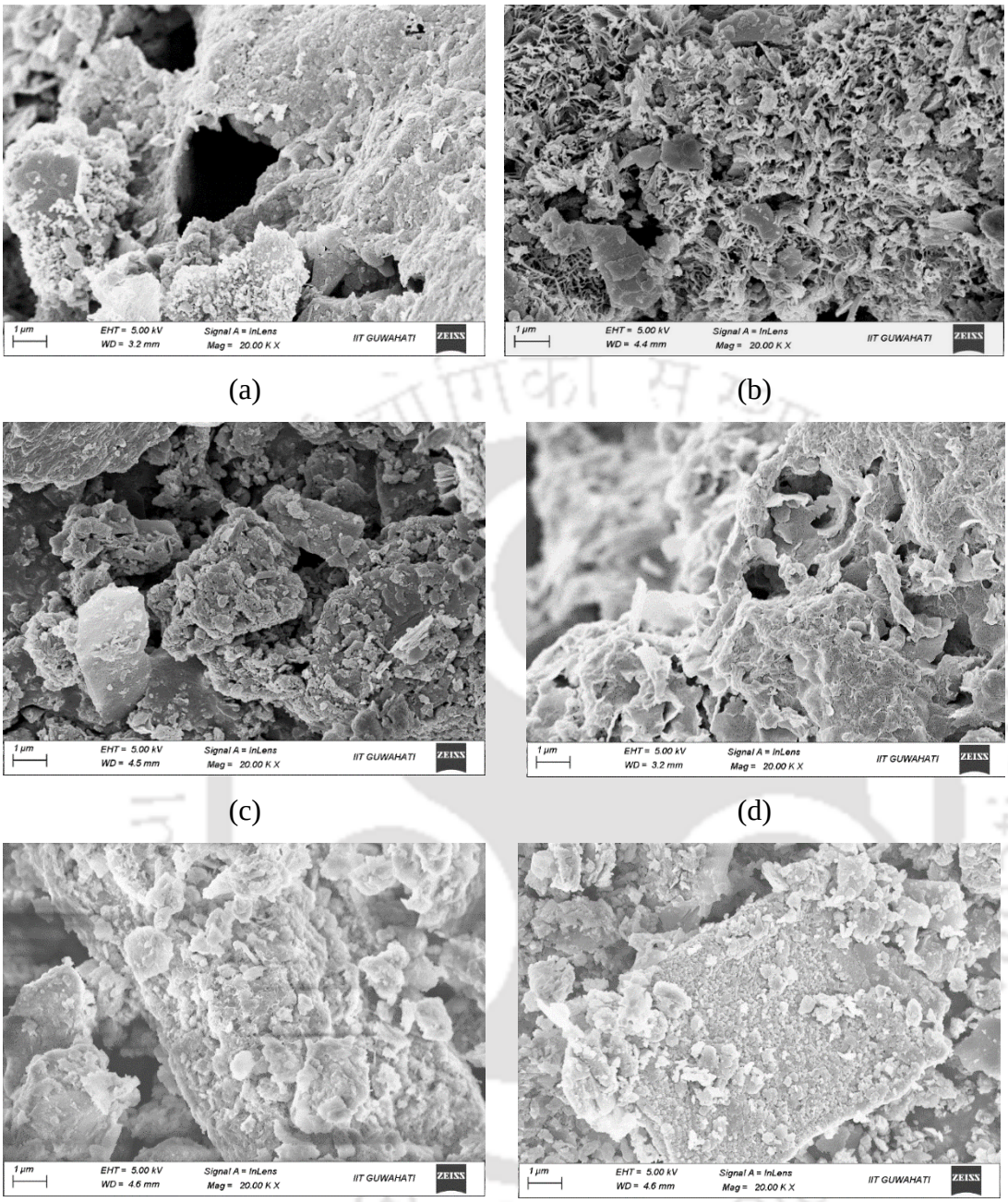

Fig. 7.2. FESEM images of activated carbon (a) AC_KOH_250°C (b) AC_KOH_350°C (c) AC_NaCl_250°C (d) AC_NaCl_350°C (e) AC_ZnCl2_250°C and (f) AC_ZnCl2_350°C

7.5 XRD ANALYSIS OF MSW-AC

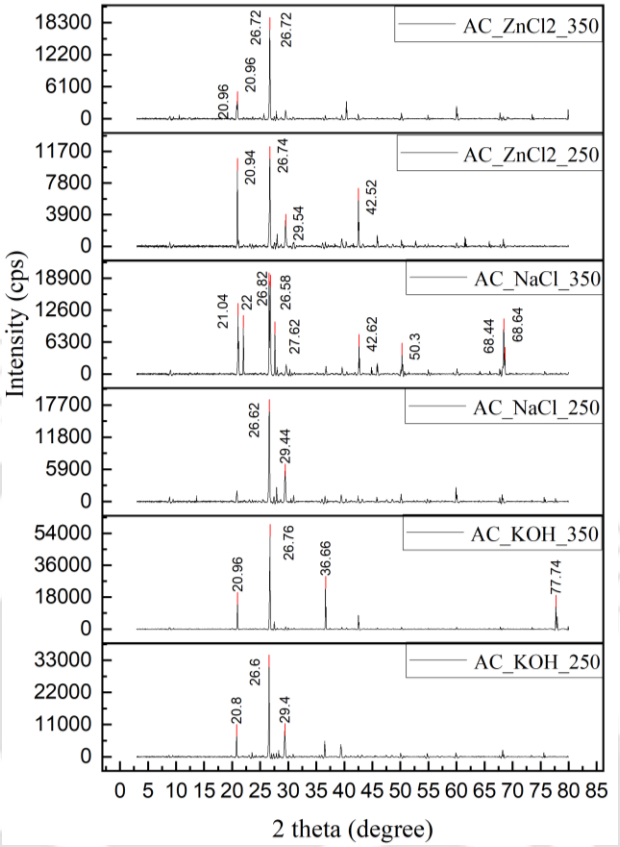

Fig. 7.3 XRD spectroscopy of activated carbon

The XRD analysis of activated carbon derived from MSW char was examined and depicted in Fig. 7.3. Using XRD analysis, the chemical composition, crystallography, and physical characteristics of MSW char-derived activated carbon were determined. The presence of SiO_2 was indicated by peaks observed at 20°, 21°, 22°, 26°, 27°, 28°, 29°, and 36° (Mészáros et al., 2007). As the temperature of MSW char production increased, there was a noticeable enhancement in the crystallinity of the resulting activated carbon. This rise in temperature facilitated the transformation of amorphous silicates into crystalline silicates (Hidayat et al., 2023). The peaks observed between 20° and 26° in the activated carbon correspond to the (002) crystallographic planes, while those between 40° and 43° represent the (100) crystallographic planes of graphite carbon. These planes suggest the amorphous carbon structure of the activated carbon

(Zhang et al., 2022). The crystallinity index was found to be highest for AC_$ZnCl_2$_350 and lowest for AC_KOH_250. Consequently, due to the amorphous nature of AC_KOH_250, produced from MSW char at a lower temperature (250°C), it can be effectively utilized as an adsorbent for the removal of heavy metals from wastewater.

7.6 AAS ANALYSIS OF ACTIVATED CARBON

The AAS analysis aimed to evaluate the concentration of heavy metals in activated carbon due to the diverse composition of MSW. Analysis revealed the presence of Pb, Fe, and Mn. Specifically, concentrations of Pb ranged from 6.22 to 22.49 mg/kg, Fe from 101.4 to 175.85 mg/kg, and Mn from 90.32 to 117.49 mg/kg. Notably, no detectable amounts of Ni and Cd were found in the MSW char, as outlined in Table 7.3. The presence of heavy metals such as Ni and Cd in char can pose significant risks, particularly in applications related to environmental remediation, agriculture, and soil amendments (Angon et al., 2024). When Ni is present in high concentrations, it is regarded as toxic. It can accumulate in water and soil, where it is absorbed by plants and moves up the food chain (Hassan et al., 2019). Ni exposure can also increase the likelihood of adverse health outcomes in people, such as allergic responses, respiratory problems, and possibly even cancer (Genchi et al., 2020). Even in minute quantities, Cd poses a serious threat to both humans and the environment. As a Group 1 carcinogen linked to lung and prostate cancer, Cd is also known to harm bones and kidneys (El-Naggar et al., 2022). Environmental factors affect the bioavailability of Cd in char. Acidic environments increase the mobility and bioavailability of Cd, which raises the possibility that it may be absorbed by plants or seep into water supplies. Food crops and groundwater may thus get contaminated by the Cd in char that is employed as a soil supplement or water filter (El-Naggar et al., 2022). Excessive Pb levels are regarded as hazardous in most environmental uses, such as soil additions, wastewater treatment, and agricultural usage, whereas Fe can have conflicting effects (Akhilesh Kumar and Agrawal, 2020). Char with high quantities of Pb is hazardous and should not be used in most environmental applications unless treated since it poses health hazards, can contaminate the environment, and poison plants (Xiang et al., 2021).

Depending on the situation, elevated Fe concentrations can have both positive and negative impacts. Although Fe can improve the removal of pollutants and provision of nutrients from char, too much Fe can cause iron toxicity in plants and complicate the dynamics of heavy metals in the environment (Harish et al., 2023). Moreover, the capacity of char to adsorb heavy metals can be strongly impacted, both favorably and adversely, by high Fe concentrations. These concentrations of heavy metals fell within the acceptable range for char application in soil amendment, heavy metal remediation in wastewater and composting, with Pb (250-500 mg/kg), Ni (75-150 mg/kg), Fe (400-500 mg/kg), and Cd (3-6 mg/kg) according to the standard permissible limits set by International Biochar Initiative (IBI), European Biochar Certificate (EBC) and US Environmental Protection Agency (EPA) (Alghobar and Suresha, 2017).

Table 7.3. Heavy metal analysis of activated carbon

Sample	Pb (mg/kg)	Ni (mg/kg)	Fe (mg/kg)	Mn (mg/kg)	Cd (mg/kg)
AC_NaCl_250	13.05 ± 0.02	ND	126.65 ± 0.46	92.21 ± 0.11	ND
AC_NaCl_350	14.68 ± 0.02	ND	154.75 ± 0.16	90.32 ± 0.04	ND
AC_KOH_250	6.22 ± 0.04	ND	101.4 ± 0.09	103.49 ± 0.05	ND
AC_KOH_350	7.13 ± 0.04	ND	105.51 ± 0.22	107.6 ± 0.04	ND
AC_$ZnCl_2$_250	20.3 ± 0.03	ND	168.13 ± 0.11	113.44 ± 0.08	ND
AC_$ZnCl_2$_350	22.49 ± 0.06	ND	175.85 ± 0.09	117.5 ± 0.11	ND

*ND: Not Detected

7.7 BATCH ADSORPTION STUDY BY USING MSW-AC

The analysis of the MSW char-activated carbon revealed that AC_KOH_250 demonstrated the characteristic of the highest efficacy in adsorption experiments. This activated carbon, prepared by chemical activation using KOH, was selected for further examination as an adsorbent for the adsorption of Pb(II). An optimization study was conducted to identify the ideal pH, dosage of activated

carbon, concentration of Pb(II), and duration of contact to maximize the efficiency of heavy metal removal.

7.7.1 Optimization of pH

The batch adsorption experiment involved using 0.5 g of AC_KOH_250, a heavy metal concentration of 100 ppm (Pb(II)), a contact time of 1 h, and a rotation speed of 150 rpm. The pH of the solution was adjusted using 0.1 N HCl. Results indicated that as the pH rises, the soluble Pb(II) gradually decreases, as depicted in Fig. 7.4 (a). However, precipitation initiates once the pH reaches 6.5. Therefore, the optimal pH for Pb(II) removal is determined to be 6.

7.7.2 Effect of contact time

The percentage removal of heavy metal by varying the contact time was studied by keeping the conditions of pH at 6, 0.5 g of AC_KOH_250, 100 ppm (Pb(II)) metal concentration, and 150 rpm rotation speed. As shown in Fig. 7.4 (b), it was clearly found that the contact time does not exert a notable influence on the adsorption process by using the activated carbon. Effective removal of the target substance is observed even at zero contact time, indicating that the adsorption capacity of the activated carbon is highly efficient and instantaneous adsorption capacity.

7.7.3 Effect of MSW-AC dose for Pb(II) removal

The effect on the percentage of heavy metal removal was studied by varying the dosage of activated carbon, provided the pH was kept at 6, the metal concentration was 100 ppm, the duration of contact was 1 h, and the agitation speed of 150 rpm, as shown in Fig. 7.4 (c). This allows to identify the optimal dose that provides the best balance between adsorption efficiency, cost-effectiveness, and practical considerations. As the dose of MSW-AC increases, there is a corresponding increase in the removal of lead until reaching a dose of 1g. At this specific dose, a 99% removal efficiency for Pb(II) has been achieved. The ion exchange, in which cations on char surfaces (such as Ca^{2+} and K^{2+} ions) are swapped out for Pb^{2+} ions, and electrostatic attraction between the negatively charged char surface and positively charged lead ions are two of the several

processes that contribute to the adsorption of Pb(II) from water. Stable metal-ligand interactions with functional groups (-COOH and -OH) cause surface complexation, whereas precipitation results in the development of insoluble lead compounds on the surface of the char. Along with the possible reduction of Pb(II) to elemental lead on char with redox-active sites, physical adsorption caused by van der Waals forces and cation interactions with aromatic structures also contribute. The efficacy of Pb(II) adsorption is greatly influenced by variables such pH, char characteristics, and the presence of competing ions.

7.7.4 Effect of heavy metal dose

According to the data presented in Fig.7.4 (d), the heavy metal removal efficiency of over 90% can be achieved for Pb(II) with concentrations up to 1000 ppm when pH is kept constant at 6, activated carbon dosage of 1 g, contact time 1 h, and rotation speed of 150 rpm.

7.7.5 Collective impact of pH, metal dosage, and activated carbon dosage

Analyzing the combined effect of metal dose, activated carbon, and pH provides valuable insights into the intricate relationship among these factors and their impact on the adsorption process. This knowledge is essential for optimizing the adsorption process and devising efficient strategies for metal removal. Fig. 7.4 (e) indicates that a pH of 6.5, an activated carbon dose of 1 g, and a metal dose of 500 mg/L represent the most suitable conditions for heavy metal adsorption by using MSW char-activated carbon. These conditions strike a balance between high adsorption efficiency and the cost-effectiveness of heavy metal removal from water.

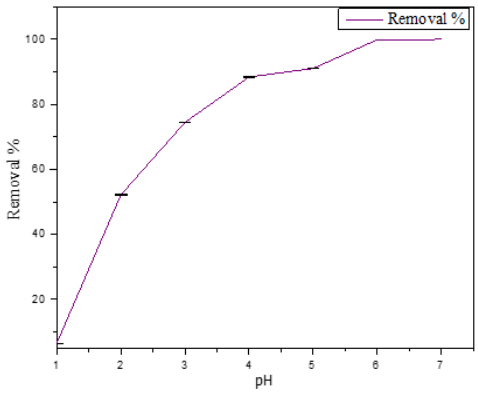

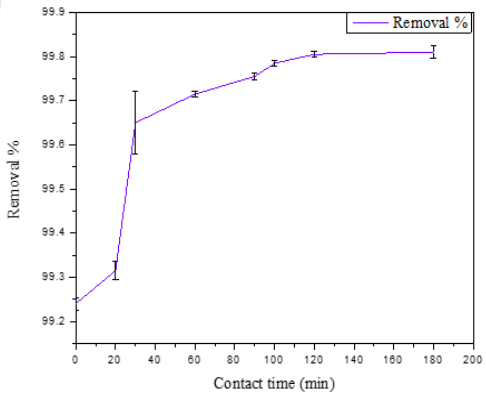

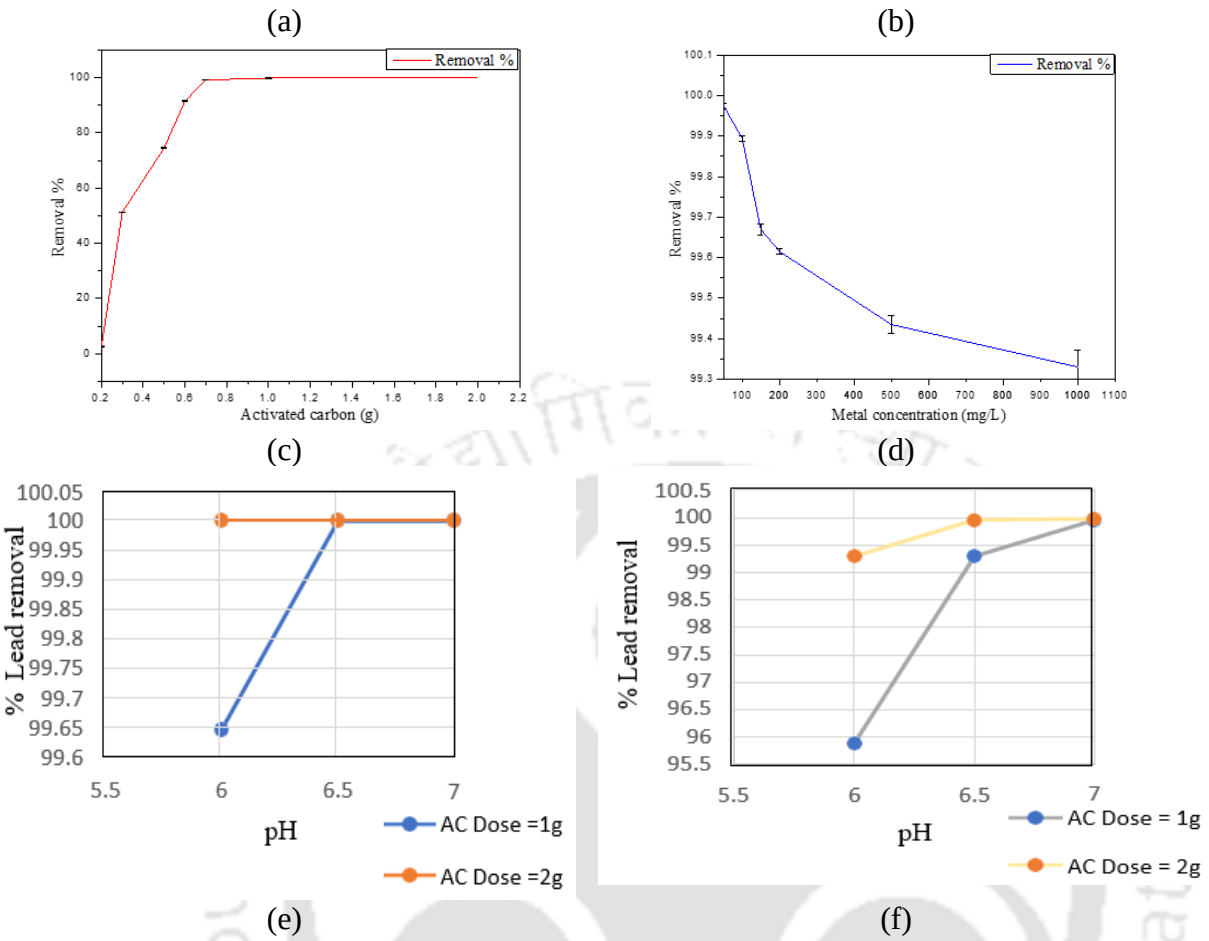

Fig. 7.4. Effect on the percentage of heavy metal removal at varying (a) pH, (b) contact time, (c) activated carbon dosage, (d) metal concentration on removal efficiency by using activated carbon and with respect to pH and activated carbon dose at a metal concentration of (e) 1000 mg/L and (f) 500 mg/L

7.8 ADSORPTION KINETICS AND ISOTHERMS

To evaluate the efficacy of the adsorption, the linearized versions of both first and second-order kinetics were computed and are detailed in Table 7.4. Table 7.4 presents a comparison of the outcomes from the two models, revealing that the second-order model, with an R^2 value of 0.99, demonstrates a superior fit compared to the first-order model, as depicted in Fig. 7.5 (a) and (b). Consequently, the kinetics analysis suggests that equilibrium was attained within an hour.

Adsorption isotherms provide insights into the concentration of adsorbate

adsorbed and the concentration in the solution at equilibrium and constant temperatures (Al-Ghouti and Da'ana, 2020). This visual representation offers valuable insights into the suitability of the adsorbent. Table 4 summarizes the parameters of Langmuir and Freundlich found from analyzing experimental data. The results indicate that the adsorption pattern of the prepared carbon sample for Pb(II) aligns well with the Langmuir model (R^2 = 0.956), as shown in Fig. 7.5 (c) and (d), suggesting effective adsorption of Pb(II) onto MSW char-activated carbon in a monolayer based on optimized parameters. According to the Langmuir isotherm hypothesis, the adsorption process is confined to the first layer of the adsorbent, where all existing sites on the surface are identical and bind one molecule of the adsorbate each (El-Bery et al., 2022).

Table 7.4. Comparison of Pseudo-first and second-order models

Initial concentration of Pb (II) (mg/L)	**Pseudo-first-order kinetics**			**Pseudo-second-order kinetics**		
	q_e (mg/g)	**k_1**	**R^2**	**q_e (mg/g)**	**k_2**	**R^2**
1000	3.27	5.34×10^{-7}	0.821	2.98	1.232	0.99
	Langmuir isotherm			**Freundlich isotherm**		
	q_{max} (mg/g)	**K_L**	**R^2**	**K_F**	**1/n**	**R^2**
	51.07	0.65	0.95	0.18	0.93	0.70

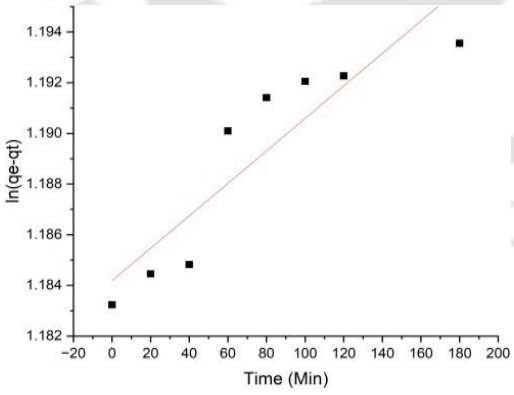

(a)

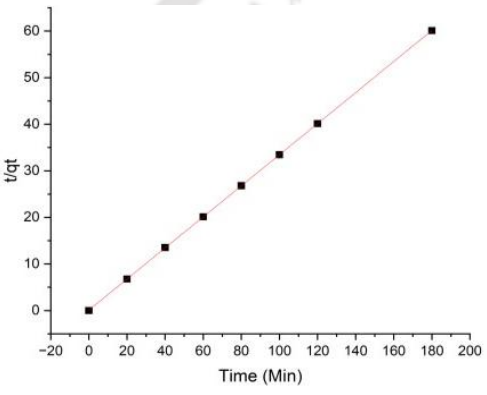

(b)

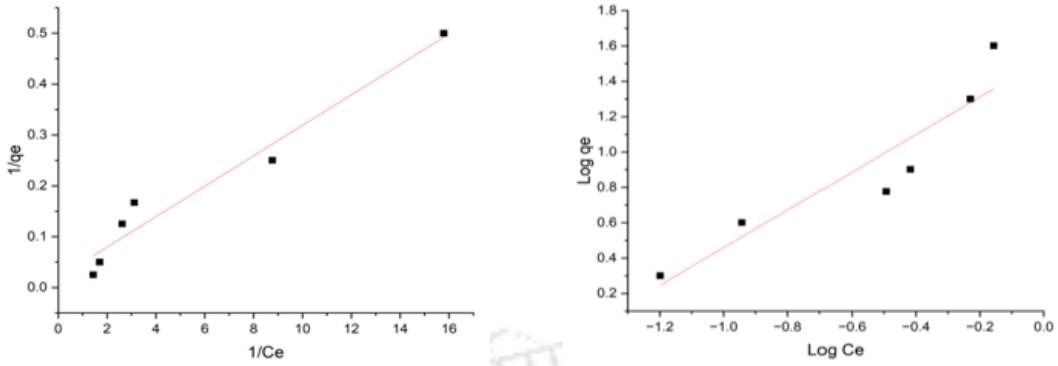

(c) (d)

Fig. 7.5. (a) Pseudo First order (b) Pseudo Second order (c) Langmuir and (b) Freundlich isotherm model plot

7.9 VALIDATION OF ADSORPTION STUDY

The FTIR spectra, SEM micrographs, and EDX spectra of MSW-AC were taken before and after the Pb(II) adsorption, as represented in Fig. 7.6. Fig. 7.6 (a) and (b) illustrate shifts occurring in the functional groups of the activated carbon. These shifts indicate alterations in the chemical environment or bonding of these functional groups due to the interaction with Pb(II) ions. Additionally, the peaks corresponding to the functional groups display both increases and decreases in intensity. This could be attributed to the participation of specific functional groups in the adsorption process or changes in their concentration on the surface of the activated carbon. The SEM micrographs revealed that the activated carbon possessed a highly porous and regular shape prior to its interaction with Pb(II). However, after the removal of Pb(II), the surface of the activated carbon appeared rough. The EDX analysis further supported this observation, as shown in Fig. 7.6 (e) and (f). The EDX spectra displayed peaks in the energy range of 2 to 16 KeV and a significant presence of peaks corresponding to Pb (II). This indicates that Pb (II) ions were adsorbed onto the activated carbon, leading to the appearance of distinct peaks in the EDX spectra.

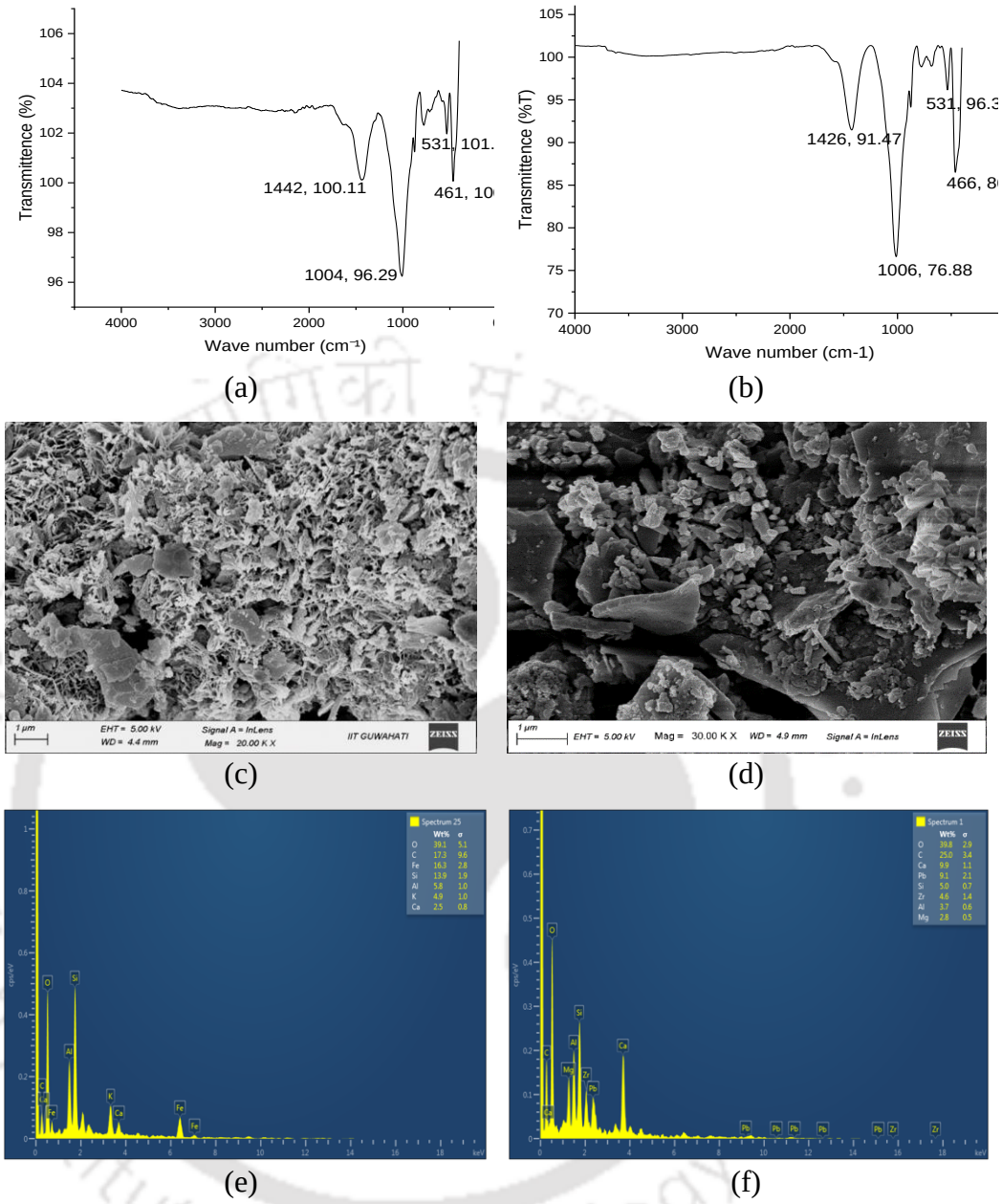

Fig. 7.6. (a) and (b) FTIR spectroscopy, (c) and (d) FESEM, and (e) and (f) EDX spectroscopy of activated carbon before and after adsorption, respectively

7.10 CYCLE STUDY USING ACTIVATED CARBON

The cycle study was conducted under precise parameters, comprising a pH level of 6, a rotation speed of 150 rpm, a contact duration of 1 h, a metal concentration of 1000 ppm, and 1 g of activated carbon. It was observed that a total of three cycles could be executed with an efficiency of 80%, as shown in Fig. 7.7, with two of

these cycles surpassing an efficiency of 90% and a decline in the removal percentage of Pb (II) during the fourth cycle.

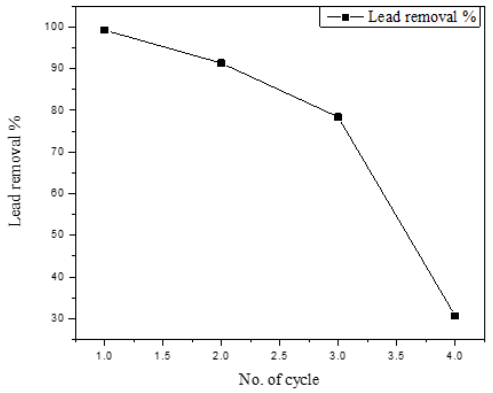

Fig. 7.7. Cycle study for Pb (II) removal using activated carbon

7.11 DESORPTION, RECOVERY, AND REUSE STUDY

The desorption study revealed that HNO_3 emerged as the most efficient eluent for removing contaminants, as shown in Fig. 7.8. Optimal desorption outcomes were achieved under acidic conditions with a pH of 1 across all eluent types. Interestingly, when using HNO_3, the duration of contact had a relatively minimal impact, possibly due to a higher recovery rate associated with HNO_3. Notably, after 2 h, the recovery rate in HNO_3 remained fairly constant. Conversely, H_2SO_4 demonstrated slower desorption kinetics, necessitating a longer desorption period for effectiveness. The recovery rates of activated carbon after desorption were 43.05, 50.60, and 64.89% for HNO_3, HCl, and H_2SO_4, respectively.

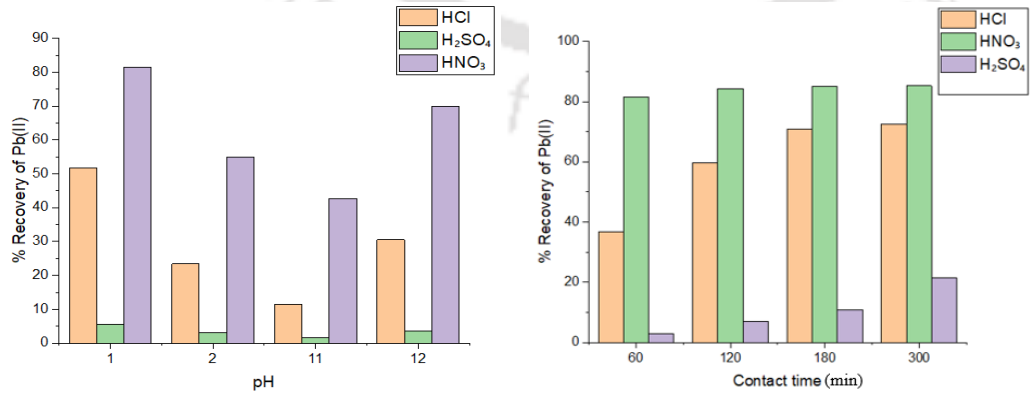

Fig. 7.8. Effect of (a) pH and (b) Contact time in desorption study

7.12 CONCLUSION OF ADSORPTION STUDY USING MSW-AC

The activated carbon derived from MSW char displayed similar properties to commercially available activated carbon. Various analyses, including proximate analysis, FTIR spectroscopy, pH, iodine number, FESEM, and XRD spectroscopy, indicated that MSW char produced at 250°C and chemically activated with KOH was highly effective in the adsorption of Pb(II). In batch adsorption tests, more than 90% of Pb(II) could be removed from water under optimized conditions using KOH-activated carbon. Kinetic studies suggested that the adsorption followed Lagrange's pseudo-second-order model, and equilibrium was reached within an hour. The adsorption isotherm supported the Langmuir model, indicating monolayer adsorption. Validation studies using FTIR, FESEM, and EDX confirmed the adsorption of Pb(II) ions onto the activated carbon. The activated carbon could be reused for about two cycles with a removal efficiency of more than 90%. Desorption experiments showed that the highest metal recovery rate was achieved using HNO_3 as an eluent. Given its impressive performance in adsorption, desorption, and cycle studies, MSW char-activated carbon appears to be a viable option for removing heavy metals from wastewater. This study not only highlights the effectiveness of MSW char-activated carbon but also presents a cost-effective and sustainable solution for waste minimization at dumpsites and wastewater treatment by utilizing MSW.

CHAPTER 8

APPLICATION OF MSW CHAR IN COMPOSTING

8.6 INITIAL CHARACTERIZATION OF SUBSTRATE

The preliminary characterization of the composting material char is shown in Table 8.1. The moisture content of vegetables was very high (89.23 %), whereas the moisture content of MSW char was very low, about 1.14%. To avoid leachate formation during the composting process and to optimize the C/N ratio, bulking agent sawdust was used. The presence of optimum moisture is significant for regulating temperature within the compost pile. Composting is characterized as an exothermic phenomenon, signifying its capacity to produce thermal energy. The presence of appropriate moisture levels promotes the effective dispersion of heat inside the pile, hence sustaining the optimal temperature range required for decomposition. The initial pH values of vegetable waste, cow dung, sawdust, and MSW char were 5.87, 6.2, 6.35, and 7.10, respectively. These values fell within the optimal range for fungal growth (5.0-8.5) and bacterial development (6.0-7.5) (Meena et al., 2021). The electrical conductivity of vegetable waste measured at 1.93 mS/cm indicates a low presence of soluble salts, reflecting the material salinity arising from exchangeable chloride, sodium, sulfate, nitrate, potassium, and soluble salts or due to the presence of highly conductivity metal ions (Feng et al., 2021). The sBOD of vegetable waste was higher than cow dung, indicating more degradable carbonaceous materials (Mangkoedihardjo et al., 2006). Vegetable waste also contained 79.84% volatile solids, 2.45% TKN, and 18.51 g/kg of total phosphorus, which resembles nutrient richness and is a feasible option for composting. The C/N ratio of sawdust indicated a higher amount of carbonaceous matter. The Fecal coliform of cow dung was 2.4×10^{11}, which determines the high concentrations of pathogenic bacteria (Hazarika and Khwairakpam, 2018). The concentration of Ca, K, Mg, and Na was in the order of Ca>K>Mg>Na for control, trial 1, and trial 2. The initial concentration of metals in MSW char was observed to be high, as depicted in Table 8.1.

Table 8.1 Initial characterization of substrate

Parameters	Vegetable waste	Cow dung	Saw dust	MSW Char
Moisture Content %	89.23 ± 0.23	90.08 ± 1.24	13.2 ± 0.2	1.14 ± 0.13
pH (1:10)	5.87± 0.09	6.2 ±0.12	6.35 ± 0.14	7.10 ± 0.04
EC (1:10)	1.93 ± 0.08	2.93 ±0.11	1.29 ± 0.08	3.57 ± 0.15
Oxygen uptake rate	30.4 ± 0.7	21.9 ±0.61	8.90 ± 0.9	-
CO_2 Evolution rate	21 ± 1.12	13 ± 1.30	9 ± 1.23	-
Volatile matter %	79.84 ± 1.23	84.8 ± 2.78	91.27 ±1.25	21.13 ± 0.31
Ash Content %	20.16 ± 1.11	15.2 ± 2.33	8.73 ± 0.98	2.83 ± 0.36
TOC %	44.36 ± 1.23	47.11 ± 2.79	50.71 ± 1.21	1.83 ± 0.67
TKN %	2.45 ± 0.14	0.84 ± 0.14	0.28 ± 0.07	0.42 ± 0.02
C/N Ratio	18.1 ± 0.45	56.1 ± 0.23	181.1 ± 3.87	5.07 ± 0.03
Ammonia (mg/kg)	106.26 ± 0.41	179.4 ± 1.5	88.93 ± 0.11	18.91 ± 0.23
Nitrate (mg/kg)	20.54 ± 0.12	2.46 ± 0.19	17.07 ± 0.67	61.78 ± 0.13
sCOD (mg/l)	2880 ± 17	1152 ± 23	768 ± 12	-
sBOD (mg/l)	1020 ± 19	645 ± 14	195 ± 19	-
Total phosphorus (g/kg)	18.51 ± 0.32	12.25 ± 0.4	2.5 ± 0.2	7.23 ± 0.29
Available phosphorus (g/kg)	1.04 ± 0.23	2.45 ± 1.01	0.87 ± 0.42	3.14 ± 0.13
Fecal Coliform	-	2.4×10^{11}	-	-
Mg (g/kg)	2.75 ± 0.65	3.12 ± 0.4	1.28 ± 0.3	4.25 ± 0.28
K (g/kg)	5.23 ± 0.8	0.16 ± 0.12	0.8 ± 0.14	9.18 ± 0.3
Ca (g/kg)	39.39 ± 2.21	39.23 ± 3.40	21.9 ± 1.76	7.46 ± 0.12
Na (g/kg)	3.72 ± 0.8	3.23 ± 0.7	1.67 ± 0.9	3.05 ± 0.3
Mn (mg/kg)	996.15 ± 3.2	521.55 ± 4.5	483.55 ± 2.1	204.12 ± 0.5
Fe (mg/kg)	10229 ± 7.67	9547.75 ± 8.98	6439.4 ± 7.43	2234.81 ± 61
Cr (mg/kg)	78.3 ± 0.97	142.8 ± 0.87	40.8 ± 0.78	83.42 ± 2.65

Pb (mg/kg)	996.5 ± 1.23	525 ± 3.12	483.55 ± 5.23	345 ± 2.12
Cd (mg/kg)	< BDL	< BDL	< BDL	< BDL
Cu (mg/kg)	101.8 ± 1.67	57.5 ± 2.12	205.1 ± 2.34	117.63 ± 0.12
Ni (mg/kg)	365.1 ± 4.23	320.9 ± 6.12	244.25 ± 2.89	213.45 ± 1.45
Zn (mg/kg)	213 ± 2.10	156.7 ± 7.55	143.54 ± 5.97	419.24 ± 4.12

Note: The data is presented in *xx* ± *yy* format where xx denotes the average value *yy* denotes the standard deviation, BDL: below detection level

8.7 VARIATION OF TEMPERATURE AND MOISTURE CONTENT DURING THE COMPOSTING PROCESS

The vegetable waste, which contains the highest quantity of organic content, triggers the activity of microbes at the onset of the composting process, resulting in a rise in temperature. This temperature increase was observed during the initial phases of composting, i.e., within 12 hours in Control, Trial 1, and Trial 2. The highest temperature of 53.8°C was observed when 5% MSW char was applied in Trial 2, followed by 50.8°C in Trial 1 and 46.8°C in Control, as shown in Fig. 8.1 (a). The thermophilic phase lasted longer in Trial 2 due to the cumulative increase of MSW char, which was comparable to biochar amendment during composting (Jain et al., 2018). The rise in temperature during the composting process is attributed to the destruction of pathogenic bacteria and a higher rate of decomposition of biodegradable carbon. The introduction of MSW char elevates the maximum temperature and accelerates the timeframe to attain high temperatures. This is attributed to the increased porosity caused by the addition of MSW char during the composting, facilitating greater oxygen availability. Consequently, the heightened porosity boosts the metabolic activities of microorganisms, leading to increased heat release. Additionally, the incorporation of char extends the duration of the high-temperature phase, as MSW char effectively sustains elevated temperatures owing to its microporous structure.

However, excessive MSW char can elevate temperatures excessively, leading to undesirable moisture loss, which is unfavorable for composting (Jain et al., 2018).

The moisture content of vegetable waste (89%) and cow dung (90%) was very high. To avoid leachate formation due to organic waste with high moisture content and for proper circumferential degradation, bulking agents such as grass cutting, dry leaves, sawdust, and MSW char were minced with inoculum and the substrate. (Kalamdhad et al., 2008) reported that microbial activity decreases at low moisture content, and at high moisture content, the composting process slows down to anaerobic conditions. The rise in temperature was observed in a few days due to readily biodegradable matter, and there was no formation of leachate during the process of composting. The heat produced due to biological decomposition results in vaporization or moisture loss due to the rise in the rate of the decomposition process (Jain et al., 2018). The inclusion of MSW char led to a decrease in moisture content, as depicted in Fig. 8.1 (b). This occurred as the addition of char lowered bulk density, promoting improved aeration and enhanced microbial activity. Consequently, there was increased heat loss, leading to greater moisture evaporation comparable to the moisture loss with biochar application during composting (Jain et al., 2018). Additionally, char contributed to the loosening of the compost structure, facilitating enhanced ventilation. This, in turn, boosted microbial activity, resulting in increased water absorption by the microbes.

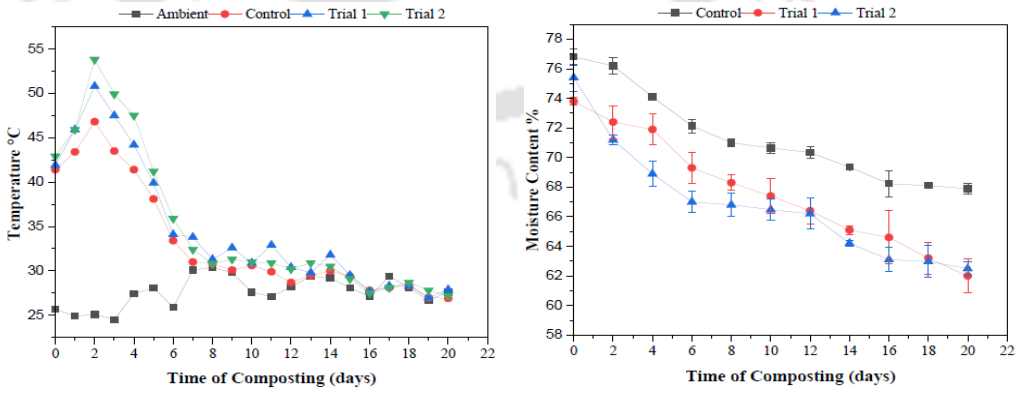

(a) (b)

Fig. 8.1. Changes in (a) Temperature and (b) Moisture content during the process of composting

8.8 VARIATION OF PH AND ELECTRICAL CONDUCTIVITY

The pH has a significant impact on microbial activity, and it has been observed that a neutral pH is optimal for the composting process. Metabolic process is more at 7.5-8.5 (Wong et al., 2009). The initial pH of mixes was recorded as 6.6, 6.72, and 6.84, which was increased to 7.5, 7.87, and 8.2 in Control, Trial 1, and Trial 2, respectively, as shown in Fig. 8.2 (a). The introduction of MSW char in the process of composting elevates the pH values in all treatments during the initial warming stage compared to the control. The pH of the final compost with the addition of MSW char was within the range of the pH of the biochar-added compost (7.4-8.5) (Jain et al., 2018). In the warming phase, NH_3 is generated, facilitating the breakdown of organic matter by bacteria and fungi. Subsequently, the pH gradually decreases in the middle and concluding stages of composting as bacteria and fungi convert some organic matter into organic acids, aiding the breakdown of lignocellulosic structures. During the cooling period, the pH stabilizes. Additionally, the ash content of char, containing Na^+, Ca^+, K^+, and Mg^+, undergoes ion exchange with H^+ ions, further contributing to an increase in pH.

The EC value higher than 4 $mScm^{-1}$ causes a toxic effect on plants after its application (Qu et al., 2022). At the beginning of the composting process, the EC value was maximum, resulting from the release of ammonium ions and salts due to increased biodegradation of organic matter during the thermophilic phase. As shown in Fig. 8.2 (b), with the application of MSW char in Trial 1, it was detected that the EC values reduced in the later stage of composting as compared to control due to precipitation of mineral salts, volatilization of ammonia and conversion of NH_4^+ into nitrate. Moreover, humification might bind small molecules during the maturation phase, lowering their abundance in the solutions obtained from solid samples through water extraction for EC analysis (Feng et al., 2021).

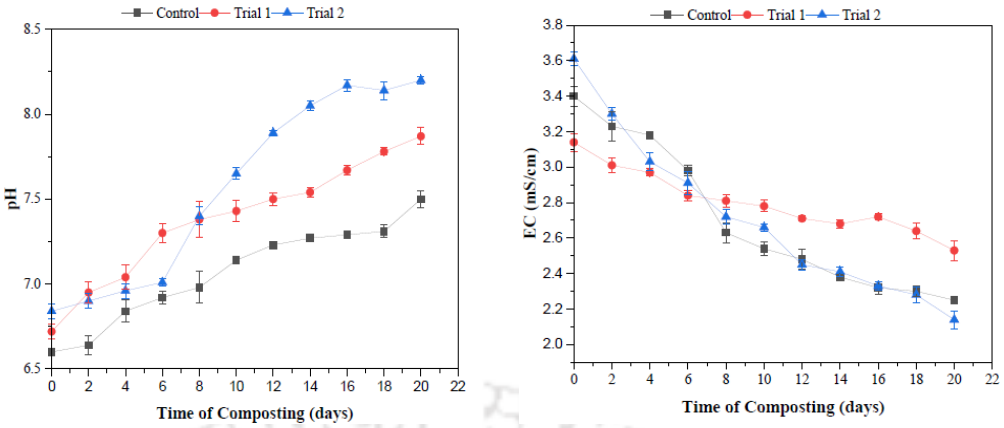

(a) (b)

Fig. 8.2. Variation of (a) pH and (b) Electrical conductivity

8.9 VARIATION OF VOLATILE SOLID, TOTAL ORGANIC CARBON, AND ASH CONTENT DURING THE COMPOSTING PERIOD

The greater the volatile solids concentration, the higher the content of organic matter. When MSW char was introduced, Trial 2 exhibited a maximum reduction of 21.02% in volatile solids, in contrast to 19.11% in Trial 1 and 17.67% in the Control, as shown in Fig. 8.3 (a). Maximum reduction of volatile solids was observed in the thermophilic phase as thermophilic bacteria decompose the organic matter rapidly (Jain et al., 2018). Initially, TOC was in the range of 27.28, 33.26 and 26.82%; after the application of MSW char, it finally reduced to 22.35, 26.17 and 21.18% in Control, Trial 1, and Trial 2, respectively, during the co-composting process, as depicted in Fig. 8.3 (b). Consumption of organic carbon as an energy source by microbes and CO_2 produced by bacteria during the metabolic process are causes of the decrease of TOC during the process of composting (Daga et al., 2018). As shown in Fig. 8.3 (c), the ash content increases by 14.82, 26.65 and 19.62% in Control, Trial 1, and Trial 2, respectively, due to organic matter degradation and high ash content of MSW char. The decrease in volatile solids synchronized with an increase in ash content in all three treatments.

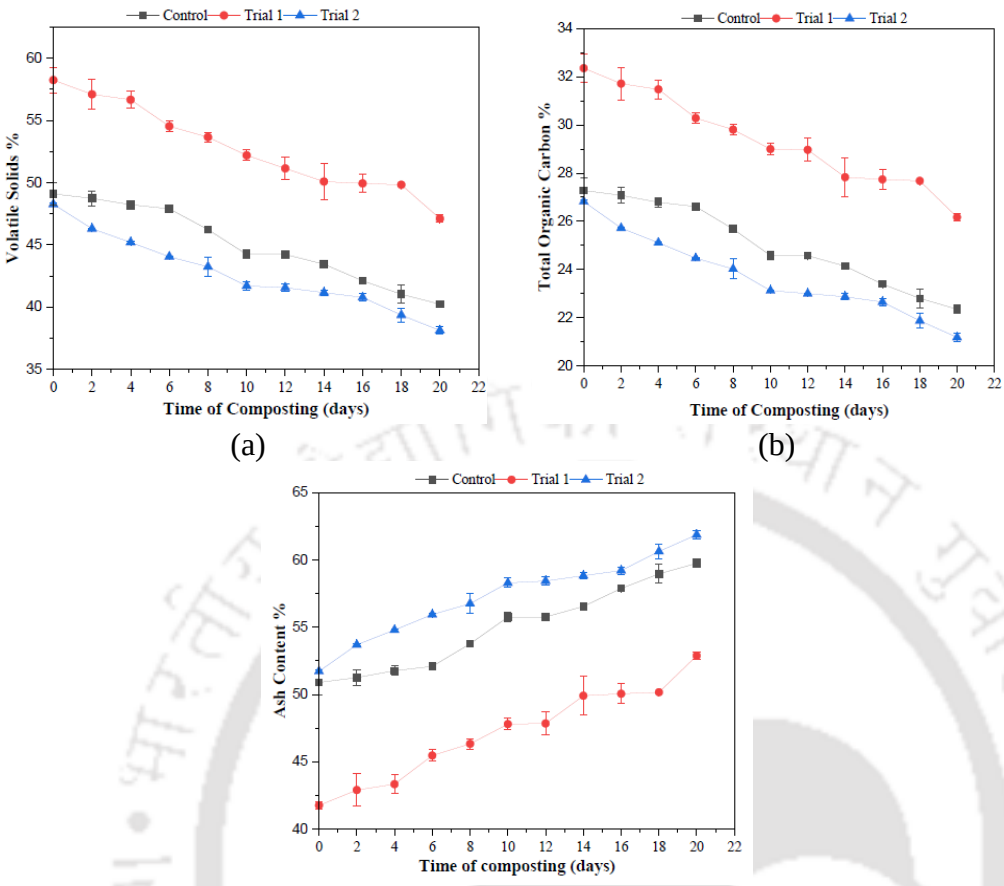

Fig. 8.3. Variation of (a) Volatile solid, (b) Total organic Carbon, and (c) Ash Content during the process of composting

8.10 NITROGEN DYNAMICS (TKN & NH_4-N) AND PHOSPHORUS (TOTAL PHOSPHORUS AND AVAILABLE PHOSPHORUS) DYNAMICS DURING THE COMPOSTING PERIOD

Nitrogen and Phosphorus are the essential macronutrients that are required by the plant for its growth. The TKN was observed in the range of 0.96, 1.12 and 1.19% on day 0, increases to 2.17, 2.24 and 2.35% on day 20 in Control, Trial 1, and Trial 2, respectively, as shown in Fig. 8.4, which was in the range of increase in the percentage of TKN value with the amendment of biochar during composting (Jain et al., 2018). Because of the overall loss of dry mass caused by CO_2 emission and water loss due to evaporation resulting from the heat generated during the oxidation of organic material, TKN increased during the rotary drum composting

process. In the cooling phase, there is a gradual rise in TKN content. The inclusion of MSW char facilitates the breakdown of cellulose, supplying nutrients to the composting process. Additionally, char contributes to nitrogen fixation, serving as a source of nitrogen for the growth and reproduction of microorganisms (Qu et al., 2022). The NH_4 was observed in the range 94.12, 102.49, and 93.41 mg/kg on day 0, reducing to 34.1, 38, and 32.37 mg/kg on day 20 in Control, Trial 1, and Trial 2, respectively, which was comparable to the biochar application during composting of various substrate (Guo et al., 2020). The result shows that the concentration of NH_4-N has significantly decreased throughout all treatments, and the decrease was greater when 2.5% MSW char was added in Trial 1. As the temperature increases rapidly with the addition of MSW char, the composting enters the high-temperature phase where volatilization of NH_3 takes place, which results in a decrease of the NH_4^+-N content, which is similar to the case of biochar amendment (Agyarko-Mintah et al., 2017). The organic nitrogen transforms to ammoniacal nitrogen in the initial period of the composting process. Due to intense aeration, a significant rise in pH, and the loss of CO_2 during the process, NH_4^+-N decreases during the maturation stage (Kauser et al., 2020). The high amount of Total Phosphorus was observed on the initial day, which may have been caused by a higher concentration of vegetable waste, cow dung, and MSW char (Kalamdhad et al., 2008). During the process of composting, total phosphorus increased from 14.13, 14.1, and 16.79 mg/kg to 20.1, 20.89, and 23.48 mg/kg in Control, Trial 1, and Trial 2, respectively. The percentage increase of total phosphorus was highest about 6.7%, when 5% of MSW char was applied. Available phosphorus increased from 0.84, 0.95 and 1.02 mg/kg to 2.28, 2.38, and 2.49 mg/kg in Control, Trial 1, and Trial 2, respectively, as shown in Fig. 8.4. The maximum increment of available phosphorus and total phosphorus was observed in Trial 2, when 5% MSW char was co-composted with vegetable waste, compared to Trial 1 and Control which was comparable to biochar addition with compost (Doan et al., 2015). Bacterial mineralization and the decomposition of organic biomass during the composting process lead to an increase in phosphorus (Kauser et al., 2020).

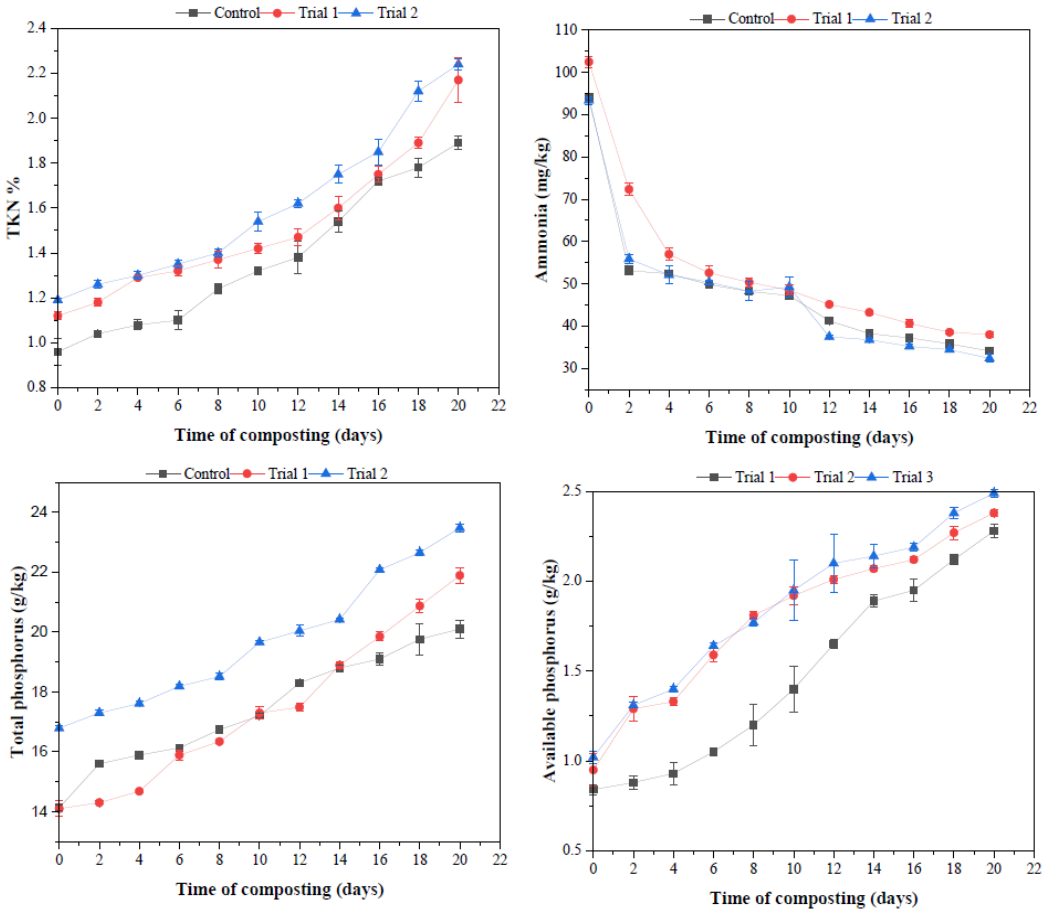

Fig. 8.4. Nitrogen Dynamics (TKN & NH_4-N) and Phosphorus (TP and AP) dynamics during the co-composting period

8.11 VARIATION IN C/N RATIO DURING COMPOSTING PERIOD

Another important parameter that is crucial for nutrient balance and microbial growth during the composting process is the C/N ratio. Microorganisms mostly obtain their resources from carbon, while nitrogen is crucial for the synthesis of the protozoa that make up cells. Analyzing the alterations in the C/N ratio allows for the measurement of organic matter decomposition and the stabilization of compost. A C/N ratio exceeding 30/1 could lead to a reduction in the activity of microbes, and below 18/1 may result in nitrogen loss to the atmosphere as ammonia. Therefore, the C/N ratio between 19-30 is ideal for microbes during composting (Kauser et al., 2020). In the present study, C/N reduced from 28.55, 28.9, and 22.54 to 11.83, 12.09, and 10 in Control, Trial 1, and Trial 2, respectively, as shown in

Fig. 8.5. Final Compost with a C/N ratio between 10-15 indicates good degree of maturity (Varma and Kalamdhad, 2015). It was observed that when 2.5% of MSW char was added during the co-composting of vegetable waste, the final product had much better maturity as compared to 5% MSW char and control. The range C/N ratio for a matured compost was within the range when MSW char was applied during composting akin to biochar (Guo et al., 2020).

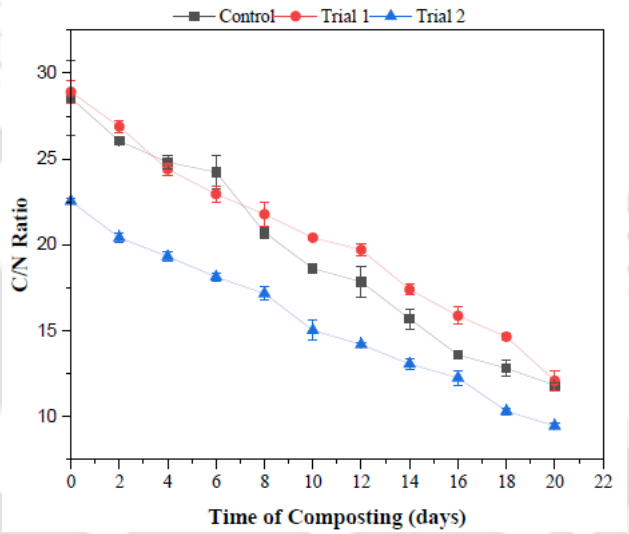

Fig. 8.5. Variation in C/N ratio during composting

8.12 VARIATION OF MACRONUTRIENTS DURING THE COMPOSTING PERIOD

Potassium is the third most important macronutrient required by the plants for its growth whereas magnesium is required by the plants for chlorophyll production. Calcium is the secondary macronutrient required by the plant for the cell division. It was observed that with the addition of MSW char, the total potassium increased from 3.08, 3.01, and 3.12 g/kg to 5.86, 6.9, 6.13 g/kg in Control, Trial 1, and Trial 2, respectively, as shown in Fig. 8.6. The other macronutrients such as total Na, Mg, and Ca exhibited an upward trend during composting for all trials. The final values found to be 4.23 g/kg (Control), 4.73 g/kg (Trial 1), 4.58 g/kg (Trial 2) of sodium, 40.89 g/kg (Control), 44.9 g/kg (Trial 1), 51.79 g/kg (Trial 2) of Calcium and 3.14 g/kg (Control), 3.3 g/kg (Trial 1), 3.32 g/kg (Trial 2) of Magnesium. The

highest concentration of macronutrients was observed in Trial 2 when 5% of MSW char was added, which also indicated the highest reduction of volatile solids and was comparable with the co-composting of biochar (Jain et al., 2018). The concentration of total Mg, Na, Ca, and K increased due to the loss of dry mass of materials caused by the decomposition of Organic matter and subsequent mineralization during the composting process.

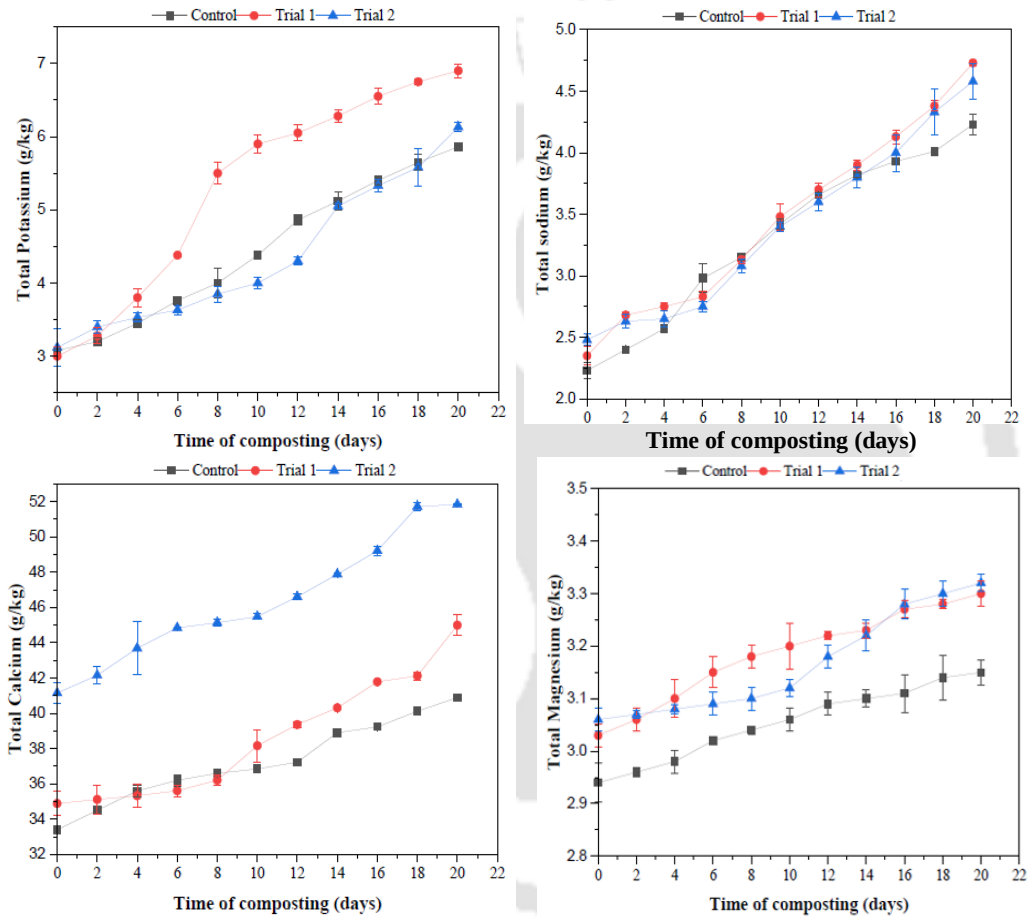

Fig. 8.6. Variation of Macronutrients: Potassium, Sodium, Calcium and Magnesium during composting period

8.13 sCOD, sBOD, AND VARIATION OF CO_2 EVOLUTION RATE DURING THE COMPOSTING PERIOD

Composting involves the aerobic decomposition of organic matter. Changes in sBOD and sCOD levels depend on the organic material degradation. The sBOD

and sCOD decreased in all trials during the composting process due to vegetable waste degradation, as shown in Fig. 8.7. In Trial 2, there was a maximum reduction in sBOD (89.33%) followed by Trial 1 (84.68%) and Control (83%). There was no significant difference in the reduction of the body after 18 days of composting in Trial 1 and Trial 2. Initially, sCOD was in the range of 505, 568, and 450 mg/l, finally reduced to 90, 87, and 48 mg/l in Control, Trial 1, and Trial 2, respectively, during composting. The degradation of organic matter by microbes during the composting reduces sBOD and sCOD, which in turn lowers carbon dioxide emissions. The emission of CO_2 decreased because of a decrease in sBOD and sCOD, indicating that the compost had stabilized.

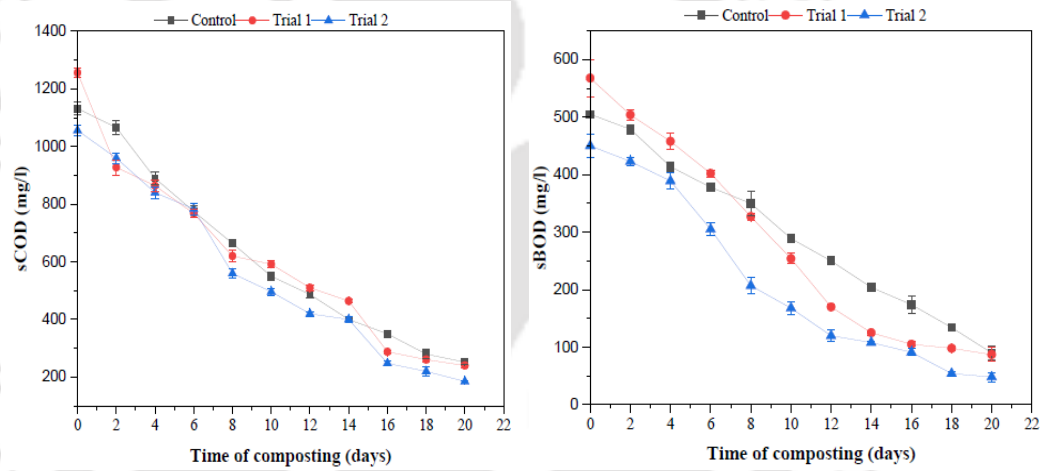

Fig. 8.7. sCOD and sBOD during composting period

The most accurate method for assessing the stability of compost is CO_2 evolution, as it detects carbon that comes directly from the compost under evaluation. Aerobic respiration has a direct relationship with CO_2 emission. As shown in Fig. 8.8, CO_2 emission decreases at the final stages of composting due to a decrease in degradable organic matter and lower microbial activity.

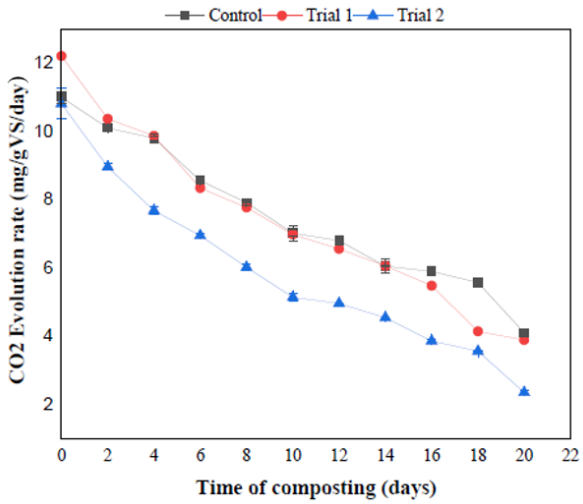

Fig. 8.8. Variation CO_2 Evolution rate during composting period

8.14 VARIATION OF HEAVY METALS (Fe, Pb, Mn, Zn, Cr, Cu, and Ni) DURING THE COMPOSTING PERIOD

Throughout composting, an increase in heavy metal concentration has been noted, attributed to material loss resulting from organic matter mineralization. Fig. 8.9 illustrates the total concentration of heavy metal during rotary drum composting in Control, Trial 1, and Trial 2. According to Singh and Kalamdhad, (2012), the increase in total heavy metal content is the result of mass degradation during composting due to organic matter breakdown, CO_2, and moisture emission.

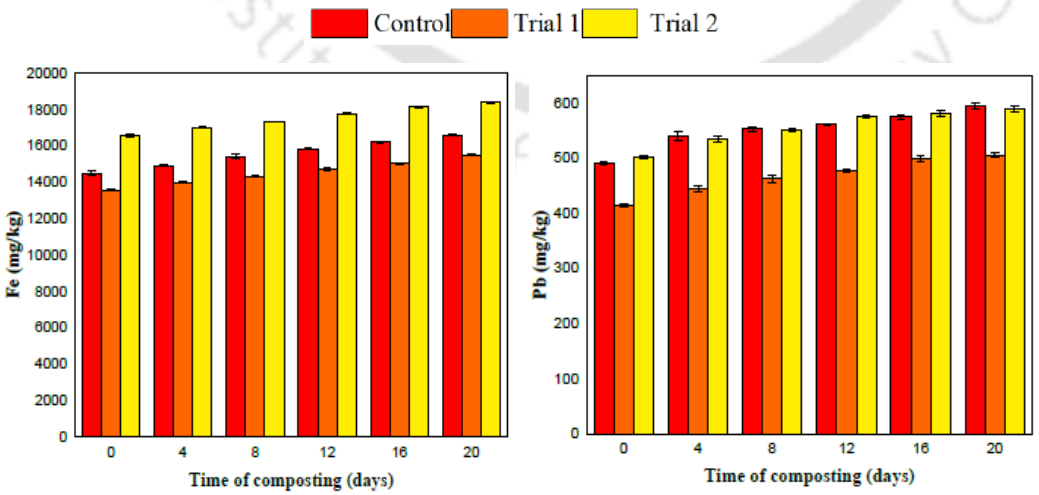

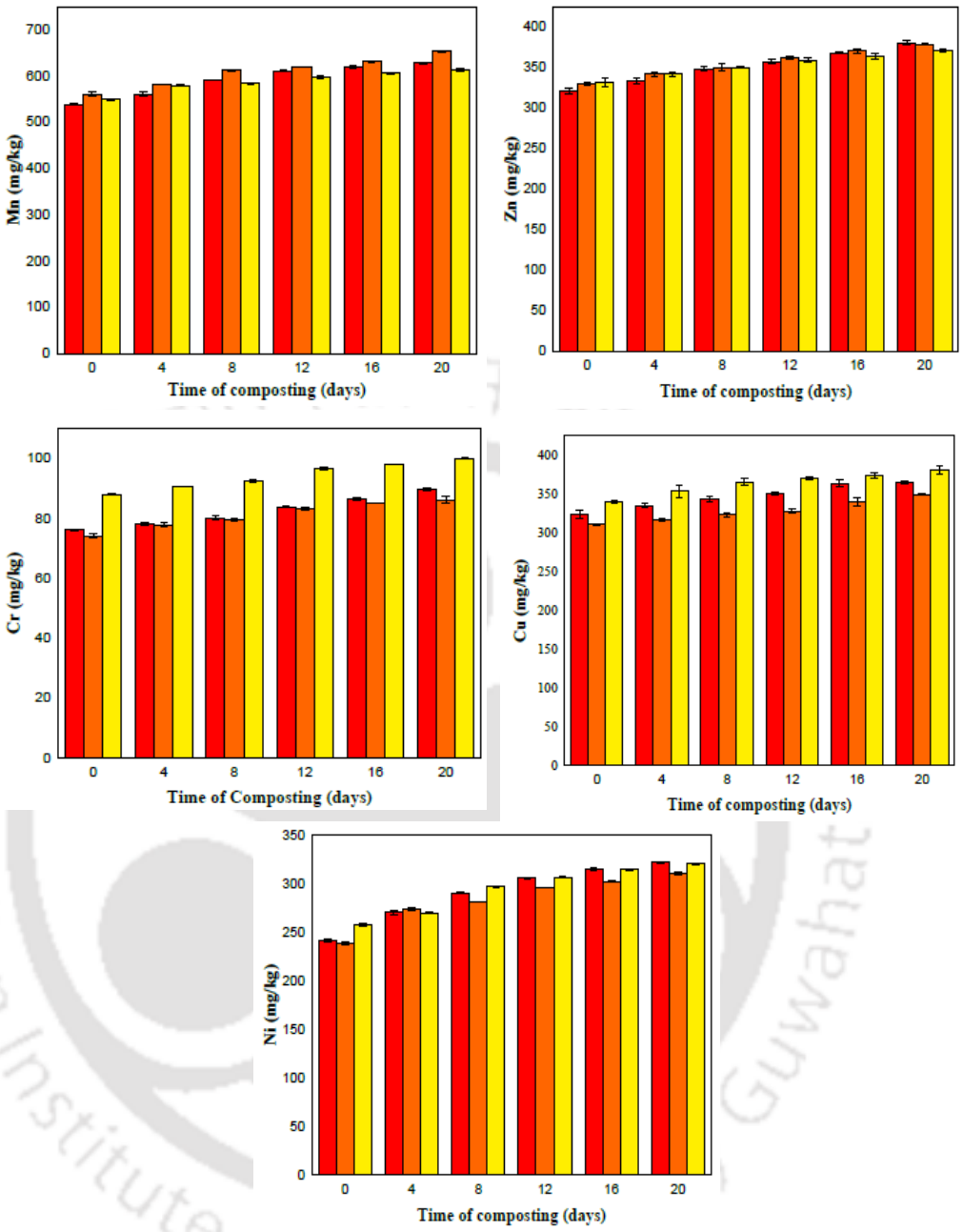

Fig. 8.9. Variation of Heavy Metals (Fe, Pb, Mn, Zn, Cr, Cu, and Ni) during composting period

8.15 MICROBIAL COUNTS

The hygiene of compost can be determined by the presence of coliform bacteria. The recommended value of Fecal density for compost hygienization are 5×10^2 and 5×10^3 MPN/g dry weight (Sudharsan Varma and Kalamdhad, 2015). The average

number of total coliforms was observed in the range of 2.1×10^7, 1.7×10^7 and 3.3×10^7 MPN/g dry weight and finally reduced to 3.3×10^4, 2.4×10^4 and 2.4×10^4 MPN/g dry weight in Control, Trial 1 and Trial 2, respectively, as shown in Table 8.2. However, Fecal coliform was in the order of 2.1×10^6, 1.4×10^6 and 2.0×10^6 MPN/g dry weight reduced to 2.0×10^3, 2.1×10^3 and 1.1×10^3 MPN/g dry weight in Control, Trial 1 and Trial 2. Maximum reduction of total coliform and Fecal coliform was observed in Trial 2 due to high temperature (53.8°C).

Table 8.2. Total and Fecal Coliforms count during composting

Trials	**Total coliform**			**Fecal coliform**		
	0^{th} day	10^{th} day	20^{th} day	0^{th} day	10^{th} day	20^{th} day
Control	2.1×10^7	1.1×10^5	3.3×10^4	2.1×10^6	2.1×10^4	2.0×10^4
Trial 1	1.7×10^7	2.0×10^5	2.4×10^4	1.4×10^6	1.7×10^4	2.1×10^3
Trial 2	3.3×10^7	2.2×10^5	2.4×10^4	2.0×10^6	1.0×10^5	1.1×10^3

8.16 HETEROTROPHIC PLATE COUNT

Due to the high amount of initial waste composition, the microbial population was very high during the initial phase of composting. The mesophilic heterophilic bacteria utilize the highly biodegradable organic matter for cell energy and cell division, thereby increasing the temperature of the composting environment. Therefore, there is a gradual decrease in heterotrophic bacteria after the thermophilic phase. The number of heterotrophs was detected as 1.84×10^{11}, 2.12×10^{12} and 2.72×10^{12} CFU/g dry weight and finally reduced to 2.1×10^6, 1.23×10^6 and 1.04×10^6 CFU/g dry weight in Control, Trial 1 and Trial 2 respectively, as shown in Table 8.3. Maximum reduction of total heterotrophic was observed in Trial 2 due to high temperature (53.8°C).

Table 8.3. Total Heterotrophic colonies during composting

Trials	**Total Heterotrophs (CFU/g)**	
	0-day	20-day
Control	1.84×10^{11}	2.1×10^6
Trial 1	2.12×10^{12}	1.23×10^6
Trial 2	2.72×10^{12}	1.04×10^6

8.17 CONCLUSION FROM CO-COMPOSTING STUDY OF CHAR

The findings of the study suggest that utilizing rotary drum composting for vegetable waste, in conjunction with MSW char, has proven to be a successful approach in terms of biodegradation, nutrients, and heavy metals adsorption. This process allows for the production of nutrient-rich compost in just 20 days. The introduction of MSW char into the mix enhances the aeration of the composting materials, which accelerates the decomposition process. During the initial composting stages, there was a noticeable increase in temperature, with Trial 2 reaching the highest temperature recorded at 53.8°C. Trial 2 also exhibits a prolonged thermophilic phase due to the higher quantity of MSW char, signifying greater organic matter degradation during this phase. Additionally, incorporating MSW char into the composting process raises the pH levels in all treatments compared to the control, indicating strong buffering capacity. Trial 2 demonstrates a more pronounced increase in electrical conductivity compared to the control and Trial 1, although it decreased in the later stages of composting. furthermore, all trials exhibit improved nutritional properties when MSW char is added during composting, and there is a reduction in the concentration of heavy metals compared to the control. Therefore, the inclusion of MSW char not only enhances the quality and speed of composting but also encourages the transformation of mixed MSW into valuable products.

Chapter 9

CHAR APPLICATION IN ALLUVIAL SOIL

9.6 ALLUVIAL SOIL, MSW CHAR, AND COMPOST CHARACTERIZATION

The Initial characteristics of alluvial soil, MSW char, and compost are given in Table 9.1. The alluvial soil used in the study was characterized as nutrient-deficient soil. The moisture content of alluvial soil was 13.37%, which was comparatively less than that required for agriculture (Nepal et al., 2023). The moisture content of compost was 63%, which can be added to the alluvial soil to maintain the ideal moisture content, promoting plant growth. The percentage of volatile matter in alluvial soil was very low, which specifies that it was unbefitting for microbial activity and resulted in slow bio-oxidation (Beesley et al., 2010). The ash content in char and compost was 2.9 and 55.27%, respectively, which is beneficial as it encompasses essential nutrients such as calcium, magnesium, potassium, and trace elements that promote soil fertility (Demeyer et al., 2001). The fixed carbon content of MSW char was 65.8%, which can be amended in the soil to improve its structure by enhancing the porosity, water, and nutrient retention capacity by adsorbing the nutrients and making them available to plants for longer periods of time (Lehmann et al., 2011a). The SOM in the alluvial soil was very low (0.41%), whereas MSW char and compost had 43.66 and 50.21%, respectively. Amendment of char and compost can improve the organic matter by reserving the essential nutrients in soil which are gradually released through microbial activities. Also, SOM improves soil porosity, penetration to roots, and water infiltration (Malone et al., 2023). The initial pH values of alluvial soil, char, and compost were 6.22, 7.53, and 6.9, respectively, which were within the ideal range for fungal growth (5.0-8.5) and bacterial development (6.0-7.5) (Meena et al., 2021). The EC of alluvial soil measured at 0.71 dS/m indicates a low presence of soluble salts. However, the addition of char (2.09 dS/m) and compost (2.30 dS/m) can enhance the EC of the soil, which indicates material salinity arising from exchangeable salts or due to the

presence of highly conductivity metal ions (Feng et al., 2021). The SOC was very low in the soil, approximately 0.22%, while char and compost had 57.23 and 26.31%, respectively. The SOC in soil plays a significant role in carbon sequestering by reducing the carbon dioxide in the atmosphere as a carbon sink (Lal, 2004). The amendment of mixed MSW char and compost can enhance the SOC in the soil, which in turn sustains buffer soil pH, thus maintaining soil health and fertility (Torsvik and Øvreås, 2002). The WHC must be high to retain moisture in the soil, as it will lessen the frequency of irrigation (Patra et al., 2022). The WHC of alluvial soil (13.5%) can be enhanced with the addition of char and compost.

Bulk density serves as a measure of soil compaction and overall soil health. It influences infiltration, rooting depth limitations, water-holding capacity, soil porosity, the availability of plant nutrients, and the activity of soil microorganisms, all of which play a crucial role in soil processes and productivity (USDA NRCS, 1998). Generally, loose soil, which is aggregated in a well and porous structure with high organic matter, generally has low bulk density. The bulk density of alluvial soil was high, about 1.35 g/cm^3, with a low porosity of 49.05%. Meanwhile, char and compost had bulk densities of 0.51 and 0.6 g/cm^3 and porosity of 79 and 63% porosity, respectively. Incorporating char and compost into the soil reduces the bulk density by enhancing its porosity. Earlier studies have indicated that the optimal porosity range for aerobic decomposition is between 85 and 90%, with the minimum required being 30% (Ruggieri et al., 2009). Therefore, having less dense soil is beneficial for effective agricultural practices. The specific gravity of the alluvial soil was higher than that of char and compost, with an approximate value of 2.65. Specific gravity plays a significant role in the movement of solutes, supports water retention, and contributes to aeration in the soil. Increased specific gravity in the soil can negatively affect plant development, which can be reduced by applying char and compost (Rai and Chatrath, 2019). The nitrate concentration of the alluvial soil was 54.58 mg/kg. A healthy soil must have nitrate concentration so as to promote plant growth without leaching into the environment. A nitrate concentration of more than 30 mg/kg can risk the environment by leaching into the

groundwater (Sanchez et al., 2003). The concentration of ammonia in the tested soil was 16.75 mg/kg, which was more than the concentration in natural, undisturbed soil ranging from 1-5 mg/kg (ASTDR, 2004). The higher concentration of ammonia can lead to toxicity in the plant (chlorosis) (Britto and Kronzucker, 2002), inhibition of microbial activity (Yenigün and Demirel, 2013), and leaching into groundwater causing water pollution. The CEC of the soil was 14.67 meq/100 g, which was much lower than clay and organic soil, which have 26 to 40 meq/100 g of CEC (Räty et al., 2021). The high CEC in the soil can hold the essential nutrients for a longer period of time without the requirement of frequent application of fertilization (Räty et al., 2021). The available phosphorus in the alluvial soil was 0.41 mg/kg, whereas MSW char and compost had 2.05 and 2.26, respectively. The available phosphorus in natural soil is generally 0.94 to 32.56 mg/kg (Tian et al., 2021). The deficiency of phosphorus has an adverse impact on plant growth. Also, high concentration of available phosphorus leads to nutrient imbalance, hindering the uptake of essential nutrients such as iron and zinc (Grant et al., 2005). The TKN in alluvial soil was 0.14%, but this can be improved by adding char and compost, which have TKN values of 0.46% and 0.88%, respectively, to support plant growth. The TKN of alluvial soil was 0.14%, which can be enhanced by the addition of char and compost with TKN of 0.46 and 0.88%, respectively. The alluvial soil tested had a deficit of nutrients such as total Na, K, Ca, and Mg as compared to the requirement of nutrients for physiological functions, building of cell walls and stability, and photosynthesis (Kang et al., 2023). The exchangeable metals in the soil were within the range required for plant growth, except for Mg (Niu et al., 2021). The balance in the exchangeable metals for plant uptake can be maintained by amendment of char and compost in the soil for healthy plant growth and to avoid antagonistic interaction. The concentration of Fe, Cr, and Ni in the soil was much higher than the optimal concentration of essential micronutrients required for the healthy growth of plants, avoiding toxicity (Vondráčková et al., 2014). The DTPA-extracted metals in the soil, such as Pb, Cr, Zn, Cu, and Cd, were within the limit to prevent the leaching and uptake of metals by plants, whereas Fe and Ni concentrations were high (Wang et al., 2018). The MSW char and compost used in

the study depicted a higher value of the mineral nutrients. The amendment of char and compost can enhance nutrient uptake and promote plant growth by storing the nutrients for longer periods in the soil and reducing the metal availability in the soil.

Table 9.1. Initial characterization of the samples

Parameters	Units	Alluvial soil	MSW char	Compost
Moisture content	(%)	13.37 ± 0.2	1.17 ± 0.10	63 ± 0.22
Volatile matter	(%)	0.16 ± 0.11	29.80 ± 0.12	36.43 ± 0.1
Ash content	(%)	-	2.90 ± 0.06	55.27 ± 0.26
Fixed carbon	(%)	-	65.80 ± 0.03	0.13 ± 0.1
SOM	(%)	0.41 ± 0.08	43.66 ± 1.01	50.21 ± 0.27
pH	-	6.22 ± 0.01	7.53 ± 0.01	6.9 ± 0.1
EC	dS/m	0.71 ± 0.04	2.09 ± 0.04	2.30 ± 0.45
SOC	(%)	0.22 ± 0.07	57.23 ± 0.16	26.31 ± 1.05
Water holding capacity	(%)	13.5 ± 0.4	26.39 ± 1.28	46.16 ± 0.2
Bulk density	g/cm^3	1.35 ± 0.1	0.51 ± 1.1	0.6 ± 1.07
Specific gravity	-	2.65 ± 0.01	2.13 ± 0.12	1.1 ± 0.4
Porosity	(%)	49.05 ± 3	79 ± 1.5	63 ± 1.26
Nitrate	mg/kg	54.58 ± 0.12	-	-
Ammonia	mg/kg	16.75 ± 0.17	15.24 ± 1.09	21.66 ± 1.27
CEC	meq/100 g	14.67 ± 0.9	26.05 ± 0.88	59.61 ± 0.25
Available phosphorus	mg/kg	0.41 ± 0.09	2.05 ± 0.09	2.26 ± 1.10
TKN	(%)	0.14 ± 0.00	0.46 ± 0.0	1.88 ± 1.16
Total sodium	mg/kg	1.5 ± 0.15	2.25 ± 0.23	4.25 ± 0.32
Total potassium	mg/kg	8.9 ± 1.14	8.05 ± 1.74	5.75 ± 2.1
Total calcium	mg/kg	17.98 ± 0.87	8.25 ± 1.94	40.12 ± 0.83
Total magnesium	mg/kg	5.04 ± 0.67	3.87 ± 1.27	3.14 ± 0.58
Exchangeable Na	mg/kg	50 ± 1.21	982 ± 2.23	645 ± 0.7
Exchangeable K	mg/kg	121 ± 2.35	1182 ± 0.30	7940.24 ± 0.23
Exchangeable Ca	mg/kg	330 ± 0.65	3636 ± 0.55	11392.1 ± 1.06

Exchangeable Mg	mg/kg	325.46 ± 0.00	545.78 ± 2.38	4839.41 ± 0.5
Zn	mg/kg	165 ± 0.67	719.25 ± 13.24	326 ± 0.87
Cu	mg/kg	63.75 ± 0.24	67.86 ± 4.13	353.03 ± 0.25
Fe	mg/kg	3300.25 ± 0.98	1392.75 ± 0.98	17480.26 ± 1.2
Cr	mg/kg	1985 ± 11.78	94.45 ± 7.27	88.4 ± 0.53
Ni	mg/kg	304.67 ± 1.24	213.45 ± 1.45	320 ± 1.11
Cd	mg/kg	<DL	<DL	<DL
DTPA Pb	mg/kg	3.019 ± 0.55	18.08 ± 0.55	15 ± 0.4
DTPA Fe	mg/kg	1311.76 ± 0.98	1202.88 ± 0.87	1168 ± 0.56
DTPA Ni	mg/kg	7.28 ± 0.92	7.90 ± 0.87	6.21 ± 0.32
DTPA Cr	mg/kg	1.23 ± 0.21	1.85 ±0.02	1.03 ± 0.6
DTPA Zn	mg/kg	2.185 ± 0.024	14.54 ± 1.12	69.44 ± 0.73
DTPA Cu	mg/kg	4.74 ± 1.24	3.56 ± 0.28	11.07 ± 1.02
DTPA Cd	mg/kg	<DL	< DL	<DL

Note: The data is presented in *xx ±yy* format where xx denotes the average value, *yy* denotes the standard deviation

9.7 EFFECT ON SOIL PHYSICAL AND CHEMICAL PROPERTIES

The soil with lower bulk density (< 1.5 g/cm^3) is generally preferred for agriculture purposes (Jain and Kalamdhad, 2020). Insufficient aeration can occur in wet conditions when the bulk density rises, while excessive strength in the soil can occur in dry conditions. As a result, root penetration and elongation get restricted in dry conditions, while the microbial decomposition of soil organic matter and supply of oxygen to roots get decreased under reduced aeration conditions (Tomobe et al., 2023). Therefore, bulk density is important for plant growth. The bulk density of alluvial soil was 1.41 gm/cm^3, but with the application of char and compost, it was decreased by 4.26% on the 0th day, as depicted in Fig. 9.1. The rate of decrease of bulk density of the soil increased with the rate of the application of the compost and MSW char. MSW Char generally enhances soil

structure by expanding pore spaces and decreasing bulk density because of its porous nature. It makes voids and channels in the soil, which improves water infiltration, root growth, and general soil health (Nguyen et al., 2023). The addition of compost and MSW char increased the total porosity of the soil. The soil bulk density decreased by 12%, and total porosity increased by 14% on adding a combination of 10% MSW char and 20% compost to the soil by the 120th day. The bulk density of all the treatments was less than 1.5 g/cm^3. There was an inverse effect seen on the total porosity of the soil compared to the bulk density of the soil. It increased with the rate of application of char. In short, the addition of MSW char and compost in the soil increases water and air circulation and improves the porosity and bulk density of the soil. The addition of char and compost initially reduces bulk density due to their lower density compared to mineral soil. Over time, microbial decomposition and humification lead to structural rearrangements, influencing aggregation and compaction dynamics. Increased microbial activity may enhance soil aggregation and increase porosity, while subsequent mineralization of organic matter may cause compaction, leading to fluctuations in bulk density.

The nutrient-holding capacity of soil increases after the addition of char and compost due to the increase in cation exchange capacity in all the treatments. Treatment with a higher percentage of MSW char has higher CEC due to a greater amount of negative charge that developed on the surface of organic matter and char. The CEC of soil increased by 6.14-folds when amended with 10% char and 20% compost on the 120th day. The pH is one of the most important parameters in the soil as it affects the CEC and nutrient availability in the soil. With the decrease in pH, the CEC of the soil decreases as most of the negative adsorption sites available for exchangeable cations, such as Na^+, K^+, Mg^{2+}, Ca^{2+}, and Al^{3+} in soil, are taken away by H^+ ions (Yadav et al., 2023). The available phosphorus in the soil is also affected by the soil pH. At pH below 6, phosphorus precipitates as solid Al or Fe phosphate mineral, while at pH above 7, phosphorus precipitates as Ca or Mg phosphate mineral (Wolka and Melaku, 2015). The pH also affects the mobility, concentration, and availability of micronutrients in the plant. The pH of the alluvial

soil was 6.74, which was slightly acidic in nature. The pH of the MSW char and compost was between 7-8 and its alkaline character directly affects soil pH after its application. The pH of the soil roses on the 120th day by 11.3% when 20% compost and 10% MSW char was applied due to the release of cations. Due to the increase in pH, the bioavailability fraction of metal decreased. The EC of the alluvial soil was 0.71 mS/cm. The specific crop and its tolerance to salt determine the ideal EC range for plant growth. High EC values, which indicate excessive salinity, might harm plant development and output by reducing water intake and nutrient availability. The EC in all treatments increased with the application rate of MSW char with compost. After 120 days, the EC of the soil in all treatments was below 1.5 mS/cm, indicating less presence of water-soluble salt (USDA (United States Department of Agriculture), 2011).

The SOC accounts for over 70% of the worldwide terrestrial carbon stock (Jobbágy et al., 2001). The addition of MSW char in the soil can enhance carbon sequestration due to the abundance of carbon. The addition of 10% MSW char and 20% compost increases SOC of the soil by 5.68-fold on the 0th day but decreases with time, resulting in an increase of 2.27-fold on the 120th day, due to the intricate balance between input of carbon from char and compost and the dynamic microbial activity that directs the SOC level (Ding et al., 2023). The percentage increase in SOC of alluvial soil with the amendment of mixed MSW char and compost was quite higher than that reported on the application of biochar and compost in soil (Nobile et al., 2022). The high variability in SOC could be due to differential decomposition rates of organic amendments. Char is relatively stable, while compost is more biodegradable, leading to variations in carbon loss and accumulation. Microbial community composition, enzyme activity, and soil moisture variations could also contribute to the observed fluctuations. Initially, SOM of the alluvial soil increased by 5.49-fold with the amendment of 10% char and 20% compost but decreased with time due to mineralization and leaching (Jain and Kalamdhad, 2020).

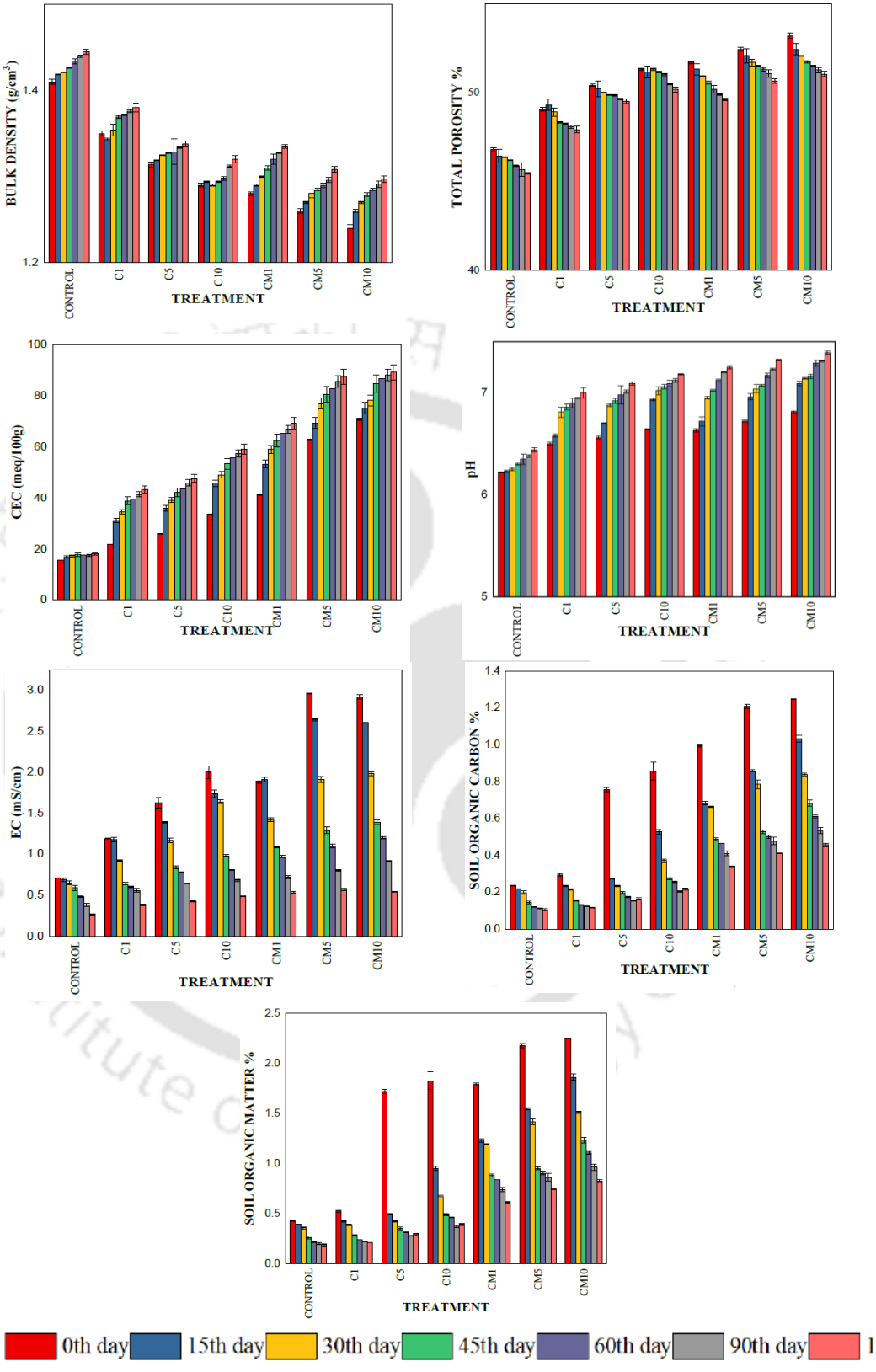

Fig. 9.1. Variation in the soil physical properties

9.8 EFFECT OF MACRO AND MICRONUTRIENTS WITH THE APPLICATION OF MSW CHAR AND COMPOST IN ALLUVIAL SOIL

Nitrogen, phosphorus, potassium, magnesium, and sodium are the most important macronutrients that are required by plants. Amino acids, proteins, enzymes, and chlorophyll are all vital for plant growth and contain nitrogen as one of their main constituents (Wany et al., 2020). The application of compost and MSW char together influences the TKN value by increasing 3.57-fold on 0-day, as shown in Fig. 9.2. The TKN of alluvial soil increased by 43% with the addition of 10% MSW char and 20% compost. Decline in TKN with time occurs due to nitrification or leaching process. Throughout 120 days, the TKN was higher in all treatments compared to the control. Available phosphorus increased with the rate of application of compost and MSW char. CM10 shows the maximum increase in available phosphorus by 4.63-fold, and the availability decreases with time. This is because the available phosphorus is converted to unavailable phosphorus due to rapid phosphorus fixation. The mineralization and leaching process also affect the available phosphorus with time (Johan et al., 2021). Potassium is the third most important macronutrient required by the plant after nitrogen and phosphorus (Hasanuzzaman et al., 2018). The amendment of compost and MSW char in the soil increases the total potassium concentration of the soil. The treatment CM10 shows a maximum increase in the concentration of potassium (2.09-fold) by the 120th day as compared to the studies reported on the amendment of biochar in soil (Bekchanova et al., 2024). Magnesium is essential for the production of chlorophyll, which is needed for the photosynthesis process. It reduces the crop stress caused by exposure to sunlight (Verbruggen and Hermans, 2013). The amendment of compost and MSW char in the soil increases the total magnesium concentration of the soil. With time it reduces due to mineralization of organic matter in soil. The CM10 shows an increase in total magnesium in the alluvial soil by 2.6-fold on the 120^{th} day. Thus, the combined application of 10% MSW char and 20% compost was effective for enhancing the essential macro and micronutrients in alluvial soil for the growth of plants.

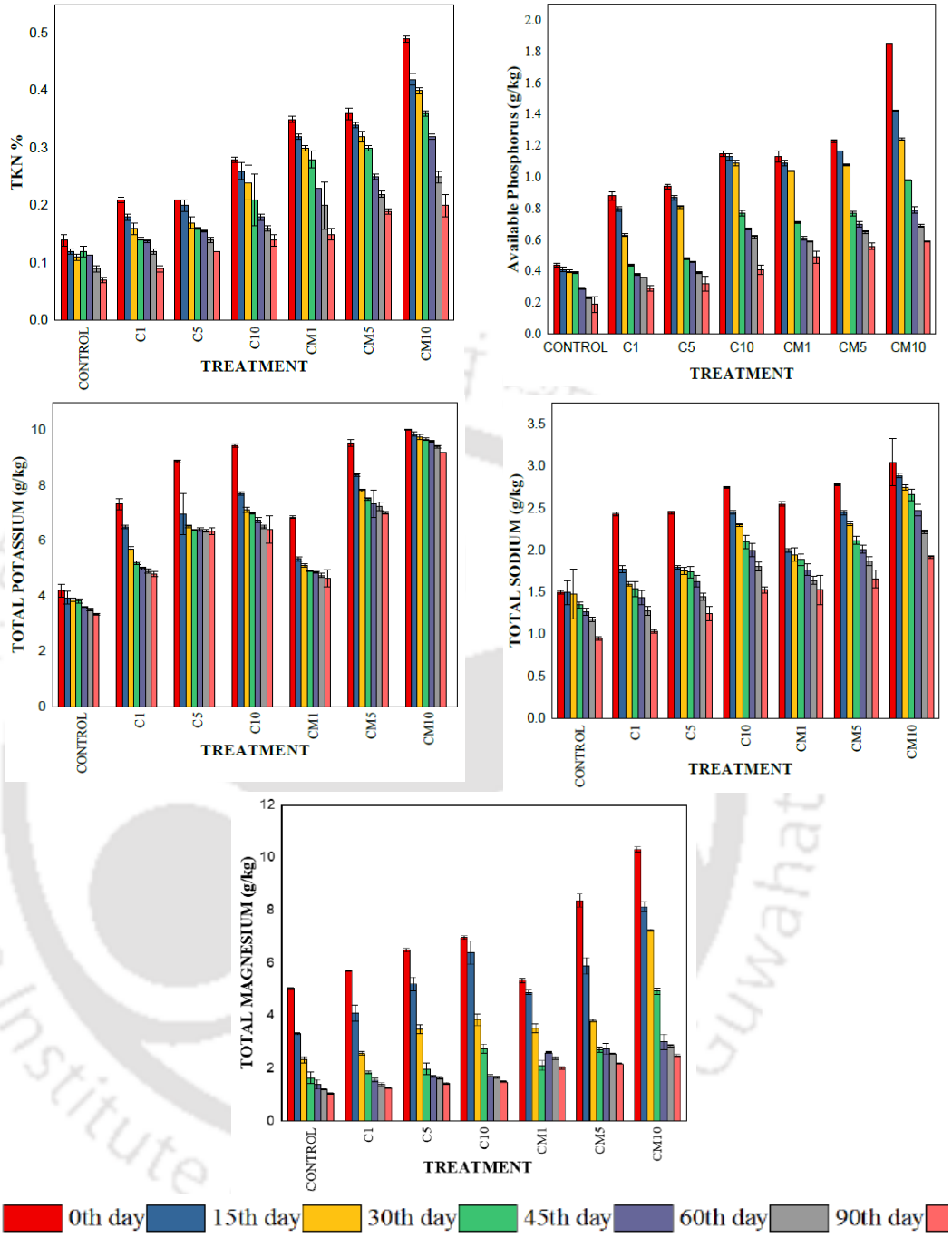

Fig. 9.2. Variation in the macro and micro-nutrients in soil with the application of char and compost

9.9 EFFECT ON THE TOTAL HEAVY METALS IN ALLUVIAL SOIL WITH THE AMENDMENT OF MSW CHAR AND COMPOST

The concentration of total heavy metals availability decreased with the sole application of MSW char but then increased when char and compost were applied together in the alluvial soil, as shown in Table 9.2. The availability of Cr dropped by 90% in C1, whereas the availability increased with the rate of application of char and compost, which was beyond Indian standards (Rajkumar et al., 2019) but was lesser than control. Similarly, the availability of Pb reduced with the C1 treatment by 31% and was within the Indian standards until the treatment CM5 and CM10. The availability of Cd was below detection level (<DL) in control as well as in all the treatments. The availability of heavy metals initially decreased in the soil when 1% MSW char was applied due to the high surface area and CEC, which immobilized metals by precipitation and adsorption. However, the availability increased with the increase in the rate of char application as it altered the organic matter and pH which releases back the previously adsorbed metals in the soil (Alaboudi et al., 2019). When the combination of MSW char and compost was amended in the soil, the metals availability increased due to the addition of organic matter, which binds the heavy metals, creating more competition for sites of binding, releasing metals back into the soil (Cheng et al., 2023). The increase in the rate of the combined amendment also tends toward the pH level that triggered the availability by increasing the solubility of heavy metals in soil (Oustriere et al., 2017). Also, the addition of both char and compost not only increases the nutrients in the soil but also forms complexes with heavy metals, which enhances mobility (Zheng et al., 2022). Thus, a 1% MSW char dose was effective in reducing the availability of heavy metals in alluvial soil.

Table 9.2. Variation in heavy metals in alluvial soil with different treatments

Metals	Control	C1	C5	C10	CM1	CM5	CM10	Indian standard (Rajkumar et al., 2019)
Cr (mg/kg)	1980 ± 9.66	202.30 ± 5.12	234.5 ± 7.23	273.56 ± 1.67	305.56 ± 8.21	329.63 ± 6.89	333.56 ± 7.21	<150
Pb (mg/kg)	412 ± 5.23	285.5 ± 2.37	308.25 ± 9.31	247.80 ± 6.62	415.75 ± 3.78	508.25 ± 4.6	662.23 ± 12.8	250-500
Cd (mg/kg)	< DL	< DL	< DL	< DL	< DL	< DL	< DL	3-6

9.10 BIOAVAILABILITY OF METALS

The availability of exchangeable Na and K was reduced by 6 and 43%, respectively, with the C1 treatment, but there was an increase in Mg and Ca with all the treatments, as given in Table 9.3. The reduction in the exchangeable metals with the application of 1% MSW char was due to the high CEC of char, which promotes adsorption initially and retains cations, reducing the immediate availability of Na and K in soil. Due to the difference in hydration energy and radii of ions, the adsorption of Na and K is stronger than Ca and Mg (Garau et al., 2024). The implementation of char increases the pH of the soil, which makes Ca and Mg more soluble and available than Na and K, which remain on the exchange site (Hailegnaw et al., 2019). Moreover, the compost and char together contribute to organic matter, which enhances microbial activity through organic acid production and mineralization (Nobile et al., 2022). Initially, the availability of DTPA extractable Fe, Pb, and Cu was reduced by 99, 52, and 15%, respectively, with the sole application of 1% char. The availability of Ni and Cr was reduced, with Cd being below the detection level, and the availability of Zn increased with all the amendments. The decrease in the availability of DTPA metals was due to the high surface area and functional groups in char, which helps in the adsorption and formation of heavy metal complexes that immobilize metals (Ma et al., 2022). There was precipitation of heavy metals as carbonates and hydroxides due to the increase in pH of the soil with the addition of char, which reduces their

bioavailability (Vithanage et al., 2017). Whereas the combination of char and compost releases organic acid and nutrients that mobilize and chelate heavy metals, increasing their bioavailability (Ma et al., 2022). The C1 treatment showed a significant reduction in the bioavailability of the metals in the alluvial soil.

Table 9.3. Bioavailability of metals and macronutrients in the soil after MSW char and compost application

Metals	Control	C1	C5	C10	CM1	CM5	CM10
Exchangeable Na (mg/kg)	50 ± 1.21	47 ± 1.3	69 ± 2.45	97 ± 4.23	235 ± 2.10	302 ± 3.5	446 ± 3.45
Exchangeable K (mg/kg)	121 ± 2.35	69 ± 1.65	109 ± 1.27	162 ± 1.21	547 ± 2.21	797 ± 2.23	682 ± 2.1
Exchangeable Mg (mg/kg)	325.46	367 ± 1.65	278.8 ± 1.70	383 ± 1.95	609.78 ± 3.08	687.23 ± 1.51	717.93 ± 2.79
Exchangeable Ca (mg/kg)	17.98 ± 0.87	1768 ± 2.42	1986 ± 0.84	2565 ± 3.09	1879 ± 13.11	2130 ± 15.89	3438 ± 2.03
DTPA Fe (mg/kg)	1311.76 ± 0.98	18.68 ± 0.17	14.68 ± 0.39	16.56 ± 0.42	19.22 ± 0.06	20.3 ± 0.49	22.69 ± 0.23
DTPA Pb (mg/kg)	3.02 ± 0.55	1.45 ± 0.14	3.56 ± 0.09	4.02 ± 0.06	4.53 ± 0.04	5.05 ± 0.01	5.21 ± 0.01
DTPA Cu (mg/kg)	4.74 ± 1.24	4.02 ± 0.04	3.8 ± 0.12	4.93 ± 0.06	5.12 ± 0.28	4.54 ± 0.07	5.09 ± 0.06
DTPA Ni (mg/kg)	7.28 ± 0.92	2.11 ± 0.04	3.54 ± 0.05	3.80 ± 0.01	4.04 ± 0.7	3.95 ± 0.3	4.35 ± 0.05
DTPA Zn (mg/kg)	2.19 ± 0.02	2.37 ± 0.02	5.14 ± 0.01	12.84 ± 0.17	11.51 ± 0.61	10.33 ± 0.21	11.83 ± 0.24
DTPA Cr (mg/kg)	1.23 ± 0.21	0.55 ± 0.02	0.54 ± 0.04	0.68 ± 0.01	0.60 ± 0.05	0.48 ± 0.02	0.43 ± 0.03
DTPA Cd (mg/kg)	<DL	< DL	< DL	< DL	< DL	< DL	< DL

9.11 RESULTS OF THE POT STUDY

Plants absorb essential nutrients and metals through their roots via various uptake pathways such as passive diffusion and active transport processes. Nutrient

uptake is facilitated by specific transporters and channels present in the root membranes that selectively absorb essential elements from the soil solution. These nutrients are then transported through the plant's vascular system to different plant parts, including fruits. Plants regulate nutrient uptake based on their physiological needs and the availability of nutrients in the soil. Excess nutrients can be stored in different plant tissues, including fruits, serving as reserves for future growth and development. This regulatory mechanism helps plants maintain nutrient homeostasis and ensures the proper accumulation of metals and nutrients in fruits (Clemens, 2006). In the pot study of *Abelmoschus esculentus* (Okra) using different amendment percentages of MSW char and compost in alluvial soil, it was found that the concentration of heavy metal uptake by the fruit of Okra was less than that of control, as shown in Table 9.4. The concentration of Cr, Zn, K, and Mg in the fruit was reduced by 15, 13, 16, and 10%, respectively, with the only application of MSW char, as shown in Table 9.4. Whereas, the concentration of Cd in the fruit was in the undetected level with all the treatments. The heavy metals such as Pb, Mn, Cu, Ni, and Fe were reduced by 22, 91, 47, 29, and 55% with the increase in the rate of application of MSW char and compost. The metal uptake by fruit was reduced with the application of MSW char due to the high surface area and functional groups in char that can adsorb heavy metals, reducing their bioavailability in the soil (Choppala, et al., 2011). The differential reduction in the uptake of metals by fruits with increasing rates of char and compost, as opposed to char alone, can be attributed to the synergistic effects of char and compost on soil properties and metal availability. The MSW char and compost together enhance the soil's capacity to adsorb heavy metals more effectively than char alone. The compost adds organic matter, which increases the formation of metal-organic complexes, while char provides additional adsorption sites (Choppala, et al., 2011). Both char and compost increase the soil's CEC. The addition of compost further enhances this effect, leading to greater retention of cations such as Pb, Mn, Cu, Ni, and Fe on soil particles and char surfaces (Lehmann and Joseph, 2009). Moreover, compost is rich in organic acids and humic substances that form stable complexes with heavy metals, reducing their free ionic forms and, thus, their bioavailability

for plant uptake (Izilan et al., 2022). Compost and char addition stimulate microbial activity, which can lead to increased microbial immobilization of metals. Microbes can uptake and sequester metals, reducing their availability to plants (Lehmann et al., 2011a).

Table 9.4. Concentration of heavy metals and nutrients in Fruits of *Abelmoschus esculentus* (Okra) in different treatment

Metals	**Control**	**C1**	**C5**	**C10**	**CM1**	**CM5**	**CM10**
Pb (mg/kg)	419.59 ± 0.4	378.20 ± 1.2	370.9 ± 2.31	375.90 ± 2.9	330.45 ± 1.1	328.0 ± 1	325.91 ± 1.67
Cd (mg/kg)	< DL	< DL	< DL	< DL	< DL	< DL	< DL
Cr (mg/kg)	80.6 ± 0.4	73.95 ± 0.09	68.45 ± 0.3	76.55 ± 0.41	75.4 ± 0.81	74.5 ± 0.55	73.6 ± 0.01
Mn (mg/kg)	174.65 ± 0.3	19.95 ± 0.1	20.55 ± 0.1	21.3 ± 1.9	23.59 ± 1.1	20.34 ± 0.6	16.45 ± 0.9
Cu (mg/kg)	85.2 ± 2.3	66.45 ± 1.5	52.9 ± 0.4	51.89 ± 0.9	57.35 ± 0.7	49.08 ± 0.5	45.20 ± 0.16
Zn (mg/kg)	251.7 ± 0.8	218.2 ± 2.9	220.75 ± 0.78	225.78 ± 0.3	239.3 ± 1.4	241.7 ± 0.17	231.98 ± 0.02
Ni (mg/kg)	326.5 ± 0.05	310.7 ± 0.15	296.8 ± 0.22	287.9 ± 0.11	291.76 ± 0.5	273.25 ± 0.2	232.1 ± 2.31
Fe (mg/kg)	1162.35 ± 9.47	1071.3 ± 7.23	532.67 ± 3.56	576.9 ± 1.5	927.8 ± 4.12	517.75 ± 6.25	637.5 ± 1.3
K (g/kg)	20.4 ± 0.4	22.93 ± 0.01	19.8 ± 0.08	17.1± 0.014	24.5 ± 0.021	24.23 ± 0.7	21.27 ± 0.14
Ca (g/kg)	1.56 ± 0.01	2.13 ± 0.03	2.22 ± 0.01	2.49 ± 0.05	3.76 ± 0.01	3.42 ± 0.4	3.50 ± 0.8
Mg (g/kg)	3.57 ± 0.68	3.48 ± 0.2	3.22 ± 0.03	3.42 ± 0.04	3.67 ± 0.12	3.54 ± 0.2	3.73 ± 0.05
Na (mg/kg)	4.78 ± 0.07	5.38 ± 0.21	5.83 ± 1.29	5.42 ± 0.41	5.82 ± 0.012	5.98 ± 0.05	6.16 ± 0.03

9.12 MORPHOLOGICAL RESULT

The application of MSW char and compost in alluvial soil affected the growth of plants, as shown in Fig. 9.3. The addition of compost and MSW char decreases the bulk density. As a result, roots are deeper in all treatments compared to the control. CM5 shows a better morphological parameter compared to all treatments. The root length increased by 63% vertically and 60% horizontally on the 120th day when 5% MSW char and 20% compost were applied together. The plant height increases by 31 cm on the 120th day with CM5 treatment. C5 gave a maximum number of leaves on the 90th day, and then the shedding of leaves started, whereas CM1 had the maximum number of leaves on the 120th day. It is worth noting that the shape and size of fruits on treatments with biochar alone were more uniform during the trials. The increase in root length with the combined application of biochar and compost, compared to biochar alone, can be attributed to several synergistic effects that enhance soil quality and root growth. Compost addition improves soil aggregation and structure, which enhances soil aeration and water infiltration. Char contributes to these benefits by providing a porous structure that helps maintain soil porosity (Lehmann et al., 2011a). Compost provides a slow-release source of essential nutrients that are crucial for root development. Char, while enhancing nutrient retention, also improves the efficiency of nutrient use. The combined use of char and compost enhances the availability of nutrients through increased microbial activity and improved nutrient cycling (Agegnehu et al., 2016). The presence of diverse microbial communities facilitated by compost can interact with char to enhance root growth-promoting processes (Lehmann et al., 2011b). The combined application of char and compost enhances plant height and the number of leaves more than char alone due to improved soil structure, increased nutrient availability, enhanced microbial activity, better water retention, reduced soil toxicity, and stabilized pH. These synergistic effects create an optimal environment for plant growth, leading to taller plants with more leaves (Lehmann et al., 2011a).

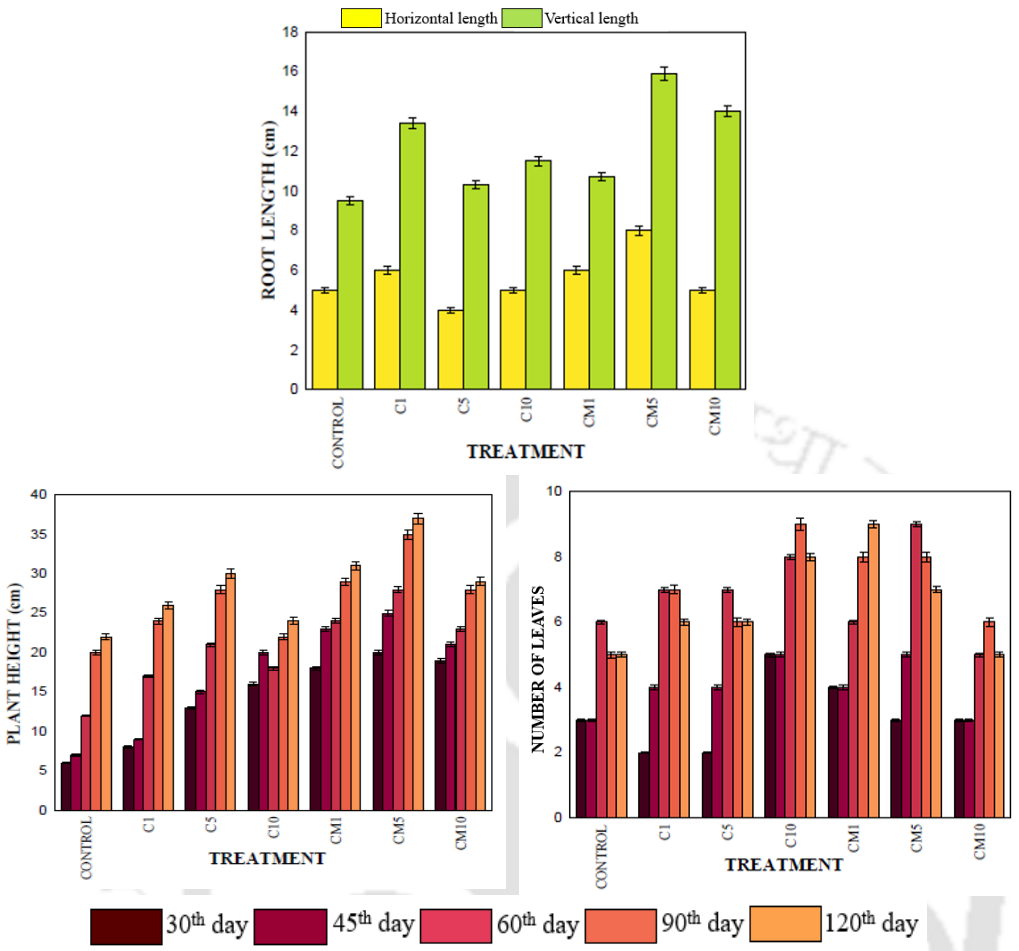

Fig. 9.3. Effect on plant morphology with the amendment of char and compost in alluvial soil

9.13 HEAVY METALS IN FRUITS OF *ABELMOSCHUS ESCULENTUS* (OKRA)

The surface physicochemical features of MSW char has an affinity for certain heavy metals. The decrease in the heavy metal uptake by the plant grown under the influence of MSW char and compost is related to the diluting impact of enhanced plant growth, heavy metal immobilization in soil, and the development of stable metal-organic complexes. When more MSW char and compost were added, the metal's bioavailability decreased, which can be explained by raising the pH of the soil and the action of MSW char in reducing metal uptake. The bioaccumulation factor (BF) is defined as the ratio of the concentration of metals in fruits to the

concentration of metals in the soil. BF of Zn, Pb, Ni, and Mn decrease in all treatments, as shown in Fig. 9.4 with the application of compost and MSW char as compared to control due to a decrease in the bioavailable concentration of heavy metals in soil with the addition of MSW char, resulting in lower uptake by the roots (Ibrahim et al., 2022). Char adsorbs metals on its surfaces, reducing their concentrations and mobilization in the soil as well as their translocation in plants. There was no significant BF of Fe and Cu.

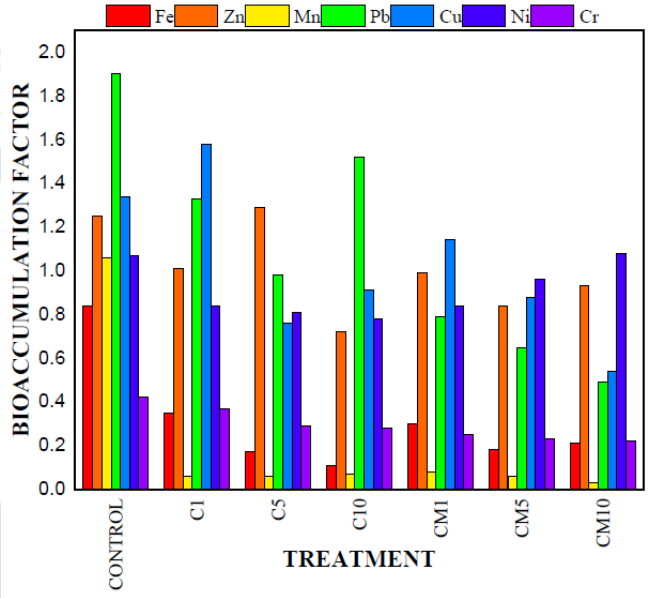

Fig. 9.4. Variation of bioaccumulation factor in fruit

9.14 CONCLUSION FROM THE APPLICATION OF MSW CHAR IN ALLUVIAL SOIL

The study demonstrates that amending alluvial soil with a combination of MSW char and compost significantly improves soil nutrients and physicochemical properties, leading to healthier plant growth. By the 120th day, the physical and chemical properties of the alluvial soil, such as bulk density, porosity, CEC, pH, EC, SOM, and SOC, were significantly enhanced with the combined application of 10% MSW char and 20% compost. This improvement was attributed to the synergistic effects promoting the healthy growth of plants. The essential micro and macronutrients in the soil increased with higher doses of the amendments. The application of MSW char solely proves effective in reducing the bioavailability of

heavy metals in the soil, thereby minimizing their uptake by plants. These findings suggest that utilizing MSW char, either alone or in combination with compost, can be a viable strategy for enhancing soil quality and promoting sustainable agriculture, especially in soils prone to heavy metal contamination.

Chapter 10

APPLICATION OF MSW CHAR IN MINE TAILING SOIL

10.1 PRELIMINARY CHARACTERIZATION OF SUBSTRATE

The characterization of the MTS, MSW char, and VC is shown in Table 10.1. The initial pH values of MTS, char, and VC were 3.25, 7.11, and 6.7, respectively. The value of MTS is very low, but the pH of char and VC were within the ideal range for bacterial development (6.0-7.5) and fungal growth (5.0-8.5) (Meena et al., 2021). The material salinity resulting from exchangeable sodium, potassium, sulfate, chloride, nitrate, and soluble salts or because of the existence of highly conductivity metal ions is reflected through the electrical conductivity of MTS, which was found to be 0.29 mS/cm (Feng et al., 2021). Whereas the addition of char (3.55 mS/m) and VC (2.2 mS/m) can enhance the EC of the mined soil. Bulk density is a sign of both healthy and compacted soil. It has an impact on plant nutrient availability, soil porosity, available water capacity, infiltration, rooting depth/restrictions, and soil microbe activity, all of which are important soil processes and productivity (USDA NRCS, 1998). Generally, loose soil, which is aggregated in a well and porous structure with high organic matter, generally has low bulk density. The bulk density of MTS was high at about 1.20 g/cm3, with a low porosity of 48%. Whereas char and VC had 0.6 and 0.67 g/cm^3 bulk density and 78 and 71% porosity, respectively. The addition of char and VC will lower the bulk density by improving the porosity of the soil. Previous researchers have reported that the optimum and minimum range of porosity for aerobic decomposition was 85–90%, and 30%, respectively (Ruggieri et al., 2009). Hence, it is desirable to have less dense soil for good agricultural practices. The moisture content of MTS was maximum (12%), whereas MSW char was very low, about 1.16%. The moisture level of good soil is in the range of 20 to 60% (Nepal et al., 2023). Thus, adding VC, which has a moisture content of 62%, can enhance the moisture content in the soil. Appropriate moisture content encourages heat to be dispersed effectively throughout the pile, maintaining the ideal temperature range

needed for decomposition. The specific gravity helps in the movement of solute, supports water, and provides aeration in the soil. Higher specific gravity in the soil affects plant growth (Rai and Chatrath, 2019). The application of char and VC can improve the specific gravity of MTS, thus making it more suitable for plantation. The volatile solid of MTS was very low, which indicates unsuitable for microbial activity, resulting in slow bio-oxidation. Whereas char and VC have volatile solids of 30.31 and 36.27%. To counteract the lower volatile solids, char and VC can be amended in MTS. The TKN of MTS was 0.13%, which can be enhanced by the addition of char and VC with TKN of 0.2 and 0.56%, respectively, for plant growth. TOC specifically refers to the carbon content in organic compounds, while OM encompasses the entire range of organic materials in soil (Bisutti et al., 2004). Both TOC and OM are critical for soil fertility, nutrient cycling, soil structure, and overall soil health. Monitoring and managing these parameters can help optimize agricultural productivity, support sustainable land management practices, and mitigate environmental challenges. The TOC of MTS was 0.11%, which can be improved by the application of char and VC. The WHC is desirable to be high because it will retain the moisture in the soil, and the irrigation frequency required will not be very high if the WHC is good enough. The WHC of MTS (18.5%) can be enhanced with the addition of char and VC.

Table 10.1. Initial characterization of soil, MSW char, and VC

Parameters	**Units**	**Soil**	**MSW Char**	**VC**
pH	-	3.25 ± 0.02	7.11 ± 0.1	6.7 ± 0.2
EC	dS/m	0.29 ± 0.01	3.55 ± 0.14	2.2 ± 0.15
Bulk density	g/cm^3	1.20 ± 0.02	0.60 ± 0.04	0.67 ± 0.12
Porosity	%	48 ± 0.4	78 ± 0.02	67 ± 0.3
Moisture content	%	12 ± 0.02	1.16 ± 0.03	62 ± 0.05
Specific gravity	-	2.56 ± 0.01	2.1 ± 0.01	1.06 ± 0.22
Volatile solids	%	5.3 ± 0.11	30.31 ± 0.02	36.27 ± 0.06
TKN	%	0.13 ± 0.02	0.2 ± 0.1	0.56 ± 0.07
TOC	%	0.11 ± 0.02	8 ± 0.22	4.3 ± 0.2
WHC	%	18.5 ± 2.12	25 ± 0.02	45.12± 0.6

10.2 EFFECT OF THE PHYSIO-CHEMICAL PARAMETERS OF MTS WITH THE APPLICATION OF CHAR AND VC

With the application of MSW char (10 and 20%) and a combination of char (5%) and VC (20 and 30%) in MTS, there was variation in the physiochemical parameters from the 0^{th} day to the 45^{th} day, as shown in Fig. 10.1. The pH of the MTS, which was initially 3.25, increased with the amendment of char and VC. The maximum pH of MTS was 6.4 when 10% char was applied, followed by the combination of 5% char and 30% VC in MTS, which was 6.2. But with the due course of time, the pH of the MTS decreased to 5.25 on the 45^{th} day. The average increase in the pH of MTS was 45.44% on the 0^{th} day with the application of 10% char, and the trend was similar to the studies on the application of biochar and VC in soil (Wang et al., 2021). The char produced at lower temperatures generally increases the EC of soil on its application (Singh et al., 2022). In this study, the char produced at 350°C was used, and the EC significantly increased in the 0^{th} day by 76% with the amendment of the combination of 5% char and 30% VC, and then a decrease in EC was observed with the increase in time to the 45^{th} day, which had the lowest average values of 0.65 dS/m in the 10% and 20% char treated soil. A similar trend was observed with the implementation of biochar produced at 550°C on soil (Singh et al., 2022). The bulk density of MTS was observed to be increasing with the number of days but with the amendment of char and VC, the bulk density declined as compared to control. The bulk density was decreased by 3.3% on the 0^{th} day with the application of 30% VC and 5% char, and the value obtained was 1.17 g/cm^3, which was comparable to the bulk density obtained with the addition of biochar in soil (Blanco-Canqui, 2017), thus improving the MTS properties. The specific gravity of soil is a significant index attribute that is intimately related to its chemistry or mineralogy (Oyediran and Durojaiye, 2011). In terms of the physical characteristics of soil, it is quite significant and helpful for classifying soil minerals; iron minerals, for instance, have a higher specific gravity level than silicas (Tuncer and Lohnes, 1977). It gives an idea about the suitability of the soil as a construction material; the higher value of specific gravity gives more strength to roads and foundations. Typically, soil with iron, inorganic clay, and silty sand has a specific

gravity of 2.67-3 (Roy and Bhalla, 2017). In this study the value of specific gravity was less as compared to healthy soil. With the implementation of 10% MSW char, the specific gravity of the MTS increased by 4% on the 45th day. The volatile solids in the MTS decreased over time but increased by 2.45-fold with the application of a combination of 30% VC and 5% MSW char on the 0th day, as VC and char itself are high in volatile solids of 36.27 and 30.31%, respectively. The increase in volatile solids enhances microbial activity in the soil, thus making MTS suitable for agriculture (Ameloot et al., 2013). The WHC of untreated MTS was 18.25% which was comparatively less than sandy and sandy loam soil (21 and 25%, respectively). The WHC decreased from the 0th to the 45th day but increased by 2.96 fold in the MTS with the application of a combination of 5% MSW char and 30% VC, which was much higher than unsorted biochar prepared at 550°C when applied to sandy loam soil (Verheijen et al., 2019). The application of VC and char can have a positive impact on TKN in soil by improving nitrogen retention, enhancing microbial activity, and acting as a slow-release fertilizer. In this study, it was observed that the TKN of MTS reduced with the increase in time but increased on the initial day by 2.79-fold with the amendment of 30% VC and 5% MSW char. Studies have shown that the application of biochar to soil can increase TKN by enhancing nitrogen retention and reducing losses due to leaching and volatilization. For instance, research has demonstrated that biochar-amended soils can exhibit higher TKN levels compared to unamended soil (Zhang et al., 2021).

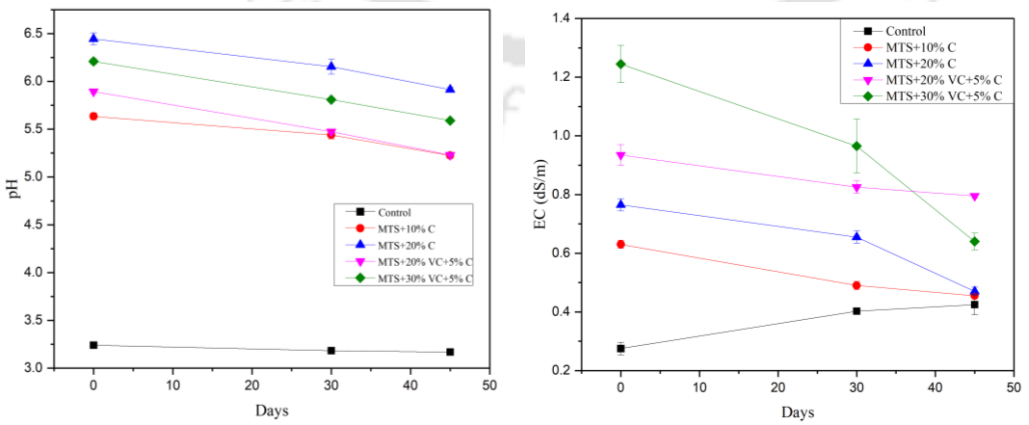

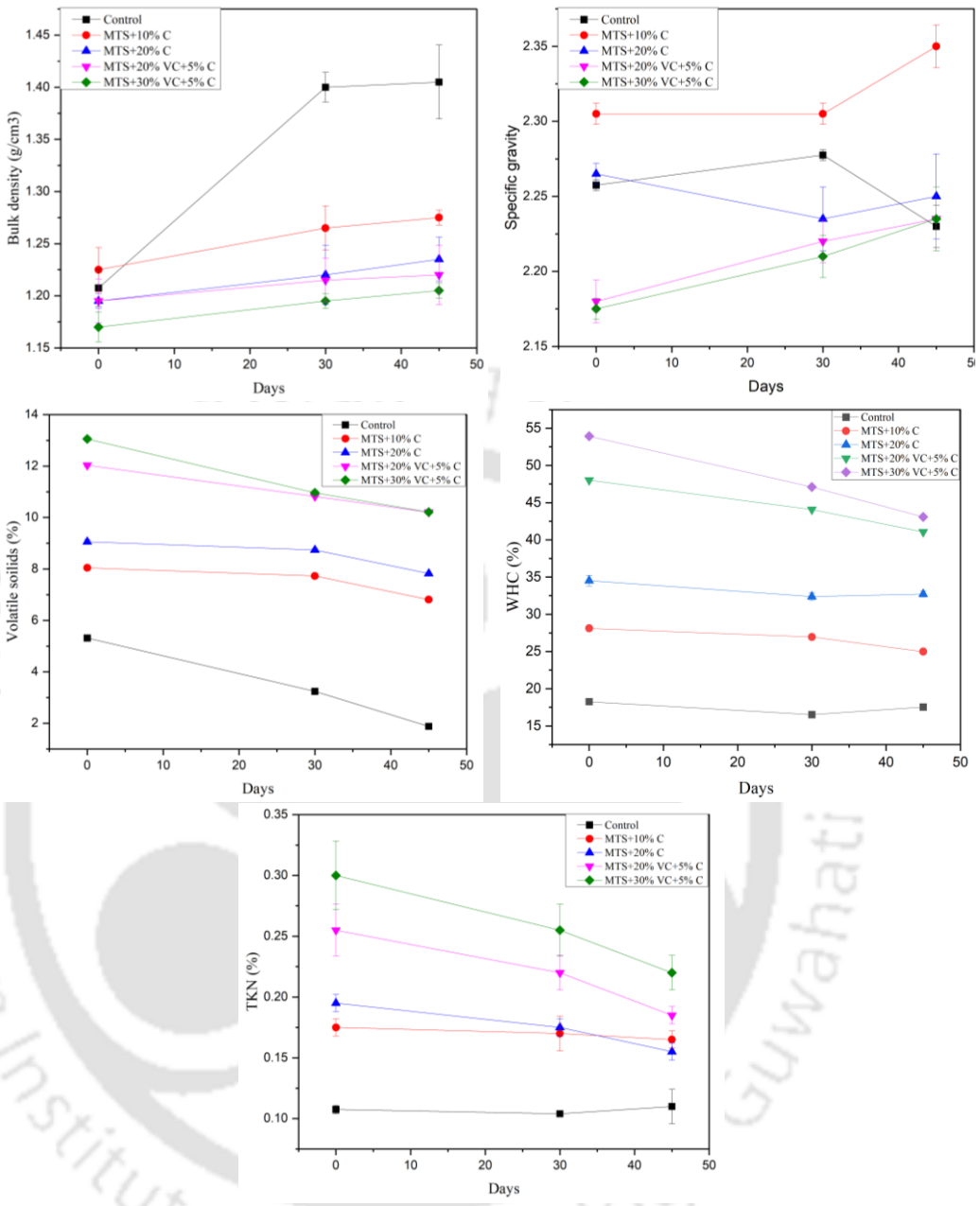

Fig. 10.1. Variation in physiochemical parameters with the amendment of char and VC in MTS

10.3 TOTAL METALS

The amendment of char and VC in soil has a synergistic effect which reduces the availability of total metals (Munir et al., 2020). The availability of Fe was decreased with the increase in time when a combination of 30% VC and 5% char

were applied to MTS, as depicted in Fig. 10.2. The amendment of VC and char reduced the availability of Fe in soil by 28% on the 30th day. The availability of Ni was reduced by 22% with the addition of 20% VC and 5% char on the 45th day. In the case of Pb, the highest reduction was by 9% on the 45th day with the application of 20% char. The reduction of available total metals with the amendment of char and VC was primarily due to the large surface area, porosity, and presence of functional groups that adsorb heavy metals (Beesley et al., 2011). Meanwhile, the availability of Zn and Mn increased with time because of the presence of these metals in higher concentrations in compost and char and mineralization with the increase in the number of days. Also, the increasing pH of MTS with the application of MSW char led to the precipitation of metals and reduced solubility, thus limiting the availability to plants (Wei et al., 2023).

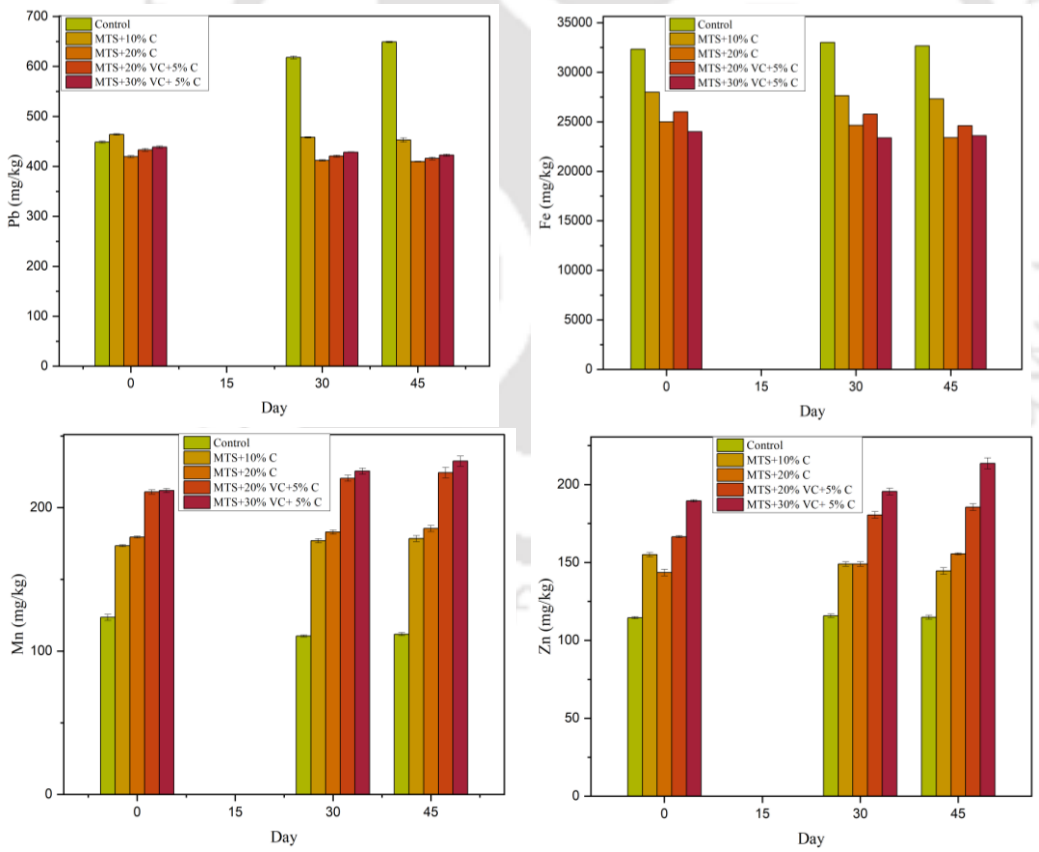

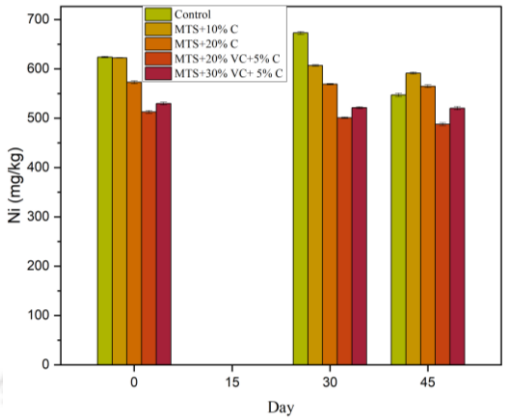

Fig. 10.2. Variation in the availability of total metals in MTS

10.4 WATER SOLUBLE METALS

The application of char and VC to soil can significantly affect the behavior of water-soluble metals by reducing the mobility and bioavailability of metals in soil. Fig. 10.3 illustrates the amendment of char and VC, and it was observed that the bioavailability of the water-soluble metals decreased with the increase in time. The availability of water-soluble fraction of Fe with the amendments increases than that of control but later reduces with the application of 30% VC and 5% char from 0^{th} day to 45^{th} day by 19%. The data shows that biochar alone can significantly increase the availability of a water-soluble portion of Fe, indicating that char can enhance the solubility of iron in the soil. Adding VC along with char also increases the metal availability, though to a slightly lesser extent compared to char alone. This suggests that while VC contributes to the increase in water-soluble Fe, its effect might be moderated when combined with MSW char. Over the 45-day period, the availability of Fe tends to decrease slightly but remains significantly elevated in amended soils compared to the control. This indicates that the amendments provide a sustained release of metal, though the peak availability may diminish over time. Char, due to its high surface area and porous structure, likely enhances the retention and gradual release of Fe. VC rich in organic matter and nutrients, further contributes to this effect, though the combination with char may moderate the peak availability levels slightly. These amendments provide a more sustained release of

water-soluble portion of Fe, which can be beneficial for improving soil fertility and plant nutrition over time.

Similar to Fe, the addition of char and VC significantly increases the water-soluble Mn. The immediate increase is likely due to the nutrient content of char and VC. The Mn fraction decreases over time, which could be due to natural processes such as leaching or binding to soil particles. The water-soluble Mn levels remain elevated compared to the control and show a slight decrease over time. Char continues to release Mn, maintaining its availability. The presence of VC initially boosts water-soluble Mn availability. However, there was a decrease over time, similar to Fe. This could be due to a reduction in microbial decomposition activity or Mn becoming bound in less soluble forms. The reduction in Mn levels at day 30 and day 45 across all the treatments suggests a similar process affecting Mn as Fe, including plant uptake, leaching, and binding. The water-soluble fraction of Ni, Zn, and Pb was found to be reduced to undetected levels with the amendment of char and VC.

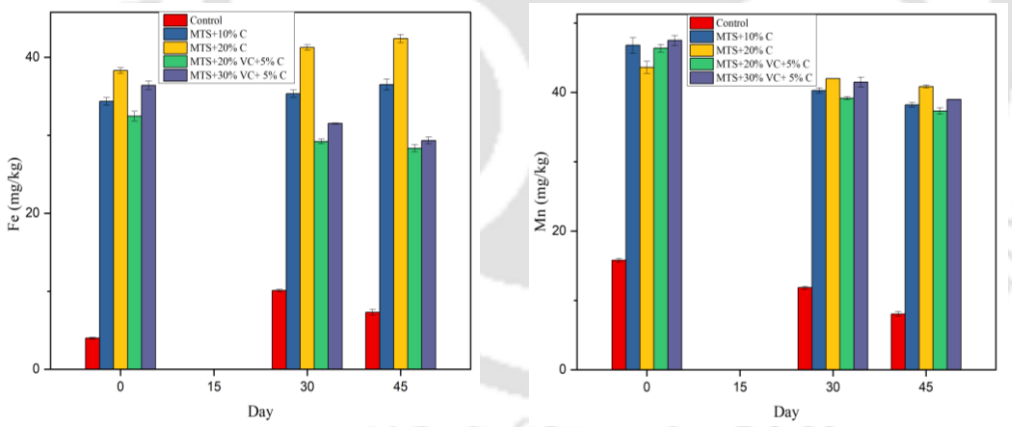

Fig. 10.3. Variation of water-soluble metals with the application of MSW char and VC

10.5 BIOAVAILABILITY OF HEAVY METALS (DTPA)

DTPA metal fraction in soil is significant for understanding metal availability to plants, nutrient management, soil testing, environmental risk assessment, and regulatory compliance. It is a chelating agent used to extract bioavailable forms of

metals from soil, which provides valuable information for optimizing plant nutrition, assessing soil fertility, managing metal contamination, and ensuring sustainable land use practices (Jafarnejadi et al., 2013). Initially, DTPA-extractable Fe was higher in soil amended with MSW char and VC compared to control, indicating that these amendments increased the availability of Fe, as shown in Fig. 10.4. The availability of Fe increased over time in the MTS by 91% on day 45. The amendment of 20% char shows a drastic reduction in Fe availability by 89% on the 45th day, indicating a significant immobilization effect over time. The DTPA-extractable Zn on the 0th day was higher in the amended MTS compared to the control. The application of 30% VC and 5% char has the highest Zn availability due to the presence of metal in VC. The availability of Zn increases on the 30^{th} day and then decreases slightly by the 45^{th} day in control, whereas, with the amendment of 30% VC and 5% char, the Zn availability increases by 45%. Similarly, DTPA extractable Mn increased in the amended MTS but decreased over time, indicating natural reduction processes (Tebo et al., 2005). Other metals, such as Ni and Pb, remained at the undetectable level with the application of MSW char and VC. The initial increase in the DTPA-extractable Fe, Zn, and Mn with MSW char and VC amendments can be attributed to the release of nutrients from char and VC (Lehmann et al., 2003). The high surface area and porosity, combined with the rich nutrient content of VC, enhance the metal's availability. Over time, the availability of these metals generally decreases, which is due to the adsorption by char and, hence, the immobilization of heavy metals, reducing their bioavailability (Ahmad et al., 2014). The increase in pH with the application of char leads to the precipitation of metals, reducing their solubility (Lu et al., 2014). Also, the metals form complexes with organic matter from VC and char, reducing their extractability (Park et al., 2011). The combined use of MSW char and VC can provide a balanced approach to enhancing soil fertility while mitigating heavy metal availability.

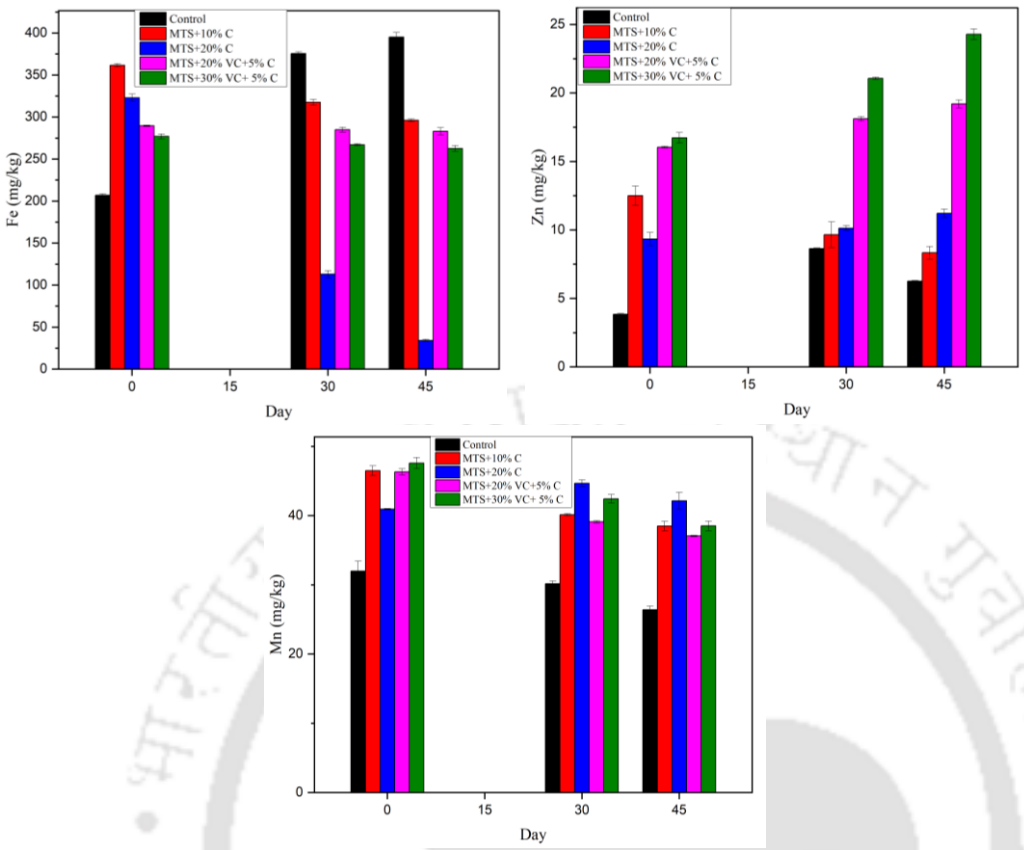

Fig. 10.4. Variation of DTPA metals in MTS

10.6 LEACHABILITY OF HEAVY METALS

To evaluate the leachability of heavy metals, one popular method is to calculate the heavy metal leached fraction, which is the ratio of the quantity of heavy metal liberated from the toxicity characteristics leaching procedure (TCLP) assay to its total content. The purpose of TCLP is to measure the mobility of both inorganic and organic analogs in solid, liquid, and multiphase waste, sediments, and soil. The TCLP test is primarily used to evaluate the potential environmental impact of solid waste materials, such as industrial byproducts, municipal solid waste, and hazardous wastes. The test assesses the leaching potential of metals and other contaminants from the waste under specific conditions that simulate environmental conditions, particularly those found in landfills. From Fig. 10.5, it was observed that the availability of leachable heavy metals such as Fe, Zn, and Mn increased on the 0th day, whereas Ni and Pb decreased with the amendments as compared to the

control. The availability of leachable metal fractions of Fe, Zn, and Mn in MTS increases with time from 0 to 45 days since char and VC are packed with nutrients, which follows a similar trend to the studies reported on compost amendment in soil (Pathak and Rao, 1998). The availability of a leachable fraction of Ni was reduced by 30% on the initial day with the amendment of 20% VC and 5% char. Similarly, the availability of leachable Pb in MTS reduced on the 45th day by 61% with the application of 30% VC and 5% char. The Fe and Pb are less soluble in alkaline conditions, which explains the observed reduction in the leachability data. The alkaline nature of char contributes to the precipitation and adsorption of heavy metals, thus reducing their leachability (Méndez et al., 2012). Also, VC increases microbial activity and organic matter in the soil, which can lead to the formation of stable metal-organic complexes. These complexes reduce the mobility and leachability of metals (Liu et al., 2018). Similar studies on biochar amendments showed a general trend of reducing heavy metals leachability, though the effectiveness varies with different metals (Ahmad et al., 2014). Studies showed that the reduction in heavy metals leachability in soil was contributed by the synergistic effect of char and VC (Liu et al., 2018). The data shows that a combination of char and VC amendments can effectively reduce the leachability of heavy metals in MTS. These findings are consistent with other studies, underscoring the potential of these amendments in soil remediation efforts (Glaser et al., 2002).

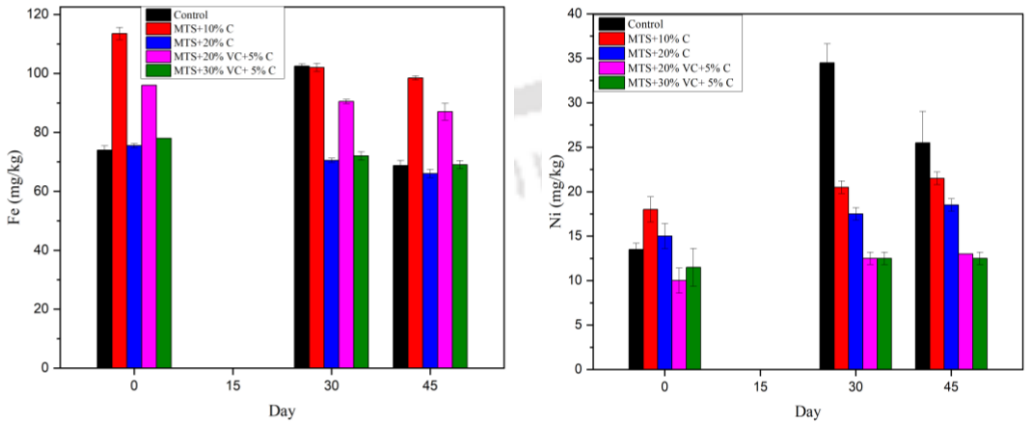

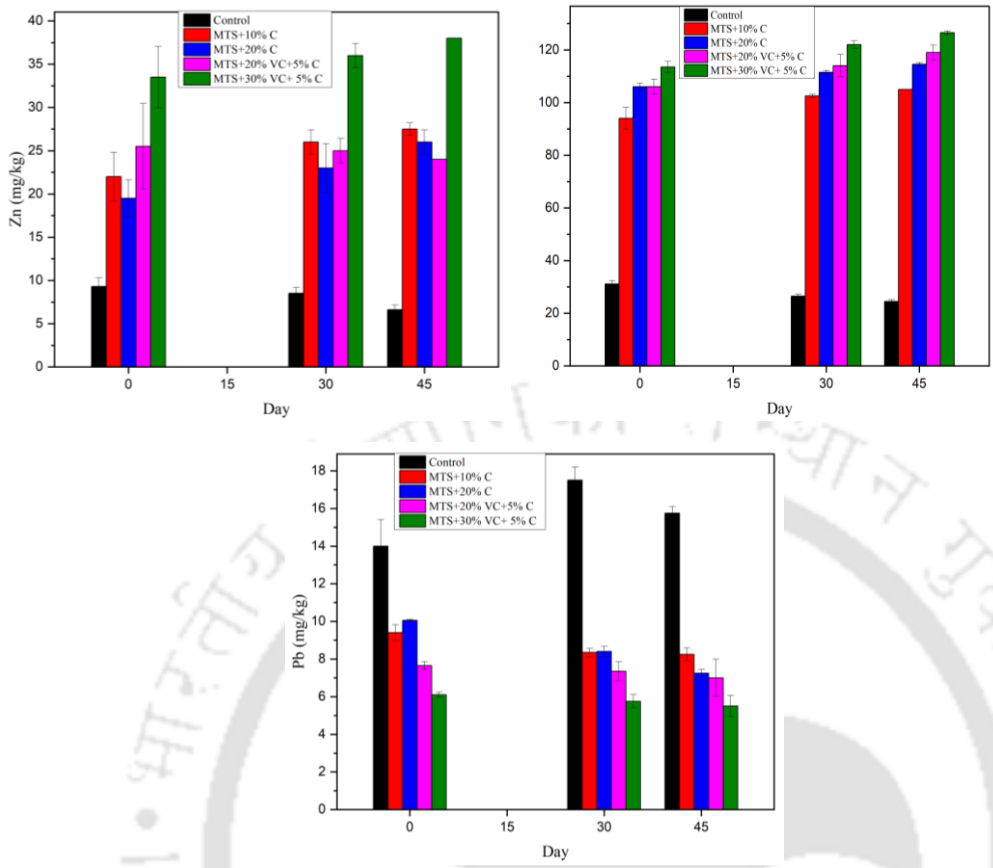

Fig. 10.5. Leachability of heavy metals in MTS

10.7 METAL SPECIATION IN MINE TAILING SOIL

The impact of metal speciation in soil with the amendment of char and VC can vary. Each fraction may be influenced differently, potentially affecting the bioavailability, mobility, and overall metal behavior in the soil. The F3, F4, and F5 fractions of Fe were found to be prominent in all the amendments and control on the initial day to the 45th day, whereas F1 and F2 were negligible levels throughout the amendments, as shown in Fig. 10.6. The order of the Fe fractions was F3>F4>F5. The F3 was highest mostly due to the reduction and oxidation reaction in the MTS with the application of char and VC, thus affecting the binding of metal to Fe oxides. The VC is rich in organic matter and increases the F4 by complexing metals with organic compounds (Beesley et al., 2011). The F5 is the least affected initially, as these metals are tightly bound within the soil matrix (Liu et al., 2022).

There were only changes in metal fractions in control, and the percentage of fraction of metals in the amendments remains the same.

In the case of Ni, the F5 was highest (99%) in control on the initial day, whereas the F4, F3, F2, and F1 were at the lowest level but increased the availability with the amendments. The highest reduction in the F5 fraction availability was 73%, and the F4 fraction increased by 48% with the amendment of 20% VC and 5% char in MTS. The F1 was reduced to 0% with the application of 20% VC and 5% char, as well as 30% VC and 5% char. On the 45th day, the availability of F1 was reduced to 0%, but F2 increased with all the amendments. The F1 fraction is the most bioavailable and mobile form of Ni in soil. The addition of char and VC reduced the exchangeable fraction of Ni due to the high surface area and presence of functional groups that adsorb Ni, thereby reducing its availability. VC contains organic matter that can be complex with Ni, further reducing its mobility (Beesley et al., 2011). The F2 involves Ni bound to carbonates and is moderately available. The presence of char increased the carbonate bound fractions due to its alkalizing effect, which promotes the precipitation of Ni as carbonate minerals. VC also helps in buffering soil pH, which enhances the formation of carbonate-bound Ni (Park et al., 2011). The Ni in F3 is associated with iron and manganese oxides. Char and VC can influence soil redox conditions, potentially stabilizing Fe-Mn oxides and enhancing Ni sorption onto these oxides. This leads to an increase in the Fe-Mn oxide-bound fraction of Ni (Tang et al., 2013). Similarly, the F4 of Ni is bound to the organic matter of VC, forming stable complexes with Ni. Char, with its surface area and functional groups, can also enhance the binding of Ni to organic matter (Liang et al., 2006). The availability of F5 decreased the maximum by 50% on the 45th day with the amendment of 20% char in MTS. The overall decrease of the residual fraction of Ni was due to the strong bond within the mineral matrix and is the least available form. However, char and VC have a minimal effect on this fraction, but the changes in soil chemistry and microbial activity slowly affect the residual Ni fraction (Liu et al., 2022).

The availability of F1 and F5 of Zn decreased in control from the initial day to the 45th day due to the adsorption and complexation, and also the bonding of Zn to

carbonates, Fe-Mn oxide, or organic matter (Méndez et al., 2012). The F2 remains the same over time in control but decreases to 0% with the application of char in MTS. This further increases on the 45th day with all the amendments due to the presence of Zn in both char and VC. The availability of F3 in Zn reduces with the amendment of 10% and 20% MSW char by 6% and up to 4% with the application of 20% VC and 5% char. On the 0th day, F3 increased by 12% with the application of 30% VC and 5% char in MTS. With the increase in time, the F3 decreases with the amendments due to the surfaces and functional groups that promote the adsorption of Zn to Fe-Mn oxides (Beesley et al., 2011). Organic matter in VC can interact with Fe-Mn oxides, creating organic Fe-Mn oxide complexes that have a high affinity for Zn, which increases the amount of Zn associated with Fe-Mn oxide (Liang et al., 2006). The F4 increases with all the amendments initially, and the highest was 51% with the application of 20% char. On the 45th day, the F4 decreased due to the breakdown of organic matter, resulting in the disruption of a complex between Zn and organic compounds, which decreases the organic bond fraction of Zn (Bernal et al., 2009). The F5 of Zn remained the same with the application of 10% char, but the availability decreased by 24% with the application of 20% VC and 5% char on the initial day. As the char and VC alter the soil pH and redox conditions, they can affect the stability of minerals that tightly bind Zn. The increase in pH enhances the dissolution of minerals, releasing Zn into a more available fraction (Beesley et al., 2011). Also, VC contains organic ligands that can chelate Zn, effectively extracting it from the mineral matrix, which decreases the residual fraction as Zn forms soluble complexes with organic molecules (Novak et al., 2009). Further, the F5 fraction increased with all the amendments on the 45th day and the highest increase in the available F5 of Zn was by 38% with the amendment of 30% VC and 5% char. This was because, over time, char becomes stable and forms complexes between Zn and char, leading to the immobilization of Zn in the residual fraction (Lehmann et al., 2011a). The presence of char and VC promotes the formation of stable mineral phases, such as Zn silicates or Zn precipitates, which are a part of the residual fraction that incorporate Zn into their structure over time (Beesley et al., 2011).

The available F1 of Mn decreased by 80% on the 45th day with the application of 20% char due to an increase in soil pH, thus leading to a decrease in the solubility and mobility of Mn (Ghodszad et al., 2021). The F2 was reduced by 17% with the application of 30% VC and 5% char. The reduction in F2 of Mn in soil over time was due to the changes in pH of soil and carbonate dynamics (Novak et al., 2009), enhanced microbial activity and organic complexation (Lehmann et al., 2011a), sorption onto char and soil organic matter (Beesley et al., 2011), precipitation and co-precipitation reactions (Mendez and Maier, 2008). These processes collectively reduce the association of Mn with carbonate minerals, leading to a decrease in the carbonate bond fraction.

In the case of Pb, the F1 and F2 were reduced by 83% on the 45th day with the amendment of 30% VC and 5% char. Due to the high surface area of char, the Pb is adsorbed onto the surface, reducing its availability in the exchangeable form (Beesley et al., 2011). Also, the char and VC can enhance the formation of stable organic complexes with Pb, which reduces the mobility and shifts it from an exchangeable fraction to a more stable form (Mendez and Maier, 2008). With the application of char, the increase in soil pH contributes to the reduction in solubility of Pb and promotes the formation of insoluble Pb compounds, thereby decreasing the exchangeable fraction (Ghodszad et al., 2021). The F3, F4, and F5 of Pb increased over time with all the amendments due to enhanced adsorption onto Fe-Mn oxides, formation of stable organic complexes, and immobilization of Pb in residual forms. These processes collectively enhance the stabilization and reduce the mobility of Pb in contaminated soil making these fractions more prevalent compared to the control. From the metal speciation study, it was observed that the availability of F1 and F2 portions of harmful metals such as Pb and Ni were reduced over time with the amendment of char and VC, which makes the MTS less risky for plant toxicity and environmental contamination (Kabata-Pendias, 1984). In contrast, the F3, F4, and F5 portions of metals were intensified with the amendments but were not threatening to the environment since these fractions are less bioavailable and pose lower risks (Ghodszad et al., 2021). Overall, the

combined use of biochar and compost can alter the distribution and stability of heavy metals across these fractions, potentially reducing their environmental risk.

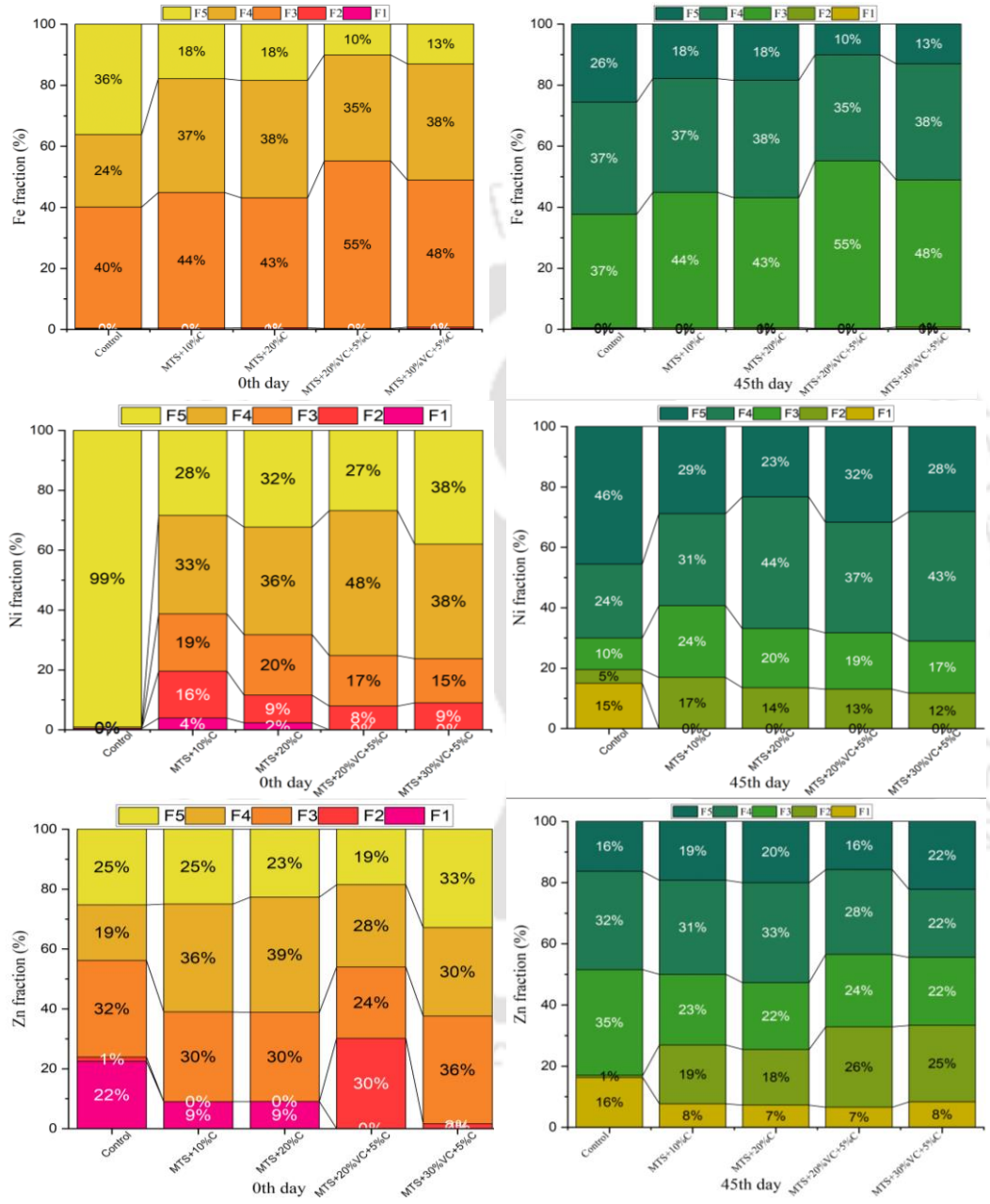

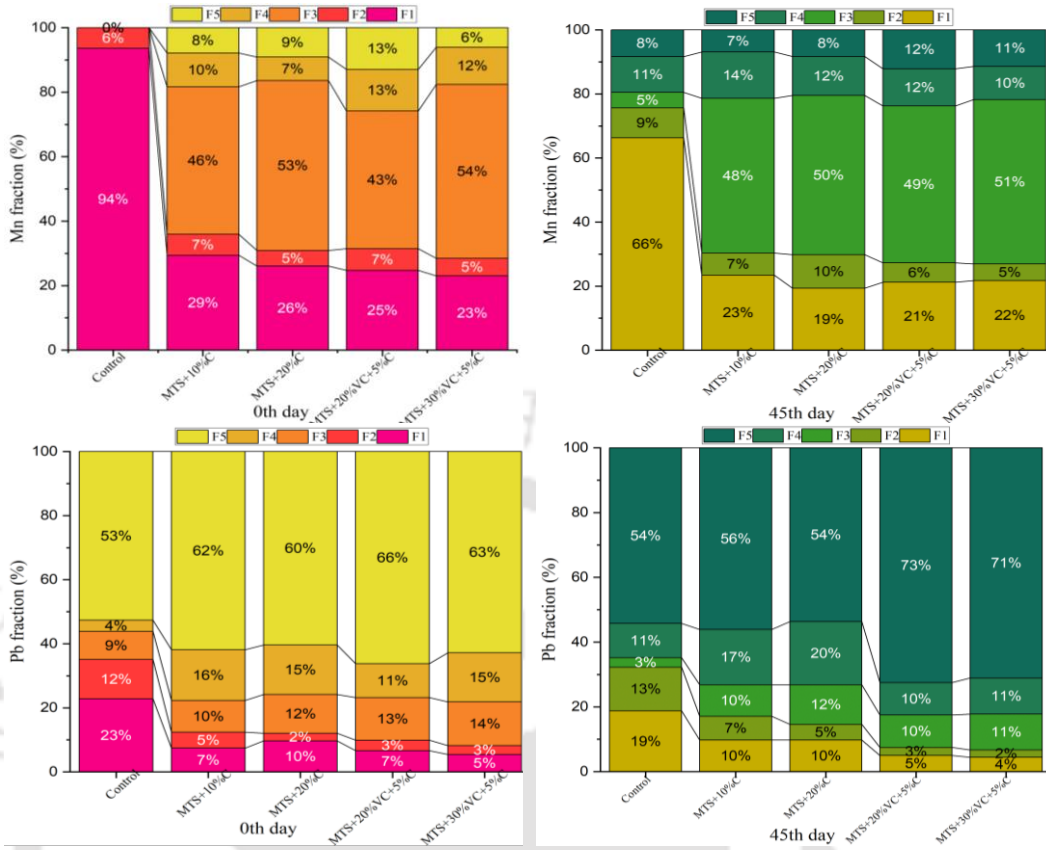

Fig. 10.6. Variation in the available fractions of metals in MTS

10.8 MOBILITY FACTOR AND RAC

The mobility of metals in soil directly impacts their bioavailability, which in turn affects their toxicity to plants and microorganisms. Metals that are highly mobile are more likely to be taken up by plant roots, potentially leading to phytotoxicity and entering the food chain. Highly mobile metals can leach through the soil profile and contaminate groundwater, posing risks to drinking water supplies and aquatic ecosystems. Of all the metals analyzed, Pb is particularly concerning due to their toxicity and persistence in the environment (Zhang et al., 2013). As shown in Table 10.2, it was observed that the mobility factor of Fe increased in MTS, but RAC was 0, with all the amendments indicating "no risk" for the environment. The mobility factor for Ni was found to increase over time in control by 52% and the percentage of mobility was decreased by 44% with the amendment of 30% VC and 5% MSW char. The RAC was reduced by 29%,

indicating the bioavailable fraction Ni in MTS to pose a "medium risk" to the environment. The mobility of Zn was reduced by 38%, and RAC was 0 with "no risk" when 30% VC and 5% char were applied in MTS. With the increase in time, mobility increased, but there was less concern due to the non-toxic effect of Zn in soil on the environment as it was within the permissible limit (Ministry of Agriculture, 2013). The maximum reduction in mobility of Mn was 26% with the application of 20% VC and 5% char initially, and the RAC of Mn in MTS was reduced by 73% with the amendment of a combination of 5% char each in 20% VC and 30% VC on the 45th day. Initially, the percentage of mobility of Pb was reduced by 50% with the amendment of 10% char and a combination of 5% char with 30% VC in MTS, with RAC indicating "low risk". Whereas the amendment of char and VC in MTS over time increased, the mobility percentage and RAC of Pb were at "high risk".

Table 10.2. Mobility percentage and RAC of metals in MTS

Days	Amendments	Fe		Ni		Zn		Mn		Pb	
		MF (%)	RAC (%)	MF (%)	RAC (%)	MF (%)	RAC (%)	MF (%)	RAC (%)	MF (%)	RAC (%)
0th day	Control	40	0	0	0	56	23	100	100	44	35
	MTS+10%C	44	0	39	20	39	9	82	36	22	12
	MTS+20%C	43	0	31	11	39	9	84	31	24	12
	MTS+20%VC +5%C	55	0	25	8	53	30	74	32	23	10
	MTS+30%VC +5%C	49	0	24	9	36	0	82	28	22	8
45th day	Control	37	0	52	17	52	17	81	76	35	32
	MTS+10%C	44	0	41	17	50	27	79	30	83	67
	MTS+20%C	43	0	34	14	47	25	80	29	54	28
	MTS+20%VC +5%C	55	0	32	13	56	33	76	27	70	41
	MTS+30%VC +5%C	49	0	29	12	56	33	79	27	53	36

10.9 CONCLUSION FROM APPLICATION OF MSW CHAR IN MINE TAILING SOIL

The amendment of MSW char for metal immobilization and reducing the available heavy metals proved to be a virtuous remediation technique for acidic coal mine tailing soil, but char amended with VC showed better results in terms of improving the soil texture and physio-chemical properties of the soil. Applying MSW char alone significantly increased pH and specific gravity, while the combination of char and VC increased volatile solids, electrical conductivity, water holding capacity, and TKN and reduced the bulk density. The availability of total metals was reduced with the amendment of char alone as well as with the combination of char and VC in MTS. Water-soluble metals initially increased with only char application but decreased over time with the combined effect of VC and char, and water-soluble fractions of Ni, Zn, and Pb were reduced to undetectable levels with all amendments. Bioavailable Fe decreased with 20% char, though Mn and Zn increased, while bioavailable Ni and Pb fell to undetectable levels with all amendments. The leachability of Fe, Zn, and Mn increased, whereas Ni and Pb decreased with 20% VC+5% char and 30% VC+5% char. F1 and F2 metal fractions decreased after char amendments with VC, reducing metal mobility, although Pb remained at "high risk." Increasing char with VC can further reduce Pb mobility and RAC. Thus, using mixed MSW char and VC together enhances soil fertility while mitigating heavy metal availability in mine tailing soil.

Chapter 11

CONCLUSIONS AND RECOMMENDATIONS

This chapter presents a thorough amalgamation of key insights from numerous studies focused on the pyrolysis of unsegregated and non-shredded MSW for char production and its diverse application as an adsorbent and in soil remediation. Additionally, it offers valuable recommendations for future research endeavors in the domain of pyrolysis of MSW and its product utilization.

11.1 OVERALL CONCLUSIONS

- In phase I, the study underscores the promising role of pyrolysis in addressing the challenges of municipal solid waste and legacy waste management. By effectively recovering resources and generating energy, pyrolysis can transform waste into valuable solid fuel, taking advantage of the favorable characteristics of MSW, such as its high heating value and bulk density. The findings from thermogravimetric analysis indicate that pyrolysis not only enhances reaction efficiency but also aligns with sustainable waste management practices. Although the adoption of pyrolysis technology is still emerging in India, its implementation could significantly reduce landfill emissions and contribute to a cleaner environment. Embracing this "third-generation" technology offers a proactive step toward more sustainable waste solutions, paving the way for advancements in both energy recovery and waste minimization.
- Phase II successfully demonstrated the pyrolysis of commingled municipal solid waste in a fixed-bed reactor, establishing optimal operational conditions for maximizing char yield. Through a systematic approach utilizing CCD in RSM, the ideal parameters were identified as a temperature of 250°C, a heating rate of 10°C/min, a feed particle size of 50 mm, and a residence time of 180 minutes. Under these conditions, a maximum char yield of approximately 72.62% was achieved from 3 kg of waste. The analysis revealed that temperature was the most influential factor affecting char yield, followed by feed particle size, heating rate, and residence time. These findings underscore

the feasibility of achieving high char yields under relatively low operating temperatures and conditions, contributing valuable insights for optimizing waste-to-energy processes.

- In phase III, the pyrolysis of mixed municipal solid waste in a fixed-bed reactor has proven to be an effective method for producing high-quality char comparable to biomass-derived biochar. Characterization of the MSW char revealed promising properties making it suitable for applications in adsorption and as a soil amendment. The char produced at both 250°C and 350°C exhibits characteristics similar to biochar, enhancing its viability for heavy metal adsorption and soil enhancement. Overall, this study highlighted the potential of transforming waste into valuable carbon products, contributing to waste reduction efforts, and promoting sustainable practices in waste management. The activated carbon derived from MSW char demonstrated comparable effectiveness to commercially available activated carbon, particularly in the removal of Pb(II) from water. Characterization through various analyses confirmed that the MSW char, produced at 250°C and chemically activated with KOH, exhibited strong adsorptive properties, achieving over 90% removal of Pb(II) under optimized conditions. Kinetic studies indicated that the adsorption process followed a pseudo-first-order model and reached equilibrium within an hour, while isotherm analysis supported monolayer adsorption per the Langmuir model. The activated carbon maintained over 90% removal efficiency across two reuse cycles, with HNO_3 yielding the highest metal recovery during desorption. This research highlights the potential of MSW char-activated carbon as a cost-effective and sustainable solution for heavy metal removal in wastewater treatment, contributing to waste minimization at dumpsites. The co-composting of MSW char with vegetable waste effectively enhanced biodegradation, nutrient content, and heavy metal adsorption. The process yields nutrient-rich compost in just 20 days, with MSW char improving aeration and accelerating decomposition, exemplified by Trial 2, which achieved a peak temperature of 53.8°C and a prolonged thermophilic phase. The incorporation of MSW char also raised pH levels and enhanced the

buffering capacity while improving electrical conductivity and reducing heavy metal concentrations. Overall, the use of MSW char significantly enhanced both the efficiency and quality of composting, facilitating the conversion of mixed MSW into valuable products. The study of the application of char in alluvial soil highlighted its effectiveness with a combined application of 10% MSW char and 20% compost, which significantly enhances soil nutrients and physicochemical properties, ultimately promoting healthier plant growth. By the 120th day, improvements in bulk density, porosity, cation exchange capacity, pH, electrical conductivity, soil organic matter, and soil organic carbon were observed. Additionally, the amendments increased essential nutrients and, notably, MSW char reduced the bioavailability of heavy metals, minimizing plant uptake. The combination of MSW char and VC effectively remediates acidic coal mine tailing soil, improving soil texture and physicochemical properties. While both amendments reduce heavy metal availability, the char-VC mixture notably decreases water-soluble fractions of Ni, Zn, and Pb to undetectable levels, enhancing soil nutrients and mitigating risks associated with heavy metals.

11.2 FUTURE RECOMMENDATIONS

- Optimization of the pyrolysis process parameters for maximizing the yield of pyrolysis oil and syngas and its characterization can be studied.
- Further modification of the fixed bed pyrolizer for proper collection of pyrolysis oil and syngas and improvement in the efficiency of the pyrolysis process could be explored.
- Upgradation of char quality to improve its specific surface area for further application in the adsorption of multi-metals from wastewater.
- Application of MSW char as a combustible fuel by briquetting to a charcoal-like material.
- Modification of the fixed bed pyrolizer by integrating it into a gasifier for utilization of syngas.

BIBLIOGRAPHY

Abidli, S., Antunes, J. C., Ferreira, J. L., Lahbib, Y., Sobral, P., & Trigui El Menif, N. (2018). Microplastics in sediments from the littoral zone of the north Tunisian coast (Mediterranean Sea). *Estuarine, Coastal and Shelf Science*, *205*, 1–9. https://doi.org/10.1016/j.ecss.2018.03.006

Adeolu, A. T., Okareh, O. T., & Dada, A. O. (2016). Adsorption of Chromium Ion from Industrial Effluent Using Activated Carbon Derived from Plantain (Musa paradisiaca) Wastes. *American Journal of Environmental Protection*, *4*(1), 7–20. https://doi.org/10.12691/env-4-1-2

Agarwal, M., Tardio, J., & Venkata Mohan, S. (2013). Critical analysis of pyrolysis process with cellulosic based municipal waste as renewable source in energy and technical perspective. *Bioresource Technology*, *147*, 361–368. https://doi.org/10.1016/j.biortech.2013.08.011

Agarwal, M., Tardio, J., & Venkata Mohan, S. (2015). Pyrolysis of activated sludge: Energy analysis and its technical feasibility. *Bioresource Technology*, *178*, 70–75. https://doi.org/10.1016/j.biortech.2014.09.134

Agegnehu, G., Bass, A. M., Nelson, P. N., & Bird, M. I. (2016). Benefits of biochar, compost and biochar-compost for soil quality, maize yield and greenhouse gas emissions in a tropical agricultural soil. *Science of the Total Environment*, *543*, 295–306. https://doi.org/10.1016/j.scitotenv.2015.11.054

Aghaei Chadegani, A., Salehi, H., Md Yunus, M. M., Farhadi, H., Fooladi, M., Farhadi, M., & Ale Ebrahim, N. (2013). A comparison between two main academic literature collections: Web of science and scopus databases. *Asian Social Science*, *9*(5), 18–26. https://doi.org/10.5539/ass.v9n5p18

Agyarko-Mintah, E., Cowie, A., Van Zwieten, L., Singh, B. P., Smillie, R., Harden, S., & Fornasier, F. (2017). Biochar lowers ammonia emission and improves nitrogen retention in poultry litter composting. *Waste Management*, *61*(May 2016), 129–137. https://doi.org/10.1016/j.wasman.2016.12.009

Ahmad, M., Rajapaksha, A. U., Lim, J. E., Zhang, M., Bolan, N., Mohan, D., Vithanage, M., Lee, S. S., & Ok, Y. S. (2014). Biochar as a sorbent for contaminant management in soil and water: A review. *Chemosphere*, *99*, 19–33. https://doi.org/10.1016/j.chemosphere.2013.10.071

Akyürek, Z. (2021). Carbon dioxide sequestration assessment through pyrogenic biomass: Case for Turkey. *Polish Journal of Environmental Studies*, *30*(3), 2467–2475. https://doi.org/10.15244/pjoes/129688

Al-Ghouti, M. A., & Da'ana, D. A. (2020). Guidelines for the use and interpretation of adsorption isotherm models: A review. *Journal of Hazardous Materials*, *393*(November 2019), 122383. https://doi.org/10.1016/j.jhazmat.2020.122383

Al-Qodah, Z., & Shawabkah, R. (2009). Production and characterization of granular activated carbon from activated sludge. *Brazilian Journal of Chemical Engineering*, *26*(1), 127–136. https://doi.org/10.1590/S0104-66322009000100012

Al-Salem, S. M., Antelava, A., Constantinou, A., Manos, G., & Dutta, A. (2017). A review

on thermal and catalytic pyrolysis of plastic solid waste (PSW). *Journal of Environmental Management*, *197*(1408), 177–198. https://doi.org/10.1016/j.jenvman.2017.03.084

Al-Salem, S. M., Lettieri, P., & Baeyens, J. (2009). Recycling and recovery routes of plastic solid waste (PSW): A review. *Waste Management*, *29*(10), 2625–2643. https://doi.org/10.1016/j.wasman.2009.06.004

Alaboudi, K. A., Ahmed, B., & Brodie, G. (2019). Effect of biochar on Pb, Cd and Cr availability and maize growth in artificial contaminated soil. *Annals of Agricultural Sciences*, *64*(1), 95–102. https://doi.org/10.1016/j.aoas.2019.04.002

Albalasmeh, A. A., Quzaih, M. Z., Gharaibeh, M. A., Rusan, M., Mohawesh, O. E., Rababah, S. R., Alqudah, A., Alghamdi, A. G., & Naserin, A. (2024). Significance of pyrolytic temperature, application rate and incubation period of biochar in improving hydro-physical properties of calcareous sandy loam soil. *Scientific Reports*, *14*(1), 1–13. https://doi.org/10.1038/s41598-024-57755-y

Alghobar, M. A., & Suresha, S. (2017). Evaluation of metal accumulation in soil and tomatoes irrigated with sewage water from Mysore city, Karnataka, India. *Journal of the Saudi Society of Agricultural Sciences*, *16*(1), 49–59. https://doi.org/10.1016/j.jssas.2015.02.002

Amalina, F., Razak, A. S. A., Krishnan, S., Zularisam, A. W., & Nasrullah, M. (2022). A comprehensive assessment of the method for producing biochar, its characterization, stability, and potential applications in regenerative economic sustainability – A review. *Cleaner Materials*, *3*(January), 100045. https://doi.org/10.1016/j.clema.2022.100045

Ambaye, T. G., Vaccari, M., van Hullebusch, E. D., Amrane, A., & Rtimi, S. (2021). Mechanisms and adsorption capacities of biochar for the removal of organic and inorganic pollutants from industrial wastewater. *International Journal of Environmental Science and Technology*, *18*(10), 3273–3294. https://doi.org/10.1007/s13762-020-03060-w

Ameloot, N., De Neve, S., Jegajeevagan, K., Yildiz, G., Buchan, D., Funkuin, Y. N., Prins, W., Bouckaert, L., & Sleutel, S. (2013). Short-term CO2 and N2O emissions and microbial properties of biochar amended sandy loam soils. *Soil Biology and Biochemistry*, *57*, 401–410. https://doi.org/10.1016/j.soilbio.2012.10.025

Amini, Z., Hatami-Manesh, M., Aazami, J., & Savabieasfahani, M. (2024). Ecological risk assessment of heavy metals (Pb, Cd, Cr, Ni, Zn, Fe) and metalloid (As) in surface sediment of Anzali International Wetland, Iran. *Geology, Ecology, and Landscapes*, *00*(00), 1–19. https://doi.org/10.1080/24749508.2024.2373488

Anca-Couce, A. (2016). Reaction mechanisms and multi-scale modelling of lignocellulosic biomass pyrolysis. In *Progress in Energy and Combustion Science* (Vol. 53, Issue March 2016). https://doi.org/10.1016/j.pecs.2015.10.002

Angon, P. B., Islam, M. S., KC, S., Das, A., Anjum, N., Poudel, A., & Suchi, S. A. (2024). Sources, effects and present perspectives of heavy metals contamination: Soil, plants and human food chain. *Heliyon*, *10*(7), e28357. https://doi.org/10.1016/j.heliyon.2024.e28357

Ashiq, A., Adassooriya, N. M., Sarkar, B., Rajapaksha, A. U., Ok, Y. S., & Vithanage, M.

(2019). Municipal solid waste biochar-bentonite composite for the removal of antibiotic ciprofloxacin from aqueous media. *Journal of Environmental Management*, *236*(September 2018), 428–435. https://doi.org/10.1016/j.jenvman.2019.02.006

Ashiq, A., Sarkar, B., Adassooriya, N., Walpita, J., Rajapaksha, A. U., Ok, Y. S., & Vithanage, M. (2019). Sorption process of municipal solid waste biochar-montmorillonite composite for ciprofloxacin removal in aqueous media. *Chemosphere*, *236*, 124384. https://doi.org/10.1016/j.chemosphere.2019.124384

ASTDR, 2004. (2004). Ammonia Ammonia. *The Agency for Toxic Substances and Disease Registry (ATSDR)*, 1–7.

Awasthi, M. K., Wang, M., Chen, H., Wang, Q., Zhao, J., Ren, X., Li, D. sheng, Awasthi, S. K., Shen, F., Li, R., & Zhang, Z. (2017). Heterogeneity of biochar amendment to improve the carbon and nitrogen sequestration through reduce the greenhouse gases emissions during sewage sludge composting. *Bioresource Technology*, *224*, 428–438. https://doi.org/10.1016/j.biortech.2016.11.014

Awasthi, M. K., Wang, Q., Chen, H., Wang, M., Ren, X., Zhao, J., Li, J., Guo, D., Li, D. sheng, Awasthi, S. K., Sun, X., & Zhang, Z. (2017). Evaluation of biochar amended biosolids co-composting to improve the nutrient transformation and its correlation as a function for the production of nutrient-rich compost. *Bioresource Technology*, *237*, 156–166. https://doi.org/10.1016/j.biortech.2017.01.044

Ayeni, A. O., Adeeyo, O. A., Oresegun, O. M., & Oladimeji, T. E. (2015). Compositional analysis of lignocellulosic materials: Evaluation of an economically viable method suitable for woody and non-woody biomass. *American Journal of Engineering Research*, *44*, 2320–2847. www.ajer.org

Ayiania, M., Terrell, E., Dunsmoor, A., Carbajal-Gamarra, F. M., & Garcia-Perez, M. (2019). Characterization of solid and vapor products from thermochemical conversion of municipal solid waste woody fractions. *Waste Management*, *84*, 277–285. https://doi.org/10.1016/j.wasman.2018.11.042

Aysu, T., & Küçük, M. M. (2014). Biomass pyrolysis in a fixed-bed reactor: Effects of pyrolysis parameters on product yields and characterization of products. *Energy*, *64*, 1002–1025. https://doi.org/10.1016/j.energy.2013.11.053

Babu, B. V., & Chaurasia, A. S. (2003). Modeling, simulation and estimation of optimum parameters in pyrolysis of biomass. *Energy Conversion and Management*, *44*(13), 2135–2158. https://doi.org/10.1016/S0196-8904(02)00237-6

Badger, P. C., & Fransham, P. (2006). Use of mobile fast pyrolysis plants to densify biomass and reduce biomass handling costs - A preliminary assessment. *Biomass and Bioenergy*, *30*(4), 321–325. https://doi.org/10.1016/j.biombioe.2005.07.011

Badran, A. M., Utra, U., Yussof, N. S., & Bashir, M. J. K. (2023). Advancements in Adsorption Techniques for Sustainable Water Purification: A Focus on Lead Removal. *Separations*, *10*(11), 1–26. https://doi.org/10.3390/separations10110565

Baghurst, D. R., & Mingos, D. M. P. (1992). Superheating effects associated with microwave dielectric heating. *Journal of the Chemical Society, Chemical Communications*, *9*, 674–677. https://doi.org/10.1039/C39920000674

Bakshi, S., Banik, C., & Laird, D. A. (2020). Estimating the organic oxygen content of

biochar. *Scientific Reports*, *10*(1), 1–12. https://doi.org/10.1038/s41598-020-69798-y

Barampouti, E. M., Mai, S., Malamis, D., Moustakas, K., & Loizidou, M. (2019). Liquid biofuels from the organic fraction of municipal solid waste: A review. *Renewable and Sustainable Energy Reviews*, *110*(April), 298–314. https://doi.org/10.1016/j.rser.2019.04.005

Beesley, L., Inneh, O. S., Norton, G. J., Moreno-Jimenez, E., Pardo, T., Clemente, R., & Dawson, J. J. C. (2014). Assessing the influence of compost and biochar amendments on the mobility and toxicity of metals and arsenic in a naturally contaminated mine soil. *Environmental Pollution*, *186*, 195–202. https://doi.org/10.1016/j.envpol.2013.11.026

Beesley, L., Moreno-Jiménez, E., & Gomez-Eyles, J. L. (2010). Effects of biochar and greenwaste compost amendments on mobility, bioavailability and toxicity of inorganic and organic contaminants in a multi-element polluted soil. *Environmental Pollution*, *158*(6), 2282–2287. https://doi.org/10.1016/j.envpol.2010.02.003

Beesley, L., Moreno-Jiménez, E., Gomez-Eyles, J. L., Harris, E., Robinson, B., & Sizmur, T. (2011). A review of biochars' potential role in the remediation, revegetation and restoration of contaminated soils. *Environmental Pollution*, *159*(12), 3269–3282. https://doi.org/10.1016/j.envpol.2011.07.023

Beheshti, S. M., Ghassemi, H., & Shahsavan-Markadeh, R. (2015). Process simulation of biomass gasification in a bubbling fluidized bed reactor. *Energy Conversion and Management*, *94*, 345–352. https://doi.org/10.1016/j.enconman.2015.01.060

Bekchanova, M., Campion, L., Bruns, S., Kuppens, T., Lehmann, J., Jozefczak, M., Cuypers, A., & Malina, R. (2024). Biochar improves the nutrient cycle in sandy-textured soils and increases crop yield: a systematic review. *Environmental Evidence*, *13*(1), 1–34. https://doi.org/10.1186/s13750-024-00326-5

Beneroso, D., Monti, T., Kostas, E. T., & Robinson, J. (2017). Microwave pyrolysis of biomass for bio-oil production: Scalable processing concepts. *Chemical Engineering Journal*, *316*, 481–498. https://doi.org/10.1016/j.cej.2017.01.130

Bernal, M. P., Alburquerque, J. A., & Moral, R. (2009). Composting of animal manures and chemical criteria for compost maturity assessment. A review. *Bioresource Technology*, *100*(22), 5444–5453. https://doi.org/10.1016/j.biortech.2008.11.027

Bhardwaj, G., Kumar, M., Mishra, P. K., & Upadhyay, S. N. (2021). Kinetic analysis of the slow pyrolysis of paper wastes. *Biomass Conversion and Biorefinery*. https://doi.org/10.1007/s13399-021-01363-7

Bhatnagar, A., Kaczala, F., Burlakovs, J., Kriipsalu, M., Hogland, M., & Hogland, W. (2017). Hunting for valuables from landfills and assessing their market opportunities A case study with Kudjape landfill in Estonia. *Waste Management and Research*, *35*(6), 627–635. https://doi.org/10.1177/0734242X17697816

Bhatt, M., Chakinala, A. G., Joshi, J. B., Sharma, A., Pant, K. K., Shah, K., & Sharma, A. (2021). Valorization of solid waste using advanced thermo-chemical process: A review. *Journal of Environmental Chemical Engineering*, *9*(4), 105434. https://doi.org/10.1016/j.jece.2021.105434

Bi, W., Chen, T., Zhao, R., Wang, Z., Wu, J., & Wu, J. (2015). Characteristics of a CaSO4

oxygen carrier for chemical-looping combustion:Reaction with polyvinylchloride pyrolysis gases in a two-stage reactor. *RSC Advances*, *5*(44), 34913–34920. https://doi.org/10.1039/c5ra02044a

Bisutti, I., Hilke, I., & Raessler, M. (2004). Determination of total organic carbon - An overview of current methods. *TrAC - Trends in Analytical Chemistry*, *23*(10–11), 716–726. https://doi.org/10.1016/j.trac.2004.09.003

Blanco-Canqui, H. (2017). Biochar and Soil Physical Properties. *Soil Science Society of America Journal*, *81*(4), 687–711. https://doi.org/10.2136/sssaj2017.01.0017

Blanco, P. H., Wu, C., Onwudili, J. A., Dupont, V., & Williams, P. T. (2014). Catalytic Pyrolysis/Gasification of Refuse Derived Fuel for Hydrogen Production and Tar Reduction: Influence of Nickel to Citric Acid Ratio Using Ni/SiO2 Catalysts. *Waste and Biomass Valorization*, *5*(4), 625–636. https://doi.org/10.1007/s12649-013-9254-7

Bogusz, A., Oleszczuk, P., & Dobrowolski, R. (2015). Application of laboratory prepared and commercially available biochars to adsorption of cadmium, copper and zinc ions from water. *Bioresource Technology*, *196*, 540–549. https://doi.org/10.1016/j.biortech.2015.08.006

Bosmans, A., Vanderreydt, I., Geysen, D., & Helsen, L. (2013). The crucial role of Waste-to-Energy technologies in enhanced landfill mining: A technology review. *Journal of Cleaner Production*, *55*, 10–23. https://doi.org/10.1016/j.jclepro.2012.05.032

Brandi, J., & Wilson-Wilde, L. (2013). Standard Methods. *Encyclopedia of Forensic Sciences: Second Edition*, 522–527. https://doi.org/10.1016/B978-0-12-382165-2.00237-3

Bridgwater, A. V. (2012). Review of fast pyrolysis of biomass and product upgrading. *Biomass and Bioenergy*, *38*, 68–94. https://doi.org/10.1016/j.biombioe.2011.01.048

Bridgwater, A. V., & Peacocke, G. V. C. (2000). Fast pyrolysis processes for biomass. *Renewable and Sustainable Energy Reviews*, *4*(1), 1–73. https://doi.org/10.1016/S1364-0321(99)00007-6

Briffa, J., Sinagra, E., & Blundell, R. (2020). Heavy metal pollution in the environment and their toxicological effects on humans. *Heliyon*, *6*(9), e04691. https://doi.org/10.1016/j.heliyon.2020.e04691

Britto, D. T., & Kronzucker, H. J. (2002). NH4+ toxicity in higher plants: A critical review. *Journal of Plant Physiology*, *159*(6), 567–584. https://doi.org/10.1078/0176-1617-0774

Buah, W. K., Cunliffe, A. M., & Williams, P. T. (2007). Characterization of products from the pyrolysis of municipal solid waste. *Process Safety and Environmental Protection*, *85*(5 B), 450–457. https://doi.org/10.1205/psep07024

Buah, William K., & Williams, P. T. (2010). Activated carbons prepared from refuse derived fuel and their gold adsorption characteristics. *Environmental Technology*, *31*(2), 125–137. https://doi.org/10.1080/09593330903386741

Calugaru, I. L., Neculita, C. M., Genty, T., & Zagury, G. J. (2019). Removal efficiency of As(V) and Sb(III) in contaminated neutral drainage by Fe-loaded biochar. *Environmental Science and Pollution Research*, *26*(9), 9322–9332. https://doi.org/10.1007/s11356-019-04381-1

Camps, M., & Tomlinson, T. (2015). The Use of Biochar in Composting. *International Biochar Initiative*, *February*, 1–4.

Cao, J. P., Xiao, X. Bin, Zhang, S. Y., Zhao, X. Y., Sato, K., Ogawa, Y., Wei, X. Y., & Takarada, T. (2011). Preparation and characterization of bio-oils from internally circulating fluidized-bed pyrolyses of municipal, livestock, and wood waste. *Bioresource Technology*, *102*(2), 2009–2015. https://doi.org/10.1016/j.biortech.2010.09.057

Cao, Y., Gao, Y., Qi, Y., & Li, J. (2018). Biochar-enhanced composts reduce the potential leaching of nutrients and heavy metals and suppress plant-parasitic nematodes in excessively fertilized cucumber soils. *Environmental Science and Pollution Research*, *25*(8), 7589–7599. https://doi.org/10.1007/s11356-017-1061-4

Chakraborty, M., Sharma, C., Pandey, J., & Gupta, P. K. (2013). Assessment of energy generation potentials of MSW in Delhi under different technological options. *Energy Conversion and Management*, *75*, 249–255. https://doi.org/10.1016/j.enconman.2013.06.027

Chandra, S., & Bhattacharya, J. (2019). Influence of temperature and duration of pyrolysis on the property heterogeneity of rice straw biochar and optimization of pyrolysis conditions for its application in soils. *Journal of Cleaner Production*, *215*, 1123–1139. https://doi.org/10.1016/j.jclepro.2019.01.079

Charvet, F., Silva, F., Ruivo, L., Tarelho, L., Matos, A., da Silva, J. F., & Neves, D. (2021). Pyrolysis characteristics of undervalued wood varieties in the portuguese charcoal sector. *Energies*, *14*(9), 1–16. https://doi.org/10.3390/en14092537

Chauhan, R. S., Gopinath, S., Razdan, P., Delattre, C., Nirmala, G. S., & Natarajan, R. (2008). Thermal decomposition of expanded polystyrene in a pebble bed reactor to get higher liquid fraction yield at low temperatures. *Waste Management*, *28*(11), 2140–2145. https://doi.org/10.1016/j.wasman.2007.10.001

Cheela, V. R. S., Ranjan, V. P., Goel, S., John, M., & Dubey, B. (2021). Pathways to sustainable waste management in Indian Smart Cities. *Journal of Urban Management*, *10*(4), 419–429. https://doi.org/10.1016/j.jum.2021.05.002

Chen, C., Jin, Y., & Chi, Y. (2014). Effects of moisture content and CaO on municipal solid waste pyrolysis in a fixed bed reactor. *Journal of Analytical and Applied Pyrolysis*, *110*(1), 108–112. https://doi.org/10.1016/j.jaap.2014.08.009

Chen, D., Yin, L., Wang, H., & He, P. (2015). Reprint of: Pyrolysis technologies for municipal solid waste: A review. *Waste Management*, *37*, 116–136. https://doi.org/10.1016/j.wasman.2015.01.022

Chen, X., Du, Z., Liu, D., Wang, L., Pan, C., Wei, Z., Jia, L., & Zhao, R. (2022). Biochar mitigates the biotoxicity of heavy metals in livestock manure during composting. *Biochar*, *4*(1). https://doi.org/10.1007/s42773-022-00174-x

Cheng, Y., Bu, X., Li, J., Ji, Z., Wang, C., Xiao, X., Li, F., Wu, Z. hui, Wu, G., Jia, P., & Li, J. tian. (2023). Application of biochar and compost improved soil properties and enhanced plant growth in a Pb–Zn mine tailings soil. *Environmental Science and Pollution Research*, *30*(12), 32337–32347. https://doi.org/10.1007/s11356-022-24488-2

Chhabra, V., Parashar, A., Shastri, Y., & Bhattacharya, S. (2021). Techno-economic and

life cycle assessment of pyrolysis of unsegregated urban municipal solid waste in India. *Industrial and Engineering Chemistry Research*, *60*(3), 1473–1482. https://doi.org/10.1021/acs.iecr.0c04746

Chiemchaisri, C., Charnnok, B., & Visvanathan, C. (2010). Recovery of plastic wastes from dumpsite as refuse-derived fuel and its utilization in small gasification system. *Bioresource Technology*, *101*(5), 1522–1527. https://doi.org/10.1016/j.biortech.2009.08.061

Clemens, S. (2006). Toxic metal accumulation, responses to exposure and mechanisms of tolerance in plants. *Biochimie*, *88*(11), 1707–1719. https://doi.org/10.1016/j.biochi.2006.07.003

CPCB. (2016). CPCB Bulletin Volume I. *CPCB Bulletin Vol. I*, *July*, 1–26. http://cpcb.nic.in/openpdffile.php?id=TGF0ZXN0RmlsZS9MYXRlc3RfMTIzX1NVTU1BUllfQk9PS19GUy5wZGY=%0Ahttp://cpcb.nic.in/upload/Latest/Latest_123_SUMMARY_BOOK_FS.pdf

CPCB. (2022). Annual Report 2020-21 on Implementation of Solid Waste Management Rules, 2016. *Central Pollution Control Board*, 288–446. https://cpcb.nic.in/uploads/plasticwaste/Annual_Report_2019-20_PWM.pdf

Municipal Solid Waste Management Manual Part I: An Overview, Ministry of Urban Development (2016). http://cpheeo.gov.in/upload/uploadfiles/files/Part1(1).pdf

Crombie, K., Mašek, O., Sohi, S. P., Brownsort, P., & Cross, A. (2013). The effect of pyrolysis conditions on biochar stability as determined by three methods. *GCB Bioenergy*, *5*(2), 122–131. https://doi.org/10.1111/gcbb.12030

Cutroneo, L., Reboa, A., Geneselli, I., & Capello, M. (2021). Considerations on salts used for density separation in the extraction of microplastics from sediments. *Marine Pollution Bulletin*, *166*(February), 112216. https://doi.org/10.1016/j.marpolbul.2021.112216

Dang, R., Cai, Y., Li, J., Kong, Y., Jiang, T., Chang, J., Yao, S., Yuan, J., Li, G., & Wang, G. (2024). Biochar reduces gaseous emissions during poultry manure composting: Evidence from the evolution of associated functional genes. *Journal of Cleaner Production*, *452*(March), 142060. https://doi.org/10.1016/j.jclepro.2024.142060

Demeyer, A., Voundi Nkana, J. C., & Verloo, M. G. (2001). Characteristics of wood ash and influence on soil properties and nutrient uptake: An overview. *Bioresource Technology*, *77*(3), 287–295. https://doi.org/10.1016/S0960-8524(00)00043-2

Demirbaş, A. (2001). Biomass resource facilities and biomass conversion processing for fuels and chemicals. *Energy Conversion and Management*, *42*(11), 1357–1378. https://doi.org/10.1016/S0196-8904(00)00137-0

Demirbas, M. F., & Balat, M. (2007). Biomass pyrolysis for liquid fuels and chemicals: A review. *Journal of Scientific and Industrial Research*, *66*(10), 797–804.

Deng, L., Yuan, Y., Zhang, Y., Wang, Y., Chen, Y., Yuan, H., & Chen, Y. (2017). Alfalfa Leaf-Derived Porous Heteroatom-Doped Carbon Materials as Efficient Cathodic Catalysts in Microbial Fuel Cells. *ACS Sustainable Chemistry and Engineering*, *5*(11), 9766–9773. https://doi.org/10.1021/acssuschemeng.7b01585

Dhyani, V., Kumar, J., & Bhaskar, T. (2017). Thermal decomposition kinetics of sorghum straw via thermogravimetric analysis. *Bioresource Technology*, *245*(August), 1122–

1129. https://doi.org/10.1016/j.biortech.2017.08.189

Ding, K., Zhong, Z., Zhong, D., Zhang, B., & Qian, X. (2016). Pyrolysis of municipal solid waste in a fluidized bed for producing valuable pyrolytic oils. *Clean Technologies and Environmental Policy*, *18*(4), 1111–1121. https://doi.org/10.1007/s10098-016-1102-6

Ding, X., Li, G., Zhao, X., Lin, Q., & Wang, X. (2023). Biochar application significantly increases soil organic carbon under conservation tillage: an 11-year field experiment. *Biochar*, *5*(1). https://doi.org/10.1007/s42773-023-00226-w

Doan, T. T., Henry-Des-Tureaux, T., Rumpel, C., Janeau, J. L., & Jouquet, P. (2015). Impact of compost, vermicompost and biochar on soil fertility, maize yield and soil erosion in Northern Vietnam: A three year mesocosm experiment. *Science of the Total Environment*, *514*, 147–154. https://doi.org/10.1016/j.scitotenv.2015.02.005

Dong, J., Chi, Y., Tang, Y., Ni, M., Nzihou, A., Weiss-Hortala, E., & Huang, Q. (2016). Effect of Operating Parameters and Moisture Content on Municipal Solid Waste Pyrolysis and Gasification. *Energy and Fuels*, *30*(5), 3994–4001. https://doi.org/10.1021/acs.energyfuels.6b00042

Duan, X. L., Yuan, C. G., Jing, T. T., & Yuan, X. D. (2019). Removal of elemental mercury using large surface area micro-porous corn cob activated carbon by zinc chloride activation. *Fuel*, *239*(August 2018), 830–840. https://doi.org/10.1016/j.fuel.2018.11.017

Tuncer, E. R, & Lohnes, R. A. (1977). Engineering Classification of Basalt Derived Laterites. ***Engineering Geology***, *11(4)*, 319–339.https://doi.org/10.1016/0013-7952(77)90037-0

Wu, C. H., Chang, C. Y., & Lin, J. P. (1998). Effects of moisture on pyrolysis of polypropylene, *124*(9), 892–896.

Ekpete, O. A., Marcus, A. C., & Osi, V. (2017). Preparation and Characterization of Activated Carbon Obtained from Plantain (Musa paradisiaca) Fruit Stem. *Journal of Chemistry*, *2017*(March). https://doi.org/10.1155/2017/8635615

El-Bery, H. M., Saleh, M., El-Gendy, R. A., Saleh, M. R., & Thabet, S. M. (2022). High adsorption capacity of phenol and methylene blue using activated carbon derived from lignocellulosic agriculture wastes. *Scientific Reports*, *12*(1), 1–17. https://doi.org/10.1038/s41598-022-09475-4

El-Naggar, A., Chen, Z., Jiang, W., Cai, Y., & Chang, S. X. (2022). Biochar effectively remediates Cd contamination in acidic or coarse- and medium-textured soils: A global meta-analysis. *Chemical Engineering Journal*, *442*(P1), 136225. https://doi.org/10.1016/j.cej.2022.136225

El-Naggar, A., El-Naggar, A. H., Shaheen, S. M., Sarkar, B., Chang, S. X., Tsang, D. C. W., Rinklebe, J., & Ok, Y. S. (2019). Biochar composition-dependent impacts on soil nutrient release, carbon mineralization, and potential environmental risk: A review. *Journal of Environmental Management*, *241*(September 2018), 458–467. https://doi.org/10.1016/j.jenvman.2019.02.044

Elkhalifa, S., Al-Ansari, T., Mackey, H. R., & McKay, G. (2019). Food waste to biochars through pyrolysis: A review. *Resources, Conservation and Recycling*, *144*(January), 310–320. https://doi.org/10.1016/j.resconrec.2019.01.024

Enders, A., Hanley, K., Whitman, T., Joseph, S., & Lehmann, J. (2012). Characterization of biochars to evaluate recalcitrance and agronomic performance. *Bioresource Technology*, *114*, 644–653. https://doi.org/10.1016/j.biortech.2012.03.022

Eze, W. U., Umunakwe, R., Obasi, H. C., Ugbaja, M. I., Uche, C. C., & Madufor, I. C. (2021). Plastics waste management: A review of pyrolysis technology. *Clean Technologies and Recycling*, *1*(1), 50–69. https://doi.org/10.3934/ctr.2021003

Fan, S., Li, H., Wang, Y., Wang, Z., Tang, J., Tang, J., & Li, X. (2018). Cadmium removal from aqueous solution by biochar obtained by co-pyrolysis of sewage sludge with tea waste. *Research on Chemical Intermediates*, *44*(1), 135–154. https://doi.org/10.1007/s11164-017-3094-1

Fan, Y., Li, Y., Yu, M., Yang, T., & Huang, Y. (2018). Effects of different combustible municipal solid waste components without/with additives on co-pyrolysis. *Energy Sources, Part A: Recovery, Utilization and Environmental Effects*, *40*(20), 2379–2387. https://doi.org/10.1080/15567036.2018.1495784

Fang, S., Gu, W., Chen, L., Yu, Z., Dai, M., Lin, Y., Liao, Y., & Ma, X. (2018). Ultrasonic pretreatment effects on the co-pyrolysis of municipal solid waste and paper sludge through orthogonal test. *Bioresource Technology*, *258*(February), 5–11. https://doi.org/10.1016/j.biortech.2018.02.120

Fang, S., Yu, Z., Lin, Y., Lin, Y., Fan, Y., Liao, Y., & Ma, X. (2016). Effects of additives on the co-pyrolysis of municipal solid waste and paper sludge by using thermogravimetric analysis. *Bioresource Technology*, *209*, 265–272. https://doi.org/10.1016/j.biortech.2016.03.027

Fang, S., Yu, Z., Lin, Y., Lin, Y., Fan, Y., Liao, Y., & Ma, X. (2017). A study on experimental characteristic of co-pyrolysis of municipal solid waste and paper mill sludge with additives. *Applied Thermal Engineering*, *111*, 292–300. https://doi.org/10.1016/j.applthermaleng.2016.09.102

Fantozzi, F., Colantoni, S., Bartocci, P., & Desideri, U. (2007). Rotary kiln slow pyrolysis for syngas and char production from biomass and waste - Part I: Working envelope of the reactor. *Journal of Engineering for Gas Turbines and Power*, *129*(4), 901–907. https://doi.org/10.1115/1.2720521

FAO. (2019). Standard operating procedure for soil organic carbon Walkley-Black method. *Food and Agriculture Organization of the United Nations*, *1*(20), 27.

Fatih Demirbas, M., Balat, M., & Balat, H. (2011). Biowastes-to-biofuels. *Energy Conversion and Management*, *52*(4), 1815–1828. https://doi.org/10.1016/j.enconman.2010.10.041

Feng, Y., Wang, G., Zhen, Liu, Y., Wang, Cheng, D., Miao, Fan, S., Hu, Zhao, Q., Sheng, Xue, J., Zhang, S., Qing, & Li, Z., Jun. (2021). The impacts of oxytetracycline on humification during manure composting can be alleviated by adjusting initial moisture contents as illustrated by NMR. *Journal of Integrative Agriculture*, *20*(8), 2277–2288. https://doi.org/10.1016/S2095-3119(20)63332-9

USDA NRCS (1998). *Inherent Factors Affecting Bulk Density and Available Water Capacity*, (*1*), 1–9.

Fisher, T., Hajaligol, M., Waymack, B., & Kellogg, D. (2002). *Pyrolysis behavior and kinetics of biomass derived materials*. *62*, 331–349.

Font, R., Marcilla, A., Devesa, J., & Verdú, E. (1993). Kinetic study of the flash pyrolysis of almond shells in a fluidized bed reactor at high temperatures. *Journal of Analytical and Applied Pyrolysis*, *27*(2), 245–273. https://doi.org/10.1016/0165-2370(93)80012-O

Gao, N., Wang, F., Quan, C., Santamaria, L., Lopez, G., & Williams, P. T. (2022). Tire pyrolysis char: Processes, properties, upgrading and applications. *Progress in Energy and Combustion Science*, *93*(September), 101022. https://doi.org/10.1016/j.pecs.2022.101022

Garau, M., Pinna, M. V., Nieddu, M., Castaldi, P., & Garau, G. (2024). Mixing Compost and Biochar Can Enhance the Chemical and Biological Recovery of Soils Contaminated by Potentially Toxic Elements. *Plants*, *13*(2). https://doi.org/10.3390/plants13020284

Gayathri, R., Gopinath, K. P., & Kumar, P. S. (2021). Adsorptive separation of toxic metals from aquatic environment using agro waste biochar: Application in electroplating industrial wastewater. *Chemosphere*, *262*, 128031. https://doi.org/10.1016/j.chemosphere.2020.128031

Gedam, V. V., & Regupathi, I. (2012). Pyrolysis of Municipal Solid Waste for Syngas Production by Microwave Irradiation. *Natural Resources Research*, *21*(1), 75–82. https://doi.org/10.1007/s11053-011-9161-1

Genchi, G., Carocci, A., Lauria, G., Sinicropi, M. S., & Catalano, A. (2020). Nickel: Human health and environmental toxicology. *International Journal of Environmental Research and Public Health*, *17*(3). https://doi.org/10.3390/ijerph17030679

Geng, N., Kang, X., Yan, X., Yin, N., Wang, H., Pan, H., Yang, Q., Lou, Y., & Zhuge, Y. (2022). Biochar mitigation of soil acidification and carbon sequestration is influenced by materials and temperature. *Ecotoxicology and Environmental Safety*, *232*, 113241. https://doi.org/10.1016/j.ecoenv.2022.113241

Ghodszad, L., Reyhanitabar, A., Maghsoodi, M. R., Asgari Lajayer, B., & Chang, S. X. (2021). Biochar affects the fate of phosphorus in soil and water: A critical review. *Chemosphere*, *283*(April), 131176. https://doi.org/10.1016/j.chemosphere.2021.131176

Ghosh, A., Debnath, B., Ghosh, S. K., Das, B., & Sarkar, J. P. (2018). Sustainability analysis of organic fraction of municipal solid waste conversion techniques for efficient resource recovery in India through case studies. *Journal of Material Cycles and Waste Management*, *20*(4), 1969–1985. https://doi.org/10.1007/s10163-018-0721-x

Ghosh, A., & Kartha, S. A. (2024). Landfill Biomining of Legacy Waste Dumpsites in India: Process, Challenges and Future Perspective. In V. Kumar, S. A. Bhat, S. Kumar, & P. Verma (Eds.), *Environmental Engineering and Waste Management: Recent Trends and Perspectives* (pp. 377–390). Springer Nature Switzerland. https://doi.org/10.1007/978-3-031-58441-1_13

Glaser, B., Lehmann, J., & Zech, W. (2002). Ameliorating physical and chemical properties of highly weathered soils in the tropics with charcoal - A review. *Biology and Fertility of Soils*, *35*(4), 219–230. https://doi.org/10.1007/s00374-002-0466-4

Gohain, S. B., & Bordoloi, S. (2021). Impact of municipal solid waste disposal on the

surface water and sediment of adjoining wetland Deepor Beel in Guwahati, Assam, India. *Environmental Monitoring and Assessment*, *193*(5), 1–19. https://doi.org/10.1007/s10661-021-09040-y

Goli, V. S. N. S., Singh, D. N., & Baser, T. (2021). A critical review on thermal treatment technologies of combustible fractions from mechanical biological treatment plants. *Journal of Environmental Chemical Engineering*, *9*(4), 105643. https://doi.org/10.1016/j.jece.2021.105643

Gopinath, A., Divyapriya, G., Srivastava, V., Laiju, A. R., Nidheesh, P. V., & Kumar, M. S. (2021). Conversion of sewage sludge into biochar: A potential resource in water and wastewater treatment. *Environmental Research*, *194*(May 2020), 110656. https://doi.org/10.1016/j.envres.2020.110656

Götze, R., Pivnenko, K., Boldrin, A., Scheutz, C., & Astrup, T. F. (2016). Physico-chemical characterisation of material fractions in residual and source-segregated household waste in Denmark. *Waste Management*, *54*, 13–26. https://doi.org/10.1016/j.wasman.2016.05.009

Grace, J. R., & Bi, H. (1997). Introduction to Circulating Fluidized Beds. *Circulating Fluidized Beds*, 1–20. https://doi.org/10.1007/978-94-009-0095-0_1

Grant, C., Bittman, S., Montreal, M., Plenchette, C., & Morel, C. (2005). Soil and fertilizer phosphorus: Effects on plant P supply and mycorrhizal development. *Canadian Journal of Plant Science*, *85*(1), 3–14. https://doi.org/10.4141/P03-182

Gulab, H., Jan, M. R., Shah, J., & Manos, G. (2010). Plastic catalytic pyrolysis to fuels as tertiary polymer recycling method: Effect of process conditions. *Journal of Environmental Science and Health - Part A Toxic/Hazardous Substances and Environmental Engineering*, *45*(7), 908–915. https://doi.org/10.1080/10934521003709206

Guo, X., Liu, H., & Zhang, J. (2020). The role of biochar in organic waste composting and soil improvement : A review. *Waste Management*, *102*, 884–899. https://doi.org/10.1016/j.wasman.2019.12.003

Guo, X., Wang, Z., Li, H., Huang, H., Wu, C., Chen, Y., & Li, B. (2001). A study on combustion characteristics and kinetic model of municipal solid wastes. *Energy and Fuels*, *15*(6), 1441–1446. https://doi.org/10.1021/ef010068f

Gupta, B., & Arora, S. K. (2016). Municipal Solid Waste Management in Delhi—The Capital of India. *International Journal of Innovative Research in Science, Engineering and Technology*, *5*(4), 5130–5138. https://doi.org/10.15680/IJIRSET.2016.0504106

Gupta, N., Yadav, K. K., & Kumar, V. (2015). A review on current status of municipal solid waste management in India. *Journal of Environmental Sciences (China)*, *37*(August), 206–217. https://doi.org/10.1016/j.jes.2015.01.034

Hailegnaw, N. S., Mercl, F., Pračke, K., Száková, J., & Tlustoš, P. (2019). Mutual relationships of biochar and soil pH, CEC, and exchangeable base cations in a model laboratory experiment. *Journal of Soils and Sediments*, *19*(5), 2405–2416. https://doi.org/10.1007/s11368-019-02264-z

Hamilton, J., Seyedmahmoudian, M., Jamei, E., Horan, B., & Stojcevski, A. (2020). A systematic review of solar driven waste to fuel pyrolysis technology for the Australian

state of Victoria. *Energy Reports*, *6*, 3212–3229. https://doi.org/10.1016/j.egyr.2020.11.039

Han, Z., Li, J., Gu, T., Yang, R., Fu, Z., Yan, B., & Chen, G. (2021). Effects of torrefaction on the formation and distribution of dioxins during wood and PVC pyrolysis: An experimental and mechanistic study. *Journal of Analytical and Applied Pyrolysis*, *157*(January), 105240. https://doi.org/10.1016/j.jaap.2021.105240

Harish, V., Aslam, S., Chouhan, S., Pratap, Y., & Lalotra, S. (2023). Iron toxicity in plants: A Review. *International Journal of Environment and Climate Change*, *13*(8), 1894–1900. https://doi.org/10.9734/ijecc/2023/v13i82145

Hasan, M. M., Rasul, M. G., Khan, M. M. K., Ashwath, N., & Jahirul, M. I. (2021). Energy recovery from municipal solid waste using pyrolysis technology: A review on current status and developments. *Renewable and Sustainable Energy Reviews*, *145*(March), 111073. https://doi.org/10.1016/j.rser.2021.111073

Hasanuzzaman, M., Bhuyan, M. H. M. B., Nahar, K., Hossain, M. S., Al Mahmud, J., Hossen, M. S., Masud, A. A. C., Moumita, & Fujita, M. (2018). Potassium: A vital regulator of plant responses and tolerance to abiotic stresses. *Agronomy*, *8*(3). https://doi.org/10.3390/agronomy8030031

Hassan, M. U., Chattha, M. U., Khan, I., Chattha, M. B., Aamer, M., Nawaz, M., Ali, A., Khan, M. A. U., & Khan, T. A. (2019). Nickel toxicity in plants: Reasons, toxic effects, tolerance mechanisms, and remediation possibilities—a review. *Environmental Science and Pollution Research*, *26*(13), 12673–12688. https://doi.org/10.1007/s11356-019-04892-x

Hassanzadeh M. O., Nabi, B. G., Daryabeigi, Z. A., Rabiee, A. M., & Nabi, B. A. (2023). Effect of forest-based biochar on maturity indices and bio-availability of heavy metals during the composting process of organic fraction of municipal solid waste (OFMSW). *Scientific Reports*, *13*(1), 1–10. https://doi.org/10.1038/s41598-023-42835-2

Hazarika, J., & Khwairakpam, M. (2018). Evaluation of biodegradation feasibility through rotary drum composting recalcitrant primary paper mill sludge. *Waste Management*, *76*, 275–283. https://doi.org/10.1016/j.wasman.2018.03.044

He, X., Chen, L., Han, L., Liu, N., Cui, R., Yin, H., & Huang, G. (2017). Evaluation of biochar powder on oxygen supply efficiency and global warming potential during mainstream large-scale aerobic composting. *Bioresource Technology*, *245*(August), 309–317. https://doi.org/10.1016/j.biortech.2017.08.076

Hemavathy, R. V., Kumar, P. S., Kanmani, K., & Jahnavi, N. (2020). Adsorptive separation of Cu(II) ions from aqueous medium using thermally/chemically treated Cassia fistula based biochar. *Journal of Cleaner Production*, *249*, 119390. https://doi.org/10.1016/j.jclepro.2019.119390

Hendrawan, Y., Sajidah, N., Umam, C., Fauzy, M. R., Wibisono, Y., & Hawa, L. C. (2019). Effect of Carbonization Temperature Variations and Activator Agent Types on Activated Carbon Characteristics of Sengon Wood Waste (Paraserianthes falcataria (L.) Nielsen). *IOP Conference Series: Earth and Environmental Science*, *239*(1). https://doi.org/10.1088/1755-1315/239/1/012006

Hidayat, R. A., Nissa, R. C., Sukamto, N. L., Nurtanto, M., & Ramadhani, W. S. (2023).

Analysis of rice husk biochar characteristics under different pyrolysis temperature. *IOP Conference Series: Earth and Environmental Science*, *1201*(1), 012095. https://doi.org/10.1088/1755-1315/1201/1/012095

Higashikawa, F. S., Conz, R. F., Colzato, M., Cerri, C. E. P., & Alleoni, L. R. F. (2016). Effects of feedstock type and slow pyrolysis temperature in the production of biochars on the removal of cadmium and nickel from water. *Journal of Cleaner Production*, *137*, 965–972. https://doi.org/10.1016/j.jclepro.2016.07.205

Himbane, P. B., Ndiaye, L. G., Napoli, A., Goli, T., Rozis, J. F., Ba, M. S., & Ndioukane, R. (2022). Influence of binder rate, pyrolysis temperature and volume of biochar briquettes on CO and PM2.5 emission factors and thermal efficiency. *Energy for Sustainable Development*, *68*, 525–531. https://doi.org/10.1016/j.esd.2022.04.012

Hoornweg, D. (2015). A Cities Approach to Sustainability. *Department of Civil Engineering University of Toronto*, 351. http://search.proquest.com/docview/1711716893?accountid=10673%5Cnhttp://openurl.ac.uk/athens:_edu?url_ver=Z39.88-2004&rft_val_fmt=info:ofi/fmt:kev:mtx:dissertation&genre=dissertations+&+theses&sid=ProQ:ProQuest+Dissertations+&+Theses+Global&atitle=&titl

Hoslett, J., Ghazal, H., Ahmad, D., & Jouhara, H. (2019). Removal of copper ions from aqueous solution using low temperature biochar derived from the pyrolysis of municipal solid waste. *Science of the Total Environment*, *673*, 777–789. https://doi.org/10.1016/j.scitotenv.2019.04.085

Hrabovsky, M., Konrad, M., Kopecky, V., Hlina, M., Kavka, T., Chumak, O., Van Oost, G., Beeckman, E., & Defoort, B. (2006). Pyrolysis of wood in arc plasma for syngas production. *High Temperature Material Processes*, *10*(4), 557–570. https://doi.org/10.1615/HighTempMatProc.v10.i4.70

Hu, B., Huang, Q., Bourtsalas, A. C. T., Ali, M., Chi, Y., & Yan, J. (2017). Effect of Chlorine on the Structure and Reactivity of Char Derived from Solid Waste. *Energy and Fuels*, *31*(7), 7606–7616. https://doi.org/10.1021/acs.energyfuels.7b01042

Hu, M., Deng, W., Hu, M., Chen, G., Zhou, P., Zhou, Y., & Su, Y. (2021). Preparation of binder-less activated char briquettes from pyrolysis of sewage sludge for liquid-phase adsorption of methylene blue. *Journal of Environmental Management*, *299*(August), 113601. https://doi.org/10.1016/j.jenvman.2021.113601

Hu, X., Xu, J., Wu, M., Xing, J., Bi, W., Wang, K., Ma, J., & Liu, X. (2017). Effects of biomass pre-pyrolysis and pyrolysis temperature on magnetic biochar properties. *Journal of Analytical and Applied Pyrolysis*, *127*(August), 196–202. https://doi.org/10.1016/j.jaap.2017.08.006

Huang, H., & Tang, L. (2007). Treatment of organic waste using thermal plasma pyrolysis technology. *Energy Conversion and Management*, *48*(4), 1331–1337. https://doi.org/10.1016/j.enconman.2006.08.013

Huang, Q., Tang, Y., Lu, S., Wu, X., Chi, Y., & Yan, J. (2015). Characterization of Tar Derived from Principle Components of Municipal Solid Waste. *Energy and Fuels*, *29*(11), 7266–7274. https://doi.org/10.1021/acs.energyfuels.5b01152

Hwang, I. H., Matsuto, T., Tanaka, N., Sasaki, Y., & Tanaami, K. (2007). Characterization of char derived from various types of solid wastes from the standpoint of fuel

recovery and pretreatment before landfilling. *Waste Management*, *27*(9), 1155–1166. https://doi.org/10.1016/j.wasman.2006.05.013

Iannello, S., Morrin, S., & Materazzi, M. (2020). Fluidised bed reactors for the thermochemical conversion of biomass and waste†. *KONA Powder and Particle Journal*, *37*(37), 114–131. https://doi.org/10.14356/kona.2020016

Ibrahim, E. A., El-Sherbini, M. A. A., & Selim, E. M. M. (2022). Effects of biochar on soil properties, heavy metal availability and uptake, and growth of summer squash grown in metal-contaminated soil. *Scientia Horticulturae*, *301*(February), 111097. https://doi.org/10.1016/j.scienta.2022.111097

Inyang, M. I., Gao, B., Yao, Y., Xue, Y., Zimmerman, A., Mosa, A., Pullammanappallil, P., Ok, Y. S., & Cao, X. (2016). A review of biochar as a low-cost adsorbent for aqueous heavy metal removal. *Critical Reviews in Environmental Science and Technology*, *46*(4), 406–433. https://doi.org/10.1080/10643389.2015.1096880

Iribarren, D., Peters, J. F., & Dufour, J. (2012). Life cycle assessment of transportation fuels from biomass pyrolysis. *Fuel*, *97*, 812–821. https://doi.org/10.1016/j.fuel.2012.02.053

Izilan, N. I. S., Sari, N. A., Othman, N. M. I., & Mustaffha, S. (2022). The effects of biochar-compost on soil properties and plant growth performance grown in a sandy-loam soil. *IOP Conference Series: Earth and Environmental Science*, *1059*(1). https://doi.org/10.1088/1755-1315/1059/1/012021

Jafarnejadi, A. R., Sayyad, G., Homaee, M., & Davamei, A. H. (2013). Spatial variability of soil total and DTPA-extractable cadmium caused by long-term application of phosphate fertilizers, crop rotation, and soil characteristics. *Environmental Monitoring and Assessment*, *185*(5), 4087–4096. https://doi.org/10.1007/s10661-012-2851-2

Jain, M. S., Daga, M., & Kalamdhad, A. S. (2018). Composting physics: A science behind bio-degradation of lignocellulose aquatic waste amended with inoculum and bulking agent. *Process Safety and Environmental Protection*, *116*, 424–432. https://doi.org/10.1016/j.psep.2018.03.017

Jain, M. S., Jambhulkar, R., & Kalamdhad, A. S. (2018). Biochar amendment for batch composting of nitrogen rich organic waste: Effect on degradation kinetics, composting physics and nutritional properties. *Bioresource Technology*, *253*(January), 204–213. https://doi.org/10.1016/j.biortech.2018.01.038

Jain, M. S., & Kalamdhad, A. S. (2018). Efficacy of batch mode rotary drum composter for management of aquatic weed (Hydrilla verticillata (L.f.) Royle). *Journal of Environmental Management*, *221*(June 2017), 20–27. https://doi.org/10.1016/j.jenvman.2018.05.055

Jain, M. S., & Kalamdhad, A. S. (2020). Soil revitalization via waste utilization: Compost effects on soil organic properties, nutritional, sorption and physical properties. *Environmental Technology and Innovation*, *18*, 100668. https://doi.org/10.1016/j.eti.2020.100668

Jin, H., Capareda, S., Chang, Z., Gao, J., Xu, Y., & Zhang, J. (2014). Biochar pyrolytically produced from municipal solid wastes for aqueous As(V) removal: Adsorption property and its improvement with KOH activation. *Bioresource Technology*, *169*,

622–629. https://doi.org/10.1016/j.biortech.2014.06.103

Jindo, K., Mizumoto, H., Sawada, Y., Sanchez-Monedero, M. A., & Sonoki, T. (2014). Physical and chemical characterization of biochars derived from different agricultural residues. *Biogeosciences*, *11*(23), 6613–6621. https://doi.org/10.5194/bg-11-6613-2014

Jobbágy, E. G., Jackson, R. B., Biogeochemistry, S., & Mar, N. (2001). The Distribution of Soil Nutrients with Depth. *Biogeochemistry*, *53*(1), 51–77. https://doi.org/10.1023/A:1010760720215

Johan, P. D., Ahmed, O. H., Omar, L., & Hasbullah, N. A. (2021). Phosphorus transformation in soils following co-application of charcoal and wood ash. *Agronomy*, *11*(10), 1–25. https://doi.org/10.3390/agronomy11102010

Jones, S., Valkenburg, C., & Walton, C. (2009). Production of gasoline and diesel from biomass via fast pyrolysis, hydrotreating and hydrocracking: a design case. *Energy*, *February*, 76. https://doi.org/PNNL-22684.pdf

Joshi, R., & Ahmed, S. (2016). Status and challenges of municipal solid waste management in India: A review. *Cogent Environmental Science*, *2*(1), 1–18. https://doi.org/10.1080/23311843.2016.1139434

Jung, H., Sewu, D. D., Ohemeng-Boahen, G., Lee, D. S., & Woo, S. H. (2019). Characterization and adsorption performance evaluation of waste char by-product from industrial gasification of solid refuse fuel from municipal solid waste. *Waste Management*, *91*, 33–41. https://doi.org/10.1016/j.wasman.2019.04.053

Kabata-Pendias, A. (1984). *Trace elements in soils and plants*. https://api.semanticscholar.org/CorpusID:94259065

Kalamdhad, A. S., Pasha, M., & Kazmi, A. A. (2008). Stability evaluation of compost by respiration techniques in a rotary drum composter. *Resources, Conservation and Recycling*, *52*(5), 829–834. https://doi.org/10.1016/j.resconrec.2007.12.003

Kalargaris, I., Tian, G., & Gu, S. (2018). Experimental characterisation of a diesel engine running on polypropylene oils produced at different pyrolysis temperatures. *Fuel*, *211*(October 2017), 797–803. https://doi.org/10.1016/j.fuel.2017.09.101

Kalivodová, M., Baláš, M., Milčák, P., Lisá, H., Lisý, M., Lachman, J., Kracík, P., Križan, P., & Vejražka, K. (2022). the Determination of Higher Heating Value By Calculation Based on Elemental Analysis. *Paliva*, *14*(1), 8–20. https://doi.org/10.35933/paliva.2022.01.02

Kambo, H. S., & Dutta, A. (2015). A comparative review of biochar and hydrochar in terms of production, physico-chemical properties and applications. *Renewable and Sustainable Energy Reviews*, *45*, 359–378. https://doi.org/10.1016/j.rser.2015.01.050

Kang, N. Q., Hu, Y. Y., Zhang, Z. W., & Lü, X. T. (2023). Changes of mineral nutrition (K, Ca, and Mg) in soil and plants following historical nitrogen inputs in a temperate steppe: the implications for grass tetany. *Plant and Soil*, *491*(1–2), 57–68. https://doi.org/10.1007/s11104-023-06012-8

Karajgi, S. B., Yaragatti, U. R., & Kamalapur, G. D. (2012). Modeling of Power Generation using Municipal Solid Waste in India. *International Journal of Electrical and Computer Engineering (IJECE)*, *2*(2). https://doi.org/10.11591/ijece.v2i2.270

Kasim, N. N., Mohamed, A. R., Ishak, M. A. M., Ahmad, R., Nawawi, W. I., Ismail, K.,

& Salleh, N. H. M. (2018). Optimization of pyrolysis process parameters of torrefied demineralized palm empty fruit bunch (TDEFB) by response surface methodology. *AIP Conference Proceedings*, *2013*(October). https://doi.org/10.1063/1.5054202

Kataki, R., Bordoloi, N. J., Saikia, R., Sut, D., Narzari, R., Gogoi, L., & Bhuyan, N. (2018). Waste Valorization to Fuel and Chemicals Through Pyrolysis: Technology, Feedstock, Products, and Economic Analysis. In *Energy, Environment, and Sustainability*. https://doi.org/10.1007/978-981-10-7431-8_21

Kaur, R., Gera, P., Jha, M. K., & Bhaskar, T. (2018). Pyrolysis kinetics and thermodynamic parameters of castor (Ricinus communis) residue using thermogravimetric analysis. *Bioresource Technology*, *250*(September 2017), 422–428. https://doi.org/10.1016/j.biortech.2017.11.077

Kauser, H., Pal, S., Haq, I., & Khwairakpam, M. (2020). Evaluation of rotary drum composting for the management of invasive weed Mikania micrantha Kunth and its toxicity assessment. *Bioresource Technology*, *313*(April), 123678. https://doi.org/10.1016/j.biortech.2020.123678

Kaushal, R. K., Chabukdhara, M., & Varghese, G. K. (2012). Municipal Solid Waste Management in India-Current State and Future Challenges: A Review Heavy metal(loid)s in soil-rice system View project battery waste management View project Municipal Solid Waste Management in India-Current State and Future Challenges. *Article in International Journal of Engineering Science and Technology*, *4*(04), 1473–1489. https://www.researchgate.net/publication/233894305

Kaza, S., Lisa, Y., Perinaz, B. T., and F. V. W. (2018). What a Waste 2.0 Introduction - "Snapshot of Solid Waste Management to 2050." Overview booklet. *World Bank, Washington, DC. License: Creative Commons Attribution CC BY 3.0 IGO.*, 1–38. https://openknowledge.worldbank.org/handle/10986/30317

Khare, P., & Baruah, B. P. (2014). Thermogravimetric analysis of perhydrous Indian coals. *Energy Sources, Part A: Recovery, Utilization and Environmental Effects*, *36*(7), 774–782. https://doi.org/10.1080/15567036.2010.547919

Klemetsrud, B., Ukaew, S., Thompson, V. S., Thompson, D. N., Klinger, J., Li, L., Eatherton, D., Puengprasert, P., & Shonnard, D. (2016). Characterization of Products from Fast Micropyrolysis of Municipal Solid Waste Biomass. *ACS Sustainable Chemistry and Engineering*, *4*(10), 5415–5423. https://doi.org/10.1021/acssuschemeng.6b00610

Klute, A. (1986). Water retention: laboratory methods. *Methods of Soil Analysis: Part 1 Physical and Mineralogical Methods*, *5*, 635–662.

Koelsch, F., Fricke, K., Mahler, C., & Damanhuri, E. (2005). Stability of Landfills – the Bandung Dumpsite Desaster. *10th International Waste Management and Landfill Symposium*, *2000*(March 2003), 1–10.

Komilis, D., Evangelou, A., Giannakis, G., & Lymperis, C. (2012). Revisiting the elemental composition and the calorific value of the organic fraction of municipal solid wastes. *Waste Management*, *32*(3), 372–381. https://doi.org/10.1016/j.wasman.2011.10.034

Kondoh, K., & Umeda, J. (2018). C–O bond enhancing direct bonding strength between plastic and pure titanium. *Materials Letters*, *211*, 331–334.

https://doi.org/10.1016/j.matlet.2017.10.042

Korai, M. S., Mahar, R. B., & Uqaili, M. A. (2016). Optimization of waste to energy routes through biochemical and thermochemical treatment options of municipal solid waste in Hyderabad, Pakistan. *Energy Conversion and Management*, *124*(2016), 333–343. https://doi.org/10.1016/j.enconman.2016.07.032

Kosakowski, W., Bryszewska, M. A., & Dziugan, P. (2020). Biochars from post-production biomass and waste from wood management: Analysis of carbonization products. *Materials*, *13*(21), 1–13. https://doi.org/10.3390/ma13214971

Kulikov, E. (2016). Determination of elemental nutrients in DTPA extracted soil using the Agilent 5110 SVDV ICP-OES. *Agilent Technologies*. http://hpst.cz/sites/default/files/attachments/5991-6854en-pudy-5110-svdv.pdf

Kumar, A., & Agrawal, A. (2020). Recent trends in solid waste management status, challenges, and potential for the future Indian cities – A review. *Current Research in Environmental Sustainability*, *2*, 100011. https://doi.org/10.1016/j.crsust.2020.100011

Kumar, Ashwani. (2013). Existing Situation of Municipal Solid Waste Management in NCT of Delhi, India. *Research Forum: International Journal of Social Sciences*, *ISSN*(1), 2347–9272. http://ijss.publicationsupport.com/docs/paper/Volume-1/issue_1/IJSS-104.pdf

Kuśmierek, K., Świątkowski, A., Kotkowski, T., Cherbański, R., & Molga, E. (2020). Adsorption Properties of Activated Tire Pyrolysis Chars for Phenol and Chlorophenols. *Chemical Engineering and Technology*, *43*(4), 770–780. https://doi.org/10.1002/ceat.201900574

Lal, R. (2004). Soil carbon sequestration impacts on global climate change and food security. *Science*, *304*(5677), 1623–1627. https://doi.org/10.1126/science.1097396

Langmuir. (1918). *The adsorption of gases on plane surfaces of glass, mica and platinum*. *345*(1914).

Law, K. L., Starr, N., Siegler, T. R., Jambeck, J. R., Mallos, N. J., & Leonard, G. H. (2020). The United States' contribution of plastic waste to land and ocean. *Science Advances*, *6*(44), 1–7. https://doi.org/10.1126/sciadv.abd0288

Lee, J., Kim, K. H., & Kwon, E. E. (2017). Biochar as a Catalyst. *Renewable and Sustainable Energy Reviews*, *77*(February), 70–79. https://doi.org/10.1016/j.rser.2017.04.002

Lee, T., Jang, S. H., Jung, S., Kim, S., Park, Y. K., Moon, D. H., & Kwon, E. E. (2020). CO2 effects on catalytic pyrolysis of yard trimming over concrete waste. *Chemical Engineering Journal*, *396*(February), 125331. https://doi.org/10.1016/j.cej.2020.125331

Lehmann, J., & Joseph, S. (2009). 书2015-Biochar for Environmental Management. *Science And Technology*, *1*(7), 449. https://doi.org/10.1016/j.forpol.2009.07.001

Lehmann, J., Pereira da Silva, J., Steiner, C., Nehls, T., Zech, W., & Glaser, B. (2003). Nutrient availability and leaching in an archaeological Anthrosol and a Ferralsol of the Central Amazon basin: fertilizer, manure and charcoal amendments. *Plant and Soil*, *249*(2), 343–357. https://doi.org/10.1023/A:1022833116184

Lehmann, J., Rillig, M. C., Thies, J., Masiello, C. A., Hockaday, W. C., & Crowley, D.

(2011a). Biochar effects on soil biota - A review. *Soil Biology and Biochemistry*, *43*(9), 1812–1836. https://doi.org/10.1016/j.soilbio.2011.04.022

Lehmann, J., Rillig, M. C., Thies, J., Masiello, C. A., Hockaday, W. C., & Crowley, D. (2011b). Biochar effects on soil biota - A review. *Soil Biology and Biochemistry*, *43*(9), 1812–1836. https://doi.org/10.1016/j.soilbio.2011.04.022

Lehto, J., Oasmaa, A., Solantausta, Y., Kytö, M., & Chiaramonti, D. (2013). Fuel oil quality and combustion of fast pyrolysis bio-oils. *VTT Publications*, *87*, 79. https://doi.org/http://dx.doi.org/10.1016/j.apenergy.2013.11.040

Leng, L., Xiong, Q., Yang, L., Li, H., Zhou, Y., Zhang, W., Jiang, S., Li, H., & Huang, H. (2021). An overview on engineering the surface area and porosity of biochar. *Science of the Total Environment*, *763*, 144204. https://doi.org/10.1016/j.scitotenv.2020.144204

Letters, P. R., & Paths, F. (1984). *«2. 5 «2. 5. 52*(15), 1280–1283.

Li, D., Manu, M. K., Varjani, S., & Wong, J. W. C. (2023). Role of tobacco and bamboo biochar on food waste digestate co-composting: Nitrogen conservation, greenhouse gas emissions, and compost quality. *Waste Management*, *156*(June 2022), 44–54. https://doi.org/10.1016/j.wasman.2022.10.022

Li, H., Zhang, S., Zhao, X., & Eiji, S. (2005). Pyrolysis characteristics and kinetics of municipal solid waste. *Transactions of Tianjin University*, *11*(5), 353–359.

Li, Q., Zhang, Y., Chen, M., Meng, A., & Chen, C. (2009). Study on drying and combustion process in grate-CFB incinerator. *Science in China, Series E: Technological Sciences*, *52*(5), 1153–1160. https://doi.org/10.1007/s11431-008-0182-x

Li, S., Sanna, A., & Andresen, J. M. (2011). Influence of temperature on pyrolysis of recycled organic matter from municipal solid waste using an activated olivine fluidized bed. *Fuel Processing Technology*, *92*(9), 1776–1782. https://doi.org/10.1016/j.fuproc.2011.04.026

Liang, B., Lehmann, J., Solomon, D., Kinyangi, J., Grossman, J., O'Neill, B., Skjemstad, J. O., Thies, J., Luizão, F. J., Petersen, J., & Neves, E. G. (2006). Black Carbon Increases Cation Exchange Capacity in Soils. *Soil Science Society of America Journal*, *70*(5), 1719–1730. https://doi.org/10.2136/sssaj2005.0383

Lin, Y., Ma, X., Yu, Z., & Cao, Y. (2014). Investigation on thermochemical behavior of co-pyrolysis between oil-palm solid wastes and paper sludge. *Bioresource Technology*, *166*, 444–450. https://doi.org/10.1016/j.biortech.2014.05.101

Lira, C. S., Berruti, F. M., Palmisano, P., Berruti, F., Briens, C., & Pécora, A. A. B. (2013). Fast pyrolysis of Amazon tucumã (Astrocaryum aculeatum) seeds in a bubbling fluidized bed reactor. *Journal of Analytical and Applied Pyrolysis*, *99*, 23–31. https://doi.org/10.1016/j.jaap.2012.11.005

Liu, H., Wang, Y., Zhao, S., Hu, H., Cao, C., Li, A., Yu, Y., & Yao, H. (2020). Review on the Current Status of the Co-combustion Technology of Organic Solid Waste (OSW) and Coal in China. *Energy and Fuels*, *34*(12), 15448–15487. https://doi.org/10.1021/acs.energyfuels.0c02177

Liu, J., Ding, Y., Ma, L., Gao, G., & Wang, Y. (2017). Combination of biochar and immobilized bacteria in cypermethrin-contaminated soil remediation. *International Biodeterioration and Biodegradation*, *120*, 15–20.

https://doi.org/10.1016/j.ibiod.2017.01.039

Liu, L., Li, W., Song, W., & Guo, M. (2018). Remediation techniques for heavy metal-contaminated soils: Principles and applicability. *Science of the Total Environment*, *633*, 206–219. https://doi.org/10.1016/j.scitotenv.2018.03.161

Liu, Yonglin, Huang, J., Xu, H., Zhang, Y., Hu, T., Chen, W., Hu, H., Wu, J., Li, Y., & Jiang, G. (2020). A magnetic macro-porous biochar sphere as vehicle for the activation and removal of heavy metals from contaminated agricultural soil. *Chemical Engineering Journal*, *390*(February), 124638. https://doi.org/10.1016/j.cej.2020.124638

Liu, Yucheng, Liu, Q., Chen, M., Ma, L., Yang, B., Chen, J., Lv, Z., Liang, Q., & Yang, P. (2017). Evaluation of migration of heavy metals and performance of product during co-pyrolysis process of municipal sewage sludge and walnut shell. *Environmental Science and Pollution Research*, *24*(27), 22082–22090. https://doi.org/10.1007/s11356-017-9858-8

Liu, Zhixin, Xu, Z., Xu, L., Buyong, F., Chay, T. C., Li, Z., Cai, Y., Hu, B., Zhu, Y., & Wang, X. (2022). Modified biochar: synthesis and mechanism for removal of environmental heavy metals. *Carbon Research*, *1*(1), 1–21. https://doi.org/10.1007/s44246-022-00007-3

Liu, Zishan, Asghar, A., Hou, C., Ali, I., Naqvi, S. R., Wang, N., Zhu, H., Mehmood, M. A., & Liu, C. G. (2022). Co-pyrolysis of the Chinese liquor industry waste and bamboo waste, elucidation of the pyrolysis reaction chemistry, and TG-FTIR-MS based study of the evolved gases. *Fuel*, *326*(April), 124976. https://doi.org/10.1016/j.fuel.2022.124976

Lombardi, L., Carnevale, E., & Corti, A. (2015). A review of technologies and performances of thermal treatment systems for energy recovery from waste. *Waste Management*, *37*, 26–44. https://doi.org/10.1016/j.wasman.2014.11.010

Lou, L., Luo, L., Yang, Q., Cheng, G., Xun, B., Xu, X., & Chen, Y. (2012). Release of pentachlorophenol from black carbon-inclusive sediments under different environmental conditions. *Chemosphere*, *88*(5), 598–604. https://doi.org/10.1016/j.chemosphere.2012.03.039

Lu, K., Yang, X., Shen, J., Robinson, B., Huang, H., Liu, D., Bolan, N., Pei, J., & Wang, H. (2014). Effect of bamboo and rice straw biochars on the bioavailability of Cd, Cu, Pb and Zn to Sedum plumbizincicola. *Agriculture, Ecosystems and Environment*, *191*, 124–132. https://doi.org/10.1016/j.agee.2014.04.010

Lu, P., Huang, Q., Chi, Y., Wang, F., & Yan, J. (2019). Catalytic cracking of tar derived from the pyrolysis of municipal solid waste fractions over biochar. *Proceedings of the Combustion Institute*, *37*(3), 2673–2680. https://doi.org/10.1016/j.proci.2018.06.051

Lu, S., & Zong, Y. (2018). Pore structure and environmental serves of biochars derived from different feedstocks and pyrolysis conditions. *Environmental Science and Pollution Research*, *25*(30), 30401–30409. https://doi.org/10.1007/s11356-018-3018-7

Luo, L., Wang, G., Shi, G., Zhang, M., Zhang, J., He, J., Xiao, Y., Tian, D., Zhang, Y., Deng, S., Zhou, W., Lan, T., & Deng, O. (2019). The characterization of biochars

derived from rice straw and swine manure, and their potential and risk in N and P removal from water. *Journal of Environmental Management*, *245*(May), 1–7. https://doi.org/10.1016/j.jenvman.2019.05.072

Bortolamasi, M., & Fottner, J. (2001). Design and sizing of screw feeders. *International Congress for Particle Technology*, *January 2001*, 27–29.

Ma, X., Ren, Q., Zhan, W., Zheng, K., Chen, R., & Wang, Y. (2022). Simultaneous stabilization of Pb, Cd, Cu, Zn and Ni in contaminated sediment using modified biochar. *Journal of Soils and Sediments*, *22*(1), 392–402. https://doi.org/10.1007/s11368-021-03086-8

Maliutina, K., Tahmasebi, A., Yu, J., & Saltykov, S. N. (2017). Comparative study on flash pyrolysis characteristics of microalgal and lignocellulosic biomass in entrained-flow reactor. *Energy Conversion and Management*, *151*(July), 426–438. https://doi.org/10.1016/j.enconman.2017.09.013

Malone, Z., Berhe, A. A., & Ryals, R. (2023). Impacts of organic matter amendments on urban soil carbon and soil quality: A meta-analysis. *Journal of Cleaner Production*, *419*(November 2022), 138148. https://doi.org/10.1016/j.jclepro.2023.138148

Mangkoedihardjo, S. (2006). Revaluation of maturity and stability indices for compost. *Journal of Applied Sciences and Environmental Management*, *10*(3). https://doi.org/10.4314/jasem.v10i3.17324

Manyà, J. J., Alvira, D., Azuara, M., Bernin, D., & Hedin, N. (2016). Effects of Pressure and the Addition of a Rejected Material from Municipal Waste Composting on the Pyrolysis of Two-Phase Olive Mill Waste. *Energy and Fuels*, *30*(10), 8055–8064. https://doi.org/10.1021/acs.energyfuels.6b01579

Marcilla, A., Catalá, L., García-Quesada, J. C., Valdés, F. J., & Hernández, M. R. (2013). A review of thermochemical conversion of microalgae. *Renewable and Sustainable Energy Reviews*, *27*, 11–19. https://doi.org/10.1016/j.rser.2013.06.032

Masud, M. A. Al, Shin, W. S., Sarker, A., Septian, A., Das, K., Deepo, D. M., Iqbal, M. A., Islam, A. R. M. T., & Malafaia, G. (2023). A critical review of sustainable application of biochar for green remediation: Research uncertainty and future directions. *Science of the Total Environment*, *904*(June), 166813. https://doi.org/10.1016/j.scitotenv.2023.166813

Maturi, K. C., Haq, I., & Kalamdhad, A. S. (2022). Biodegradation of an intrusive weed Parthenium hysterophorus through in-vessel composting technique: toxicity assessment and spectroscopic study. *Environmental Science and Pollution Research*, *29*(56), 84600–84615. https://doi.org/10.1007/s11356-022-21816-4

Maulina, S., & Iriansyah, M. (2018). Characteristics of activated carbon resulted from pyrolysis of the oil palm fronds powder. *IOP Conference Series: Materials Science and Engineering*, *309*(1). https://doi.org/10.1088/1757-899X/309/1/012072

Meena, A. L., Karwal, M., & Dutta, D. (2021). *Composting: Phases and Factors Responsible for Efficient and Improved Composting Network Project on Organic Farming View project*. *January*. https://doi.org/10.13140/RG.2.2.13546.95689

Meena, M. D., Dotaniya, M. L., Meena, B. L., Rai, P. K., Antil, R. S., Meena, H. S., Meena, L. K., Dotaniya, C. K., Meena, V. S., Ghosh, A., Meena, K. N., Singh, A. K., Meena, V. D., Moharana, P. C., Meena, S. K., Srinivasarao, C., Meena, A. L., Chatterjee, S.,

Meena, D. K., … Meena, R. B. (2023). Municipal solid waste: Opportunities, challenges and management policies in India: A review. *Waste Management Bulletin*, *1*(1), 4–18. https://doi.org/10.1016/j.wmb.2023.04.001

Meier, S., Curaqueo, G., Khan, N., Bolan, N., Cea, M., Eugenia, G. M., Cornejo, P., Ok, Y. S., & Borie, F. (2017). Chicken-manure-derived biochar reduced bioavailability of copper in a contaminated soil. *Journal of Soils and Sediments*, *17*(3), 741–750. https://doi.org/10.1007/s11368-015-1256-6

Méndez, A., Gómez, A., Paz-Ferreiro, J., & Gascó, G. (2012). Effects of sewage sludge biochar on plant metal availability after application to a Mediterranean soil. *Chemosphere*, *89*(11), 1354–1359. https://doi.org/10.1016/j.chemosphere.2012.05.092

Mendez, M. O., & Maier, R. M. (2008). Phytostabilization of mine tailings in arid and semiarid environments - An emerging remediation technology. *Environmental Health Perspectives*, *116*(3), 278–283. https://doi.org/10.1289/ehp.10608

Mészáros, E., Jakab, E., Várhegyi, G., Bourke, J., Manley-Harris, M., Nunoura, T., & Antal, M. J. (2007). Do all carbonized charcoals have the same chemical structure? 1. Implications of thermogravimetry-mass spectrometry measurements. *Industrial and Engineering Chemistry Research*, *46*(18), 5943–5953. https://doi.org/10.1021/ie0615842

Miao, M., Deng, B., Kong, H., Yang, H., Lyu, J., Jiang, X., & Zhang, M. (2021). Effects of volatile matter and oxygen concentration on combustion characteristics of coal in an oxygen-enriched fluidized bed. *Energy*, *220*, 119778. https://doi.org/10.1016/j.energy.2021.119778

Ministry of Agriculture. (2013). Fertilizer Control Order. *J Conserv Dent. 2013*, *16*(4), 2013. https://pubmed.ncbi.nlm.nih.gov/23956527/

Mohamed, A. R., Hamzah, Z., & Daud, M. Z. M. (2014a). Optimization of the pyrolysis process of empty fruit bunch (EFB) in a fixed-bed reactor through a central composite design (CCD). *AIP Conference Proceedings*, *1605*(Ccd), 1172–1177. https://doi.org/10.1063/1.4887756

Mohamed, A. R., Hamzah, Z., & Daud, M. Z. M. (2014b). Optimization of the pyrolysis process of empty fruit bunch (EFB) in a fixed-bed reactor through a central composite design (CCD). *AIP Conference Proceedings*, *1605*(1), 1172–1177. https://doi.org/10.1063/1.4887756

Mohan, D., Pittman, C. U., & Steele, P. H. (2017). Pyrolysis of wood /biomass for Bio-oil. *Progress in Energy and Combustion Science*, *62*(4), 848–889. http://dx.doi.org/10.1016/j.pecs.2017.05.004

Mohanty, S. K., Valenca, R., Berger, A. W., Yu, I. K. M., Xiong, X., Saunders, T. M., & Tsang, D. C. W. (2018). Plenty of room for carbon on the ground: Potential applications of biochar for stormwater treatment. *Science of the Total Environment*, *625*, 1644–1658. https://doi.org/10.1016/j.scitotenv.2018.01.037

Mohee, R., Mauthoor, S., Bundhoo, Z. M. A., Somaroo, G., Soobhany, N., & Gunasee, S. (2015). Current status of solid waste management in small island developing states: A review. *Waste Management*, *43*, 539–549. https://doi.org/10.1016/j.wasman.2015.06.012

Moiseenko, K. V., Glazunova, O. A., Savinova, O. S., Vasina, D. V., Zherebker, A. Y., Kulikova, N. A., Nikolaev, E. N., & Fedorova, T. V. (2021). Relation between lignin molecular profile and fungal exo-proteome during kraft lignin modification by Trametes hirsuta LE-BIN 072. *Bioresource Technology*, *335*(April), 125229. https://doi.org/10.1016/j.biortech.2021.125229

Moroń, W., & Rybak, W. (2015). NOx and SO2 emissions of coals, biomass and their blends under different oxy-fuel atmospheres. *Atmospheric Environment*, *116*(x), 65–71. https://doi.org/10.1016/j.atmosenv.2015.06.013

Moustakas, K., Rehan, M., Loizidou, M., Nizami, A. S., & Naqvi, M. (2020). Energy and resource recovery through integrated sustainable waste management. *Applied Energy*, *261*(December 2019). https://doi.org/10.1016/j.apenergy.2019.114372

Mu, L., Chen, J., Yin, H., Song, X., Li, A., & Chi, X. (2015). Pyrolysis behaviors and kinetics of refining and chemicals wastewater, lignite and their blends through TGA. *Bioresource Technology*, *180*, 22–31. https://doi.org/10.1016/j.biortech.2014.12.090

Mujtaba Munir, M. A., Liu, G., Yousaf, B., Ali, M. U., Abbas, Q., & Ullah, H. (2020). Synergistic effects of biochar and processed fly ash on bioavailability, transformation and accumulation of heavy metals by maize (Zea mays L.) in coal-mining contaminated soil. *Chemosphere*, *240*, 124845. https://doi.org/10.1016/j.chemosphere.2019.124845

Musale, H. K., Bhattacharyulu, Y. C., Bhoyar, R. K., Student, P. G., & Professor, A. (2013). " Design Consideration Of Pyrolysis Reactor For Production Of Bio-Oil ". *International Journal of Engineering Trends and Technology*, *5*(2), 83–85. http://www.ijettjournal.org

Mushtaq, S., Bareen, F. e., & Tayyeb, A. (2023). Equilibrium kinetics and thermodynamic studies on biosorption of heavy metals by metal-resistant strains of Trichoderma isolated from tannery solid waste. *Environmental Science and Pollution Research*, *30*(4), 10925–10954. https://doi.org/10.1007/s11356-022-22860-w

Namasivayam, C., & Kavitha, D. (2002). *Removal of Congo Red from water by adsorption onto activated carbon prepared from coir pith, an agricultural solid waste*. *54*, 47–58.

Narwal, R. P., Singh, B. R., & Salbu, B. (1999). Association of cadmium, zinc, copper, and nickel with components in naturally heavy metal-rich soils studied by parallel and sequential extractions. *Communications in Soil Science and Plant Analysis*, *30*(7–8), 1209–1230. https://doi.org/10.1080/00103629909370279

Nepal, J., Ahmad, W., Munsif, F., Khan, A., & Zou, Z. (2023). Advances and prospects of biochar in improving soil fertility, biochemical quality, and environmental applications. *Frontiers in Environmental Science*, *11*(February). https://doi.org/10.3389/fenvs.2023.1114752

Nguyen, M. K., Lin, C., Hoang, H. G., Sanderson, P., Dang, B. T., Bui, X. T., Nguyen, N. S. H., Vo, D. V. N., & Tran, H. T. (2022). Evaluate the role of biochar during the organic waste composting process: A critical review. *Chemosphere*, *299*(January), 134488. https://doi.org/10.1016/j.chemosphere.2022.134488

Nguyen, T. B., Sherpa, K., Bui, X. T., Nguyen, V. T., Vo, T. D. H., Ho, H. T. T., Chen, C. W., & Dong, C. Di. (2023). Biochar for soil remediation: A comprehensive review of

current research on pollutant removal. *Environmental Pollution*, *337*(September), 122571. https://doi.org/10.1016/j.envpol.2023.122571

Ni, N., Song, Y., Shi, R., Liu, Z., Bian, Y., Wang, F., Yang, X., Gu, C., & Jiang, X. (2017). Biochar reduces the bioaccumulation of PAHs from soil to carrot (Daucus carota L.) in the rhizosphere: A mechanism study. *Science of the Total Environment*, *601–602*, 1015–1023. https://doi.org/10.1016/j.scitotenv.2017.05.256

Nilai, P., Kalorifik, N., Proses, B. M., Sisa, T., Perbandaran, P., Isa, K., Kasim, F. H., Ali, U. F., & Rashid, R. A. (2017). Characterization, Calculation of Calorific Values, and Bio-Oil Production Via Thermochemical Processes of Municipal Solid Waste in Perlis, Malaysia. *Malaysian Journal of Analytical Science*, *21*(4), 801–809. https://doi.org/10.17576/mjas-2017-2104-06

Nithikul, J. (2007). Potential of Refuse Derived Fuel Production. *Evaluation*, *Master of*(December), 2005–2008.

Niu, G., Wang, R., Hasi, M., Wang, Y., Geng, Q., Wang, C., Jiang, Y., & Huang, J. (2021). Availability of soil base cations and micronutrients along soil profile after 13-year nitrogen and water addition in a semi-arid grassland. *Biogeochemistry*, *152*(2–3), 223–236. https://doi.org/10.1007/s10533-020-00749-5

Nizam, N. U. M., Hanafiah, M. M., Mahmoudi, E., Halim, A. A., & Mohammad, A. W. (2021). The removal of anionic and cationic dyes from an aqueous solution using biomass-based activated carbon. *Scientific Reports*, *11*(1), 1–17. https://doi.org/10.1038/s41598-021-88084-z

Nobile, C., Lebrun, M., Védère, C., Honvault, N., Aubertin, M. L., Faucon, M. P., Girardin, C., Houot, S., Kervroëdan, L., Dulaurent, A. M., Rumpel, C., & Houben, D. (2022). Biochar and compost addition increases soil organic carbon content and substitutes P and K fertilizer in three French cropping systems. *Agronomy for Sustainable Development*, *42*(6). https://doi.org/10.1007/s13593-022-00848-7

Novak, J. M., Busscher, W. J., Laird, D. L., Ahmedna, M., Watts, D. W., & Niandou, M. A. S. (2009). Impact of biochar amendment on fertility of a southeastern coastal plain soil. *Soil Science*, *174*(2), 105–112. https://doi.org/10.1097/SS.0b013e3181981d9a

Nuraisyah, S., Khairunnisa, M. P., Norruwaida, J., Ali, A. H. M., Dewika, M., & Rashid, M. (2020). Soil with high porosity as an excellent carbon dioxide adsorbent carbon-rich soil as an effective adsorbent for carbon dioxide. *IOP Conference Series: Earth and Environmental Science*, *476*(1). https://doi.org/10.1088/1755-1315/476/1/012124

O'Connor, D., Peng, T., Li, G., Wang, S., Duan, L., Mulder, J., Cornelissen, G., Cheng, Z., Yang, S., & Hou, D. (2018). Sulfur-modified rice husk biochar: A green method for the remediation of mercury contaminated soil. *Science of the Total Environment*, *621*, 819–826. https://doi.org/10.1016/j.scitotenv.2017.11.213

Ohmukai, Y., Hasegawa, I., & Mae, K. (2008). Pyrolysis of the mixture of biomass and plastics in countercurrent flow reactor Part I: Experimental analysis and modeling of kinetics. *Fuel*, *87*(13–14), 3105–3111. https://doi.org/10.1016/j.fuel.2008.04.005

Oldfield, T. L., Sikirica, N., Mondini, C., López, G., Kuikman, P. J., & Holden, N. M. (2018). Biochar, compost and biochar-compost blend as options to recover nutrients and sequester carbon. *Journal of Environmental Management*, *218*, 465–476.

https://doi.org/10.1016/j.jenvman.2018.04.061

Onay, O. (2007). Influence of pyrolysis temperature and heating rate on the production of bio-oil and char from safflower seed by pyrolysis, using a well-swept fixed-bed reactor. *Fuel Processing Technology*, *88*(5), 523–531. https://doi.org/10.1016/j.fuproc.2007.01.001

Onay, O., & Kockar, O. M. (2003). Slow, fast and flash pyrolysis of rapeseed. *Renewable Energy*, *28*(15), 2417–2433. https://doi.org/10.1016/S0960-1481(03)00137-X

Oustriere, N., Marchand, L., Rosette, G., Friesl-Hanl, W., & Mench, M. (2017). Wood-derived-biochar combined with compost or iron grit for in situ stabilization of Cd, Pb, and Zn in a contaminated soil. *Environmental Science and Pollution Research*, *24*(8), 7468–7481. https://doi.org/10.1007/s11356-017-8361-6

Oyediran, I. A., & Durojaiye, H. F. (2011). Variability in the Geotechnical properties of some residual clay soils from southwestern Nigeria. *International Journal of Scientific and Engineering Research*, *2*(9), 235–240. https://doi.org/10.14299/ijser.2011.09.001

Park, J. H., Choppala, G. K., Bolan, N. S., Chung, J. W., & Chuasavathi, T. (2011). Biochar reduces the bioavailability and phytotoxicity of heavy metals. *Plant and Soil*, *348*(1–2), 439–451. https://doi.org/10.1007/s11104-011-0948-y

Park, J. H., Lamb, D., Paneerselvam, P., Choppala, G., Bolan, N., & Chung, J. W. (2011). Role of organic amendments on enhanced bioremediation of heavy metal(loid) contaminated soils. *Journal of Hazardous Materials*, *185*(2–3), 549–574. https://doi.org/10.1016/j.jhazmat.2010.09.082

Pasangulapati, V., Ramachandriya, K. D., Kumar, A., Wilkins, M. R., Jones, C. L., & Huhnke, R. L. (2012). Effects of cellulose, hemicellulose and lignin on thermochemical conversion characteristics of the selected biomass. *Bioresource Technology*, *114*, 663–669. https://doi.org/10.1016/j.biortech.2012.03.036

Pathak, H., & Rao, D. L. N. (1998). Carbon and nitrogen mineralization from added organic matter in saline and alkali soils. *Soil Biology and Biochemistry*, *30*(6), 695–702. https://doi.org/10.1016/S0038-0717(97)00208-3

Patra, S. K., Poddar, R., Brestic, M., Acharjee, P. U., Bhattacharya, P., Sengupta, S., Pal, P., Bam, N., Biswas, B., Barek, V., Ondrisik, P., Skalicky, M., & Hossain, A. (2022). Prospects of Hydrogels in Agriculture for Enhancing Crop and Water Productivity under Water Deficit Condition. *International Journal of Polymer Science*, *2022*. https://doi.org/10.1155/2022/4914836

Patumsawad, S., & Cliffe, K. R. (2002). Experimental study on fluidised bed combustion of high moisture municipal solid waste. *Energy Conversion and Management*, *43*(17), 2329–2340. https://doi.org/10.1016/S0196-8904(01)00179-0

Peacocke, G. V. C., Madrali, E. S., Li, C. Z., Güell, A. J., Wu, F., Kandiyoti, R., & Bridgwater, A. V. (1994). Effect of reactor configuration on the yields and structures of pine-wood derived pyrolysis liquids: A comparison between ablative and wire-mesh pyrolysis. *Biomass and Bioenergy*, *7*(1–6), 155–167. https://doi.org/10.1016/0961-9534(94)00055-X

Peces, M., Astals, S., & Mata-Alvarez, J. (2014). Assessing total and volatile solids in municipal solid waste samples. *Environmental Technology (United Kingdom)*,

35(24), 3041–3046. https://doi.org/10.1080/09593330.2014.929182

Periathamby, A., Hamid, F. S., & Sakai, S. I. (2012). Disaster waste management challenges. *Waste Management and Research*, *30*(2), 113–114. https://doi.org/10.1177/0734242X11434630

Phan, A. N., Ryu, C., Sharifi, V. N., & Swithenbank, J. (2008). Characterisation of slow pyrolysis products from segregated wastes for energy production. *Journal of Analytical and Applied Pyrolysis*, *81*(1), 65–71. https://doi.org/10.1016/j.jaap.2007.09.001

PIB. (2023). *Press Information Bureau Government of India Ministry of New and Renewable Energy Generation Based Incentive Scheme*. 1–2. https://pib.gov.in/newsite/PrintRelease.aspx?relid=78829

Pottipati, S., Kundu, A., & Kalamdhad, A. S. (2022). Process optimization by combining in-vessel composting and vermicomposting of vegetable waste. *Bioresource Technology*, *346*(November 2021), 126357. https://doi.org/10.1016/j.biortech.2021.126357

Powar, R. V., & Gangil, S. (2015). Effect of temperature on iodine value and total carbon contain in bio-char produced from soybean stalk in continuous feed reactor. *International Journal of Agricultural Engineering*, *8*(1), 26–30. https://doi.org/10.15740/has/ijae/8.1/26-30

Puranik, P. R., & Paknikar, K. M. (1999). Biosorption of lead, cadmium, and zinc by Citrobacter strain MCM B-181: Characterization studies. *Biotechnology Progress*, *15*(2), 228–237. https://doi.org/10.1021/bp990002r

Qian, T. T., Wu, P., Qin, Q. Y., Huang, Y. N., Wang, Y. J., & Zhou, D. M. (2019). Screening of wheat straw biochars for the remediation of soils polluted with Zn (II) and Cd (II). *Journal of Hazardous Materials*, *362*(August 2018), 311–317. https://doi.org/10.1016/j.jhazmat.2018.09.034

Qiu, B., Shao, Q., Shi, J., Yang, C., & Chu, H. (2022). Application of biochar for the adsorption of organic pollutants from wastewater: Modification strategies, mechanisms and challenges. *Separation and Purification Technology*, *300*(June), 121925. https://doi.org/10.1016/j.seppur.2022.121925

Qu, Y., Qu, J., Yan, W., Yue, T., Zhang, Q., Yi, W., Liu, X., & Sun, Y. (2022). Influence of Biochar on Physico-Chemical, Microbial Community and Maturity during Biogas Residue Aerobic Composting Process. *Fermentation*, *8*(11). https://doi.org/10.3390/fermentation8110623

Quesada, L., Calero, M., Martín-Lara, M. A., Pérez, A., & Blázquez, G. (2019). Characterization of fuel produced by pyrolysis of plastic film obtained of municipal solid waste. *Energy*, *186*(2019). https://doi.org/10.1016/j.energy.2019.115874

Rai, P., & Chatrath, H. (2019). Effects of Soil Viscosity, Soil Temperature, and Specific Gravity on Plants Growth Sown in Soil Prepared From Laboratory Chemical Waste. *International Journal of Students' Research in Technology & Management*, *7*(2), 11–16. https://doi.org/10.18510/ijsrtm.2019.723

Rajaeifar, M. A., Ghanavati, H., Dashti, B. B., Heijungs, R., Aghbashlo, M., & Tabatabaei, M. (2017). Electricity generation and GHG emission reduction potentials through different municipal solid waste management technologies: A comparative review.

Renewable and Sustainable Energy Reviews, *79*(May), 414–439. https://doi.org/10.1016/j.rser.2017.04.109

Rajkumar, H., Naik, P. K., & Rishi, M. S. (2019). Evaluation of heavy metal contamination in soil using geochemical indexing approaches and chemometric techniques. *International Journal of Environmental Science and Technology*, *16*(11), 7467–7486. https://doi.org/10.1007/s13762-018-2081-4

Rasheed, T., Anwar, M. T., Ahmad, N., Sher, F., Khan, S. U. D., Ahmad, A., Khan, R., & Wazeer, I. (2021). Valorisation and emerging perspective of biomass based waste-to-energy technologies and their socio-environmental impact: A review. *Journal of Environmental Management*, *287*(September 2020), 112257. https://doi.org/10.1016/j.jenvman.2021.112257

Rathod, N., Jain, S., & Patel, M. R. (2023). Thermodynamic analysis of biochar produced from groundnut shell through slow pyrolysis. *Energy Nexus*, *9*(July 2022), 100177. https://doi.org/10.1016/j.nexus.2023.100177

Räty, M., Keskinen, R., Yli-Halla, M., Hyvönen, J., & Soinne, H. (2021). Estimating cation exchange capacity and clay content from agricultural soil testing data. *Agricultural and Food Science*, *30*(4), 131–145. https://doi.org/10.23986/afsci.111107

Reddy, P. J. (2016). Pyrolysis and Gasification technologies. In *Energy Recovery from Municipal Solid Waste by Thermal Conversion Technologies*. https://doi.org/10.1201/b21307-8

Rodríguez-Vila, A., Forján, R., Guedes, R. S., & Covelo, E. F. (2016). Changes on the Phytoavailability of Nutrients in a Mine Soil Reclaimed with Compost and Biochar. *Water, Air, and Soil Pollution*, *227*(12). https://doi.org/10.1007/s11270-016-3155-x

Rojas-Valencia, M. N., & Nájera-Aguilar, H. (2012). Analysis of the generation of household solid wastes, household hazardous wastes and sustainable alternative handling. *International Journal of Sustainable Society*, *4*(3), 280–299. https://doi.org/10.1504/IJSSOC.2012.047282

Rojith, G., & S, B. S. I. (2013). *Cellulose Crystallinity Change Assessment of Biochar Produced by Pyrolysis of Coir Pith*. *2*(June 2014), 98–101.

Roy, S. ., & Bhalla, S. K. (2017). Role of Geotechnical Properties of Soil on Civil Engineering Structures. *Resources and Environment*, *7*(4), 103–109. https://doi.org/10.5923/j.re.20170704.03

Ruengvilairat, P., Tanatavikorn, H., & Vitidsant, T. (2012). Bio-Oil Production by Pyrolysis of Oil Palm Empty Fruit Bunch in Nitrogen and Steam Atmospheres. *Journal of Sustainable Bioenergy Systems*, *02*(04), 75–85. https://doi.org/10.4236/jsbs.2012.24011

Ruggieri, L., Gea, T., Artola, A., & Sánchez, A. (2009). Air filled porosity measurements by air pycnometry in the composting process: A review and a correlation analysis. *Bioresource Technology*, *100*(10), 2655–2666. https://doi.org/10.1016/j.biortech.2008.12.049

Rangabhashiyam, S., & Paramasivan, B. (2019). The potential of lignocellulosic biomass precursors for biochar production: Performance, mechanism and wastewater application—A review. *Industrial Crops and Products*, *128*(November 2018), 405–423. https://doi.org/10.1016/j.indcrop.2018.11.041

Saffarzadeh, A., Shimaoka, T., Motomura, Y., & Watanabe, K. (2006). Chemical and mineralogical evaluation of slag products derived from the pyrolysis/melting treatment of MSW. *Waste Management*, *26*(12), 1443–1452. https://doi.org/10.1016/j.wasman.2005.12.005

Sahu, S., Sindhu, N. J., & Sharma, P. K. (2014). Review on Solid Waste Management of Art. *International Journal of Innovative Research and Development*, *3*(3), 261–268.

Sánchez-Monedero, M. A., Sánchez-García, M., Alburquerque, J. A., & Cayuela, M. L. (2019). Biochar reduces volatile organic compounds generated during chicken manure composting. *Bioresource Technology*, *288*(May), 121584. https://doi.org/10.1016/j.biortech.2019.121584

Sanchez, P. A., Palm, C. A., & Buol, S. W. (2003). Fertility capability soil classification: A tool to help assess soil quality in the tropics. *Geoderma*, *114*(3–4), 157–185. https://doi.org/10.1016/S0016-7061(03)00040-5

Saqib, N. U., Sharma, H. B., Baroutian, S., Dubey, B., & Sarmah, A. K. (2019). Valorisation of food waste via hydrothermal carbonisation and techno-economic feasibility assessment. *Science of the Total Environment*, *690*, 261–276. https://doi.org/10.1016/j.scitotenv.2019.06.484

Saravanakumar, A., Sudha, M. R., Chen, W. H., & Pradeshwaran, V. (2024). A review on green adsorbent from plastic waste-derived char for wastewater treatment: Production, aqueous contaminants adsorption, and applications. *Journal of the Taiwan Institute of Chemical Engineers*, *xxxx*, 105437. https://doi.org/10.1016/j.jtice.2024.105437

Saravanan, A., Kumar, P. S., & Renita, A. A. (2018). Hybrid synthesis of novel material through acid modification followed ultrasonication to improve adsorption capacity for zinc removal. *Journal of Cleaner Production*, *172*, 92–105. https://doi.org/10.1016/j.jclepro.2017.10.109

Sbrolini Tiburcio, R., Malpeli Junior, M., Tófano de Campos Leite, J., Minoru Yamaji, F., & Pereira Neto, A. M. (2021). Physicochemical and thermophysical characterization of rejected waste and evaluation of their use as refuse-derived fuel. *Fuel*, *293*(February). https://doi.org/10.1016/j.fuel.2021.120359

Sembiring, K. C., Rinaldi, N., & Simanungkalit, S. P. (2015). Bio-oil from Fast Pyrolysis of Empty Fruit Bunch at Various Temperature. *Energy Procedia*, *65*, 162–169. https://doi.org/10.1016/j.egypro.2015.01.052

Senthil Kumar, P., Ramalingam, S., Abhinaya, R. V., Thiruvengadaravi, K. V., Baskaralingam, P., & Sivanesan, S. (2011). Lead(II) adsorption onto sulphuric acid treated cashew nut shell. *Separation Science and Technology*, *46*(15), 2436–2449. https://doi.org/10.1080/01496395.2011.590174

Shah, S. H., Khan, Z. M., Raja, I. A., Mahmood, Q., Bhatti, Z. A., Khan, J., Farooq, A., Rashid, N., & Wu, D. (2010). Low temperature conversion of plastic waste into light hydrocarbons. *Journal of Hazardous Materials*, *179*(1–3), 15–20. https://doi.org/10.1016/j.jhazmat.2010.01.134

Shahbaz, M., Yusup, S., Inayat, A., Patrick, D. O., Ammar, M., & Pratama, A. (2017). Cleaner Production of Hydrogen and Syngas from Catalytic Steam Palm Kernel Shell Gasification Using CaO Sorbent and Coal Bottom Ash as a Catalyst. *Energy and*

Fuels, *31*(12), 13824–13833. https://doi.org/10.1021/acs.energyfuels.7b03237

Shakya, A., & Agarwal, T. (2019). Removal of Cr(VI) from water using pineapple peel derived biochars: Adsorption potential and re-usability assessment. *Journal of Molecular Liquids*, *293*, 111497. https://doi.org/10.1016/j.molliq.2019.111497

Shakya, A., Núñez-Delgado, A., & Agarwal, T. (2019). Biochar synthesis from sweet lime peel for hexavalent chromium remediation from aqueous solution. *Journal of Environmental Management*, *251*(97), 109570. https://doi.org/10.1016/j.jenvman.2019.109570

Shao, Q., Ju, Y., Guo, W., Xia, X., Bian, R., Li, L., Li, W., Liu, X., Zheng, J., & Pan, G. (2019). Pyrolyzed municipal sewage sludge ensured safe grain production while reduced C emissions in a paddy soil under rice and wheat rotation. *Environmental Science and Pollution Research*, *26*(9), 9244–9256. https://doi.org/10.1007/s11356-019-04417-6

Sharholy, M., Ahmad, K., Mahmood, G., & Trivedi, R. C. (2008). Municipal solid waste management in Indian cities - A review. *Waste Management*, *28*(2), 459–467. https://doi.org/10.1016/j.wasman.2007.02.008

Sharma, D., Varma, V. S., Yadav, K. D., & Kalamdhad, A. S. (2017). Evolution of chemical and biological characterization during agitated pile composting of flower waste. *International Journal of Recycling of Organic Waste in Agriculture*, *6*(1), 89–98. https://doi.org/10.1007/s40093-017-0155-9

Sharma, K. D., & Jain, S. (2019). Overview of Municipal Solid Waste Generation, Composition, and Management in India. *Journal of Environmental Engineering*, *145*(3), 04018143. https://doi.org/10.1061/(asce)ee.1943-7870.0001490

Shen, Y. (2015). Chars as carbonaceous adsorbents/catalysts for tar elimination during biomass pyrolysis or gasification. *Renewable and Sustainable Energy Reviews*, *43*, 281–295. https://doi.org/10.1016/j.rser.2014.11.061

Shinogi, Y., & Kanri, Y. (2003). Pyrolysis of plant, animal and human waste: Physical and chemical characterization of the pyrolytic products. *Bioresource Technology*, *90*(3), 241–247. https://doi.org/10.1016/S0960-8524(03)00147-0

Shrivastava, P., Palamanit, A., & Kumar, A. (2023). Isoconversional thermal decomposition reaction kinetics of oil palm trunk and rubberwood sawdust for thermochemical conversion processes. *Environmental Science and Pollution Research*, 1–11. https://doi.org/10.1007/s11356-023-28998-5

Simon, N., Raubenheimer, K., Urho, N., Unger, S., Azoulay, D., Farrelly, T., Sousa, J., van Asselt, H., Carlini, G., Sekomo, C., Schulte, M. L., Busch, P. O., Wienrich, N., & Weiand, L. (2021). A binding global agreement to address the life cy cle of plastics. *Science*, *373*(6550), 43–47. https://doi.org/10.1126/science.abi9010

Singh, E., Kumar, A., Mishra, R., You, S., Singh, L., Kumar, S., & Kumar, R. (2021). Pyrolysis of waste biomass and plastics for production of biochar and its use for removal of heavy metals from aqueous solution. *Bioresource Technology*, *320*(PA), 124278. https://doi.org/10.1016/j.biortech.2020.124278

Singh, H., Northup, B. K., Rice, C. W., & Prasad, P. V. V. (2022). Biochar applications influence soil physical and chemical properties, microbial diversity, and crop productivity: a meta-analysis. *Biochar*, *4*(1), 1–17. https://doi.org/10.1007/s42773-

022-00138-1

Singh, J., & Kalamdhad, A. S. (2012). Concentration and speciation of heavy metals during water hyacinth composting. *Bioresource Technology*, *124*, 169–179. https://doi.org/10.1016/j.biortech.2012.08.043

Singh, J., & Kalamdhad, A. S. (2016). Effect of lime on speciation of heavy metals during composting of water hyacinth. *Frontiers of Environmental Science and Engineering*, *10*(1), 93–102. https://doi.org/10.1007/s11783-014-0704-7

Singh Yadav, S. P., Bhandari, S., Bhatta, D., Poudel, A., Bhattarai, S., Yadav, P., Ghimire, N., Paudel, P., Paudel, P., Shrestha, J., & Oli, B. (2023). Biochar application: A sustainable approach to improve soil health. *Journal of Agriculture and Food Research*, *11*(January), 100498. https://doi.org/10.1016/j.jafr.2023.100498

Singhal, A., Gupta, A. K., Dubey, B., & Ghangrekar, M. M. (2022). Seasonal characterization of municipal solid waste for selecting feasible waste treatment technology for Guwahati city, India. *Journal of the Air and Waste Management Association*, *72*(2), 147–160. https://doi.org/10.1080/10962247.2021.1980450

Sipra, A. T., Gao, N., & Sarwar, H. (2018). Municipal solid waste (MSW) pyrolysis for bio-fuel production: A review of effects of MSW components and catalysts. *Fuel Processing Technology*, *175*(February), 131–147. https://doi.org/10.1016/j.fuproc.2018.02.012

Solantausta, Y., Nylund, N. O., Westerholm, M., Koljonen, T., & Oasmaa, A. (1993). Wood-pyrolysis oil as fuel in a diesel-power plant. *Bioresource Technology*, *46*(1–2), 177–188. https://doi.org/10.1016/0960-8524(93)90071-I

Song, F., Li, T., Zhang, J., Wang, X., Bai, Y., Giesy, J. P., Xing, B., & Wu, F. (2019). Novel Insights into the Kinetics, Evolved Gases, and Mechanisms for Biomass (Sugar Cane Residue) Pyrolysis. *Environmental Science and Technology*, *53*(22), 13495–13505. https://doi.org/10.1021/acs.est.9b04595

Song, Q., Zhao, H. yu, Xing, W. long, Song, L. hua, Yang, L., Yang, D., & Shu, X. (2018). Effects of various additives on the pyrolysis characteristics of municipal solid waste. *Waste Management*, *78*, 621–629. https://doi.org/10.1016/j.wasman.2018.06.033

Sotoudehnia, F., Baba Rabiu, A., Alayat, A., & McDonald, A. G. (2020). Characterization of bio-oil and biochar from pyrolysis of waste corrugated cardboard. *Journal of Analytical and Applied Pyrolysis*, *145*(October 2019), 104722. https://doi.org/10.1016/j.jaap.2019.104722

Stamatov, V., Honnery, D., & Soria, J. (2006). Combustion properties of slow pyrolysis bio-oil produced from indigenous Australian species. *Renewable Energy*, *31*(13), 2108–2121. https://doi.org/10.1016/j.renene.2005.10.004

Stefanidis, S. D., Kalogiannis, K. G., Iliopoulou, E. F., Michailof, C. M., Pilavachi, P. A., & Lappas, A. A. (2014). A study of lignocellulosic biomass pyrolysis via the pyrolysis of cellulose, hemicellulose and lignin. *Journal of Analytical and Applied Pyrolysis*, *105*, 143–150. https://doi.org/10.1016/j.jaap.2013.10.013

Steiner, C., Das, K. C., Melear, N., & Lakly, D. (2010). Reducing Nitrogen Loss during Poultry Litter Composting Using Biochar. *Journal of Environmental Quality*, *39*(4), 1236–1242. https://doi.org/10.2134/jeq2009.0337

Sudharsan Varma, V., & Kalamdhad, A. S. (2015). Evolution of chemical and biological

characterization during thermophilic composting of vegetable waste using rotary drum composter. *International Journal of Environmental Science and Technology*, *12*(6), 2015–2024. https://doi.org/10.1007/s13762-014-0582-3

Šuhaj, P., Haydary, J., Husár, J., Steltenpohl, P., & Šupa, I. (2019). Catalytic gasification of refuse-derived fuel in a two-stage laboratory scale pyrolysis/gasification unit with catalyst based on clay minerals. *Waste Management*, *85*, 1–10. https://doi.org/10.1016/j.wasman.2018.11.047

Sun, J., He, F., Pan, Y., & Zhang, Z. (2017). Effects of pyrolysis temperature and residence time on physicochemical properties of different biochar types. *Acta Agriculturae Scandinavica Section B: Soil and Plant Science*, *67*(1), 12–22. https://doi.org/10.1080/09064710.2016.1214745

Sun, Y., Gao, B., Yao, Y., Fang, J., Zhang, M., Zhou, Y., Chen, H., & Yang, L. (2014). Effects of feedstock type, production method, and pyrolysis temperature on biochar and hydrochar properties. *Chemical Engineering Journal*, *240*, 574–578. https://doi.org/10.1016/j.cej.2013.10.081

Suriapparao, D. V., & Vinu, R. (2015). Bio-oil production via catalytic microwave pyrolysis of model municipal solid waste component mixtures. *RSC Advances*, *5*(71), 57619–57631. https://doi.org/10.1039/c5ra08666c

Taherymoosavi, S., Verheyen, V., Munroe, P., Joseph, S., & Reynolds, A. (2017). Characterization of organic compounds in biochars derived from municipal solid waste. *Waste Management*, *67*, 131–142. https://doi.org/10.1016/j.wasman.2017.05.052

Takaya, C. A., Fletcher, L. A., Singh, S., Anyikude, K. U., & Ross, A. B. (2016). Phosphate and ammonium sorption capacity of biochar and hydrochar from different wastes. *Chemosphere*, *145*, 518–527. https://doi.org/10.1016/j.chemosphere.2015.11.052

Tan, X. fei, Liu, Y. guo, Gu, Y. ling, Xu, Y., Zeng, G. ming, Hu, X. jiang, Liu, S. bo, Wang, X., Liu, S. mian, & Li, J. (2016). Biochar-based nano-composites for the decontamination of wastewater: A review. *Bioresource Technology*, *212*, 318–333. https://doi.org/10.1016/j.biortech.2016.04.093

Tang, F., Yu, Z., Li, Y., Chen, L., & Ma, X. (2020). Catalytic co-pyrolysis behaviors, product characteristics and kinetics of rural solid waste and chlorella vulgaris. *Bioresource Technology*, *299*(December 2019), 122636. https://doi.org/10.1016/j.biortech.2019.122636

Tang, J., Zhu, W., Kookana, R., & Katayama, A. (2013). Characteristics of biochar and its application in remediation of contaminated soil. *Journal of Bioscience and Bioengineering*, *116*(6), 653–659. https://doi.org/10.1016/j.jbiosc.2013.05.035

Tang, Y., Alam, M. S., Konhauser, K. O., Alessi, D. S., Xu, S., Tian, W. J., & Liu, Y. (2019). Influence of pyrolysis temperature on production of digested sludge biochar and its application for ammonium removal from municipal wastewater. *Journal of Cleaner Production*, *209*, 927–936. https://doi.org/10.1016/j.jclepro.2018.10.268

Tanner, R. (1965). Die Entwicklung der Von Roll- Müllverbrennungsanlagen. *Schweizerische Bauzeitung*, *83*(16), 251–260.

Tebo, B. M., Johnson, H. A., McCarthy, J. K., & Templeton, A. S. (2005). Geomicrobiology of manganese(II) oxidation. *Trends in Microbiology*, *13*(9), 421–

428. https://doi.org/10.1016/j.tim.2005.07.009

TERI. (2014). Waste to resources: A waste management handbook. *TERI Press: The Energy and Research Institute*. http://cbs.teriin.org/pdf/Waste_Management_Handbook.pdf

Tessier, A., Campbell, P. G. C., & Bisson, M. (1979). Sequential Extraction Procedure for the Speciation of Particulate Trace Metals. *Analytical Chemistry*, *51*(7), 844–851. https://doi.org/10.1021/ac50043a017

Tian, H., Qiao, J., Zhu, Y., Jia, X., & Shao, M. (2021). Vertical distribution of soil available phosphorus and soil available potassium in the critical zone on the Loess Plateau, China. *Scientific Reports*, *11*(1), 1–10. https://doi.org/10.1038/s41598-021-82677-4

Tirkey, A., & Upadhyay, L. S. B. (2021). Microplastics: An overview on separation, identification and characterization of microplastics. *Marine Pollution Bulletin*, *170*(June), 112604. https://doi.org/10.1016/j.marpolbul.2021.112604

Tokmurzin, D., Aiymbetov, B., Abylkhani, B., Yagofarova, A., Sarbassov, Y., Inglezakis, V., Venetis, C., & Poulopoulos, S. G. (2019). Fixed-bed gasification and pyrolysis of organic fraction of MSW blended with coal samples. *Chemical Engineering Transactions*, *72*(March 2018), 163–168. https://doi.org/10.3303/CET1972028

Tokmurzin, D., Kuspangaliyeva, B., Aimbetov, B., Abylkhani, B., Inglezakis, V., Anthony, E. J., & Sarbassov, Y. (2020). Characterization of solid char produced from pyrolysis of the organic fraction of municipal solid waste, high volatile coal and their blends. *Energy*, *191*, 116562. https://doi.org/10.1016/j.energy.2019.116562

Tomobe, H., Tsugawa, S., Yoshida, Y., Arita, T., Tsai, A. Y. L., Kubo, M., Demura, T., & Sawa, S. (2023). A mechanical theory of competition between plant root growth and soil pressure reveals a potential mechanism of root penetration. *Scientific Reports*, *13*(1), 1–12. https://doi.org/10.1038/s41598-023-34025-x

Torsvik, V., & Øvreås, L. (2002). *<0222 Torsvik and Øvreås 2002.pdf>*. 240–245.

Tugov, A. N. (2021). Modern Technologies for the Thermal Treatment of Municipal Solid Waste, and Prospects for Their Implementation in Russia (Review). *Thermal Engineering* , *68*(1), 1–16. https://doi.org/10.1134/S0040601521010183

UNEP. (2024). *Beyond an age*. https://doi.org/10.59117/20.500.11822/44939

Upadhyay, V. (2012). Solid Waste Collection and Segregation: A Case Study of MNIT Campus, Jaipur. *International Journal of Engineering and Innovative Technology*, *1*(3), 144–149.

US EPA. (1992). *Method 1311: Toxicity Characteristic Leaching Procedure, part of Test Methods for Evaluating Solid Waste, Physical/Chemical Methods*. *July 1992*, 1–17.

USDA (United States Department of Agriculture). (2011). Soil Health Quality Indicators: chemical Properties, soil electrical conductivity. *USDA Natural Resources Conservation Service*, 3. https://www.nrcs.usda.gov/wps/portal/nrcs/detail/soils/health/assessment/?cid=stelprdb1237387

van Eck, N. J., & Waltman, L. (2010). Software survey: VOSviewer, a computer program for bibliometric mapping. *Scientometrics*, *84*(2), 523–538. https://doi.org/10.1007/s11192-009-0146-3

Van Vinh, N., Zafar, M., Behera, S. K., & Park, H. S. (2015). Arsenic(III) removal from

aqueous solution by raw and zinc-loaded pine cone biochar: equilibrium, kinetics, and thermodynamics studies. *International Journal of Environmental Science and Technology*, *12*(4), 1283–1294. https://doi.org/10.1007/s13762-014-0507-1

Varma, V. S., Dhamodharan, K., & Kalamdhad, A. S. (2018). Characterization of bacterial community structure during in-vessel composting of agricultural waste by 16S rRNA sequencing. *3 Biotech*, *8*(7), 1–8. https://doi.org/10.1007/s13205-018-1319-7

Verbruggen, N., & Hermans, C. (2013). Physiological and molecular responses to magnesium nutritional imbalance in plants. *Plant and Soil*, *368*(1–2), 87–99. https://doi.org/10.1007/s11104-013-1589-0

Verheijen, F. G. A., Zhuravel, A., Silva, F. C., Amaro, A., Ben-Hur, M., & Keizer, J. J. (2019). The influence of biochar particle size and concentration on bulk density and maximum water holding capacity of sandy vs sandy loam soil in a column experiment. *Geoderma*, *347*(March), 194–202. https://doi.org/10.1016/j.geoderma.2019.03.044

Verla, A. W., Horsfall, M., Verla, E. ., Spiff, A. I., & Ekpete, O. A. (2012). Preparation and Characterization of Activated Carbon From Fluted Pumpkin (Telfairia Occidentalis Hook.F) Seed Shell. *Asian Journal of Natural & Applied Sciences*, *1*(3), 39–50. www. leena-luna.co.jp

Vidu, R., Matei, E., Predescu, A. M., Alhalaili, B., Pantilimon, C., Tarcea, C., & Predescu, C. (2020). Removal of heavy metals from wastewaters: A challenge from current treatment methods to nanotechnology applications. *Toxics*, *8*(4), 1–37. https://doi.org/10.3390/toxics8040101

Vikramarjun, M. (2020). *Waste to Wealth : Municipal Solid Waste Management in Indian Scenario*. *October*, 0–3.

Vishan, I., Saha, B., Sivaprakasam, S., & Kalamdhad, A. (2019). Evaluation of Cd(II) biosorption in aqueous solution by using lyophilized biomass of novel bacterial strain Bacillus badius AK: Biosorption kinetics, thermodynamics and mechanism. *Environmental Technology and Innovation*, *14*, 100323. https://doi.org/10.1016/j.eti.2019.100323

Vithanage, M., Herath, I., Almaroai, Y. A., Rajapaksha, A. U., Huang, L., Sung, J. K., Lee, S. S., & Ok, Y. S. (2017). Effects of carbon nanotube and biochar on bioavailability of Pb, Cu and Sb in multi-metal contaminated soil. *Environmental Geochemistry and Health*, *39*(6), 1409–1420. https://doi.org/10.1007/s10653-017-9941-6

Vitolo, S., Bresci, B., Seggiani, M., & Gallo, M. G. (2001). Catalytic upgrading of pyrolytic oils over HZSM-5 zeolite: Behaviour of the catalyst when used in repeated upgrading-regenerating cycles. *Fuel*, *80*(1), 17–26. https://doi.org/10.1016/S0016-2361(00)00063-6

Vondráčková, S., Hejcman, M., Száková, J., Müllerová, V., & Tlustoš, P. (2014). Soil chemical properties affect the concentration of elements (N, P, K, Ca, Mg, As, Cd, Cr, Cu, Fe, Mn, Ni, Pb, and Zn) and their distribution between organs of Rumex obtusifolius. *Plant and Soil*, *379*(1–2), 231–245. https://doi.org/10.1007/s11104-014-2058-0

Wang, B., Wang, Z., Jiang, Y., Tan, G., Xu, N., & Xu, Y. (2017). Enhanced power generation and wastewater treatment in sustainable biochar electrodes based

bioelectrochemical system. *Bioresource Technology*, *241*, 841–848. https://doi.org/10.1016/j.biortech.2017.05.155

Wang, F., Wang, X., & Song, N. (2021). Biochar and vermicompost improve the soil properties and the yield and quality of cucumber (Cucumis sativus L.) grown in plastic shed soil continuously cropped for different years. *Agriculture, Ecosystems and Environment*, *315*(October 2020), 107425. https://doi.org/10.1016/j.agee.2021.107425

Wang, H., & Luo, P. (2020). Preparation, Kinetics, and Adsorption Mechanism Study of Microcrystalline Cellulose-Modified Bone Char as an Efficient Pb (II) Adsorbent. *Water, Air, and Soil Pollution*, *231*(7). https://doi.org/10.1007/s11270-020-04687-8

Wang, R., Wang, C., Zhao, Z., Jia, J., & Jin, Q. (2019). Energy recovery from high-ash municipal sewage sludge by hydrothermal carbonization: Fuel characteristics of biosolid products. *Energy*, *186*, 115848. https://doi.org/10.1016/j.energy.2019.07.178

Wang, S. P., Wang, L., Sun, Z. Y., Wang, S. T., Shen, C. H., Tang, Y. Q., & Kida, K. (2021). Biochar addition reduces nitrogen loss and accelerates composting process by affecting the core microbial community during distilled grain waste composting. *Bioresource Technology*, *337*(24), 125492. https://doi.org/10.1016/j.biortech.2021.125492

Wang, W., Bai, J., Lu, Q., Zhang, G., Wang, D., Jia, J., Guan, Y., & Yu, L. (2021). Pyrolysis temperature and feedstock alter the functional groups and carbon sequestration potential of Phragmites australis- and Spartina alterniflora-derived biochars. *GCB Bioenergy*, *13*(3), 493–506. https://doi.org/10.1111/gcbb.12795

Wang, X., Guo, M., Koppelaar, R. H. E. M., Van Dam, K. H., Triantafyllidis, C. P., & Shah, N. (2018). A Nexus Approach for Sustainable Urban Energy-Water-Waste Systems Planning and Operation. *Environmental Science and Technology*, *52*(5), 3257–3266. https://doi.org/10.1021/acs.est.7b04659

Wang, Yangyang, Li, F., Song, J., Xiao, R., Luo, L., Yang, Z., & Chai, L. (2018). Stabilization of Cd-, Pb-, Cu- and Zn-contaminated calcareous agricultural soil using red mud: a field experiment. *Environmental Geochemistry and Health*, *40*(5), 2143–2153. https://doi.org/10.1007/s10653-018-0089-9

Wang, Yuchuan, Villamil, M. B., Davidson, P. C., & Akdeniz, N. (2019). A quantitative understanding of the role of co-composted biochar in plant growth using meta-analysis. *Science of the Total Environment*, *685*, 741–752. https://doi.org/10.1016/j.scitotenv.2019.06.244

Wany, A., Pathak, P. K., & Gupta, K. J. (2020). Methods for Measuring Nitrate Reductase, Nitrite Levels, and Nitric Oxide from Plant Tissues. In *Methods in Molecular Biology* (Vol. 2057). https://doi.org/10.1007/978-1-4939-9790-9_2

Wei, B., Peng, Y., Jeyakumar, P., Lin, L., Zhang, D., Yang, M., Zhu, J., Ki Lin, C. S., Wang, H., Wang, Z., & Li, C. (2023). Soil pH restricts the ability of biochar to passivate cadmium: A meta-analysis. *Environmental Research*, *219*(December 2022), 115110. https://doi.org/10.1016/j.envres.2022.115110

Weil, S. A. (1980). *Thermodynamic Analysis of Coal* (Vol. 5, Issue 1, pp. 905–914).

Williams, P. T., & Williams, E. A. (1999). Interaction of plastics in mixed-plastics

pyrolysis. *Energy and Fuels*, *13*(1), 188–196. https://doi.org/10.1021/ef980163x

Windeatt, J. H., Ross, A. B., Williams, P. T., Forster, P. M., Nahil, M. A., & Singh, S. (2014). Characteristics of biochars from crop residues: Potential for carbon sequestration and soil amendment. *Journal of Environmental Management*, *146*, 189–197. https://doi.org/10.1016/j.jenvman.2014.08.003

Wolka, K., & Melaku, B. (2015). Exploring selected plant nutrient in compost prepared from food waste and cattle manure and its effect on soil properties and maize yield at Wondo Genet, Ethiopia. *Environmental Systems Research*, *4*(1). https://doi.org/10.1186/s40068-015-0035-0

Wong, J. W. C., Fung, S. O., & Selvam, A. (2009). Coal fly ash and lime addition enhances the rate and efficiency of decomposition of food waste during composting. *Bioresource Technology*, *100*(13), 3324–3331. https://doi.org/10.1016/j.biortech.2009.01.063

Wong, S. L., Ngadi, N., Abdullah, T. A. T., & Inuwa, I. M. (2015). Current state and future prospects of plastic waste as source of fuel: A review. *Renewable and Sustainable Energy Reviews*, *50*, 1167–1180. https://doi.org/10.1016/j.rser.2015.04.063

Woolf, D., Amonette, J. E., Street-Perrott, F. A., Lehmann, J., & Joseph, S. (2010). Sustainable biochar to mitigate global climate change. *Nature Communications*, *1*(5). https://doi.org/10.1038/ncomms1053

Wu, C.-H., Chang, C.-Y., Liu, Y.-F., & Yan, Y.-L. (2003). Effects of Oxygen on Pyrolysis Kinetics of Tetra Pack. *Journal of Environmental Engineering*, *129*(4), 382–386. https://doi.org/10.1061/(asce)0733-9372(2003)129:4(382)

Xiang, L., Liu, S., Ye, S., Yang, H., Song, B., Qin, F., Shen, M., Tan, C., Zeng, G., & Tan, X. (2021). Potential hazards of biochar: The negative environmental impacts of biochar applications. *Journal of Hazardous Materials*, *420*(January), 126611. https://doi.org/10.1016/j.jhazmat.2021.126611

Xing, Y., Wang, J., Xia, J., Liu, Z., Zhang, Y., Du, Y., & Wei, W. (2019). A pilot study on using biochars as sustainable amendments to inhibit rice uptake of Hg from a historically polluted soil in a Karst region of China. *Ecotoxicology and Environmental Safety*, *170*(November 2018), 18–24. https://doi.org/10.1016/j.ecoenv.2018.11.111

Xiu, S., & Shahbazi, A. (2012). Bio-oil production and upgrading research: A review. *Renewable and Sustainable Energy Reviews*, *16*(7), 4406–4414. https://doi.org/10.1016/j.rser.2012.04.028

Xu, J. L., Thomas, K. V., Luo, Z., & Gowen, A. A. (2019). FTIR and Raman imaging for microplastics analysis: State of the art, challenges and prospects. *TrAC - Trends in Analytical Chemistry*, *119*, 115629. https://doi.org/10.1016/j.trac.2019.115629

Xu, X., Hu, X., Ding, Z., Chen, Y., & Gao, B. (2017). Waste-art-paper biochar as an effective sorbent for recovery of aqueous Pb(II) into value-added PbO nanoparticles. *Chemical Engineering Journal*, *308*, 863–871. https://doi.org/10.1016/j.cej.2016.09.122

Xu, Y., Luo, G., He, S., Deng, F., Pang, Q., Xu, Y., & Yao, H. (2019). Efficient removal of elemental mercury by magnetic chlorinated biochars derived from co-pyrolysis of Fe(NO3)3-laden wood and polyvinyl chloride waste. *Fuel*, *239*(July 2018), 982–990.

https://doi.org/10.1016/j.fuel.2018.11.102

Yaashikaa, P. R., Kumar, P. S., Varjani, S., & Saravanan, A. (2020). A critical review on the biochar production techniques, characterization, stability and applications for circular bioeconomy. *Biotechnology Reports*, *28*, e00570. https://doi.org/10.1016/j.btre.2020.e00570

Yaashikaa, P. R., Senthil Kumar, P., Varjani, S. J., & Saravanan, A. (2019). Advances in production and application of biochar from lignocellulosic feedstocks for remediation of environmental pollutants. *Bioresource Technology*, *292*(August), 122030. https://doi.org/10.1016/j.biortech.2019.122030

Yang, H., Yan, R., Chen, H., Lee, D. H., & Zheng, C. (2007). Characteristics of hemicellulose, cellulose and lignin pyrolysis. *Fuel*, *86*(12–13), 1781–1788. https://doi.org/10.1016/j.fuel.2006.12.013

Yang, X., Hou, R., Fu, Q., Li, T., Li, M., Cui, S., Li, Q., & Liu, M. (2024). A critical review of biochar as an environmental functional material in soil ecosystems for migration and transformation mechanisms and ecological risk assessment. *Journal of Environmental Management*, *360*(May). https://doi.org/10.1016/j.jenvman.2024.121196

Yang, Y., Heaven, S., Venetsaneas, N., Banks, C. J., & Bridgwater, A. V. (2018). Slow pyrolysis of organic fraction of municipal solid waste (OFMSW): Characterisation of products and screening of the aqueous liquid product for anaerobic digestion. *Applied Energy*, *213*(November 2017), 158–168. https://doi.org/10.1016/j.apenergy.2018.01.018

Yang, Y., Wang, J., Chong, K., & Bridgwater, A. V. (2018). A techno-economic analysis of energy recovery from organic fraction of municipal solid waste (MSW) by an integrated intermediate pyrolysis and combined heat and power (CHP) plant. *Energy Conversion and Management*, *174*(August), 406–416. https://doi.org/10.1016/j.enconman.2018.08.033

Yargicoglu, E. N., Sadasivam, B. Y., Reddy, K. R., & Spokas, K. (2015). Physical and chemical characterization of waste wood derived biochars. *Waste Management*, *36*, 256–268. https://doi.org/10.1016/j.wasman.2014.10.029

Yenigün, O., & Demirel, B. (2013). Ammonia inhibition in anaerobic digestion: A review. *Process Biochemistry*, *48*(5–6), 901–911. https://doi.org/10.1016/j.procbio.2013.04.012

Yin, C. (2012). Microwave-assisted pyrolysis of biomass for liquid biofuels production. *Bioresource Technology*, *120*, 273–284. https://doi.org/10.1016/j.biortech.2012.06.016

Yufeng, Z., Na, D., Jihong, L., & Changzhong, X. (2003). A new pyrolysis technology and equipment for treatment of municipal household garbage and hospital waste. *Renewable Energy*, *28*(15), 2383–2393. https://doi.org/10.1016/S0960-1481(03)00065-X

Zabihi, M., Ahmadpour, A., & Haghighi Asl, A. (2009). Removal of mercury from water by carbonaceous sorbents derived from walnut shell. *Journal of Hazardous Materials*, *167*(1–3), 230–236. https://doi.org/10.1016/j.jhazmat.2008.12.108

Zaini, I. N., García López, C., Pretz, T., Yang, W., & Jönsson, P. G. (2019).

Characterization of pyrolysis products of high-ash excavated-waste and its char gasification reactivity and kinetics under a steam atmosphere. *Waste Management*, *97*, 149–163. https://doi.org/10.1016/j.wasman.2019.08.001

Zaman, A. U. (2013). Identification of waste management development drivers and potential emerging waste treatment technologies. *International Journal of Environmental Science and Technology*, *10*(3), 455–464. https://doi.org/10.1007/s13762-013-0187-2

Zhang, J., Wu, S., Xu, Z., Wang, M., Man, Y. B., Christie, P., Liang, P., Shan, S., & Wong, M. H. (2019). The role of sewage sludge biochar in methylmercury formation and accumulation in rice. *Chemosphere*, *218*, 527–533. https://doi.org/10.1016/j.chemosphere.2018.11.090

Zhang, L., Jing, Y., Chen, C., Xiang, Y., Rezaei Rashti, M., Li, Y., Deng, Q., & Zhang, R. (2021). Effects of biochar application on soil nitrogen transformation, microbial functional genes, enzyme activity, and plant nitrogen uptake: A meta-analysis of field studies. *GCB Bioenergy*, *13*(12), 1859–1873. https://doi.org/10.1111/gcbb.12898

Zhang, X., Wang, H., He, L., Lu, K., Sarmah, A., Li, J., Bolan, N. S., Pei, J., & Huang, H. (2013). Using biochar for remediation of soils contaminated with heavy metals and organic pollutants. *Environmental Science and Pollution Research*, *20*(12), 8472–8483. https://doi.org/10.1007/s11356-013-1659-0

Zhang, Y., Cheng, L., & Ji, Y. (2022). A novel amorphous porous biochar for adsorption of antibiotics: Adsorption mechanism analysis via experiment coupled with theoretical calculations. *Chemical Engineering Research and Design*, *186*, 362–373. https://doi.org/10.1016/j.cherd.2022.07.049

Zhao, H. L., Wang, L., Liu, F., Liu, H. Q., Zhang, N., & Zhu, Y. W. (2021). Energy, environment and economy assessment of medical waste disposal technologies in China. *Science of the Total Environment*, *796*, 148964. https://doi.org/10.1016/j.scitotenv.2021.148964

Zheng, J., Jin, Y. qi, Chi, Y., Wen, J. ming, Jiang, X. guang, & Ni, M. jiang. (2009). Pyrolysis characteristics of organic components of municipal solid waste at high heating rates. *Waste Management*, *29*(3), 1089–1094. https://doi.org/10.1016/j.wasman.2008.06.034

Zheng, L., Ji, H., Gao, Y., Yang, Z., Ji, L., Zhao, Q., Liu, Y., & Pan, X. (2022). Effects of Modified Biochar on the Mobility and Speciation Distribution of Cadmium in Contaminated Soil. *Processes*, *10*(5), 1–11. https://doi.org/10.3390/pr10050818

Zheng, X., Ying, Z., Wang, B., & Chen, C. (2019). Effect of Calcium Oxide Addition on Tar Formation During the Pyrolysis of Key Municipal Solid Waste (MSW) Components. *Waste and Biomass Valorization*, *10*(8), 2309–2318. https://doi.org/10.1007/s12649-018-0249-2

Zhou, C., Zhang, Q., Arnold, L., Yang, W., & Blasiak, W. (2013). A study of the pyrolysis behaviors of pelletized recovered municipal solid waste fuels. *Applied Energy*, *107*, 173–182. https://doi.org/10.1016/j.apenergy.2013.02.029

Zhou, H., Long, Y. Q., Meng, A. H., Li, Q. H., & Zhang, Y. G. (2015). Interactions of three municipal solid waste components during co-pyrolysis. *Journal of Analytical and Applied Pyrolysis*, *111*, 265–271. https://doi.org/10.1016/j.jaap.2014.08.017

Zu'amah, H., Dewi, T., Handayani, C. O., Gafur, N. A., & Arianti, F. D. (2024). Impact of compost and biochar from agricultural waste on reducing cadmium concentration and mancozeb residue in soil. *Journal of Degraded and Mining Lands Management*, *11*(4), 6307–6317. https://doi.org/10.15243/jdmlm.2024.114.6307

ANNEXURE 1

OUTCOMES OF THE THESIS

JOURNAL PUBLICATIONS

Published articles

- Saikia, S., & Kalamdhad, A. S. (2023). Response surface methodology (RSM) - based pyrolysis process parameter optimization for char generation from municipal solid waste (MSW) in a fixed bed reactor. *Sustainable Energy Technologies and Assessments*, *60*(July), 103541. https://doi.org/10.1016/j.seta.2023.103541
- Saikia, S., & Kalamdhad, A.S. (2023). Assessment of pyrolysis potential of Indian municipal solid waste and legacy waste via physicochemical and thermochemical characterization. *Bioresource Technology*. https://doi.org/10.1016/j.biortech.2023.130289
- Saikia, S., Chaitanya, K., Harsh, M., Suryateja, P., & Kalamdhad, A. S. (2024). Application of municipal solid waste (MSW) char during rotary drum co - composting (RDC) of vegetable waste and its characterization. *Environmental Science and Pollution Research*, *0123456789*. https://doi.org/10.1007/s11356-024-34332-4
- Saikia, S., Anagha, V., Khwairakpam, M., & Kalamdhad, A. S. (2024). Assessment of activated carbon derived from municipal solid waste char as a precursor for mitigation of heavy metals. Biomass and Bioenergy, 190(August), 107385. https://doi.org/10.1016/j.biombioe.2024.107385
- Saikia, S., Prit, H., Chaitanya, K., & Kalamdhad, A. S. (2025). Amendment of Nutrient - deficient Alluvial Soil by Municipal Solid Waste Char and Compost for the Remediation of Contaminants and Enhancement of Plant Growth. *Water, Air, & Soil Pollution*. https://doi.org/10.1007/s11270-025-07872-9
- Saikia, S., Kumar, S., & Kalamdhad, A. S. (2025). Application of unsegregated municipal solid waste char produced at low temperature and

vermicompost for remediation of coal mine tailing soil. *Environmental Geochemistry and Health*. https://doi.org/10.1007/s10653-025-02436-6

Articles (submitted/under review)

- Saikia, S., Anagha, V., Kalamdhad, A. S., Khwairakpam, M., (2024). Assessment of char quality produced through pyrolysis of commingled municipal solid waste at varying temperatures and its prospective utilization. *Environmental Sustainability*. **(Revisions submitted)**

BOOK CHAPTERS

- Saikia, S., & Kalamdhad, A.S. (2024). Innovative Pyrolysis Technologies for thermochemical processing of Municipal Solid Waste into products with enhanced values. *Advancement in Solid Waste Management and Treatment.* Springer, 179, doi:10.1007/978-3-031-64873-1_14

INTERNATIONAL CONFERENCES

- Saikia, S., & Kalamdhad, A.S. (2023). Characterization of char generated from pyrolysis of municipal solid waste and its potential as a carbon precursor. 4th International Conference on Recent Advances in Bio-energy Research, 9-12 October, 2023, Punjab (India).
- Saikia, S., & Kalamdhad, A.S. (2023). Pyrolysis of municipal solid waste and its product application, International Conference on Environmental Sustainability and Climate Change, 21-22 December 2023, Meghalaya (India).
- Saikia, S., & Kalamdhad, A.S. (2024). Application of municipal solid waste char in rotary drum composting and its characterization, International Conference on Waste Recycling and Environmental Technology, 8-9 February 2024, Lucknow (India).
- Saikia, S., & Kalamdhad, A.S. (2024). Pyrolysis of municipal solid waste to generate char and its prospective utilization as a carbon precursor. Research and Industrial Conclave-Integration'24, 9-11 August 2024, Indian Institute of Technology Guwahati, Guwahati, Assam, (India).

AWARDS

- Best oral presentation award for the paper, "Characterization of char generated from pyrolysis of municipal solid waste and its potential as a carbon precursor" at

4th International Conference on Recent Advances in Bio-energy Research, 9-12 October 2023, Punjab (India).

- Best paper award for the paper, "Pyrolysis of municipal solid waste and its product application" at the International Conference on Environmental Sustainability and Climate Change, 21-22 December 2023, Meghalaya (India).
- Winner of SCIENTIFIQUE: ORAL PRESENTATION entitled "Pyrolysis of municipal solid waste to generate char and its prospective utilization as a carbon precursor" at Research and Industrial Conclave-Integration'24, 9-11 August 2024, Indian Institute of Technology Guwahati, Guwahati, Assam, (India).